



The University of
Nottingham

**The role of VGF and its derived peptides in the regulation of energy
homeostasis**

Jo Edward Lewis BSc, MSc.

BSc (Hons) University of Leeds, (2004)

MSc University of Westminster, (2008)

This thesis is submitted to the University of Nottingham in accordance with
the requirements for the degree of Doctor of Philosophy

Division of Nutritional Sciences

School of Biosciences

University of Nottingham

September 2014

Abstract

The VGF gene (non-acronymic) was first implicated in energy homeostasis by VGF^{-/-} null mice, which were lean, hypermetabolic and hyperactive, suggesting an anabolic role for VGF (Hahm et al., 1999). Furthermore, VGF^{-/-} mice were resistant to obesity induced by diet and genetic manipulation (Hahm et al., 2002). While VGF mRNA was reduced in response to short photoperiod, which is associated with reduced food intake and the utilisation of intra-abdominal fat stores in the Siberian hamster (Barrett et al., 2005; Ebling, 2014). However subsequent studies in Siberian hamsters and mice have suggested a catabolic role for the VGF derived peptide TLQP-21 (Bartolomucci et al., 2006; Jethwa et al., 2007). Thus the aim of this thesis was to further investigate the role of VGF in the regulation of energy homeostasis in the mouse and Siberian hamster.

The studies presented in this thesis have shown that VGF derived peptide HHPD-41 can affect short term food intake in the Siberian hamsters, while over-expressing VGF mRNA in the hypothalamus of both Siberian hamsters and mice reduced bodyweight. However, this reduction in body weight was associated with an increase in both food intake and energy expenditure. These effects of VGF overexpression were attenuated in disrupted models of energy regulation. Finally these studies identified novel regulators of the VGF gene *in vitro* to postulate a possible mechanism for the seasonal regulation of appetite in the Siberian hamster. Collectively, the studies described in this thesis demonstrate a role for VGF in the regulation of energy homeostasis and contribute to increasing our understanding of how the brain regulates food intake.

Acknowledgements

Firstly, I would like to thank my PhD supervisors Drs Preeti Jethwa, John Brameld and Phil Hill. Without their expertise and guidance this body of work would not have been possible. I would also like to thank Professor Fran Ebling and Dr Dylan Sweetman for their generous advice and assistance.

I feel very fortunate to have worked with these eminent scientists.

Furthermore I'd like to thank the technical staff (Cathy, Ian, Kirsty, Maxine, Tania and Zoe and those in the BMU at the University of Nottingham) who were instrumental in my training, as well as my friends and colleagues in the Division of Nutritional Sciences

I'd also like to thank my friends whom have kept me (relatively) sane throughout this process – you are too numerous to mention but know that your support is appreciated. A special thank you is reserved for Richard Malham for his time and effort, with only beers and friendship to show for it, and to Kowski.

Finally I wish to thank my superhumanly patient and always supportive girlfriend Miranda and my parents, Bernardette, Sam and Al. Whilst they deserve medals, I can only offer my heartfelt thanks.

This PhD is dedicated to the woman I told I didn't need a piece of paper to demonstrate I was clever.

Declaration

The candidate confirms that the work submitted is his own and that appropriate credit has been given where reference has been made to the work of others.

All of the procedures presented in this thesis have been performed by myself, with the following exceptions:

Dr Preeti Jethwa aided in the ICV cannulation studies presented in chapter 3 and the microinjection of AAV in chapter 4, while Professor Fran Ebling aided in the perfusion studies presented in chapter 3. Dr Ricardo Samms aided in the dissection studies performed in chapter 4 and Dr Dylan Sweetman aided in the *in situ* hybridisation studies performed in chapter 4.

This copy has been supplied on the understanding that it is copyright material and that no quotation from the thesis may be published without proper acknowledgement.

© The University of Nottingham and Jo Edward Lewis

The right of Jo Edward Lewis to be identified as Author of this work has been asserted by him in accordance with the Copyright, Designs and Patents Act, 1988.

Publications

Lewis JE, Brameld JM and Jethwa PH (2015) *Neuroendocrine Role of Vgf. Frontiers in Endocrinology* 6; 3 doi: 10.3389/fendo.2015.00003. eCollection 2015.

Lewis JE, Brameld JM, Hill P, Barrett P, Ebling FJP and Jethwa PH (2015) The use of a viral 2A sequence for the simultaneous over-expression of both the vgf gene and enhanced green fluorescent protein (eGFP) in vitro and in vivo (submitted).

Lewis JE, Brameld JM, Hill P, Ebling FJP and Jethwa PH (2015) Thyroid hormone and vitamin D regulates VGF expression and promoter activity in SH-SY5Y cells; a possible mechanism for the seasonal regulation in the Siberian hamster (in preparation).

Lewis JE, Brameld JM, Hill P, Barrett P, Ebling FJP and Jethwa PH (2015) Over-expression of VF mRNA within the hypothalamus of Siberian hamsters and mice reduces bodyweight and increases food intake and energy expenditure (in preparation).

Conferences

Lewis JE, Hill PJ, Brameld JM and Jethwa PH 2014 *Thyroid hormone (T3) represses VGF endogenous expression and promoter activity: a possible mechanism for the seasonal regulation of appetite*. Abstract 163, Poster at The International Congress of Neuroendocrinology. 17 – 20 August 2014, Sydney, Australia.

Lewis JE, Hill PJ, Brameld JM and Jethwa PH 2014 *Retinoic acid (RA) and nerve growth factor (NGF) induce VGF endogenous expression and promoter activity in SH-SY5Y cells*. Abstract 255, Poster at The International Congress of Neuroendocrinology. 17 – 20 August 2014, Sydney, Australia.

Lewis JE, Ebling FJ, Hill PJ, Brameld JM and Jethwa PH 2013 *The role of VGF and its derived peptides in the regulation of energy balance*. Abstract 4, Oral Presentation at Food for Thought, Full4Health. 14 -18 July 2013, Chiemsee, Germany.

Lewis JE, Ebling FJ, Hill PJ, Brameld JM and Jethwa PH 2013 *Central over-expression of VGF using adeno-associated virus increases food intake and energy expenditure*. Abstract 15, Oral Presentation and Poster at the British Society for Neuroendocrinology. 7 – 9 July 2013, Manchester, UK.

Lewis JE, Ebling FJ, Hill PJ, Brameld JM and Jethwa PH 2013 *2A or not 2A; the advantages of the viral 2A peptide in multicistronic vector strategies*. Abstract 1, Oral Presentation at the Early Stage Researchers Committee, British Society for Neuroendocrinology. 7 – 9 July 2013, Manchester, UK.

Lewis JE, Ebling FJ, Hill PJ, Brameld JM and Jethwa PH 2012 *Peptides derived from VGF pro-peptide have differential effects on food intake*. Abstract 14, Oral Presentation and Poster at the British Society for Neuroendocrinology. 8 – 10 July 2012, Aberdeen, UK.

Abbreviations

3V – Third ventricle

AAV – Adeno-associated virus

α MSH – Alpha-Melanocortin stimulating hormone

AgRP – Agouti related protein

AM – Amygdala

ANOVA – Analysis of variance

AP-2 – Activating protein 2

AR – Adrenergic receptor

ARC – Arcuate nucleus

B3-AR – Beta-3 Adrenergic receptor

BAT – Brown adipose tissue

BBB – Blood-brain barrier

BCIP – indoxyl-nitroblue tetrazolium

BDNF – Brain-derived neurotrophic factor

BMI – Body mass index

BMU – Biomedical sciences unit

BSA – Bovine serum albumin

C3AR1 – Complement C3a receptor-1

cAMP – Cyclic adenosine monophosphate

CART – Cocaine- and amphetamine-regulated transcript

CC – Corpus callosum

CCK – Cholecystokinin

CCX – Cerebral cortex

cDNA – Complementary deoxyribonucleic acid

CLAMS – Comprehensive laboratory animal monitoring system

CNS – Central nervous system

CRE – Cyclic adenosine monophosphate-response element

CREB – Cyclic adenosine monophosphate response element binding protein

DAB – Diaminobenzidine

DIG – Dioxigenin

DIO – Diet-induced obesity

DIOX – Type X iodothyronine deiodinase enzyme

DMN – Dorsomedial nucleus

DNA – Deoxyribonucleic acid

dmpARC – Dorsomedial posterior arcuate nucleus

dsDNA – Double stranded deoxyribonucleic acid

dUTP – Deoxyuridine triphosphate

E.coli – *Escherichia coli*

EGF – Epidermal growth factor

ER – Endoplasmic reticulum

EX – Embryonic day X

FGF – Fibroblast growth factor

G – Gravity

GABA – Gamma-Aminobutyric acid

Gc – Genomic copies

GPCR – G protein-coupled receptor

HEK – Human embryonic kidney

HFD – High fat diet

HI - Hippocampus

Hyb - Hybridisation

ICC – Immunocytochemistry

ICV – Intracerebroventricular

IgG – Immunoglobulin G

i.p. – Intraperitoneal

IL-6 – Interleukin 6

Ires – Internal ribosome entry site

ISH – *In situ* hybridisation

JM 109 – Bacterial strain of *E.coli*

KO – Knockout

LD – Long day

LH – Luteinising hormone

LHA – Lateral hypothalamic area

MABT – Maleic acid buffer containing Tween20

MASH-1 – Mammalian achaete-scute homologue-1

MC4R – Melanocortin 4 receptor

MCS – Multiple cloning site

ME – Medial eminence

MSG – Monosodium glutamate

NERP – Neuroendocrine regulatory peptide

NGF – Nerve growth factor

NHS – National Health Service

NPY – Neuropeptide Y

NMTT – 1-methyl-5-thiotetrazole

NT-3 – Neurotrophin 3

NTS – Solitary nucleus

OC – Olfactory chiasm

OCT – Optimal temperature compound

PBS – Phosphate buffered saline

PBSTw – Phosphate buffered saline containing Tween20

PC – Prohormone convertases

PC12 – rat pheochromocytoma cell line

PCR – Polymerase chain reaction

PFA – Paraformaldehyde

PG – Prostaglandin

PMT – Photomultiplier tube

PNS – Peripheral nervous system

POMC – Proopiomelanocortin

PPAR- δ – Peroxisome proliferator-activated receptor- δ

PVN – Paraventricular nucleus

rAAV – recombinant adeno-associated virus

RE – Restriction enzyme

RER – Respiratory exchange ratio

RNA – Ribonucleic acid

RPM – Revolutions per minute

rT3 – Reverse triiodothyronine

s.c. – subcutaneous

SCN – Suprachiasmatic nucleus

SD – Short day

SE – Septum

SEM – Standard error mean

SH-SY5Y – subclone of SK-N-SH cell line

Sp-1 – Specificity protein 1

T2DM – Type 2 diabetes mellitus

T3 – Triiodothyronine

T4 - Thyroxine

TH - Thalamus

TRH – Thyrotropin-releasing hormone

TSH – Thyroid-stimulating hormone

UCP-1 – Uncoupling protein-1

VCO₂ – Carbon dioxide production

VGF – Non-acronymic, plate V of NGF-induced PC12 cDNA library

VMN – Ventomedial nucleus

VO₂ – Oxygen consumption

WAT –White adipose tissue

WHO – World Health Organisation

Contents

Abstract.....	1
Acknowledgements	2
Declaration	4
Publications	5
Conferences.....	5
Abbreviations.....	7
Contents.....	13
List of Figures.....	21
List of Tables	24
1 Chapter 1 – GENERAL INTRODUCTION.....	25
1.1 OBESITY – AN OVERVIEW	26
1.2 THE CENTRAL CONTROL OF ENERGY HOMEOSTASIS	29
1.2.1 The structure of the hypothalamus.....	29
1.2.1.1 Arcuate nucleus (ARC)	32
1.2.1.2 Paraventricular nucleus (PVN).....	33
1.2.1.3 Dorsomedial nucleus (DMN).....	34
1.2.1.4 Ventromedial nucleus (VMN)	34
1.2.1.5 Lateral hypothalamic area (LHA)	34
1.2.1.6 Perifornical area.....	35
1.2.2 The hypothalamic regulation of food intake and energy expenditure	36
1.2.3 Peripheral Control of appetite.....	37
1.2.3.1 Cholecystinin (CCK)	39
1.2.3.2 Glucagon-like peptide (GLP)-1	39
1.2.3.3 Peptide YY (PYY).....	39
1.2.3.4 Adiposity signals: Insulin and leptin.....	40
1.2.3.5 Neuropeptides and adiposity signals.....	41
1.3 ANIMAL MODELS UTILISED IN THE STUDY OF OBESITY.....	47
1.3.1 The Siberian hamster.....	47
1.3.2 The C57BL/6J Mouse	51
1.4 VGF – A NEUROTROPHIN-INDUCED GENE.....	54
1.4.1 The transcriptional regulation of VGF	55
1.4.2 The structure of the VGF polypeptide	61
1.4.3 VGF expression	65

1.4.3.1	VGF mRNA.....	65
1.4.3.2	Peptides	67
1.4.4	VGF ^{-/-} null mouse	68
1.4.5	VGF and obesity	70
1.4.6	Physiological roles of VGF and VGF derived peptides	73
1.4.6.1	VGF expression in states of altered energy balance.....	74
1.4.6.2	VGF in response to season.....	74
1.4.6.3	The VGF derived peptide TLQP-21.....	75
In Mice		75
In Mice switched to a High Fat Diet (HFD).....		76
In Siberian hamsters		77
In Rats		79
1.4.6.4	The VGF derived peptides neuroendocrine regulatory peptides (NERP)-1 and NERP-2	79
1.5	AIMS AND OBJECTIVES	80
1.5.1	Chapter 3 Objectives.....	81
1.5.2	Chapter 4 Objectives.....	81
1.5.3	Chapter 5 Objectives.....	82
2	CHAPTER 2 – MATERIALS AND METHODS	84
2.1	INTRODUCTION.....	85
2.2	NUCLEIC ACID EXTRACTIONS AND PROCEDURES	86
2.2.1	Extraction of total genomic DNA	86
2.2.2	Phenol: Chloroform extraction	86
2.2.3	Removal of contaminating DNA	87
2.2.4	DNA/RNA quality assessment and quantification	87
2.2.5	Agarose gel electrophoresis	87
2.3	CLONING	88
2.3.1	PCR amplicon clean-up	88
2.3.2	pGEM T-Easy Vector cloning of PCR amplicons	88
2.3.3	Ligation	88
2.3.4	Transformation	89
2.3.4.1	JM109 cells.....	89
2.3.4.2	SURE 2 Supercompetent cells.....	89
2.3.5	Plasmid miniPrep	90

2.3.6	Plasmid maxiPrep	90
2.3.7	Glycerol stocks	90
2.3.8	Restriction enzyme digestion of DNA	90
2.3.9	DNA sequencing.....	91
2.4	SUBCLONING.....	91
2.4.1	Alkaline phosphatase treatment	91
2.5	ANIMALS	91
2.5.1	Siberian hamsters	92
2.5.2	C57BL/6J Mice.....	92
3	Chapter 3 – THE VGF DERIVED PEPTIDES HHPD-41 AND TLQP-21 HAVE DIFFERENTIAL EFFECTS ON FOOD INTAKE IN SIBERIAN HAMSTERS.....	93
3.1	THE ROLE OF VGF IN THE REGULATION OF ENERGY HOMEOSTASIS.....	94
3.1.1	VGF null mouse	94
3.2	VGF EXPRESSION IN ALTERED ENERGY BALANCE.....	94
3.2.1	In response to fasting	94
3.2.2	In response to season in the Siberian hamster	95
3.3	VGF POLYPEPTIDE	95
3.3.1	Roles of VGF derived peptides.....	95
3.3.1.1	TLQP-21.....	95
3.3.1.2	Neuroendocrine regulatory peptide-1 and -2 (NERP-1 and -2).....	96
3.4	AIMS AND OBJECTIVES	97
3.5	MATERIALS AND METHODS.....	98
3.5.1	Peptides	98
3.5.2	Siberian hamsters	98
3.5.3	ICV Cannulation and infusion	98
3.5.4	Palatable diet	100
3.5.5	Determining the optimum working dose of HHPD-41	100
3.5.6	The effects of ICV infusion of HHPD-41 on food intake, bodyweight and behaviour.....	101
3.5.7	Investigating the site of action of HHPA-41 and TLQP-21	101
3.5.8	Statistics.....	102
3.6	RESULTS	104
3.6.1	Determining the optimum working dose of HHPD-41	104
3.6.2	The effects of ICV infusion of HHPD-41 on food intake and bodyweight	106

3.6.3	c-Fos.....	108
3.7	DISCUSSION	110
3.8	CONCLUSION	116
4	Chapter 4 – CENTRAL OVER-EXPRESSION OF VGF USING A RECOMBINANT ADENO-ASSOCIATED VIRUS INCREASES FOOD INTAKE AND ENERGY EXPENDITURE IN THE SIBERIAN HAMSTER AND MOUSE	118
4.1	INTRODUCTION.....	119
4.1.1	rAAV and energy homeostasis.....	119
4.2	THE VIRAL 2A PEPTIDE; A SUITABLE ALTERNATIVE TO THE INTERNAL RIBOSOME ENTRY SITE (ires)	122
4.3	AIMS AND OBJECTIVE	123
4.4	METHODS.....	124
4.4.1	Preparation of AAV	124
4.4.2	The SH-SY5Y cell line.....	126
4.4.3	Typhoon Trio+.....	127
4.4.4	ImageQuant	127
4.4.5	Animals	127
4.4.5.1	Siberian hamsters	127
4.4.5.2	C57Bl/6J Mice	127
4.4.6	Viral infusion	127
4.4.7	Comprehensive Laboratory Animal Monitoring System (CLAMS).....	128
4.4.8	Dissection.....	129
4.4.9	Cryostat.....	129
4.4.10	<i>In situ</i> hybridisation	129
4.4.10.1	Generation of riboprobes	130
4.4.10.2	Detection of mRNA	130
4.4.11	Statistics.....	132
4.5	EXPERIMENTAL DESIGN.....	133
4.5.1	Siberian hamsters	133
4.5.1.1	Study 1: The effects of VGF over-expression in the hypothalamus of Siberian hamsters	133
4.5.1.2	Study 2: The effects of VGF over-expression in the hypothalamus of Siberian hamsters transferred to SD	133
4.5.2	Mice	133

4.5.2.1	Study 3: The effects of VGF over-expression in the hypothalamus of mice	133
4.5.2.2	Study 4: The effects of VGF over-expression in the hypothalamus of the mice transferred to a HFD	134
4.6	RESULTS	135
4.6.1	Construct expression in SH-SY5Y cells	135
4.6.1.1	Transfection of the SH-SY5Y cell line with pAAV-CBA-VGF-2A-eGFP-WPRE significantly increased eGFP expression	135
4.6.1.2	Transfection of the SH-SY5Y cell line with pAAV-CBA-VGF-2a-eGFP-WPRE significantly increased VGF mRNA	137
4.6.1.3	AAV-VGF infection of SH-SY5Y cells significantly increased eGFP expression	138
4.6.2	Study 1: The effects of VGF over-expression in the hypothalamus of Siberian hamsters	139
4.6.2.1	Over-expression of VGF mRNA significantly increased food intake, but bodyweight remained constant	139
4.6.2.2	Over-expression of VGF mRNA significantly increased oxygen consumption	142
4.6.2.3	Over-expression of VGF mRNA results in an increase in brown adipose tissue	145
4.6.3	Study 2: The effects of VGF over-expression in the hypothalamus of Siberian hamsters transferred to SD	146
4.6.3.1	Over-expression of VGF mRNA in SD has no effect on body weight, however food intake was significantly increased	147
4.6.3.2	Over-expression of VGF mRNA increased oxygen consumption and carbon dioxide production, RER was significantly increased	150
4.6.3.3	eGFP expression in the hypothalamus of Siberian hamsters was widespread	154
4.6.3.4	VGF mRNA expression was higher in Siberian hamsters receiving the over-expression vector	157
4.6.4	Study 3: The effects of VGF over-expression in the hypothalamus of the mouse	159
4.6.4.1	Over-expression of VGF mRNA significantly affects food intake and body weight	159
4.6.4.2	Over-expression of VGF mRNA significantly increased oxygen consumption	162
4.6.4.3	Over-expression of VGF mRNA significantly affected the epididymal fat weight	165

4.6.5	Study 4: The effects of VGF over-expression in the hypothalamus of mice transferred to a HFD	167
4.6.5.1	Over-expression of VGF mRNA significantly increased body weight but food intake was unaffected.....	167
4.6.5.2	Over-expression of VGF mRNA significantly increased RER	170
4.6.5.3	Hypothalamic expression of eGFP is similar to Siberian hamsters	172
4.6.5.4	In situ hybridisation revealed similar expression to Siberian hamsters	172
4.7	DISCUSSION	173
4.7.1	The timecourse studies in the Siberian hamster and C57Bl/6J mouse	175
4.7.2	VGF over-expression in disrupted models of energy homeostasis ...	180
4.8	CONCLUSION	184
5	Chapter 5 – THYROID HORMONE (T3), IN VITRO, REPRESSES VGF ENDOGENOUS EXPRESSION AND PROMOTER ACTIVITY; A NOVEL, POSSIBLE MECHANISM FOR THE SEASONAL REGULATION OF APPETITE	185
5.1	THE HYPOTHALAMUS-PITUITARY-THYROID (HPT) AXIS	186
5.2	THYROID HORMONE RECEPTOR (TR).....	188
5.3	THYROID HORMONE RESPONSE ELEMENT (TRE)	189
5.4	VITAMIN D (1,25-DIHYDROXYVITAMIN D3 (1,25D3)).....	190
5.5	AIMS AND OBJECTIVES	190
5.6	MATERIALS AND METHODS.....	192
5.6.1	Cell Culture	192
5.6.1.1	The SH-SY5Y cell line.....	192
5.6.1.2	Differentiation	193
5.6.1.3	Adhesion	193
5.6.1.4	Endogenous expression	194
5.6.1.5	RNA extraction.....	194
5.6.1.6	Generation of first strand complimentary DNA	194
5.6.1.7	Oligonucleotide primer design	195
5.6.1.8	Polymerase chain reaction	196
5.6.1.9	Quantitative PCR.....	197
5.6.1.10	Data normalisation	197
5.6.1.11	Transfection	198
5.6.1.12	Typhoon Trio+	198

5.6.1.13	ImageQuant	199
5.6.1.14	Statistics	199
5.6.2	Cloning	200
5.6.2.1	Development of a reporter construct.....	200
5.6.2.2	Development of the promoter constructs.....	200
5.7	RESULTS	203
5.7.1	Characterisation of the SH-SY5Y cell line.....	203
5.7.1.1	Nerve growth factor (NGF) treatment of the SH-SY5Y cell line increased proliferation	203
5.7.1.2	Retinoic acid (RA) treatment of the SH-SY5Y cell line reduces proliferation and increased differentiation	204
5.7.1.3	Long term treatment of the SH-SY5Y cell line with RA resulted in a heterogeneous population of neuronal cells	205
5.7.1.4	Exposure of the SH-SY5Y cell line to RA and subsequently NGF resulted in a homogenous population of neuronal cells.....	205
5.7.1.5	Collagen increased neurite outgrowth in the SH-SY5Y cell line	208
5.7.1.6	RA treatment of the SH-SY5Y cell line increased neuronal markers of differentiation.....	209
5.7.2	The response of endogenous VGF expression to RA, NGF, T3 and 1,25D3 treatment of the SH-SY5Y cell line	210
5.7.2.1	RA and NGF treatment of undifferentiated SH-SY5Y cells significantly increased endogenous VGF expression.....	210
5.7.2.2	T3 treatment of undifferentiated and differentiated SH-SY5Y cells significantly reduced endogenous VGF expression	211
5.7.2.3	1,25D3 treatment of undifferentiated and differentiated SH-SY5Y cells significantly increased endogenous VGF expression.....	211
5.7.3	The response of the VGF promoter to RA, NGF, T3 and 1,25D3 treatment.....	213
5.7.3.2	T3 reduced vgf promoter activity in undifferentiated and differentiated SH-SY5Y cells.....	216
5.7.3.3	1,25 D3 increased vgf promoter activity in undifferentiated and differentiated SH-SY5Y cells.....	218
5.8	DISCUSSION	220
5.8.1	NGF, RA and 1,25D3: Transcriptional activators of the VGF gene and promoter	224
5.8.2	T3: A transcriptional repressor of the VGF gene and promoter.....	226
5.9	CONCLUSION	231

6	Chapter 6 – GENERAL DISCUSSION.....	232
6.1	SUMMARY.....	233
6.1.1	The ICV infusion of HHPD-41 demonstrated an initial opposing role of VGF derived peptides in food intake	234
6.1.2	The over-expression of VGF mRNA in the hypothalamus of Siberian hamsters and mice demonstrates a function beyond food intake	235
6.1.3	VGF over-expression in disrupted models of energy homeostasis ...	239
6.1.4	Thyroid hormone represses endogenous VGF expression and promoter activity <i>in vitro</i>	241
6.2	MAIN IMPLICATIONS, LIMITATIONS AND FUTURE WORK.....	242
6.3	CLOSING REMARKS	245
	Appendix 1 – Buffers and Solutions.....	246
	REFERENCES.....	251

List of Figures

Figure 1.2.1 Schematic of the rat brain displaying the major hypothalamic regions implicated in the regulation of food intake.....	31
Figure 1.2.3.5 The hypothalamus and leptin - their role in the regulation of energy homeostasis.....	45
Figure 1.3.1 The Siberian hamster shown in long days and short days.....	48
Figure 1.4.1 The nucleotide sequence of the 5' region of the mouse <i>vgf</i> gene.....	60
Figure 1.4.2 A Pairwise sequence alignment of the human and mouse VGF protein sequence.....	62-63
Figure 1.4.2 B The <i>vgf</i> gene and its derived peptides.....	64
Figure 1.4.5 The VGF ^{-/-} mouse with a wildtype littermate.....	73
Figure 3.6.1 Effects of acute ICV infusion of the VGF derived peptide HHPD-41 on food intake, body weight and behaviour.....	105
Figure 3.6.2 Effects of acute ICV infusion of the VGF derived peptides HHPD-41 and TLQP-21 on food intake.....	107
Figure 3.6.3 Neuronal activation, indicated by c-fos expression, in the PVN of Siberian hamsters treated with saline (A), HHPD-41 (B) or TLQP-21 (C)	109
Figure 4.4.1 A schematic of the pAAV-CBA-VGF-2a-eGFP-WPRE.....	127
Figure 4.6.1.1 eGFP expression in SH-SY5Y cells following transfection with pAAV-CBA-VGF-2a-eGFP-WPRE.....	137
Figure 4.6.1.2 SH-SY5Y cells transfected with pAAV-CBA-VGF-2A-eGFP-WPRE results in significantly increased VGF mRNA expression.....	138
Figure 4.6.1.3 Increased MOI increases eGFP expression in SH-SY5Y cells....	139
Figure 4.6.2.1 Over-expression of VGF mRNA in the hypothalamus of Siberian hamsters significantly increased food intake, while body weight was significantly reduced.....	141
Figure 4.6.2.1 F Over-expression of VGF mRNA in the hypothalamus of Siberian hamsters significantly affected feeding behaviour.....	142
Figure 4.6.2.3 The metabolic parameters of Siberian hamsters over-expressing VGF mRNA in the hypothalamus was significantly altered...144-145	
Figure 4.6.3.1 Despite no differences in body weight of Siberian hamsters over-expressing VGF mRNA within the hypothalamus, cumulative food intake was significantly increased.....	149

Figure 4.6.3.1 F Over-expression of VGF mRNA in the hypothalamus of Siberian hamsters significantly affected feeding behaviour.....	150
Figure 4.6.3.2 The metabolic parameters of Siberian hamsters over-expressing VGF mRNA in the hypothalamus was altered.....	152-153
Figure 4.6.3.3 A eGFP expression in the hypothalamus of Siberian hamsters	156
Figure 4.6.3.3 B eGFP expression in the PVN of Siberian hamsters.....	157
Figure 4.6.3.4 Examples of the distribution of eGFP and VGF mRNA in the Siberian hamster following SD exposure.....	159
Figure 4.6.4.1 Despite significantly increased food intake in mice over-expressing VGF mRNA within the hypothalamus, body weight was reduced	161
Figure 4.6.4.1 F Over-expression of VGF mRNA in the hypothalamus of mice significantly affected feeding behaviour.....	162
Figure 4.6.4.2 The metabolic parameters of mice over-expressing VGF mRNA in the hypothalamus were significantly altered.....	164-165
Figure 4.6.5.1 The over-expression of VGF mRNA in the hypothalamus of mice fed a high fat diet (HFD) resulted in significantly increased body weight but unaltered food intake.....	169
Figure 4.6.5.1 F Over-expression of VGF mRNA in the hypothalamus of mice significantly affected feeding behaviour.....	170
Figure 4.6.5.2 The metabolic parameters of mice over-expressing VGF mRNA in the hypothalamus was significantly altered 8 weeks post exposure to HFD	172-173
Figure 5.6.2.2 Plasmid map of pVGFCBG992AmRFP containing 1Kb of the VGF promoter.....	203
Figure 5.7.1.1 Treatment of the SH-SY5Y cell line with NGF increased cell proliferation.....	204
Figure 5.7.1.2 Treatment of the SH-SY5Y cell line with RA reduced cell proliferation and increased differentiation.....	205
Figure 5.7.1.3 Long term treatment of the SH-SY5Y cell line with RA resulted in a heterogeneous population of neuronal cells.....	206
Figure 5.7.1.4 Treatment of the SH-SY5Y cell line with RA and NGF resulted in a more homogenous population of N-type cells.....	208
Figure 5.7.1.5 The effect of extracellular matrices on neurite outgrowth in the differentiated SH-SY5Y cell line.....	209

Figure 5.7.1.6 RA treatment of the SH-SY5Y cell line increased neuronal markers of differentiation.....	210
Figure 5.7.2.1 Endogenous VGF mRNA expression in undifferentiated SH-SY5Y cells was increased by treatment with NGF and RA.....	211
Figure 5.7.2.2 Treatment of undifferentiated and differentiated SH-SY5Y cells with T3 reduced while 1,25D3 increased endogenous VGF expression.....	213
Figure 5.7.3 The VGF promoter constructs and their promoter activities.....	214
Figure 5.7.3.1 RA and NGF treatment of undifferentiated and differentiated SH-SY5Y cells increased VGF promoter activity.....	216
Figure 5.7.3.2 T3 reduces vgf promoter activity in undifferentiated and differentiated SH-SY5Y cells.....	218
Figure 5.7.3.3 1,25D3 increased vgf promoter activity in undifferentiated and differentiated SH-SY5Y cells.....	220
Figure 5.8.2 Schematic of the proposed role of T3 and RA in the hypothalamus of Siberian hamsters as a possible mechanism for the seasonal regulation of appetite.....	228
Figure 6.1.2 A possible mechanism for the activation of BAT by VGF.....	238

List of Tables

Table 1.2.2 Hypothalamic neuropeptides implicated in the control of food intake and energy homeostasis.....	37
Table 1.3.1 Effect of SD photoperiod on hypothalamic neuropeptide gene expression at the mRNA level.....	50
Table 2 The materials and methods of relevant chapters.....	85
Table 3.3.1.1 The contrasting findings of VGF ^{-/-} mice and subsequent ICV infusion studies with the VGF derived peptide TLQP-21 in mice and Siberian hamsters	96
Table 3.5.5 The five behavioural categories of the Siberian hamster used in this study.....	101
Table 4.1.1 Comparison of the feeding and metabolic parameters affected by over-expression of AgRP and NPY in the PVN and LHA respectively...	121
Table 4.6.2.4 Over-expression of VGF mRNA in the hypothalamus of Siberian hamsters, maintained in LD, resulted in significantly increased BAT weight.	146
Table 4.6.3 Over-expression of VGF mRNA in the hypothalamus of Siberian hamsters, switched to short day (SD) photoperiod, resulted in a significant decrease in epididymal fat	147
Table 4.6.4.3 Over-expression of VGF mRNA in the hypothalamus of mice resulted in differential fat mass.....	166
Table 4.6.5.1 Despite the significant increase in body weight, VGF over-expression had no significant affect on fat depots.....	168

1 Chapter 1 - GENERAL INTRODUCTION

1.1 OBESITY – AN OVERVIEW

“At least 2.8 million adults die each year as a result of being overweight or obese”.

– World Health Organisation, 2008

The World Health Organisation (WHO) defines overweight (body mass index (BMI) $\geq 25\text{kg/m}^2$) and obesity (BMI $\geq 30\text{kg/m}^2$) as abnormal or excessive fat accumulation that presents a risk to health. Obesity is a major public health problem associated with significant morbidity and mortality, attributed to the increased risk of a number of conditions, including, but not limited to, type II diabetes mellitus (T2DM) (44% of disease burden), ischaemic heart disease (23%) and certain cancers (between 7 and 41%). Obesity is thought to reduce life expectancy by an average of 9 years and is responsible for 9000 premature deaths each year in England (The Health Survey for England, 2005).

The economic costs of treating the co-morbidities associated with obesity are vast. It is estimated that obesity costs the National Health Service (NHS) approximately £1 billion per year, with an additional £2.4 billion per year to the economy as a whole (The Foresight talking Obesity: Future Choices Project, 2007).

Obesity has reached epidemic proportions. Worldwide obesity has more than doubled since 1980. In 2008, 1.5 billion adults (20 and older) were overweight. Of these, 200 million men and nearly 300 million women were obese. Nearly 43 million children under the age of 5 were overweight in 2010 (WHO Challenges, 2010). In England, the proportion of adults with a normal BMI decreased between 1993 and 2012 from 41% to 32% among men and 50% to 41% among women. At the same time, the proportion of adults that were classified as overweight or obese increased from 58% to 67% among men and

from 49% to 57% among women. In 2012, 24% of men, 25% of women and 19% of children (aged 10-11) were classified as obese (Statistics on Obesity Physical Activity and Diet, 2014). By 2050 it is predicted that 60% of men and 50% of women could be obese (The Foresight talking Obesity: Future Choices Project, 2007).

Given the prevalence of obesity, and its danger, surprisingly little is known about its causes, and even less, its cures. Monogenic forms of obesity, in which there is a single identifiable genetic factor, are rare. The most prevalent is MC4R-linked obesity estimated to represent 2-3% of obesity cases (Mutch and Clement, 2006).

Obesity, when not attributable to a single genetic factor is a multifactorial condition, in which scores of genes have been implicated (Frayling et al., 2007). Obesity may be one of the strongest genetically influenced traits we have (Willyard, 2014). However, genetics is unlikely to have influenced the increasing prevalence of obesity. This increase is a result of the environment; with some being more susceptible to the condition than others.

Key to the remainder of obesity cases not attributable to a single identifiable genetic factor is the energy imbalance between calories consumed and calories expended (i.e. energy homeostasis). Globally, there has been:

- An increased intake of energy-dense foods that are high in fat, salt and sugars but low in vitamins, minerals and other micronutrients; and
- A decrease in physical activity due to the increasingly sedentary nature of many forms of work, changing modes of transportation and increasing urbanisation.

There have been significant upward trends in household expenditure on total fats and oils, butter, sugar and preserves, fruit juice and soft drinks, while overall purchases of fruit and vegetables reduced between 2009 and 2012. Also, 19% of men and 26% of women were classed as inactive in 2012 (Statistics on Obesity Physical Activity and Diet, 2014). However, obesity arises not simply from the passive accumulation of excess calories, stored as fat, but involves a re-calibration of the biologically defended level of body fat (Velloso and Schwartz, 2011).

The pathophysiology of obesity is not well characterised. Major advances have been made to identify the physiological factors regulating energy homeostasis. Energy homeostasis may be considered the biological process(es) that promotes stability in the amount of energy stored as fat. Efforts are aimed at increasing our understanding of how the brain regulates food intake to identify potential therapeutic targets (Dietrich and Horvath, 2012). The hypothalamus is at the core of the central networks predisposed to regulate energy homeostasis by sensing the level and activity of both central and peripheral mediators and activating catabolic/anabolic pathways (Bartolomucci et al., 2009).

The work presented in this thesis aims to explore the role of a novel gene and its derived peptides in the regulation of food intake and energy expenditure, herein referred to as energy homeostasis, both of which are fundamental to the development of obesity.

1.2 THE CENTRAL CONTROL OF ENERGY HOMEOSTASIS

Energy homeostasis is a complex physiological function co-ordinated at multiple levels and its regulation now receives increasing interest. At the centre of energy homeostasis is the hypothalamus, which was initially implicated in the control of food intake in the 19th century with the first clinical description, by Bernard Mohr, of hypothalamic-pituitary injury resulting in obesity (Williams and Elmquist, 2011). Various afferent signals from the periphery, communicate information about metabolic and nutritional status to the hypothalamus. The hypothalamus responds to these afferent signals by altering neurotransmitter systems, thereby generating efferent signals that alter appetite and energy expenditure (Lenard and Berthoud, 2008). While modification of energy intake is the traditional approach to the control of obesity, the importance of energy expenditure in the energy balance equation has become increasingly apparent over the past few years.

1.2.1 The structure of the hypothalamus

The hypothalamus, which lies in the ventral half of the diencephalons below the thalamus, contains multiple neural populations or nuclei. It surrounds the third ventricle immediately above the pituitary gland, and is connected by extensive afferent and efferent nerve fibres to the rest of the central nervous system (CNS) (Zhao et al., 2008a). In addition to the neural regulation of the autonomic nervous system, body temperature and appetite control, the hypothalamus functions as an endocrine gland. This endocrine role is closely linked to that of the pituitary gland (Elmquist, 2001). Various hypothalamic neurones secrete hormones into the hypothalamo-pituitary portal system which are then carried to their target cells in the anterior pituitary to regulate the release of anterior pituitary hormones (Morrison and Berthoud, 2007).

In the mid-20th century numerous experiments identified the hypothalamus as an important region in the regulation of food intake (Anand and Brobeck, 1951;

Hetherington and Ranson, 1940). The inference that hypothalamic sites contain neural mechanisms affecting ingestive behaviour was based on numerous studies employing either lesioning or electrical stimulation of specific nuclei within the hypothalamus (Williams et al., 2001). It was demonstrated that experimental manipulations of the ventromedial nucleus (VMN), dorsomedial nucleus (DMN) and the paraventricular nucleus (PVN) disrupted daily food intake patterns and produced permanently enhanced appetite or hyperphagia. Whilst lesions of the lateral hypothalamic area (LHA) resulted in a reduction in food intake and weight loss (Kalra et al., 1999). This led to a two-centre theory of hunger, involving the LHA 'hunger' centre and a VMN 'satiety' centre (Schwartz et al., 2000). This has subsequently been expanded; discrete neuronal pathways are thought to generate integrated responses to changes in body fuel stores (Schwartz et al., 2000).

Recently it has become apparent that several extra hypothalamic brain regions are also important in the control of food intake, for example, the nucleus tractus solitarius (NTS) and the area postrema in the brainstem (Flatt, 2001) (see Figure 1.2.1). Within the hypothalamus, however, other important structures include the PVN and the arcuate nucleus (ARC) (see Figure 1.2.1) (Gold, 1977). These hypothalamic areas, in particular the neurones localised within them (which are a target for peripheral factors), produce an array of both orexigenic (increase food intake) and anorexigenic (decrease food intake) peptides that constitute a major part of the neuronal network regulating energy homeostasis (Sahu, 2004).

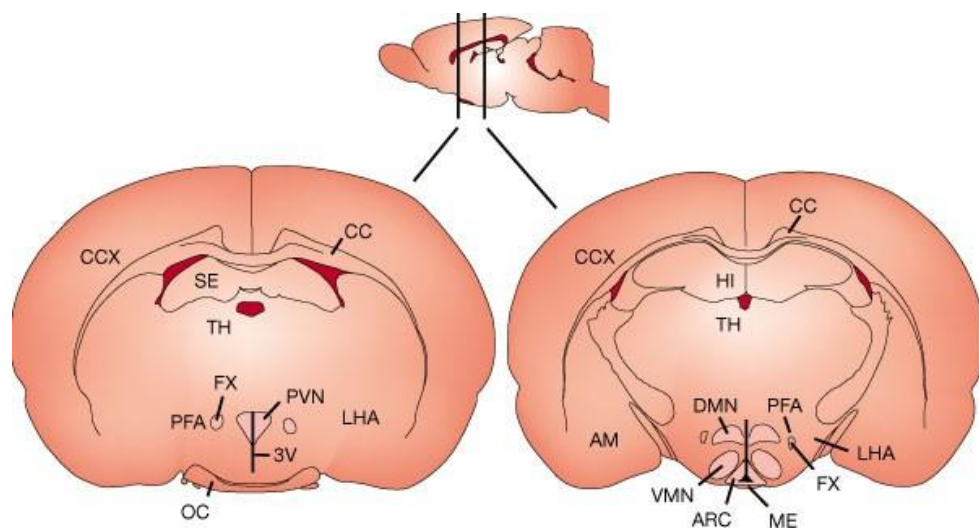


Figure 1.2.1: **Schematic of the rat brain displaying the major hypothalamic regions implicated in the regulation of food intake.** The smaller figure at the top is a longitudinal view of the rat brain, with olfactory bulb at the anterior end (to the left) and the caudal hindbrain (to the right). Cross sections of the brain at two levels are shown beneath (indicated by black lines). The following nuclei are involved in regulating food intake; PVN, paraventricular nucleus; ARC, arcuate nucleus; VMN, ventromedial hypothalamus; DMN, dorsomedial hypothalamus; LHA, lateral hypothalamic area. Other brain structures include 3V, third ventricle; ME, median eminence; OC, optic chiasm; CCX, cerebral cortex; CC, corpus callosum; HI hippocampus; SE, septum; TH, thalamus and AM, amygdala (adapted from Schwartz et al., 2000).

1.2.1.1 Arcuate nucleus (ARC)

The ARC is situated around the base of the third ventricle and lies immediately above the median eminence, effectively outside of the blood brain barrier (BBB) (Broadwell et al., 1976). Therefore it is positioned to integrate a number of signals from the periphery (Hewson et al., 2002). The ARC is an elongated collection of neuronal cell bodies occupying nearly one-half of the length of the hypothalamus and is sub-divided into several functional domains. Neuropeptide Y (NPY) and agouti related protein (AgRP), both potent stimulators of food intake, are co-localised in a population of neurones in the medial ARC (see 1.1.3.5). Pro-opiomelanocortin (POMC; the precursor of alpha melanocortin stimulating hormone (α MSH)) and cocaine amphetamine-regulated transcript (CART), which induce an anorexic response, are co-localised in a lateral subset of ARC neurones (Dhillon et al., 2002) (see 1.2.3.5).

It has been established that the ARC is important in the regulation of energy homeostasis, indeed the first neuropeptides discovered to be involved are located in this nuclei (Sainsbury and Zhang, 2010). The neurones contained in the ARC are the major elements in the central control of feeding and metabolism. The major neuronal populations thought to mediate the integration of peripheral signals are thought to be the NPY/AgRP neurones and the POMC/CART neurones (Simpson et al., 2009). These neurones alter energy homeostasis and appetite, as well as neuroendocrine function (Leibowitz and Wortley, 2004). The ARC is considered the site of synthesis while the PVN is the site of action. These two neuronal populations have opposing effects on feeding. POMC expressing neurones are activated by anorexigenic stimuli and release α MSH, a derivative of POMC and an agonist of melanocortin-4-receptors (MC4R). These receptors are expressed in neurones in various target nuclei which inhibit feeding behaviour (Millington, 2007). NPY/AgRP expressing neurones are activated by orexigenic stimuli. They inhibit both POMC-expressing neurones and MC4R expressing neurones through the release of γ -aminobutyric acid (GABA) and AgRP, resulting in the induction of feeding (Tong

et al., 2008). AgRP acts as a potent endogenous antagonist of MC4Rs, in opposition to α MSH. Projections from NPY/AgRP expressing neurones are mostly coupled to projections from POMC expressing neurones, so that MC4R expressing target neurones receive both positive and negative signals (Dietrich and Horvath, 2010). ARC containing cell bodies project to several other hypothalamic nuclei and also have extensively reciprocal connections with other hypothalamic regions, including the PVN, DMH, VMH, LHA and perifornical area.

1.2.1.2 Paraventricular nucleus (PVN)

The PVN is richly supplied by axons from the ARC NPY/AgRP and POMC/CART neurones (see Figure 1.2.3.5). Neurones within this region ‘fan out’ from either side of the roof of the 3V (see Figure 1.2.1) allowing hormones to be released into the circulation (Stanley et al., 2005). Therefore the PVN may be considered an integrating centre for many neural pathways which influence energy homeostasis, as stimulation inhibits food intake, while bilateral lesions of the PVN result in hyperphagia and subsequent obesity (Stanley et al., 2005).

Consistent with these findings, neuropeptides synthesised in the neurones of the PVN reduce food intake and body weight when administered centrally. These include corticotrophin-releasing hormone (CRH), which causes anorexia and also activates the sympathetic nervous system in addition to its role as a major regulator of the hypothalamic-pituitary-adrenal axis (O’Connor, 2000). Similarly, thyrotropin-releasing hormone (TRH) reduces food intake, in addition to stimulating the thyroid axis (Schuhler et al., 2007). Furthermore, oxytocin reduces food intake in addition to regulating uterine function (Blevins and Ho, 2013), while microinjections of all known orexigenic signals (see Table 1.2.2) into the PVN increase appetite and food intake (Kalra et al., 1999).

1.2.1.3 Dorsomedial nucleus (DMN)

The DMN, which is located dorsally to the VMN (see Figure 1.2.1), has extensive and direct connections with other hypothalamic nuclei such as the PVN, the LHA and the brainstem (Simpson et al., 2009). It contains high levels of NPY immunoreactivity and injections of NPY as well as the orexigens, galanin and GABA, increase food intake (Kelly et al., 1979; Kyrkouli et al., 1990; Stanley et al., 1985). In contrast, dopamine signalling in the hypothalamus via neurones situated in the DMN and ARC inhibit food intake (Suzuki et al., 2012). Destruction of the DMN results in hyperphagia and obesity (Bernardis and Bellinger, 1987).

1.2.1.4 Ventromedial nucleus (VMN)

Chemical and physical lesioning of the VMN results in hyperphagia and obesity (Gillies et al., 1982), however there is no evidence for the production of appetite regulatory factors within the area itself. Electrical stimulation of the VMN suppressed food intake (Hetherington and Ranson, 1940). Direct microinjection of NPY and galanin, however, stimulates appetite while leptin and urocortin inhibit feeding; suggesting receptors are present within the VMN (Kelly et al., 1979; Kyrkouli et al., 1990; Stanley et al., 1985), unless the observed effects of administration are a result of diffusion to neighbouring nuclei. Brain-derived neurotrophic factor (BDNF) is highly expressed in the VMN, and administration results in the reduction of food intake and body weight (Pellemounter et al., 1995).

1.2.1.5 Lateral hypothalamic area (LHA)

Stimulation of the LHA increases food intake, while bilateral lesioning of the LHA causes anorexia and weight loss (Anand and Brobeck, 1951). It contains subpopulations of neurones which express orexigenic peptides, such as orexin and melanocortin concentrating hormone (MCH), and NPY terminals.

The second-order neurone hypothesis for the LHA is supported by studies conducted with MCH, an orexigenic peptide located within this region of the hypothalamus (Schwartz et al., 2000). MCH synthesis is elevated by energy restriction and leptin deficiency, and knockout (KO) mice have reduced food intake and are excessively lean. The ‘hypocretins’ or ‘orexins’ (two groups’ simultaneous discovery, the latter is used throughout this thesis) also increase food intake and cause arousal when administered centrally. Targeted deletion results in narcolepsy, suggesting a role in the onset of sleep, as well as a potential role in the control of food intake (Tsujino and Sakurai, 2013).

1.2.1.6 Perifornical area

The perifornical area, which lies adjacent to the LHA, is also richly supplied by axons from the ARC NPY/AgRP and POMC/CART neurones. Stimulation of the perifornical area, like the LHA, results in increased food intake. NPY release in the perifornical area stimulates food intake (Dailey and Bartness, 2008). The aforementioned orexins are also expressed in the perifornical area (Fadel et al., 2002).

Much experimentation is required to test this model of second-order neurones in the regulation of energy homeostasis. Specific neuronal subsets have yet to be identified within the PVN and LHA. However, rather than being passive recipients of information from the arcuate nucleus, it is thought that neuronal traffic flows bidirectionally between the two hypothalamic sites (Orlando et al., 2005).

The number of hypothalamic areas involved in the regulation of food intake and therefore energy homeostasis is vast – it communicates with the periphery with regards the metabolic and nutritional status and responds accordingly, by

altering neurotransmitter systems. The studies presented in this thesis aim to explore the role of one such system.

1.2.2 The hypothalamic regulation of food intake and energy expenditure

Significant progress has been made over the past decade in elucidating the hypothalamic network regulating food intake and energy expenditure. The hypothalamic nuclei are complex and involve a number of well-known peptides as well as recently identified hypothalamic peptides (see Table 1.2.2).

Orexigenic neuropeptides	Anorectic neuropeptides
Agouti related protein (AgRP)	Alpha-melanocortin stimulating hormone (α MSH)
Endocannabinoids	Amylin
Galanin	Calcitonin gene related peptide (CGRP)
Ghrelin	Cholecystokinin (CCK)
Growth hormone release hormone (GHRH)	Cocaine amphetamine regulated transcript (CART)
Melanin concentrating hormone (MCH)	Glucagon like peptide -1 and -2 (GLP-1, -2)
Neuropeptide Y (NPY)	Insulin
Noradrenaline	Leptin
Opioid peptides (β -endorphins)	Neuromedin U (NMU)
	Neurotensin
	Oxyntomodulin
	Polypeptide YY (PYY)
	Serotonin
	Urocortin

Table 1.2.2: **Hypothalamic neuropeptides implicated in the control of food intake and energy homeostasis.** Orexigenic hypothalamic neuropeptides increase food intake whilst anorectic hypothalamic neuropeptides decrease food intake.

1.2.3 Peripheral Control of appetite

Kennedy (1953) proposed that inhibitory signals generated in proportion to the body's stores of fat act in the brain to reduce food intake i.e. when caloric restriction induces weight loss, levels of inhibitory signals are reduced and food intake increases, until the energy deficit is corrected. This elegant model,

however, did not explain how energy intake is controlled in the short term, during individual meals. Gibbs and Smith, (1973) proposed 'satiety factors', peptides secreted from the gastrointestinal (GI) tract, which informed the brain to terminate food intake.

Exo- and endo-crine secretions are stimulated by visual, olfactory and gustatory stimuli, along with gut motility before food enters the mouth (Ahima and Antwi, 2008). The ingestion of food stimulates mechanoreceptors, for example gastric stretch and chemoreceptors, which results in the co-ordinated process of distension and propulsion to accommodate meals, and to ensure maximum digestion and subsequent absorption of nutrients. These signals are transmitted via the vagus nerve to the dorsal vagal complex in the medulla, terminating in the medial and dorsomedial parts of the NTS (Berthoud, 2008). Projections from this area of the brainstem innervate the paraventricular, dorsomedial and arcuate nuclei of the hypothalamus, LHA and AM. Furthermore, the NTS projects to the visceral sensory thalamus, which communicates with the sensory cortex and mediates the conscious perception of gastrointestinal fullness i.e. satiety (Ahima and Antwi, 2008). These processes have been investigated using surgical and chemical approaches, for example, gastric vagal stimulation induces satiety, while infusions of solutions rich in fat, carbohydrates and proteins into the proximal small intestine regulates subsequent meal size – an affect which in turn is blocked by the neurotoxin capsaicin being delivered to the vagus, or by surgical denervation (Schwartz, 2000; Smith et al., 1985; South and Ritter, 1988). A number of hormones are secreted by the GI tract which control feeding and access the brain partly through the area postrema, located at the tip of the fourth ventricle, situated above the NTS (Stanley et al., 2005).

1.2.3.1 Cholecystinin (CCK)

CCK decreases meal size (Kraly et al., 1978) and was the first gut-secreted peptide to be identified as a satiety factor (Liebling et al., 1975). Antagonists of its receptor block the satiety effects associated with nutrient infusions into the gut and stimulate further feeding in fed animals (Bi et al., 2007).

1.2.3.2 Glucagon-like peptide (GLP)-1

GLP-1, in response to meals, is cleaved from proglucagon and released from the L-cells of the intestine. GLP-1, and its receptor agonist exendin-4, decrease food intake in rodents when injected peripherally (Baggio and Drucker, 2007; Murphy and Bloom, 2006).

1.2.3.3 Peptide YY (PYY)

PYY₃₋₃₆ is co-secreted with GLP-1 (Batterham et al., 2002; Murphy and Bloom, 2006). Initially it was thought to decrease food intake in rodents by inhibiting NPY/AgRP neurones within the hypothalamus, however, this has not been confirmed by others (Halatchev et al., 2005; Tschop et al 2000).

These gut derived peptides are an attractive target for obesity treatment as they induce satiety and/or limit meal size. However, there are significant obstacles which have hampered their development as potential drugs. Firstly, their half-life is relatively short and stable analogues have eluded researchers (de Silva and Bloom, 2012). In the case of GLP-1 and CCK, which induce nausea, there are side effects which limit their therapeutic potential (Holst and Deacon, 2013). Furthermore, the system is highly redundant – genetic manipulation of anorexigenic gut hormones rarely results in beneficial changes in feeding and subsequently body weight and/or metabolism (Diano et al., 2006; Scrocchi et al., 2000; Sun et al., 2006). The gut functions as a neuroendocrine organ that responds rapidly to food intake, and influences not only the size of meals by producing satiety factors but sends messages to the brain via the ingestive-

vagus pathway, that modulate hypothalamic neurotransmitters and peptides (Ahlman and Nilsson, 2001).

1.2.3.4 Adiposity signals: Insulin and leptin

Insulin, a pancreatic hormone, enters the brain from the circulation, and reduces food intake. It was the first hormonal signal to be implicated in the control of energy homeostasis by the central nervous system (CNS) (Woods et al., 1979; Woods et al., 2006). The subsequent discovery that the hyperphagia and obesity in *ob/ob* mice, resulted from an autosomal recessive mutation in the gene encoding leptin, a hormone secreted by adipocytes, provided further evidence for the role of adiposity signals in energy homeostasis (Schwartz et al., 1999). Both insulin and leptin circulate at levels proportional to body fat content, and enter the CNS in proportion to their plasma level – their receptors are expressed in brain neurones involved in energy homeostasis (Havel, 2001). Administration of either of these peptides, directly into the brain, reduces food intake (Air et al., 2002).

However, different mechanisms underlie the association of insulin and leptin with body fat. As body weight increases, insulin secretion undergoes similar increases in the basal state and in response to food intake. Failure of this system to respond results in hyperglycaemia and is likely to contribute to the development of T2DM (Yamada et al., 2006). The mechanism of leptin, however, is not completely understood – it may involve glucose flux through the hexosamine pathway. The rate of insulin-stimulated glucose utilisation in adipocytes is a key factor linking leptin secretion to body fat mass (Denroche et al., 2012).

Leptin deficiency results in severe obesity and is therefore thought to have a more important role in the CNS control of energy homeostasis than insulin, a

deficiency in which does not result in obesity (Ahima, 2008). For example, in uncontrolled diabetes mellitus in both rats and humans, food intake is markedly increased, but levels of fat remain low, as does leptin (German et al., 2010).

Elevated levels of leptin within the plasma of obese humans suggested that resistance to the hormone was associated with the condition. It led to the suggestion that human obesity may be due to reduced leptin action in the brain and affected individuals are unlikely to respond to pharmacological intervention with leptin (Morton and Schwartz, 2011). Leptin resistance is well documented in mice, for example *db/db* mice, which have mutations within the leptin receptor gene. Whether dysfunction in the transport process or reduced receptor signalling leads to obesity remains to be determined (Morris and Rui, 2009).

1.2.3.5 Neuropeptides and adiposity signals

In the CNS, several distinct hypothalamic neuropeptide pathways have emerged as candidates for the mediation of the adiposity signals, leptin and insulin (see Table 1.2.2).

Neuropeptide Y (NPY)

Direct injection of NPY into the hypothalamus or cerebral ventricles of rats stimulates food intake, while subsequently decreasing energy expenditure (Clark et al., 1984). Repeat administration of the neuropeptide results in weight gain and obesity (Stanley et al., 1989). Leptin inhibits ARC NPY expression, while *NPY^{-/-} ob/ob* mice have reduced hyperphagia and obesity, indicating the requirement of NPY signalling for the obese phenotype (Stanley et al., 2005) (see Figure 1.2.3.5). NPY is expressed widely throughout the brain, with notably high expression in the ARC (Morris, 1989), where it is co-expressed with AgRP.

Systemic or direct delivery of insulin into the brain blocks the hyperphagic response to insulin-deficient diabetes in hypothalamic NPY synthesis and release (Kalra, 1997).

Agouti related protein (AgRP)

AgRP is expressed exclusively within the ARC, where it colocalises with NPY. When intracerebroventricular (ICV) infused, AgRP is an orexigenic peptide (Parker and Bloom, 2012) and acts as an endogenous antagonist of the MC3 and MC4Rs.

Melanocortins

Neuronal synthesis of the melanocortins, namely α MSH and CRH, increases in response to increased adiposity signalling in the brain. The neuropeptides are cleaved from the POMC precursor molecule and exert their effects by binding to members of a family of melanocortin receptors, of which MC3- and MC4-receptor genes are expressed primarily in the brain. α MSH has been demonstrated to be an anorectic peptide when delivered directly to the PVN, DMH and ARC, as well as the fourth ventricle (4V) (Kim et al., 2000; Zhang et al., 2005). There are two α MSH receptors within the brain MC3 and MC4; the latter is more widely expressed and is localised to the hypothalamus, where expression is particularly high in the aforementioned areas, the amygdala, thalamus, cortex, striatum, hippocampus and brainstem (Parker and Bloom, 2012). As a result, the MC4 receptor is considered more important in relation to energy homeostasis. MC4R^{-/-} mice are severely hyperphagic and, as a result, obese, indicating that signalling via the receptor limits food intake and body weight; while mutations in the MC4R gene have been linked to human obesity (Farooqi et al., 2000). A synthetic agonist of the MC3- and MC4-receptors suppresses food intake, whereas an antagonist has the opposite effect. The *Agrp* gene produces AgRP peptide which acts as an antagonist of the MC3 and

MC4 receptors (Dhillon et al., 2003). Its expression is up-regulated by fasting and leptin deficiency. AgRP when delivered via ICV infusion increases food hoarding and intake in Siberian hamsters, whilst its over-expression results in significantly increased food intake and body weight (Day and Bartness, 2003; Jethwa et al., 2010).

Cocaine- and amphetamine-regulated transcript (CART)

CART decreases food intake following ICV infusion, however, it has an orexigenic effect when injected into discrete hypothalamic nuclei (Dhillon et al., 2002).

Thyrotrophin-releasing hormone (TRH)

TRH decreases food intake, whilst increasing body temperature, activity and oxygen consumption in Siberian hamsters (Schuhler et al., 2007).

Orexins

Highly expressed in the LHA (Sakurai et al., 1998), much like MCH, orexins A and B are produced from the same precursor and are orexigenic when infused via ICV cannulation. However, the distribution of its receptors within the hypothalamus is different. OX1 is highly expressed in the VMN, whereas OX2 is highly expressed in the PVN (Trivedi et al., 1998). Orexin KO mice are hypophagic (Willie et al., 2001), but this may be a result of their profound narcolepsy (Chemelli et al., 1999).

Secretions from the periphery, for example the pancreas, white adipose tissue (WAT) and the GI tract, are integrated by the CNS, mainly the hypothalamus, to regulate energy homeostasis (Woods and D'Alessio, 2008). The actions of

leptin are mediated via its receptor (LepR-b), which is expressed in several areas of the CNS including the hypothalamus. It has relatively high expression in the AgRP and POMC neurones of the ARC (Cheung et al., 1997; Cowley et al., 2001; Konner et al., 2007; Lin et al., 2010). Upon binding to its receptor, Leptin activates an array of signalling cascades, mainly activating Janus kinase (JAK), which in turn phosphorylates the leptin receptor, activating STAT3 (Vaisse et al., 1996). Upon phosphorylation, STAT3 binds to *pomc* and *agrp* promoters, an affect which stimulates POMC and inhibits AgRP expression (Ernst et al., 2009; Mesaros et al., 2008). Deletion and over-expression studies of LepR in POMC or AgRP neurones results in changes in body weight, food intake and glucose homeostasis (Balthasar et al., 2004; Hill et al., 2010; Huo et al., 2009). Interestingly, these studies have demonstrated that deletion of the receptor within these neurones results in obesity, without changes in food intake or energy expenditure (see Figure 1.2.3.5) (Varela and Horvath, 2012).

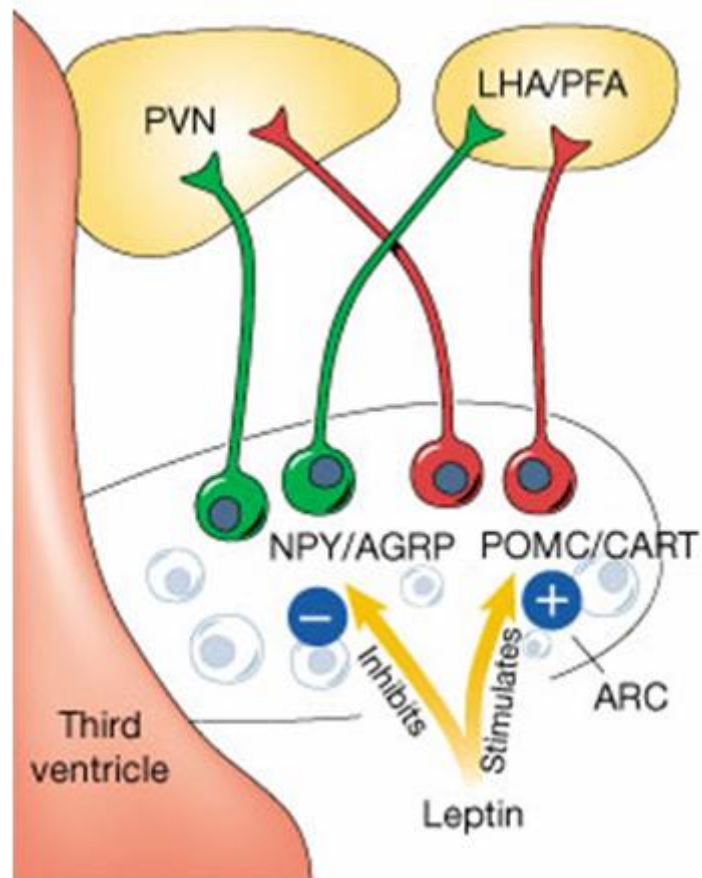


Figure 1.2.3.5: **The hypothalamus and leptin - their role in the regulation of energy homeostasis.** Leptin, secreted by white adipose tissue (WAT), informs the hypothalamus of the energy status of the organism. When the LepR-b is activated in these neurones, they promote changes in hypothalamic neuropeptide expression, resulting in alterations in peripheral functions to restore energy homeostasis.

As yet no “magic bullet” has been found for the treatment of obesity. The discovery of leptin (Zhang et al., 1994), whilst revolutionising the understanding of body weight regulation, also raised expectations for a breakthrough therapeutic for obesity. And although the role of leptin is pivotal in energy regulation, as an anti-obesity treatment it has proven unsuccessful (overweight/obesity is associated with ‘leptin resistance’) (Heymsfield et al., 1999). NPY provides a further example of discoveries made in the lab failing to transmit to the clinic. NPY stimulates feeding and weight gain, but knockout mice bred on a mixed genetic background are not affected in terms of food intake and body weight. NPY deficiency, it would seem, has no significant effect in mice fed a normal diet (Patel et al., 2006). Subsequent studies have tested agonists and antagonists of NPY receptor subtypes as anti-obesity agents, but results are equivocal and somewhat controversial (Feletou et al., 2006). Furthermore, dysregulation of NPY signalling has been linked to alterations in bone formation and alcohol consumption, as well as seizure susceptibility (Lin et al., 2004). More recent clinical studies have focused on combining long term adiposity and short term satiety endocrine signals (e.g. leptin and amylin, a 37 amino acid peptide hormone co-secreted with insulin from pancreatic β -cells that activates CNS regions to regulate glucose and energy homeostasis), but with limited success (Roth et al., 2008).

The number of genes involved in the regulation of nutrition and metabolism in general, and catabolic energy dissipating pathways in particular are vast and the identification of peptides associated with higher or lower risk of obesity is rising exponentially. The work presented in this thesis aims to explore the role of one such gene and its derived peptides.

1.3 ANIMAL MODELS UTILISED IN THE STUDY OF OBESITY

The prevalence of obesity and the substantial costs of its management and associated co-morbidities, along with the relative failure to adopt healthier lifestyles, have resulted in the need to develop pharmacological interventions to reduce appetite. At present, there are no centrally-acting drugs fit for this purpose, after the withdrawal of sibutramine and rimonabant, a monoamine reuptake inhibitor and endocannabinoid receptor antagonist respectively (James et al., 2010; Rothman and Baumann, 2009). Therefore the need to understand the complex mechanisms behind energy homeostasis, in order to identify feasible drug targets, is huge. Currently this is skewed towards a few 'model' species (Ebling, 2014).

Martin et al., (2010) summated the limitations of mice and rats as experimental models for human conditions, stating most strains are sedentary, overweight, insulin resistant, hypertensive and prone to premature death. And whilst single gene mutations, either spontaneous or as a result of genetic manipulation (e.g. *ob/ob* and those in the melanocortin system) have identified mechanisms in energy homeostasis, relatively few cases of human obesity reflect these (Farooqi and O'Rahilly, 2006).

Therefore, in these studies, we have utilised a nonstandard laboratory species that undergoes a natural seasonal cycle of altered appetite and body weight and one which reflects the human obese condition more accurately.

1.3.1 The Siberian hamster

Siberian hamsters (*Phodopus sungorus*), as an adaptation to survive winter, express profound seasonal cycles of energy metabolism, mainly through a gain/loss of intra-abdominal fat stores (Ebling, 2014). Its increasing popularity as a rodent model for understanding the long-term central control of caloric

intake and expenditure is due to its ease in maintenance in animal husbandry units, the exploitation of seasonal cycles which can be regulated by photoperiod, and most importantly for energy homeostasis studies, displays a striking seasonal change in body weight (see Figure 1.3.1) (Barrett et al., 2007).



Figure 1.3.1: **The Siberian hamster shown in long days (right) and short days (left).** The dark pelage moults under decreasing photoperiod to produce a denser, light pelage. Photo courtesy of Gregory Demas, Indiana University.

Under increasing photoperiod (long days (LD)), the Siberian hamster reaches its maximum body weight, but under decreasing photoperiod (short days (SD)), it enters a profound catabolic state, decreases its food intake and gradually loses bodyweight (between 25 and 35%), mainly through a loss of intra-abdominal fat stores (Schuhler and Ebling, 2006). The catabolic state is associated with a decrease in both peripheral leptin concentrations and in leptin mRNA levels in WAT (Jethwa et al., 2007).

Homeostatic regulators of food intake and energy expenditure were initially postulated as responsible for the seasonal changes observed in the Siberian hamster (Adam et al., 2000; Archer et al., 2007). However, despite the destruction of the ARC, Siberian hamsters exposed to SD still displayed the characteristic reduction in food intake and body weight (Ebling et al., 1998).

Subsequently Adam et al., (2000), Mercer et al., (2001) and Robson et al., (2002) reported conflicting results when comparing the differential gene expression in LD versus SD Siberian hamsters. The growth and reproductive axes are regulated by photoperiod in seasonal mammals. Adam et al. (2000), demonstrated that Siberian hamsters kept in LD from weaning displayed faster growth and body weight gain, increased adiposity and leptin gene expression in adipose tissue, and attained puberty earlier when compared to those transferred to SD. In the ARC, expression of the leptin receptor, POMC and MC3R genes increased dramatically in LD post weaning. However, this was not apparent in the group transferred to SD. Furthermore, CART gene expression was higher in SD when compared to LD (Adam et al., 2000). Mercer et al. (2001), demonstrated that Siberian hamsters transferred to SD resulted in reduced POMC and leptin receptor mRNA in the ARC, with elevated levels of CART. Gene expression of the MC3R was reduced in the ARC but elevated in the VMN compared with LD controls. The subsequent weight loss in an LD restricted food intake group resulted in a gene expression profile typical of negative energy balance (i.e. low CART mRNA and elevated leptin receptor mRNA). Robson et al. (2002) reported that photoperiod did not affect CART expression in Siberian hamsters, however, fasting produced a significant decrease in CART mRNA in the ARC of Siberian hamsters in both LD and SD. This inferred that known homeostatic regulators of energy homeostasis are unlikely to regulate seasonality in the Siberian hamster (Ebling and Barrett, 2008).

Several transcripts have subsequently been identified as altered between the obese/lean states of the Siberian hamster (see Table 1.3.1). Many of which have been shown to alter short term changes in food intake or body weight. For example, histamine 3 receptor antagonists decrease food intake for up to one hour (Jethwa et al., 2009), while inverse agonists prevent the nocturnal rise in body temperature, indicating additional effects on energy expenditure. TRH increases energy expenditure (Schuhler et al., 2007) via increased locomoter activity, body temperature and oxygen consumption in the Siberian hamster, while simultaneously decreasing food intake.

Gene	In response to SD	Reference
Deiodinase 2 (DIO-2)	Decrease	Herwig et al., (2009)
DIO-3	Increase	Barrett el., (2007)
VGF	Increase	Barrett et al., 2005
TRHr-1	Decrease	Ebling et al., 2008
H3r	Decrease	Barrett et al., (2006)

Table 1.3.1: **Effect of SD photoperiod on hypothalamic neuropeptide gene expression at the mRNA level.** DIO, deiodinase -2 and -3, VGF, non-acronymic, TRHr-1, thyrotropin-releasing hormone receptor-1, H3r, Histamine 3 receptor.

However more recent studies have shown that manipulation of hypothalamic thyroid hormone availability may play a key role in the seasonal changes in

energy homeostasis (Barrett and Ebling, 2008). Indeed it has been shown that Siberian hamsters in the long days have increased levels of the deiodinase 2 (DIO2) enzyme, which is required for the activation of thyroxine (T4) into triiodothyronine (T3) increasing the availability of thyroid hormones, while Siberian hamsters maintained on short photoperiod have an increase in deiodinase 3 (DIO3) enzyme which converts T4 to reverse T3 (rT3) mRNA (Barrett et al., 2007; Herwig et al., 2009; Watanabe et al., 2004), thereby decreasing thyroid hormone availability.

In further support of this, Barrett et al. (2007) reported that ICV infusion of T3 into the hypothalamus of Siberian hamsters transferred to SD prevented the characteristic SD-induced reduction in food intake and body weight. Similarly, increasing T3 availability using silastic implants into the hypothalamus of Siberian hamsters exposed to SD for 10 weeks increased food intake, whole-body fat mass and body weight (Murphy et al., 2012).

1.3.2 The C57BL/6J Mouse

In rodents, a number of autosomal recessive gene mutations that result in the obese phenotype have been described, including but not limited to the *ob/ob* and *db/db* mice (Tartaglia et al., 1995; Zhang et al., 1994). The products of these genes represent a hormone – receptor pair, namely leptin (see section 1.1.3.4). Mice unable to produce leptin (*ob/ob*) or to respond to the hormone (*db/db*) display hyperphagia and decreased energy expenditure, as well as hyperinsulinaemia, hyperlipidaemia, insulin resistance, glucose intolerance and diabetes (Lin et al., 2000). Therefore the efficacy of such models of obesity remains to be seen as there is currently no evidence that mutations within the genes are involved in the aetiology of common obesity in humans (Lin et al., 2000).

However, leptin resistance has recently been described in a rodent model of obesity which may reflect more accurately the human condition, namely diet-induced obese (DIO) C57Bl/6J mouse (Van Heek et al., 1997). The DIO C57Bl/6J mouse is therefore used as a model of human obesity (Surwit et al., 1988).

The increased susceptibility to develop diet-induced obesity in C57Bl/6 mice is associated with their failure to regulate hypothalamic POMC and NPY gene expression. Bergen et al. (1999) showed that resistance to DIO is associated with increased POMC mRNA and decreased NPY mRNA in the hypothalamus. An alternation in these neuropeptides is thought to not only promote the development, but also the maintenance of the obese state. Three strains of mice, namely C57Bl/6J, CBA and A/J, were fed either normal rodent chow or a high fat diet (HFD) for 14 weeks, after which hypothalamic gene expression was measured. In response to HFD, C57Bl/6J mice gained the greatest amount of weight and NPY and POMC mRNA did not significantly decrease and increase (respectively) in C57Bl/6J mice. Compensatory changes in response to a HFD would suggest that other strains of mice are resistant to DIO but not in C57Bl/6J mice which are susceptible to the condition (Bergen et al., 1999).

Lin et al. (2000) reported that significant increases in body weight in C56Bl/6J mice fed a HFD was evident after 2 weeks post dietary switch and this continued throughout the duration of the study (19 weeks). However, significant changes in epididymal and perirenal fat depots were not significant until 8 weeks post HFD. Inguinal fat mass was not significantly altered until 19 weeks feeding. Interestingly, energy intake in the HFD group paralleled that of the controls for 4 weeks, before a decrease in energy intake in the HFD group. However, by week 8, the HFD group began a gradual increase in energy intake, which increased further at 15 weeks, persisting to 19 weeks. Plasma leptin concentrations were significantly raised in the HFD group at 8, 15 and 19 weeks post HFD feeding. One week post transfer to HFD, mice retained the ability to

respond to exogenous leptin. However, by week 8, exogenous leptin did not affect body weight or cumulative energy intake. By 19 weeks, 0.1 μ g of leptin, infused by ICV cannulation, had no significant effect on body weight and cumulative energy intake in the HFD group. These results demonstrate that C57BL/6J mice develop obesity and progressive peripheral and central leptin resistance (Lin et al., 2000). They are therefore an excellent model for the study of the development of obesity, akin to that in humans.

1.4 VGF – A NEUROTROPHIN-INDUCED GENE

Neurotrophins are a family of closely related proteins, first identified as survival factors for sympathetic and sensory neurones and subsequently implicated in survival, development and function of neurones in the central and peripheral nervous system (Skaper, 2010). VGF is a neurotrophin-induced gene, which encodes for a precursor polypeptide that is expressed in neuronal and neuroendocrine cells (Levi et al., 2004). The precursor polypeptide, pro-VGF, is stored in dense core vesicles, cleaved by prohormone convertases (PC), namely PC1/3 and PC2, which are typical of neuronal/endocrine tissues, and then released post depolarisation (Trani et al., 2002).

VGF was first identified as VGF8a (Levi et al., 1985), NGF33.1 (Salton et al., 1991) and $\alpha 2$ (Cho et al., 1989) on the basis of its rapid induction in PC12 cells by nerve growth factor (NGF) (Levi et al., 1985), its non-acronymic name being based on its selection from plate V of an NGF-induced PC12 cell cDNA library and should not be confused with vascular endothelial growth factor (VEGF). Subsequent studies demonstrated that VGF is similarly up-regulated by numerous neurotrophins including BDNF and neurotrophin-3 (NT-3) in neuronal targets such as cortical or hippocampal neurones (Bonni et al., 1995). Consistent with VGF being a gene that is activated selectively in response to neurotrophin treatment, VGF mRNA levels are only marginally increased by other growth factors, including epidermal growth factor (EGF), fibroblast growth factor (FGF), interleukin-6 (IL-6) and insulin, despite the capacity of these proteins to robustly induced transcription of other immediate early genes in the PC12 cell line (Hawley et al., 1992; Possenti et al., 1992; Salton, 1991; Salton et al., 1991).

1.4.1 The transcriptional regulation of VGF

Cloning of the rat cDNA and genomic sequences was followed by the isolation of the mouse and human homologues. The gene itself is highly conserved across mammalian species (see Figure 1.4.2 A) in respect to the coding region and the promoter and the flanking 5' regulatory sequences (see Figure 1.4.1). VGF is a single copy gene, assigned to chromosome 7q22 in humans (Canu et al., 1997) and chromosome 5 in mice (Hahm et al., 1999), and has a relatively simple organisation. The entire protein sequence is encoded by a single exon (exon 3), while the 5' untranslated region contains two small introns. This differs in the rat, where alternative splicing produces two distinct mature mRNAs – one of which includes the sequence of the second, 116-bp, exon (Hawley et al., 1992). The functional relevance of this is unknown; the splice donor and acceptor sites are conserved in the human gene, however only the shorter transcript has been detected (Canu et al., 1997).

The *vgf* promoter is highly conserved; the human and mouse sequences display greater than 80% sequence identity over a length of 1Kb. This region contains a number of consensus motifs for the binding of transcriptional regulators (see Figure 1.4.1). A number of consensus motifs for the binding of transcriptional regulators have been identified 5' to the transcription initiation site of VGF and include a CCAAT box, various specificity protein I (SP-1) and activating protein 2 (AP-2) consensus binding sites and a putative silencer element similar to the one involved in tissue-specific expression of neuronal genes (Canu et al., 1997; Li et al., 1993; Salton, 1992).

Luc and Wagner, (1997) subsequently identified two cis elements, namely V1 and V2, within the -208 +55 fragment of the VGF promoter (sites in respect to the initiation of transcription) that are essential for NGF dependent gene activation. Their data also indicates that the V1 and V2 elements are required

for basal expression and for transcriptional activation in response to EGF and dibutyryl cyclic adenosine monophosphate (dbcAMP). The V1 region, mutation of which significantly impairs basal expression/promoter activity, contains the overlapping specificity protein-1 (SP-1) and activating protein-2 (AP-2) regions. V1 was shown to contain a cAMP response element (CRE), which binds cAMP response element binding protein (CREB), activating transcription factor -1 and -2 (ATF -1 and -2), as well as JunD- and JunB-related proteins, via electrophoretic mobility shift assay (EMSA) (Luc and Wagner, 1997). This element is necessary for the Ras-mediated, NGF-dependent induction of the promoter. At position -76 (in respect to the transcriptional start site), the CRE is embedded within a 14bp palindromic sequence - mutations of which abolish NGF and cAMP responses (Hawley et al., 1992). It is likely that tuning VGF expression in response to neurotrophin requires the combinatorial action of several regulatory complexes which bind to distinct promoter motifs. For example, in addition to the CRE, the CCAAT box was shown to be important for NGF induction (D'Arcangelo et al., 1996), possibly in association with the activity of a large complex containing a CREB, mammalian achaete-scute homologue-1 (MASH-1) and p300 (Mandolesi et al., 2002). A consensus mRNA destabilisation sequence ATTTA is located 300-bp downstream of the stop codon and 100-bp upstream of the polyadenylation site (Salton et al., 1991). It has been postulated that this motif may be responsible for the observed reduction of VGF mRNA stability following NGF treatment (Baybis and Salton, 1992). Previously removal of the AP-2 binding site via site directed mutagenesis has been demonstrated to reduce retinoic acid (RA) mediated transcriptional activation of genes (Doerksen et al., 1996).

Transgenic mice, which contained the *lac z* reporter gene driven by the *vgf* promoter, indicated that 200-bp of the promoter was sufficient to drive β -galactosidase gene expression within the embryonic nervous system (Piccioli et

al., 1995). A genomic fragment extending from 800-bp 5' to the transcriptional start site and including the first 700-bp of 5'-untranslated sequence was used to drive the expression of a reporter gene in transgenic mice. The transgene was shown to be expressed with a tissue-restricted pattern similar to that of the endogenous VGF gene (Picciolo et al., 1995). Interestingly, this region of the promoter contains the previously mentioned putative silencer element that is located 400-bp 5' to the transcriptional start site.

Molecular cloning and detailed characterisation of the human *vgf* promoter was initially performed in the PC12 cells line (Canu et al., 1997). Inspection of the human sequence revealed, upstream of the +1 transcriptional start site, a TATA box-like sequence, starting at -29 and a CCAAT box at -135. Further to this, Canu et al., (1997) described a CRE-binding protein element at -76, as well as several GC boxes, inverted GC motifs, numerous AP-2 and SP-1 sites, as well as several neurospecific elements, with the core motif CCAGGAG, common to genes encoding mouse neurofilament (Lewis and Cowan, 1986), rat GAP-43 (Nedivi et al., 1992) and mouse synapsin II (Chin et al., 1994). Furthermore, they identified a silencer region, at -411, similar to the human and rat synapsin I (Li et al., 1993) and the human dopamine β -hydroxylase gene (Ishiguro et al., 1993). In order to ascertain the promoter sequences required for neuronal specific expression, Canu et al., (1997) a series of progressive deletions were made to the human *vgf* promoter, which controlled chloramphenicol acetyltransferase (CAT) vector expression/activity. These constructs were transfected in the neuronal SK-N-BE cell line and the non-VGF expression cell line BOSC23. The results were expressed as percentages of transcriptional activity relative to RSV-CAT, which expressed the aforementioned gene in the front of a strong promoter. Deletion of the human *vgf* promoter region -2305 to -573 resulted in a decrease in CAT activity in SK-N-BE cells, while reporter gene activity increased by 2.5 fold in the non-expressing cell line BOSC23. This increase in VGF promoter activity suggested the presence of a negative cis-acting element within this site, which represses expression in non-specific cell

lines. A similar result was achieved for a further 5' primer deletion, up to -204, with respect to the transcriptional start site. Reporter gene activity was reduced in the specific cell line, namely SK-N-BE, whilst increased in the non-specific cell line, by 3 fold. To further investigate this region, Canu et al., (1997) cloned a 369-bp PCR fragment, representative of -573 to -204, upstream to the basal thymidine kinase promoter of herpes simplex virus. The construct displayed very low activity upon transfection in SN-K-BE cells, whereas there was no activity in the non-neuronal, non-specific BOSC23 cell line. This demonstrated that this fragment of the VGF promoter functions as an enhancer in neuronal cell-specific lines. In PC12 cells VGF is transcriptionally regulated by NGF and dbcAMP and to a lesser extent by TPA (Cho et al., 1989; Possenti et al., 1992), as well as depolarisation (Salton et al., 1991). Canu et al., (1997) demonstrated that transcriptional activity of their -2.3kb promoter construct was 3-fold higher in response to dbcAMP in cell lines that express VGF. Subsequent 5' deletion analysis demonstrated that sequences upstream of -573 contributed to enhanced expression of the promoter in response to dbcAMP. Similarly treatment of the SK-N-BE cell lines with TPA resulted in a 3-fold increase in promoter construct reporter gene expression. Again deletion analysis suggested that the responsive element was located upstream of -573.

An E box located at -180 contributes to the cell-type pattern of restricted expression (Di Rocco et al., 1997) – mutation of this region results in VGF expression in non-neuronal cell lines and decreased expression in PC12 cells. This region interacts with the CRE element to form a multiprotein nuclear complex that includes HeLA E-box binding protein (HEB) (Di Rocco et al., 1997; Salton et al., 2000) and the transcriptional coactivator p300.

It is likely that these elements, in combination with others (as yet identified), 5' to the transcriptional start site are responsible for the tissue-specific expression of the *vgf* gene. *In vivo* local administration of BDNF to the PVN

results in robust ectopic expression of the VGF gene (Eagleson et al., 2001). Tetrodotoxin-mediated blockade of retinal activity and cortical aspiration lesions results in a respective decrease and increase in VGF mRNA. VGF is regulated in the hypothalamus in response to feeding (Hahm et al., 1999, 2002; Saderi et al., 2014) and circadian rhythm (Hahm et al., 1999; Barrett et al., 2005). VGF also responds to salt loading (Mahata et al., 1993), long term potentiation (Hevroni et al., 1998) and by seizure (Snyder et al., 1998).

NRE Box

CTCTGCGTCATCGCCCCCACTCCCGG AACCTCT AACTGTCCAAGCCCCAGCCCCAACCCCTCTGGGCAGGAG

TRE TRE VDRE

AT AGGTCA CCA AGGTCA GATGGCTGAGAGGGTCCATCTCTGACGTTGCAATTCACCCCCCCCCC GGTCAGG

AP-1 SP-1

TTCA GACCTCCCCTTTAAGCGGTAGAGAGAAATGGAGTT GAGTCA CCCTCTCCACCTGCTCA CCCCCTCCCA

CCTGGTCTGCTCTCGCCCTCAAATGTCCTTGGGTCAAGGGGTCGTGGGGGAGAGGGAGACAGGCTGAAGG

GTGGGAGAGTTGGATTAAGGGGGCACAACAGGAACCCCTAACAGCCACAGCAGAGCCCGCTGGCCAGA

AGGACAGACACACCTTTTTTCCCAACCCCTTCCAGACACGAACTGGTTTGAACAGACACGACCCAAAGGCAC

ACACATCGTCAATCTTCCCTTTTCTCTCTCGACTAGGACCCTTCCAAGGTGATTACCCAAACCGCAAGATCCA

CCCATCTGCGCTGACCCTGGGCGGGCATCCCGCACCGCAAATCCACCCCTCCTCTCAGGTTCAAGTTGTCCTT

GGGCGTGCTCCCTATAGACCATACTGTGGCGGAGTAGGGAGCCAGGCCCTTCCCTTTCAAACCCCTTACCCT

RXR CCAAT Silencer

CCCCCA TCCAGT ACTGATCTTTACTGGCGC CCAAT TAGATGCTGGCGGTGCCCTTCTCCTATTCT GCTCAGC

AACGCAGGCTCCGCGCGCA AGTGCTTTGTAACCCACCCTCCCGCCTTCTGGTTCCTCTGTACCCACCCTCCAT

TCATTTTACATTCATTCATTCATCCTTTTCTCCTCGTCCCTCCTTCATTCATTCATAGCCCCCTGCCCGCCGCC

TCGACATTTTCATTCATTCATTCATTCATTCATTTCCCGGAGCTCGGCTAGCGCACGCCCTCTAGCCGAGGGGCC

E box CCAAT

TACTGCG CAGGTG CAGGCCGGGAGCGACGCTTATCCT CCAAT CATTGGACTTTCACCGTCCACCAGACACCCG

CRE SP-1 AP-2

CCCGTCCCCATGAATGAACATT GACGTCA ATG GGGCGGG GCTATCCACGTGA CCCCGCGCGT TCCCTTT

TATA +1

ATAAGGCAGAGGCGGCGGGCGCTGTCCAGCGTGCTGAA GCCGGAGCGAGAGCGCTGTTGCTGACCCAGC

Figure 1.4.1: **The nucleotide sequence of the 5' region of the mouse *vgf* gene.** The transcriptional initiation site is indicated by +1. Transcription factor binding sites are boxed, their names indicated above. Through bioinformatic searches a possible T3 response element (TRE) and vitamin D response element (VDRE) were identified.

1.4.2 The structure of the VGF polypeptide

VGF is a 68kDa polypeptide (Salton et al., 2000). The *vgf* gene encodes a polypeptide comprising 615 (human) or 617 (mouse/rat) amino acids (see Figure 1.4.2 A), with a typical secretory leader sequence of 22 amino acids, which promotes translocation to the endoplasmic reticulum (ER) (Trani et al., 2002). There are many lines of evidence which suggest that the VGF polypeptide is the precursor of several biologically active peptides which are released and play a role in intercellular communication (Bartolmucci et al., 2006; Hahm et al., 1999; Jethwa et al., 2007). The gene contains a number of specific sequences which are highly conserved between the species and these represent potential cleavage sites for the convertases of the kexin/subtilisin-like serine proteinase family (Trani et al., 2002). Western blot analyses of extracts of PC12 cells using a panel of C-terminal antisera detected a number of smaller VGF derived peptides. The most prominent VGF-derived peptides have apparent molecular masses of 20 (NAPP-129) and 10kDa (TLQP-62) respectively. Prohormone convertases (PCs), which are members of the subtilisin/kexin-like serine proteases (Steiner, 1998), have been shown to produce the VGF-derived peptides – NAPP-129 by the action of PC1/3 and PC2, TLQP-62 exclusively by PC1/3 (Trani et al., 2002). Rat, mouse and human sequences contain a minimal of 10 conserved regions of basic amino acid residues which represent potential PC cleavage sites. It is therefore proposed that the number of VGF derived peptide may be greater than first thought (see Figure 1.4.2 B).


```

Human      DKRSQEETPGHRRKEAEGTEEGGEEEDD-EEMDPQTIDSLIELSTKLHLPADDVVSIIIE 475
Mouse      DKRSQEEAPGHRKDAEGAEEGGEEEDDDDEEMDPQTIDSLIELSTKLHLPADDVVSIIIE 479
*****:*****:***:*****:** *****

Human      VEEKRKRKKNAPPEPVPPRAAPATHVRSQPAPPAPARDELDPWNEVLPPWDREED 535
Mouse      VEEKRKRKKNAPPEPVPPRAAPATHVRSQPPP--PAPARDELDPWNEVLPPWDREED 537
*****

Human      EVYPPGPYHFPNYIRPRTLQPPSALRRRHYPGRQAQARRAQEEAEAEER 595
Mouse      EVFPPGPYHFPNYIRPRTLQPPASSRRRHYPGRQAQARRAQEEADAER 597
**:*:*****:*****:*****:*****:*****:*****

Human      RLQEQEELENYIEHVLLRRP 615
Mouse      RLQEQEELENYIEHVLLHRP 617
*****:**

```

Figure 1.4.2 A: **Pairwise sequence alignment of the human and mouse VGF protein sequence.** Red, small hydrophobic, including aromatic, blue, acidic, Magenta, basic, Green, hydroxy. * indicates position which have a single, fully conserved residue. : indicates conservation between groups of strongly similar properties – scoring > 0.5 in the Gonnet PAM 250 matrix. . indicates conservation between groups of weakly similar properties – scoring < 0.5 in the Gonnet PAM 250 matrix. Sequence identity > 85%.

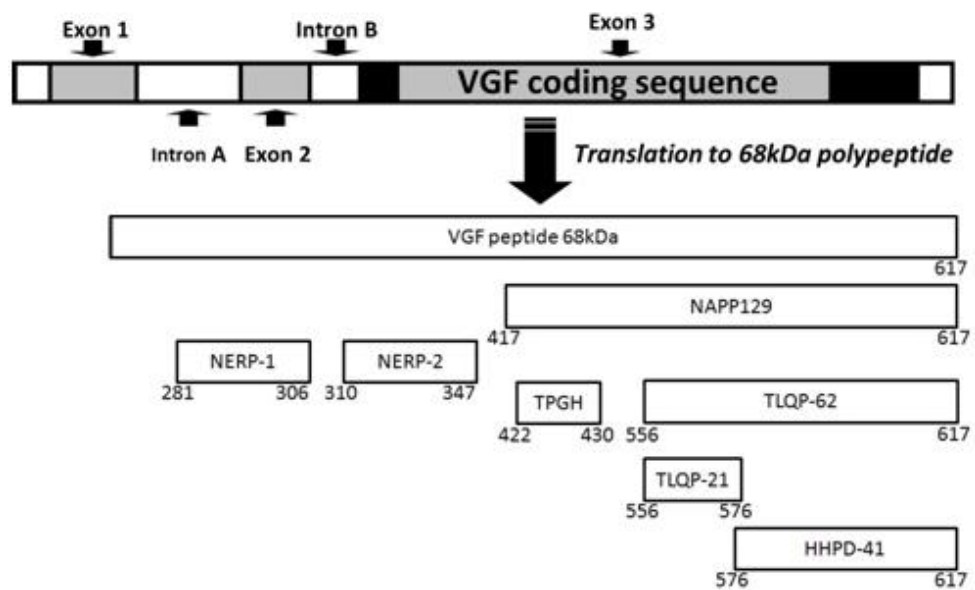


Figure 1.4.2 B: **The *vgf* gene and its derived peptides.** The VGF polypeptide is the precursor of several biologically active peptides which are released and play a role in intercellular communication. The gene contains a number of specific sequences which are highly conserved between the species and these represent potential cleavage sites for the convertases of the kexin/subtilisin-like serine proteinase family, namely prohormone convertases -1/3 and -2.

1.4.3 VGF expression

VGF mRNA is widely expressed throughout the nervous system, both in embryonic and adult tissues, but the highest expression of VGF has been detected in the ventromedial hypothalamus, in particular the ARC and in the suprachiasmatic nucleus (SCN) (van del Pol et al., 1989; Barrett et al., 2005). Immunohistochemical studies have shown that VGF immunoreactive peptides are also produced in peripheral tissues including the pituitary, adrenal, pancreas and GI tract (Snyder et al., 2003).

1.4.3.1 VGF mRNA

In the developing rat, VGF mRNA is expressed in distinct neurotrophin targets in the CNS and PNS during embryogenesis (Levi et al., 2004) – as early as embryonic day 11.5 (E11.5) in the dorsal root and sympathetic ganglia, neural crest cells migrating to enteric ganglia and in the primordium of the vagal (X) complex (Snyder et al., 1998). Subsequently, VGF mRNA is detected in the ventral spinal cord, cranial nuclei, basal forebrain, adrenal and pituitary (E13.5-15.5). VGF expression expands beyond the CNS and has been noted in the oesophagus, stomach and pancreas (E17.5-19.5) (Levi et al., 2004). In rats at birth, VGF mRNA is expressed in neurones throughout the brain, and in peripheral endocrine and neuroendocrine tissues. Whilst in the adult rat, VGF mRNA is widely distributed from the olfactory system, cerebral cortex, hypothalamus and hippocampus, and in a number of the thalamic, septal, amygdaloid and brain stem nuclei (Levi et al., 2004).

In the golden hamster, VGF mRNA levels are increased in response to light stimulation in the SCN (Wisor and Takahashi, 1997), which plays a central role in the regulation of circadian rhythms in mammals. This photic induction, however, does not occur in the PVN, despite expression of VGF in this area. Animals kept in constant darkness for 7 days were exposed to a 5 minute light pulse, resulting in a dramatic increase in VGF mRNA expression, which peaked

3 to 6 hours post exposure to the light. And whilst hybridisation, and therefore expression, was detected in the PVN, under the same experimental conditions, Wisor and Takahashi, (1997), were unable to detect an increase in gene expression.

Hahm et al., (1999) reported that VGF mRNA distribution in the mouse hypothalamus was similar to that in the rat. In addition, VGF mRNA levels were regulated in the mouse by light in the SCN and by the circadian clock in the rostral SCN (but not in the caudal SCN) as previously observed in the golden hamster (Wisor and Takahashi, 1997). Furthermore, Hahm et al., 1999 reported that VGF mRNA was induced in the ARC of fasted mice.

In leptin deficient *ob/ob* mice or leptin receptor *db/db* mice, hypothalamic VGF mRNA levels in the fed state resembled those of fasted wildtype mice, particularly in the ARC (Hahm et al., 2002). However, VGF does not appear to be an integral component of the leptin signalling pathway, as *VGF^{-/-}* mice respond to leptin administration (Hahm et al., 2002).

Snyder et al., (2003) reported the expression of VGF mRNA is detectable in the rat gastrointestinal and esophageal lumen, pancreas, adrenal and pituitary, as early as E15.5. Via *in situ* hybridisation Cocco et al., (2007) detected VGF mRNA in almost all pancreatic endocrine cells of the rat and, with less intensity of staining, in bovine islets – no staining was visible in swine pancreatic endocrine cells. VGF mRNA levels in both the PVN and SIN were up-regulated in response to water deprivation in rats (Toshinai and Nakazato, 2009).

1.4.3.2 Peptides

VGF and its derived peptides are found in dense core vesicles and are released in response to depolarising signals from neuronal and neuroendocrine cells through the regulated secretory pathways (Benson and Salton, 1996; Laslop et al., 1994; Possenti et al., 1989). Antibodies raised to synthetic peptides corresponding to the C- or N-termini of potential, or actual, cleavage products have been utilised to study VGF derived peptide distribution. In animal tissues, VGF immunoreactivity was restricted to central and peripheral neurones (Ferri et al., 1992; van den Pol et al., 1989), as well as to endocrine cells of the pituitary, adrenal medulla, gut and pancreas (Ferri et al., 1992).

The highest concentrations of VGF immunoreactivity have correspondingly been found in the medial hypothalamus, particularly in the ARC, in the SCN, and in the parvocellular and magnocellular cells of the PVN and the supraoptic nucleus (van den Pol et al., 1989). Immunostaining of serial 1 μ m rat SCN sections revealed co-localisation of VGF in cells which contain vasopressin (van den Pol et al., 1989). Weak immunoreactivity was also detected in the HI, AM, TH and CC (van den Pol et al., 1989). VGF immunoreactivity was also displayed in the female rat in the pars distalis, mainly with C-terminal antibodies (Ferri et al., 1995). This however disappeared in accordance with the estrous peak of luteinizing hormone (LH) secretion, along with an induction of VGF mRNA. Additionally, VGF-derived peptides are prominent in the adult spinal cord, in α - and γ -motorneurones of the ventral horn, and in the dorsal horn neurones as well as cells of the inner nuclear and ganglion cell layers of the retina (Zhao et al., 2008b). In the peripheral nervous system (PNS), both sympathetic ganglia and dorsal root ganglia of primary sensory neurones are important sites of localization of VGF-derived peptides (Snyder et al., 1998).

Whilst hypothalamic neurones contained the highest immunoreactivity levels, VGF derived peptide immunoreactivity was also apparent in the PNS (Ferri et

al., 1992). This is comparable to the expression of NPY, ghrelin and CCK, all of which regulate feeding, and in some cases, gastrointestinal mobility (Wren et al., 2000; Wren et al., 2002). VGF peptide levels quantified by radioimmunoassay in BAT were down-regulated by high fat diet (Watson et al., 2009).

Using double label immunofluorescence, VGF was present in 94% of α MSH neurones in the retrichiasmatic area, 84% in the anterior portion of the ARC, 69% in the mid ARC and 56% in the caudal ARC in fed rats (Hahm et al., 2002). Therefore in the fed state VGF and POMC gene expression was found to significantly overlap in the ARC. In response to fasting, a marked reduction in VGF in the trectochiasmatic area and lateral ARC in POMC-containing neurones was noted. Furthermore, increased VGF was observed in the medial part of the ARC. These increases corresponded to increases in NPY expression, a known potent stimulator of food intake (Hahm et al., 2002).

In summation, VGF derived peptides are likely to be a response to an array of stimuli and conditions, with an additional complexity given the processing of the precursor. VGF is, however, localised and regulated in a manner benefiting a gene which controls energy homeostasis, and these studies have been undertaken to further determine its action.

1.4.4 VGF^{-/-} null mouse

The function of VGF, and by extension, its derived peptides, was first assessed through the development of the VGF^{-/-} mouse via homologous recombination (Hahm et al., 1999). At birth, the homozygous VGF^{-/-} mice were indistinguishable from either their heterozygous, or even, wild-type littermates. No defects in development were detected in either the CNS or the PNS. However, in the weeks following birth, the VGF^{-/-} mice were visibly smaller

than their littermates, and adults were found to weigh 50-70% less than wild-type (see Figure 1.4.5). These initial observations led Hahm et al., (1999) to suggest that VGF may play a non-redundant role in the regulation of energy homeostasis and antagonism of the gene may constitute the basis for treatment of obesity.

The reduction on body weight was thought to be a result of a significantly elevated basal metabolic rate, as measured by oxygen consumption and carbon dioxide production. Despite these significant increases, VGF^{-/-} mice had reduced serum T4 thyroid hormone levels and thyroid-stimulating hormone (TSH). Core body temperature was normal, as was sympathetic activity as gauged by the measurement of heart rate and adrenal norepinephrine and epinephrine levels (Hahm et al., 1999). Peripheral fat stores, however, were significantly reduced in VGF^{-/-} mice, as was total body fat, which represented a smaller fraction of total body composition. Faecal levels of fat were similar in controls and VGF^{-/-} mice, suggesting that GI tract fat absorption was not altered. Expression of leptin, as measured by mRNA levels, was significantly reduced in the epididymal fat pad in VGF^{-/-} mice, as were circulating leptin levels. Therefore a compensatory increase in food intake and/or energy expenditure would be expected. *Ad libitum* VGF^{-/-} mice daily food intake was similar to that of normal littermates, which represented a significant increase in food intake per gram body weight in VGF^{-/-} mice. In addition, VGF^{-/-} mice were found to be hyperactive (Hahm et al., 1999). Fasting in normal mice results in decreased serum glucose and leptin (Ahima et al., 1996). In VGF^{-/-} mice, mean serum insulin and glucose levels were 80 and 60% respectively of the levels found in wildtype mice, while mean corticosterone level was elevated; 140% of wildtype levels, all of which is consistent with the fasted state. In addition, VGF^{-/-} mice fed *ad libitum* had high AgRP and NPY gene expression (600 and 800%, respectively) and a decrease in POMC mRNA levels similar to that observed following a 48 hour fast (Hahm et al., 1999). The mice consumed considerably more calories per gram body weight, however, this

increase in food intake was not sufficient to maintain wild-type body weight, as the VGF^{-/-} mice utilised twice as much oxygen at rest and displayed increased locomotor activity (Hahm et al., 1999), suggesting that VGF^{-/-} mice are resistant to DIO, as well as obesity induced by treatment with gold thioglucose (Hahm et al., 2002).

Targeted deletion of the VGF gene did not affect hypothalamic anatomy and/or function. Quantitative neuronal counts in the PVN of VGF^{-/-} and wildtype mice were similar, as was the overall distribution of neurones containing gonadotropin-releasing hormone, oxytocin, vasopressin, and POMC in specific hypothalamic regions. Function was assessed by circadian behaviour – heterozygous and homozygous VGF^{-/-} mice could be entrained to a light: dark cycle and both maintained a circadian rhythm of wheel running activity in constant darkness. However, the circadian period length of the VGF^{-/-} mice was shorter than wildtype littermates (Hahm et al., 1999).

1.4.5 VGF and obesity

The phenotype of the VGF^{-/-} mouse suggested that the derived peptides regulated energy homeostasis. Hahm et al., (2002) reported that *Vgf* gene deletion blocked the development of obesity from select environmental and genetic causes and suggested that VGF functions in outflow pathways, downstream of the hypothalamic melanocortin receptors, regulating energy expenditure.

VGF is required for the development of DIO – ablation of the *vgf* gene blocked the metabolic effects of HFD and resulted in a small but significant increase in fat pad weight in VGF^{-/-} mice (Hahm et al., 2002). However, there were no significant changes in leptin mRNA within adipose tissues or circulating leptin levels. Furthermore, ablation of the *vgf* gene blocked gold thioglucose (which

is taken up by and is toxic to glucose-sensitive neurons in the periarculate area of the VMN) but not monosodium glutamate (which damages the hypothalamus and the sympathetic nervous system) induced obesity (Hahm et al., 2002). None of the *VGF*^{-/-} mice developed the obesity associated via hyperphagia following gold thioglucose treatment, despite the formation of characteristic hypothalamic lesions.

However, targeted deletion of the *VGF* gene had no influence on the ability of monosodium glutamate (MSG) treatment of neonatal mice to increase body weight and develop obesity (Hahm et al., 2002). MSG treatment of postnatal animals results in a specific pattern of neural degeneration, primarily in the ARC (Ebling et al., 1998). The obesity which develops following monosodium glutamate is not a result of over-eating (Dolnikoff et al., 2001); but is instead associated with increased metabolic efficiency (Djazayery et al., 1978) and high levels of corticosterone (Tokuyama and Himms-Hagen, 1989). Furthermore, there are decreased glucose transporter protein-4 (GLUT4) (Morris et al., 1998) and uncoupling protein mRNA levels in brown adipose tissue (BAT) (Tsukahara et al., 1998) in MSG treated mice, both of which suggest an impairment of hypothalamic sympathetic output to BAT and therefore a disruption in thermogenesis. As *VGF*^{-/-} fail to develop the obesity associated with MSG treatment it suggests these thermogenic pathways, which result in the *VGF*^{-/-} phenotype, are blocked.

Further experimentation with the *VGF*^{-/-} mouse has shown that *VGF* is required for the development of obesity in the *A^{v/a}* agouti mouse, which have a mutation which blocks the function of α MSH. The mutation results in an over-expression of the agouti protein, which then has excess AgRP-like actions in the hypothalamus as it blocks melanocortin receptors (Hahm et al., 2002). Ablation of the *vgf* gene in these mice improved the obese phenotype. However, *vgf* gene ablation on *ob/ob* mice blocked the hyperphagia and increased body

weight due to leptin deficiency, but surprisingly did not prevent the development of increased adiposity or decreased body temperature (Hahm et al., 2002).

Vgf ablation blocks the development of hyperinsulinemia and hyperglycemia that results from high-carbohydrate and high-fat diets, gold thioglucose lesions and genetic defects in the hypothalamic melanocortin pathway (Watson et al., 2005). Firstly, levels of POMC mRNA, which encodes α MSH, were increased in $VGF^{-/-}$ mice fed a high calorie diet compared to those fed a regular chow, while NPY and AgRP mRNAs were decreased (Watson et al., 2005). $VGF^{-/-}$ mice fed a high fat, high carbohydrate diet had increased NPY and AgRP mRNA, and lower POMC, than similarly fed wildtype controls. The high calorie diet reversed the effect of targeted deletion of the *vgf* gene, however, the serum levels of leptin, insulin or T_4 did not increase in $VGF^{-/-}$ mice. Watson et al., (2005) therefore proposed plasma glucose, which was increased, may be responsible for the diet induced changes in hypothalamic gene expression. Furthermore, glucose tolerance was altered in $VGF^{-/-}$ mice – plasma levels increased more slowly in $VGF^{-/-}$ mice and while $VGF^{-/-}$ mice appeared more sensitive to insulin injection, which subsequently led to a greater and more prolonged decrease in plasma glucose (Watson et al., 2005). However, deletion of the VGF gene did not affect the distribution of insulin and glucagon in pancreatic islets and lack of glycogen reserves prevented a normal counter-regulatory response to insulin induced hypoglycaemia in $VGF^{-/-}$ mice.

Watson et al., (2009) demonstrated that homozygous $VGF^{-/-}$ mice on a C57Bl/6J background were hypermetabolic with similar locomoter activity levels to controls and proposed that mechanisms other than hyperactivity were responsible for their increased energy expenditure. Morphological analysis of BAT and WAT indicated decreased fat storage in both tissues and changes in gene expression were consistent with increased fatty acid oxidation and uptake

in BAT, increased lipolysis, decreased lipogenesis and brown adipocyte differentiation in WAT. Watson et al., (2009) suggested that increased sympathetic nervous system activity in $VGF^{-/-}$ mice may be associated with or responsible for alterations in energy homeostasis and fat storage. UCP-1 and -2 protein levels were up-regulated in $VGF^{-/-}$ mice, as well as mitochondrial number and cristae density. Furthermore, $VGF^{-/-}$ mice were cold intolerant (Watson et al., 2009).



Figure 1.4.5: **The $VGF^{-/-}$ mouse (left) with a wildtype littermate (right).** Size comparison of a typical 4-week old homozygous $VGF^{-/-}$ mouse (left) with a wild type littermate (right). $VGF^{-/-}$ are lean, hypermetabolic and hyperactive, relatively infertile, with markedly reduced leptin levels and fat stores. They also have altered POMC, NPY and AgRP expression (Hahm et al., 1999).

1.4.6 Physiological roles of VGF and VGF derived peptides

The lean, hypermetabolic and hyperactive phenotype of the $VGF^{-/-}$ mouse suggested that VGF and its derived peptides played a critical anabolic role in the regulation of energy homeostasis and in the normal animal may control energy storage by damping metabolic rate and/or activity (Hahm et al., 1999). However, subsequent studies have resulted in an opposing view for VGF and its derived peptides. Barrett et al., (2005), Bartolomucci et al., (2006) and Jethwa et al., (2007) suggest that VGF mRNA and its derived peptides exert a

catabolic affect. One possible explanation is that VGF derived peptides have opposing biological effects as was initially proposed for ghrelin and obestatin (Zhang et al., 2005). As receptors for the VGF derived peptides have yet to be described, and given its widespread expression throughout the body, it is possible that a global VGF^{-/-} mouse may produce a confused net phenotype that masks the function of the gene and its derived peptides.

1.4.6.1 VGF expression in states of altered energy balance

In the ARC, there are two populations of neurones whose gene expression alters in response to fasting, where VGF is co-expressed; the POMC neurones in the lateral ARC and the NPY neurones in the medial ARC. In the fed state, VGF mRNA is co-localised with POMC and there is low expression in the NPY neurones. This is reversed in the fasted state (Hahm et al., 2002). VGF expression is induced by fasting in the mouse, rat and Siberian hamster, in the ARC, which also synthesise NPY, as well as AgRP, while decreased in the neurones which synthesise POMC, and the derived feeding peptide, α MSH (Hahm et al., 2002; Ross et al., 2005; Toshinai et al., 2010). Administration of leptin attenuates the increase in VGF mRNA in response to fasting in the mouse (Hahm et al., 2002). VGF mRNA levels in the ARC match those of the fasted wild type mouse in the leptin deficient *ob/ob* mouse, as well as in the leptin unresponsive *db/db* mouse. It is suggested that VGF is an enhancer of the metabolic state of the animal.

1.4.6.2 VGF in response to season

Barrett et al., (2005) observed that VGF mRNA is regulated in response to season in the Siberian hamster. VGF mRNA is significantly increased in the winter catabolic state in the dmpARC, a region of the hypothalamus where a number of genes related to retinoic acid, histaminergic and serotonergic signalling (Barrett et al., 2005; Barrett et al., 2006; Ross et al., 2004) have been implicated in the change in body weight in response to season. Initial *in situ*

hybridisation analysis showed that the *vgf* gene had a widespread pattern of expression in the brain of the Siberian hamster, with a similar distribution pattern to that of the rat (Snyder and Salton, 1998) and mouse (Hahm et al., 1999). When exposed to SD for 14 weeks, VGF mRNA was increased by 5-fold in the dmpARC of Siberian hamsters. However, expression of VGF in the remainder of the ARC was higher in LD when compared to SD. The results from this study strengthened the view that the dmpARC is an important integrating centre mediating photoperiodic response in the Siberian hamster (Barrett et al., 2005). This finding, however, was contrary to the findings and phenotype of the VGF^{-/-} mouse, which is lean, hypermetabolic and hyperactive (Hahm et al., 1999). This may be as a result of global ablation of the VGF gene during the course of development and subsequently in the adult.

1.4.6.3 The VGF derived peptide TLQP-21

In Mice

The VGF derived peptide TLQP-21 was identified by the Bartolomucci et al., (2006) in extracts of the rat brain by immunoprecipitation and microcapillary liquid chromatography tandem mass spectrometry, with subsequent database searching. Chronic ICV infusion of TLQP-21 (15µg/day for 14 days) in mice fed normal lab chow resulted in a small increase in resting energy expenditure and rectal temperature. These were paralleled by increased serum epinephrine and decreased norepinephrine, both of which were independent of locomotor activity and free tri-iodothyronine (T3) and T4 serum levels. BAT-norepinephrine was increased by TLQP-21 treatment, while WAT-norepinephrine was inversely correlated with relative WAT/body weight. TLQP-21 also increased adrenal gland weight, whereas corticosterone levels remained unaffected. Surprisingly, TLQP-21 did not affect food intake or body weight; however, WAT/body weight and circulating leptin were slightly reduced. The changes in metabolic parameters were mirrored by increased epinephrine content in BAT, and up-regulation of BAT β2-adrenergic receptor (AR) and UCP-1 mRNA and high expression of WAT peroxisome proliferator-

activated receptor δ (PPAR- δ) and β 3-AR. However, hypothalamic neuropeptide gene expression of AgRP, NPY, α MSH, POMC and CRH was unchanged by TLQP-21 treatment.

In Mice switched to a High Fat Diet (HFD)

In mice switched to a HFD for 14 days, treatment with TLQP-21 halted the expected increased body weight, associated with an increase in WAT, and attenuated the hormonal changes, which results from a HFD (Bartolomucci et al., 2006). Despite HFD and standard diet mice consuming similar amounts, expressed as kilocalories, and displaying similar levels of activity, TLQP-21 treated mice displayed unaffected body weight and WAT weight. TLQP-21 treated mice, subject to a HFD displayed attenuated rises in leptin and a normalisation of ghrelin. Subsequent biochemical and molecular analyses suggested that TLQP-21 stimulated autonomic activation of the adrenal medulla and adipose tissues (Jethwa and Ebling, 2008). These studies demonstrated that ICV infusion of TLQP-21 prevented the DIO expected from a HFD in mice. Somewhat surprising, however, was that on mice fed a normal lab chow, TLQP-21 increased energy expenditure, yet had no effect on either food intake or body weight.

Bartolomucci et al., (2009), investigated the effect of chronic ICV infusion of TLQP-21 in male Swiss CD1 mice fed a HFD. These fast weight-gaining mice treated with TLQP-21 did not see the increases in body weight and epididymal WAT expected by a HFD, despite hyperphagia. Furthermore, TLQP-21 normalised the increase in leptin and decrease in ghrelin, while increasing epinephrine and the epinephrine/norepinephrine ratio. Mice treated with TLQP-21 also displayed increased epididymal WAT β 3-AR mRNA, PPAR- δ and hormone-sensing-lipase mRNA – all of which are catabolic markers.

The lean, hypermetabolic and hyperactive phenotype of the VGF^{-/-} mouse lead to the prediction that VGF derived peptides were anabolic neuropeptides, however, chronic ICV infusion of TLQP-21 increased resting energy expenditure and rectal temperature, without affecting body weight or food intake. Hypothalamic neuropeptide gene expression was also unaffected by treatment with TLQP-21 and while the approach was limited, whole hypothalamic semi-quantitative RT-PCR is not informative of regional gene expression, it is often enough to make an evaluation of changes in mRNA. TLQP-21 may act downstream of the hypothalamus, in the outflow pathways which project to the autonomic nervous system to peripheral metabolic tissues and is therefore able to regulate energy homeostasis.

In Siberian hamsters

Jethwa et al. (2007) demonstrated that a single ICV infusion of TLQP-21 (5 and 25 µg) dose dependently decreased food intake over a 24 hour investigative period at the onset of the dark phase. The effect occurred within 1 hour post infusion and a suppressive effect of the lowest dose was noted when the data for the entire 24 hour period was summated. As a result, ICV infusion of TLQP-21 significantly decreased body weight 24 hours post infusion compared to saline controls. No sedation or hyperactivity was observed post infusion and despite the alterations in food intake, there was no significant difference in the proportion of time Siberian hamsters spent investigating the test meal in the first hour post infusion. Whilst the mean baseline oxygen consumption in male Siberian hamsters, in the light phase, was slightly higher post TLQP-21 infusion, results were not significant. There was no significant effect of TLQP-21 infusion on the frequency of meals throughout the 24 hr period, although there was the expected, significant effect of time, with the frequency of meals higher in the dark phase in both treatment and control groups than in the light phase. There was no significant difference in locomoter activity or oxygen consumption, except for the expected circadian changes with time, indicating that oxygen consumption decreased during the light phase as anticipated when the Siberian

hamsters are at rest. There was also no effect on respiratory exchange ratio (RER: defined as carbon dioxide production divided by oxygen consumption) (Chiang et al., 2010)

Chronic infusion of TLQP-21 (5µg/day) resulted in a sustained decrease in food intake and body weight, a reflection of abdominal fat depots (Jethwa et al., 2007). By day 6, food intake was reduced by 56% in the treatment group compared to controls. A pair-fed group, whose food intake was restricted to that of the TLQP-21 treatment group, lost similar amounts of weight. Therefore, as there was no significant effect of treatment on metabolic parameters, the reduction in body weight was assumed a direct effect of reduced food intake, rather than increased energy expenditure. The observed decrease in body weight in the treatment group was a result of decreased adiposity. At day 6, epididymal WAT and paired testes weights were significantly reduced in the TLQP-21 treatment group. However, there was no significant effect of TLQP-21 treatment on the weights of the pituitary or adrenal glands. Hypothalamic gene expression (NPY, AgRP, POMC and CART) were unaffected by the chronic ICV infusion of TLQP-21. However, the orexigenic neuropeptides were significantly increased in the pair-fed group. UCP-1 mRNA expression in BAT was significantly reduced in the TLQP-21 treatment and pair-fed group. Intraperitoneal injection of TLQP-21 did not affect food intake, body weight, behaviour or oxygen consumption (Jethwa et al., 2007).

There were no observable differences in oxygen consumption; therefore weight loss was attributed to a reduced caloric intake, rather than an increase in metabolic rate, as observed by Bartolomucci et al., (2006) in mice. In support of this Jethwa et al., (2007) detected a significant decrease in UCP-1 mRNA in both the TLQP-21 treated and the pair fed hamsters in BAT. It was suggested that this was a compensatory response to reduced caloric intake. Jethwa et al.,

(2007) hypothesised that the primary role of TLQP-21, a VGF derived peptide, was therefore to induce satiety, rather than to increase energy expenditure in the Siberian hamster.

In Rats

Severini et al., (2009), examined the effects of TLQP-21 *in vitro* by measuring smooth muscle contraction in isolated preparations from the rat GI tract, and *in vivo*, by assessing gastric emptying in rats. TLQP-21 dose dependently induced smooth muscle contraction of rat longitudinal forestomach strips by release of prostaglandin (PG) E₂ and PGF_{2α} from the mucosal layer, an effect which was antagonised by indomethacin and selective inhibitors of either cyclooxygenase-1 or -2. Similarly, TLQP-21 induces contractions of gastric fundus strips (Bartolmucci et al., 2006). Interestingly, TLQP-62, AQEE-30 and LQEQ-19 failed to evoke contractions and TLQP-21 induced weak and not concentration dependent responses on oesophagus, gastric antrum and circular forestomach muscle strips, even at much higher concentrations.

TLQP-21 infused via ICV cannulation significantly decreased gastric emptying by about 40%, an effect which was blocked by ICV infusion of indomethacin, suggesting that TLQP-21 acts within the brain stimulating PG release. The results demonstrate that this VGF derived peptide plays a central and local role in the regulation of rat gastric motor functions (Severini et al., 2009).

1.4.6.4 The VGF derived peptides neuroendocrine regulatory peptides (NERP)-1 and NERP-2

Neuroendocrine regulatory peptides (NERP)-1 and -2 are distinct regions of the neurosecretory protein VGF (see Figure 1.4.2 B) (Toshinai and Nakazato, 2009). Human NERP-1 consists of 26 amino acid residues, while NERP-2 comprises 38 amino acids. The potential cleavage sites for PC are conserved across species. Radioimmunoassays using antibodies for the C terminal region of rat NERP-1

and -2 detected highly abundant species in the rat hypothalamus (Yamaguchi et al., 2007); the magnocellular neurones of the SON and PVN produces strong immunostaining of NERP-1 and -2, regions which produce the antidiuretic neuropeptide vasopressin and the reproductive neuropeptide oxytocin (Yamashita et al., 1983). Immunogold electromicroscopy revealed the colocalisation of NERPs and vasopressin in storage granules within the magnocellular neurones of both the human SON and PVN. Interestingly, NERP-1 and -2 circulate in the human plasma (Toshinai and Nakazato, 2009). Water deprivation in rats increases VGF mRNA levels in both the SON and PVN, while salt loading also increased levels, along with vasopressin mRNA (Mahata et al., 1993). Taken together, this data suggests that NERP-1 and -2 may be involved in the central control of body fluid balance. ICV infusion of hypertonic NaCl or angiotensin II increased plasma vasopressin in rats, however this was suppressed in a dose-dependent manner in ICV infusion of NERP-1 (NERP-2 had a similar, albeit weaker, effect) (Toshinai and Nakazato, 2009). ICV infusion of NERP-1 and -2 attenuated the increase in vasopressin as a result of water deprivation in rats, while immunoneutralisation via ICV infusion of anti-NERP-1 and -2 IgG reversed this suppression.

1.5 AIMS AND OBJECTIVES

Previous studies implicated VGF and its derived peptides in the regulation of food intake and body weight (Barrett et al., 2005; Bartolomucci et al., 2006; Hahm et al., 1999; Jethwa et al., 2007). The phenotype of the VGF^{-/-} mouse – lean, hypermetabolic and hyperactive – suggested an anabolic role for VGF and its derived peptides. However, Barrett et al., (2005) noted an increase in VGF mRNA in the dmPARC of Siberian hamsters switched to SD, a state which is largely catabolic, while Bartolomucci et al., (2006) suggested a role for TLQP-21 in energy expenditure and Jethwa et al., (2007) suggested a role in the control of food intake and body weight. The primary aim of this thesis was to investigate the role and regulation of VGF, and its derived peptides, in the regulation of energy homeostasis, utilising the Siberian hamster as a model of

long-term central control of caloric intake and expenditure and the mouse C57BL/6J mouse as a model for studies of diet-induced obesity.

1.5.1 Chapter 3 Objectives

While the VGF^{-/-} mouse presents a view that VGF acts as an anabolic signal (Hahm et al., 1999), data from subsequent studies utilising VGF derived peptides in mice and hamsters do not support this (Bartolomucci et al., 2006; Jethwa et al., 2007). The VGF derived peptide TLQP-21 was demonstrated to reduce food intake in Siberian hamsters (Jethwa et al., 2007), and increase energy expenditure in DIO mice (Bartolomucci et al., 2006). It has been postulated that TLQP-21 induces satiety in the Siberian hamsters, while it stimulates autonomic activation of the adrenal medulla and adipose tissues in the DIO mice. Despite the species differences the general consensus is that TLQP-21 exerts an overall catabolic action. One possible explanation between the differences observed in the functional *in vivo* studies and those in which all VGF production has been ablated may be due to the loss of multiple peptides from one large polypeptide which may have opposing effects. Indeed ghrelin and obestatin produced from the same pro-peptide have opposing roles (Zhang et al., 2005). Thus the aim of the studies presented in this chapter was to determine the effects of the VGF derived peptide HHPD-41 (which is produced following the cleavage of TLQP-21 from the larger polypeptide TLQP-62, the most abundant VGF derived species in the rat brain), on food intake, bodyweight and behaviour as well as utilising immunohistochemistry to determine sites of action of the two VGF derived peptides.

1.5.2 Chapter 4 Objectives

A possible explanation for the differences between the functional studies of VGF derived peptides (Bartolomucci et al., 2006; Jethwa et al., 2007) and the VGF^{-/-} mouse (Hahm et al., 1999), maybe a consequence of global deletion of the targeted gene during the course of development and subsequently in the

adult. Alternatively, deletion of several encoded bioactive peptides, with opposing effects (as demonstrated in chapter 3), may account for the phenotype of the VGF^{-/-} mouse. VGF is expressed and differentially processed in a number of neuronal and endocrine tissues, therefore extrapolating the findings from the VGF^{-/-} mouse is fraught with difficulties; previous findings may not be associated with loss of function in the brain. Thus the aim of the studies was to determine the effects of VGF on energy homeostasis following chronic up-regulation of the gene (via a recombinant adeno-associated virus (rAVV)) in the hypothalamus of Siberian hamsters (in LD and SD) and mice (fed a normal and HFD). These studies also assessed the feasibility of a viral 2A peptide, an alternative to the internal ribosome entry site (IRES), within a nonstandard laboratory species.

1.5.3 Chapter 5 Objectives

Tissue-specific expression of the *vgf* gene is controlled by the elements outlined in section 1.4.1, in combination with as yet unidentified elements (Levi et al., 2004). VGF mRNA expression is altered by photoperiod in Siberian hamsters, with increased levels observed in the SD in the *dmpARC* (Barrett et al., 2005). However, expression in the remainder of the ARC was higher in LD (Barrett et al., 2005; Jethwa et al., 2007). It has recently been postulated that hypothalamic thyroid hormone availability plays a key role in the seasonal regulation of appetite and bodyweight, since a reduction in the local availability of T3 in SD results in hypophagia and weight loss (Murphy et al., 2012). A heterodimer of thyroid hormone receptor (TR), retinoic acid receptor (RAR), is also significantly reduced in SD, along with components of its signalling pathway, namely cellular retinol binding protein 1 (CRBP-1) and cellular retinoic acid binding protein 2 (CRABP-2) (Ross et al., 2005). Furthermore retinaldehyde dehydrogenase-1 (RALDH-1), which is responsible for the local conversion of retinol to retinoic acid, is decreased in the ARC in response to SD in the rat (Shearer et al., 2012). Therefore, using the neuronal SH-SY5Y cell line as an *in vitro* model, the studies presented in this chapter investigated the effect of

retinoic acid (RA) and triiodothyronine (T3) on endogenous VGF expression and the VGF promoter as a mechanism for the observed decrease in VGF expression in SD in the hypothalamus as a possible mechanism for the seasonal regulation of appetite. Furthermore, having identified a vitamin D response element (VDRE) within the VGF promoter the studies investigated whether 1,25-dihydroxyvitamin D3 (1,25D3), the active metabolite of vitamin D, alters endogenous VGF expression and promoter activity. Like T3, 1,25D3's action is exerted by binding, preferentially as a heterodimer with the RXR, to the VDRE (Calle et al., 2008). Interestingly, Takeda et al., (1994) demonstrated the formation of a complex between VDRE, the active metabolite 1,25D3, RA and T3.

2 CHAPTER 2 – MATERIALS AND METHODS

2.1 INTRODUCTION

Details of a specific method can be found in the relevant chapter, outlined in Table 2 below.

Chapter 3 ICV infusion of HHPD-41 in the Siberian hamster	Chapter 4 Over-expression of VGF mRNA in the Siberian hamster and mouse	Chapter 5 A novel regulator of promoter and endogenous VGF <i>in vitro</i>
Peptides	Preparation of AAV	The SH-SY5Y cell line
Siberian hamsters	Animals – C57Bl/6J Mice	RNA Extraction
ICV cannulation and infusion	Viral infusion	cDNA synthesis
Palatable diet	CLAMS	PCR
Behaviour	Dissection	Transfection
c-Fos	Cryostat	Typhoon Trio +
Statistics	In situ hybridisation	Development of a reporter and promoter construct
	Statistics	

Table 2: **The materials and methods of relevant chapters.**

In chapter 4 the construct for over-expression was tested in the SH-SY5Y cell line. This cell line was characterised in chapter 5, where details can be found.

Routine methods are reported below.

2.2 NUCLEIC ACID EXTRACTIONS AND PROCEDURES

2.2.1 Extraction of total genomic DNA

Prior to extraction, all plastic and glassware was autoclaved to ensure sterility. All solutions were prepared in ribonuclease (RNase) and deoxyribonuclease (DNase) free water (molecular biology grade water, Sigma, UK). Total genomic DNA extraction was via the DNeasy Blood and Tissue Kit (QIAGEN, UK). Briefly, homogenised tissue was treated with proteinase K and incubated at 56°C overnight. Proprietary buffer and subsequently 100% ethanol (Fisher Scientific, UK) were added and the resultant precipitate was added to a spin column and centrifuged at 6000 x g for 1 minute. The flow-through was discarded, proprietary buffers were added to the spin column and centrifuged, firstly at 6000 x g for 1 minute, and secondly at 20000 x g for 3 minutes. The bound DNA was eluted via centrifugation at 6000 x g for 1 minute and stored at -80°C.

2.2.2 Phenol: Chloroform extraction

To extracted or digested DNA/RNA, a 1/10 volume of 3M sodium acetate (pH 5.5, Sigma, UK) was added. To this solution an equal volume of phenol (pH 8.0, Sigma, UK) was added. The mixture was vortexed and spun at 13000 x g for 5 minutes. The supernatant was transferred, to which an equal volume of chloroform (Sigma, UK) and 4µl of isoamylalcohol (Sigma, UK) was added. This mixture was vortexed and spun at 13000 x g for 5 minutes. The supernatant was transferred and 3 volumes of 100% ethanol were added. The solution was spun at 13000 x g for 30 minutes, after which the supernatant was removed and discarded. The DNA/RNA pellet was washed with 0.5ml 70% ethanol, spun

at 13000 x g for 5 minutes. The supernatant was removed and the step repeated to remove residual liquid before air drying of the pellet for 15 minutes at room temperature. The pellet was resuspended in 10µl water.

2.2.3 Removal of contaminating DNA

Prior to experimentation, all extracted total RNAs were treated with RQ1 DNase (Promega, UK) to remove contaminating genomic DNA. Total RNA (40µl as previously resuspended) was incubated with 1U DNase in 5µl of buffer comprising 400mM Tris-HCl (pH 8.0, Sigma, UK), 100mM MgSO₄ (Sigma, UK) and 10mM CaCl₂ (Sigma, UK) for 30 minutes at 37°C.

2.2.4 DNA/RNA quality assessment and quantification

The concentration of DNA/RNA in molecular biology grade water was determined spectrophotometrically using the Nanodrop system (Thermo Scientific, UK). Before measurements were taken the instrument was blanked using water as a standard. Measurements were taken at 260nm for nucleic acid and at 280nm for proteins. The ratio of these two measurements was calculated and a ratio of 1.8 – 2.0 nucleic acid to protein was deemed acceptable. DNA/RNA integrity was determined by agarose gel electrophoresis (see section 2.2.5).

2.2.5 Agarose gel electrophoresis

PCR amplicons, extracted DNA and RNA were routinely resolved by agarose gel electrophoresis. The percentage concentration of the agarose gel utilised was dependent on the size of the fragments resolved. 0.8% (w/v) agarose gels were used to resolve DNA and RNA extractions and larger PCR amplicons (≥ 1Kb). For smaller PCR fragments, 1.2% agarose gels were used. Agarose (Melford, UK) was prepared in 50ml TAE buffer (Thermo Scientific, UK), heating to boiling point in a laboratory microwave and stirred to ensure that the agarose had dissolved. Once the solution had cooled to around 50°C, the gel was poured

into a gel former (BioRad, UK) with the corresponding gel comb. The gels were then allowed to solidify at room temperature. Samples (generally 5µl) were combined with 1µl loading dye (Promega, UK) and loaded onto the gel. Samples were electrophoresed at 90 volts for 60 minutes, followed by staining in ethidium bromide (0.5µg/ml, Sigma, UK) for 30 minutes. Gels were visualised under a UV light source and images were captured using the GelDoc 2000 (BioRad, UK) with associated software. DNA markers (DNA ladder 1Kb, 100bp as appropriate, Promega, UK) were included in all runs to delineate the size of DNA electrophoresed.

2.3 CLONING

2.3.1 PCR amplicon clean-up

Where indicated, PCR amplicons were purified from contaminating reactants (primers, nucleotides and buffers) using GenElute column-based technology (Sigma, UK) prior to cloning. Briefly, PCR amplicons were bound to the silica spin column, washed in proprietary solution, and eluted in 50µl of molecular biology grade water. Products were used immediately.

2.3.2 pGEM T-Easy Vector cloning of PCR amplicons

Purified amplicons were cloned using the pGEM T-Easy vector system (Promega, UK). 5µl rapid ligation buffer, 1µl pGEM T-Easy vector, X ng amplicon (determined in section 2.3.3) and 3U of T4 ligase were mixed well and incubated at RT for 1 hour.

2.3.3 Ligation

The PCR amplicons were ligated at a molar ratio of 3:1 insert: vector to enhance the likely number of transformants. The amount of PCR product (X) to add was calculated as follows:

$$\text{Insert (ng)} = [\text{Vector (ng)} \times \text{Insert (Kb)} / \text{Vector (Kb)}] \times \text{Insert} / \text{Vector molar ratio}$$

The calculated amounts of insert and vector were added to the appropriate volume of manufacturer's buffer (Promega, UK) and 3U of DNA ligase (LigaFast™ Rapid DNA Ligation System, Proemga, UK). The reaction was incubated at 15°C overnight.

2.3.4 Transformation

2.3.4.1 JM109 cells

Following ligation, the solution of vector and insert was transformed into competent *Escherichia coli* (*E.coli*) JM109 cells (Promega, UK). Briefly, competent cells were thawed on ice, before the addition of 20ng per microlitre plasmid DNA. The reaction was maintained on ice before a 90 second heat-shock at 42°C. 800µl of LB (Sigma, UK) was added to the cells, which were incubated at 37°C for 30 minutes. The cells were centrifuged, resuspended in 200µl of LB and plated immediately on LB/agar plates containing the appropriate antibiotic (at 50µg/ml) and incubated for 37°C for 16 hours.

2.3.4.2 SURE 2 Supercompetent cells

Replicating eukaryotic DNA in prokaryotic cells can be problematic, as genes may contain inverted repeats or secondary structures, such as Z-DNA, which can be rearranged and/or deleted by *E.coli* DNA repair systems. The SURE 2 Supercomptent cells (Agilent Technologies, UK) are deficient in the *E.coli* genes involved in the rearrangement and deletion of DNA. SURE 2 cells are kanamycin, tetracycline and chloramphenicol resistant and are grown in NZY+ broth containing the following supplements: 12.5ml of 1M MgCl₂, 12.5ml 1M MgSO₄ and 20ml 20% glucose. Transformation proceeded as per JM109 cells (METHOD 2.3.4.1), with the addition of 2µl β-ME (as per the manufacturer's

instructions, supplied by Agilent Technologies, UK) and NZY⁺ medium replacing LB and appropriate antibiotic. A higher concentration of plasmid DNA (50ng per microlitre) was required.

2.3.5 Plasmid miniPrep

Plasmid mini-preparations were carried out using the GenElute Plasmid Mini-Prep Kit (Sigma, UK). Plasmid DNA was eluted in 100µl of molecular grade water. All plasmid DNA was stored at -20°C. An overnight suspension culture (3ml LB + appropriate antibiotic) of *E.coli* was purified by centrifugation and subsequent resuspension for lysis, neutralisation and washing, before elution.

2.3.6 Plasmid maxiPrep

Plasmid maxi-preparations were carried out using the GenElute Plasmid Maxi-Prep Kit (Sigma, UK). Plasmid DNA was eluted in 500µl of molecular grade water. All plasmid DNA was stored at -20°C. An overnight suspension culture (150ml of LB + appropriate antibiotic) of *E.coli* was purified by centrifugation and subsequent resuspension for lysis, neutralisation and washing, before elution.

2.3.7 Glycerol stocks

Starter cultures, those grown at 37°C for 6 hours in 3ml LB plus appropriate antibiotic, were combined with 3ml of 60% glycerol (Sigma, UK) to create a glycerol stock, which were stored at -80°C.

2.3.8 Restriction enzyme digestion of DNA

All restriction endonuclease (RE) digestion restrictions were carried out in accordance with the manufacturer's instructions (New England Biolabs and/or Promega, UK). Purified plasmid DNA was added to a reaction mixture containing 1µl of manufacturer's buffer, 1µg bovine serum albumen (BSA) (if

required), 0.5U RE and water to 10 μ l. Reactions were incubated at 37°C for 2 hours, followed by a 15 minute enzyme inactivation step at 65°C.

2.3.9 DNA sequencing

Plasmid DNA was purified by mini- or maxi-prep (sections 2.3.5 and 2.3.6 respectively), its concentration determined spectrophotometrically (via Nanodrop, section 2.2.4), diluted to 50ng/ μ l and submitted to Source BioScience, LifeSciences, UK, for bi-directional sequencing using the described oligonucleotide primers targeting the inserted sequence or utilising the T7 promoter sequences within the vector. This latter method allowed for sequencing across the cloning boundary, ensuring the full insert sequence was present and in the correct orientation.

2.4 SUBCLONING

2.4.1 Alkaline phosphatase treatment

Calf intestinal alkaline phosphatase (Promega, UK) catalyses the hydrolysis of 5'-phosphate groups from DNA and RNA. Post-RE digestion, plasmid DNA was treated with alkaline phosphatase to prevent recircularisation of linearised plasmid DNA without insert. Briefly, alkaline phosphatase was diluted in propriety reaction buffer to a final concentration of 0.01units/ μ l. Each picomole of DNA required 0.01U of alkaline phosphatase (1 μ g of 1000 bp DNA = 1.52pmol DNA = 3.03pmol of ends). Purified DNA was incubated with the aforementioned enzyme at 37°C for 30 minutes, after which another aliquot of diluted alkaline phosphatase was added and incubated at 37°C for 30 minutes. 300 μ l of propriety stop buffer was then added to the reaction, which was subsequently purified (section 2.3.1).

2.5 ANIMALS

All animal procedures were carried out in accordance with the UK Animals (Scientific Procedures) Act 1986 (under Project License PPL 40/3068 193b,

Personal License PIL 40/9973). All animal procedures were approved by the University of Nottingham Local Ethical Review Committee.

2.5.1 Siberian hamsters

Experimental Siberian hamsters (*Phodopus Sungorus*) were obtained from an in house colony, maintained at the University of Nottingham Biomedical Services Unit (BMU) (Ebling, 1994). All animals were housed at $20 \pm 2^{\circ}\text{C}$ and 40% humidity. Animals were fed ad libitum to a standard laboratory chow diet comprising 23% protein (3.17kj/g), 55% carbohydrate (7.59 kj/g), 22% fat (3.03kj/g) (Teklab no. 2019, Harlan Laboratories). Animals under long day (LD) conditions were housed in 16h light: 8h dark with lights off at 11:00 GMT, whereas those in short days (SD) conditions were exposed to 8h light: 16h dark with lights off maintained at 11:00 GMT. Body weight and food intake were measured three times a week. Pelage, on entry into SD, was measured once a week – scale 1-4 – where 4 represented a full summer LD brown coat and 1 represented a full winter (SD) white coat (Duncan and Goldman 1984).

2.5.2 C57BL/6J Mice

Experimental C57BL/6J male mice (*Mus musculus*) were supplied by the University of Nottingham BMU. They were maintained in individual cages under a 12:12 hr light/dark cycle (lights on 07:00) and controlled temperature ($21 \pm 1^{\circ}\text{C}$) with ad libitum access to food and water. The diet was a standard lab chow consisting of 19% protein, 45% carbohydrate and 9% fat (2019S Teklad Global diet, Harlan Laboratories) unless otherwise stated. Body weight and food intake were measured three times a week. The high fat diet (HFD), which was fed ad libitum, was a standard high fat diet comprising 20% protein (3.53 kj/g), 35% carbohydrate (6.18 kj/g) and 45% fat (7.95 kj/g) (D12451, New Brunswick, New Jersey, USA).

3 Chapter 3 – THE VGF DERIVED PEPTIDES HHPD-41 AND TLQP-21 HAVE DIFFERENTIAL EFFECTS ON FOOD INTAKE IN SIBERIAN HAMSTERS.

3.1 THE ROLE OF VGF IN THE REGULATION OF ENERGY HOMEOSTASIS

3.1.1 VGF null mouse

VGF was first implicated in the regulation of energy homeostasis following the development of C57BL/6 VGF^{-/-} mice, in which the VGF gene sequence was deleted via homologous recombination (Hahm et al., 1999). VGF^{-/-} mice were lean, hypermetabolic (with increased oxygen consumption and carbon dioxide production, VO₂ and VCO₂ respectively) and hyperactive, and despite significantly increased food intake had relatively low bodyweight compared to wild-type littermates (Hahm et al., 1999) (for a detailed discussion see section 1.4.4).

This prompted the hypothesis that VGF, and its derived peptides, play a non-redundant role in the regulation of energy homeostasis, that its derived peptides are anabolic and antagonism of the gene may constitute a basis for the treatment of obesity (Hahm et al., 1999). Furthermore, Hahm et al., (2002) reported that VGF^{-/-} mice were resistant to the development of obesity from selected environmental factors and genetic (see section 1.4.5).

3.2 VGF EXPRESSION IN ALTERED ENERGY BALANCE

3.2.1 In response to fasting

In neurones which synthesise NPY and AgRP in the ARC, VGF expression is induced by fasting in the mouse, rat and Siberian hamster, while decreased in the neurones which synthesise POMC, and the derived feeding peptide, α MSH (Hahm et al., 2002; Ross et al., 2005; Toshinai et al., 2010) (see section 1.4.6.1). Similarly, NPY is increased following a period of starvation, inducing hyperphagia; these increases however are attenuated by treatment with leptin (Stephens et al., 1995). In the mouse, the increase in VGF mRNA in response to fasting was attenuated by the administration of leptin (Hahm et al., 2002).

3.2.2 In response to season in the Siberian hamster

In the Siberian hamster, VGF mRNA was significantly increased in the winter catabolic state in the dmpARC, a region of the hypothalamus where a number of genes related to retinoic acid, histaminergic and serotonergic signalling (Barrett et al., 2005; Barrett et al., 2006; Ross et al., 2004) have been implicated in the change in body weight in response to season. However, expression of VGF across the remainder of the ARC was higher in LD (see section 1.4.6.2).

3.3 VGF POLYPEPTIDE

The VGF polypeptide is a 68kDa pro-peptide, selectively processed into multiple small peptides in a tissue specific manner in neuroendocrine and neuronal cells (Levi et al., 2004, see Figure 1.4.2 B) (for structure of the VGF polypeptide see section 1.3.2, for expression of the VGF derived peptides see section 1.4.3.2). VGF is localised and regulated in a manner benefiting a gene which controls energy homeostasis, and the studies presented in this chapter (and subsequent chapters) have been undertaken to further determine its action.

3.3.1 Roles of VGF derived peptides

3.3.1.1 TLQP-21

The proposed anabolic role for VGF and its derived peptides was not, however, supported by subsequent studies. Experiments with TLQP-21, a VGF derived peptide, demonstrated an opposing role in the regulation of food intake and energy expenditure in the Siberian hamster and mouse respectively (Bartolomucci et al., 2006; Jethwa et al., 2007) (see 1.3.6.3 AND Table 3.3.1.1). In rats, ICV infusion of TLQP-21 was demonstrated to decrease gastric emptying (Severini et al., 2009). A result which indicates that VGF derived peptides plays a central role in the regulation of gastric motor functions (see 1.3.6.3).

VGF	Method	Effects on food intake	Effects on body weight	Effects on energy expenditure	Effects on behaviour
VGF	VGF ^{-/-} mice (Hahm et al., 1999)	↑ (gram body weight)	↓	↑ VO ₂ consumption and VCO ₂ production	Hyperactive
TLQP-21	ICV infusion in mice (Bartolomucci et al., 2006)	Unaffected	Unaffected	↑ at rest	Unaffected
TLQP-21	ICV infusion in Siberian hamsters (Jethwa et al., 2007)	↓	↓	Unaffected	↓ meal size

Table 3.3.1.1: **The contrasting findings of VGF^{-/-} mice (Hahm et al., 1999) and subsequent ICV infusion studies with the VGF derived peptide TLQP-21 in mice (Bartolomucci et al., 2006) and Siberian hamsters (Jethwa et al., 2007).**

3.3.1.2 *Neuroendocrine regulatory peptide-1 and -2 (NERP-1 and -2)*

Neuroendocrine regulatory peptides (NERP) -1 and -2 are distinct regions of the neurosecretory protein VGF (Toshinai and Nakazato, 2009). They are a highly abundant species in the rat hypothalamus (Yamahuchi et al., 2007) and the magnocellular neurones of the SON and PVN. Furthermore, NERP-1 and -2 circulate in the human plasma (Toshinai and Nakazato, 2009) (see 1.3.6.4).

Therefore building upon the previous studies it was hypothesised that VGF derived peptides have opposing effects on energy homeostasis and possibly have alternative mechanisms of action. For example, TLQP-21 and HHPD-41 (which comprise the larger, and most abundant, VGF derived peptide TLQP-62) may act upon different subsets of neurones (or receptors) within the

hypothalamus. Global blockade of VGF, as observed in the VGF^{-/-} mouse, may obscure the particular actions of VGF derived peptides in specific brain areas or be detrimental to development. In order to investigate further the role of VGF and its derived peptides in the regulation of food intake, behaviour, and subsequently, body weight, we utilised the Siberian hamster (discussed in section 1.3.1) and HHPD-41, which is produced following the cleavage of TLQP-21 from the larger polypeptide TLQP-62.

3.4 AIMS AND OBJECTIVES

While the VGF^{-/-} mouse suggests that VGF acts as an anabolic signal (Hahm et al., 1999), data from subsequent studies utilising VGF derived peptides do not support this. Indeed the VGF derived peptide, TLQP-21, was reported to reduce food intake in Siberian hamsters (Jethwa et al., 2007), and increase energy expenditure in diet induced obese (DIO) mice (Bartolomucci et al., 2006), while decreasing gastric emptying in rats (Severini et al., 2009). It has been postulated that TLQP-21 induces satiety in the Siberian hamster, while it stimulates autonomic activation of the adrenal medulla and adipose tissues in the diet induce obese (DIO) mice (Bartolomucci et al., 2006; Jethwa et al., 2007). Despite these differences in mechanisms between species, the general sense is that TLQP-21 exerts an overall catabolic action. One possible explanation for the differences observed between the *in vivo* peptide studies and those in which all VGF production has been ablated may be due to the loss of multiple peptides from one large polypeptide which may have opposing effects. Indeed ghrelin and obestatin are produced from the same polypeptide but have opposing roles (Zhang et al., 2005). Thus the aim of the studies presented in this chapter was to determine the effects of the VGF derived peptide HHPD-41 on food intake, bodyweight and behaviour as well as utilising immunohistochemistry to determine sites of action of the two VGF derived peptides.

3.5 MATERIALS AND METHODS

3.5.1 Peptides

TLQP-21 was synthesised on an Applied Biosystems (Foster City, USA) model 433 synthesiser using FastMoc™ protocols, according to manufacturer's recommendations. All synthesis reagents were from Applied Biosystems or Novabiochem (Nottingham, UK). 5-carboxyfluorescein was coupled to the N-terminus of the resin bound peptide with no changes to the synthesis protocol. Cleavage and deprotection reactions were performed in trifluoroacetic acid (Applied Bioscience, Foster City, USA)/tri-isopropyl saline (Sigma, UK)/water (Fischer Biosciences, UK) in a ratio of 95:2.5:2.5 (v/v) at room temperature for 2 hours. The mouse amino acid sequence NH₂-TLQPPASSRRRHFFHALPPAR-OH was used. HHPD-41 was similarly synthesised and supplied by Bio-Synthesis Inc. (Lewisville, USA) using the amino acid sequence NH₂-HHPDLEAQARRAQEEADAEERRLQEQEELNYIEHVLLHRP-OH according to the mouse sequence.

3.5.2 Siberian hamsters

Details of the UK Animals (Scientific Procedures) Act 1986, Project and Personal Licenses can be found in section 2.5. Details of the experimental colony of Siberian hamsters can be found in section 2.5.1.

3.5.3 ICV Cannulation and infusion

Animal surgical procedures and handling were carried out as previously described (Jethwa et al., 2007; Schuhler et al., 2003; Schuhler et al., 2004; Stewart et al., 2003). Siberian hamsters were anaesthetised by an intraperitoneal (i.p.) injection of a mixture of ketamine (Vetalar 100mg/kg i.p., Forte Doge Animal Health Ltd, Southampton, UK) and medetomidine (Dormitor 1mg/kg i.p., Pfizer Ltd, Kent, UK) in a ratio of 1:4. While anaesthetised (prior to commencement of surgery) Siberian hamsters received a subcutaneous (s.c) injection of carprofen (Rimadyl 50mg/kg s.c., Pfizer, Kent, UK) to maintain

analgesia. Animals were placed in a stereotaxic frame (David-Kopf Instruments, supplied by Clark electromedical Instruments, Reading, UK) with the incisor bar positioned level with the interaural line. Using the sutures confluence bregma as a landmark, a small hole was drilled on midline. The dura mater was pierced just lateral to the mid-sagittal sinus and a permanent 22-gauge guide cannula (Plastic One VA, USA supplied by Bilaney Consultants Ltd, Sevenoaks, Kent, UK) was stereotactically implanted into the third ventricle 6.5mm below the surface of the dura after deflection of the superior midsagittal sinus. Two stainless steel screws (Fastenright Ltd, Wolverhampton, UK) were inserted into the cranium and the cannula was fixed to this using Permacem Smartmix refill (Henry Schein, Kent, UK). An obturator was inserted into the guide cannula to maintain patency. After surgery, the hamsters received a s.c. injection of atipamezole (Antisedan 1mg/kg s.c., Pfizer, Kent UK) to reverse the anaesthesia and were rehydrated by an i.p. injection of 0.9% sodium chloride (0.5ml/hamster). The surgically-prepared hamsters were allowed a seven day recovery period during which they were handled on a daily basis and received daily s.c. injection of analgesia (Rimadyl 50mg/kg, s.c., Pfizer, Kent, UK) and had access to a palatable diet consisting of soaked Teklab diet (see section 2.5.1) supplemented with a sunflower seed. Hamsters were habituated to the experimental process by a control vehicle infusion (1 μ l of 0.9 % saline) prior to the onset of the study. Studies on the same set of animals were performed with a minimum of seven days between study days as a wash out period.

All infusions (1 μ l total volume) were performed on conscious, free-moving hamsters. Substances were administered via a stainless steel injector (Plastic One VA, USA supplied by Bilaney Consultants Ltd, Kent, UK) placed in the cannula with the tip of the injector projecting 0.5mm below the cannula. The injector was connected by polyethylene tubing (inside diameter 0.1mm; outside diameter 0.5mm) to a 10 μ l Hamilton Syringe gas-tight syringe (VWR, Leicestershire, UK) set to dispense at a rate of 1 μ l/min. The tubing was filled with saline and a 1 μ l air bubble was drawn up to separate the saline and the

test substance. All substances were dissolved in 0.9% saline and administered in a volume of 1µl. The injection was given over 1 minute and the injector kept in position for a further 3 minutes to ensure diffusion. The cannula stylet was replaced immediately after withdrawal of the infusion cannula and the animals were returned to their home cages.

3.5.4 Palatable diet

Before infusion, lab chow was removed from the hopper and replaced by a pre-weighed amount of palatable diet (soaked Teklab diet) inside the home cage. To estimate the reduction in weight of the test meal through water evaporation, three pre-weighed dishes also containing wet Teklab diet pellets were placed in control cages alongside the experimental hamster cages. The calculation of the food intake at any given time by each hamster included the deduction of the average evaporation of water of the three control cages.

3.5.5 Determining the optimum working dose of HHPD-41

Previously, ICV infusion of 5 and 25µg of TLQP-21 was shown to reduce food intake and body weight in Siberian hamsters (Jethwa et al., 2007). To determine the working dose for HHPD-41, male Siberian hamsters (n = 4) received either a single infusion of saline or the VGF-derived peptide HHPD-41 (5 or 25 µg) in a pseudorandom order so that each animal acted as its own control over the course of 4 weeks. Infusions were carried out shortly before light outs (1100 h). Following the infusion, hamsters were observed in their home cages and offered a pre-weighed amount of the palatable diet. Food was re-weighed at 1, 2, 4, 6 and 24 hour post-infusion, while body weight was measured 24 hours post infusion using a Fisher Scientific FP-300 series balance (Fisher Scientific Ltd, Leicester, UK). On each experimental occasion, the behaviour of each hamster was monitored in its home cage for 5 seconds in every minute for one hour after lights off. Behaviour was classified into 5 categories - feeding, locomotion, grooming, drinking and inactive (definitions are based on Halford et al., 1998) - in this study (Table 3.5.5).

Behaviour	Description
Feeding	Observed to be investigating / eating the test meal of palatable chow
Drinking	hamster at / drinking from water bottle
Grooming	hamster grooming
Locomotion	ambulatory, climbing on cage bars, burrowing, rearing
Inactive	hamster at rest /sleeping

Table 3.5.5: **The five behavioural categories of the Siberian hamster used in this study.** Behaviour as defined by Halford et al., (1998), were scored, as described in 3.5.5.

3.5.6 The effects of ICV infusion of HHPD-41 on food intake, bodyweight and behaviour

Once a working dose of HHPD-41 was established, a second group of Siberian hamsters (n = 8) received either a single infusion of saline, the VGF derived peptide HHPD-41 (5µg) or TLQP-21 (5µg) in a pseudorandom order, so that each animal acted as its own control over the course of 3 weeks. Food intake was monitored as previously described.

3.5.7 Investigating the site of action of HHPA-41 and TLQP-21

At the onset of the dark phase, Siberian hamsters were euthanized by injection of pentobarbital sodium (Euthantal; Rhone Merieux, UK) and transcardially perfused with 0.01M phosphate buffered saline (PBS) (pH 7.2), followed by 4% paraformaldehyde in 0.1M PBS (pH 7.2). The skull was removed and the frontal lobes lifted to reveal the optic chiasma. The optic chiasma nerves were cut and the whole brain was immediately removed and placed in 4% paraformaldehyde overnight and then washed and stored in to 0.01M PBS. The dorsal section of the brain was notched for the purposes of identification/orientation and the brain mounted on a platform using phosphazene base P₄-t-optimal cutting

temperature (OCT) (Sigma, UK) with the optic nerve facing the blade. Twenty micrometer sections were cut using a freezing microtome from the optic nerve/chiasm through to the substantia nigra. Sections were stored in anti-freeze at -20°C. For immunohistochemistry, free floating sections (20 µm thick) were immersed in blocking solution (1% wt/vol bovine serum albumin (BSA), 0.2% Triton X in PBS) for 1 hour at room temperature. Sections were incubated overnight at 4°C with the primary antibody DCH-1 (1: 4000, buffer; 0.5 g BSA in 50 ml PBS, 150 µl Triton X, 0.01% sodium azide). Sections were subsequently incubated with biotinylated anti-rabbit IgG antibody (0.5g BSA in 167ml PBS, 167µl Triton X, 1:4000 antibody) for 1 hour at room temperature, followed by incubation with Avidin-Biotin (0.5 g BSA in 167 ml PBS, 167 µl Triton X, 1:4000 antibody) for 1 hour at room temperature. The sections were washed twice with 0.01M PBS before reaction with 3,3'-diaminobenzidine (DAB) solution (10 mg DAB in 20 ml PBS, 6.6 µl 30% H₂O₂) for 5 minutes at room temperature. The sections were washed twice in PBS before being mounted on slides, air dried, dehydrated with ethanol and histoclear before coverslipped with DPX (Sigma, UK). Brain sections were always stained in groups containing sections of each treatment, so that intra-assay variation would not cause systematic group differences. We investigated different hypothalamic nuclei identified on the basis of the stereotaxic mouse brain atlas: ARC, dmpARC, PVN, DMN and VMN. We selected these sites because their involvement in food intake has been established (Olszewski et al., 2008). Pictures from slices were obtained by optic microscope then transferred to a PC for image capture, using the Image Pro 4 software.

3.5.8 Statistics

GenStat (14th Edition, VSN International, London, UK) was used to determine the sample size for the *in vivo* experimentation. The software calculates the power (probability of detection) and the replication (sample size) required to detect an effect of treatment. In these studies, each animal acted as its own control to reduce the impact of inter-subject variability and to reduce the total

number of animals required to achieve the objective of the study. Power analyses are not considered suitable to assess group sizes for studies with a repeated measure design (Rosner, 2006). However, by assuming that the treatment groups were independent, and that HHPD-41 would produce a similar effect as TLQP-21, and if we desire a level of significance to be at least 5% (p equal to or less than 0.05) and a power of 80%, using the software a minimum group size of 4 is required for the dose response study and 8 in the acute study.

Descriptive statistics (means and standard error mean (SEM)) were generated using PRISM (Prism 6.0, GraphPad, San Diego, USA). Body weight and home cage food intake data were analysed using one way analysis of variance (ANOVA) with repeated measures and Bonferroni tests for post-hoc comparisons (Prism 6.0, GraphPad) unless otherwise stated. Data from the behavioural observations were compared using the non-parametric Kruskal-Wallis test.

3.6 RESULTS

3.6.1 Determining the optimum working dose of HHPD-41

The ICV infusion of HHPD-41 at the onset of the dark phase dose-dependently increased food intake 1 hour post infusion [0-1 h; saline, $0.22 \pm 0.06\text{g}$; HHPD-41 $5\mu\text{g}$, $1.03 \pm 0.30\text{g}$; HHPD-41 $25\mu\text{g}$, $1.28 \pm 0.30\text{g}$] (one way ANOVA $F = 4.44$, $p < 0.05$ vs. saline] (see Figure 3.6.1. A). However, this effect of increased food intake did not persist beyond this time point. There was a trend towards a suppressive effect of HHPD-41 at 6-24 hours (see Figure 3.6.1. E) [6-24h; saline, $5.64 \pm 1.83\text{g}$; HHPD-41 $5\mu\text{g}$, $1.18 \pm 0.82\text{g}$; HHPD-41 $25\mu\text{g}$, $1.44 \pm 0.24\text{g}$] (one way ANOVA $F = 2.91$, $p = 0.09$). When the data for the entire 24 hour period post infusion was summated, a significant suppressive effect of HHPD-41 was apparent [0-24h; saline, $7.06 \pm 2.27\text{g}$; HHPD-41 $5\mu\text{g}$, $2.41 \pm 1.21\text{g}$; HHPD-41 $25\mu\text{g}$, $4.03 \pm 1.67\text{g}$] (two way ANOVA repeated measures, interaction $F = 3.50$, $p < 0.01$) (see Figure 3.6.1. F). However, there was no effect on bodyweight over the 24 hour period (one way ANOVA $F = 2.68$, $p = 0.11$) (see Figure 3.6.1. F).

The number of observations made for each defined behaviour was calculated and expressed as a percentage of the total number of observations in 1 hour post infusion of HHPD-41 or saline into the third ventricle. No sedation or hyperactivity was observed after ICV infusion of the VGF derived peptide HHPD-41 (5 or $25\mu\text{g}$) when compared to saline controls. Despite the increase in food intake in the first hour after 5 and $25\mu\text{g}$ HHPD-41 infusion, there was no significant difference in the proportion of time that the hamsters were observed to be investigating or eating the test meal. There were no adverse behaviours observed in any group (see Figure 3.6.1 H).

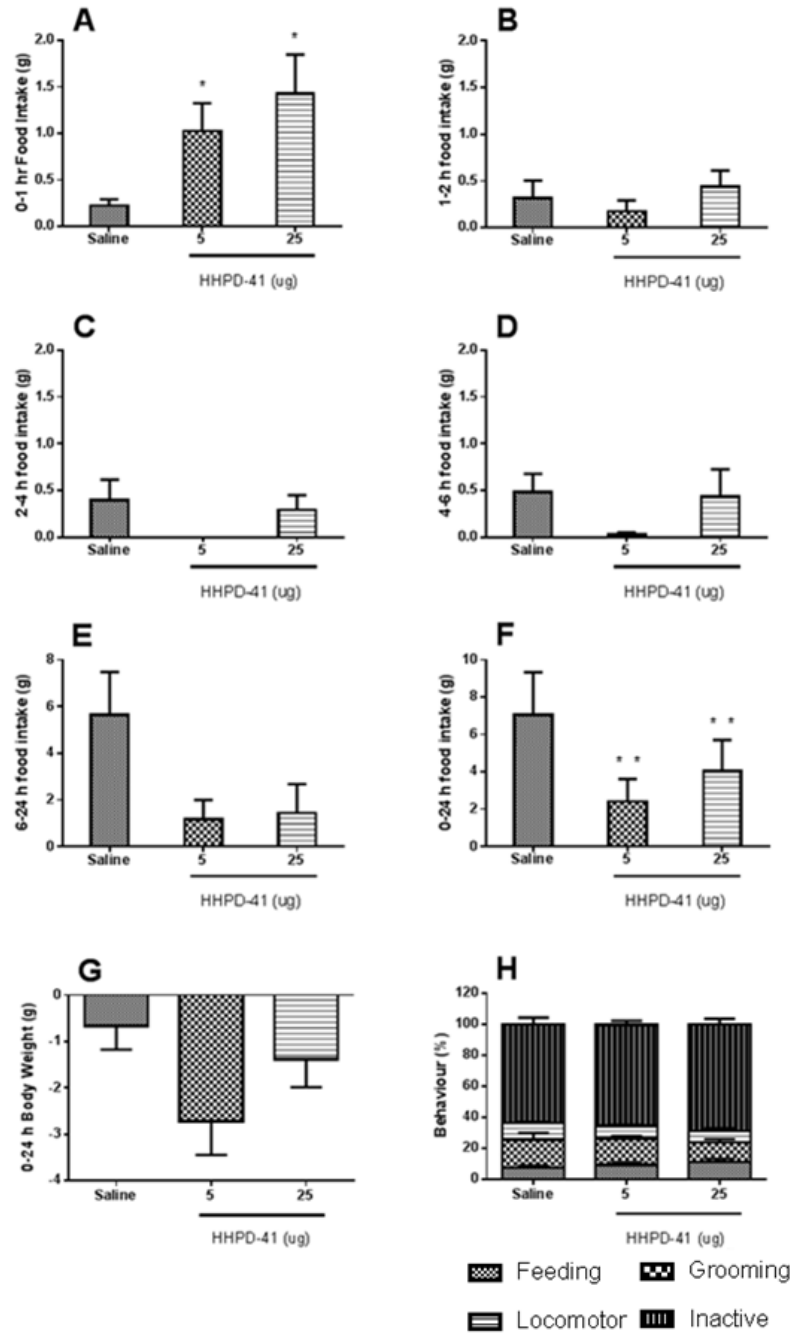


Figure 3.6.1: **Effects of acute ICV infusion of the VGF derived peptide HHPD-41 on food intake, body weight and behaviour.** *Ad libitum* fed male Siberian hamsters received a single 1 µl ICV infusion of either saline or HHPD-41 (5 or 25 µg) in a pseudorandom order so that each animal acted as its own control. Food intake was measured 0-1 h (A), 1-2 h (B), 2-4 h (C), 4-6 h (D), 6-24 h (E) and 0-24 h (F) post infusion. Body weight was measured 24 hours post infusion (G). Behaviour was measured 1 hour post infusion (H), as defined by Halford et al., (1998). Bars are expressed as mean + SEM (n =4). Significance values are as indicated * p < 0.05, **p < 0.01.

3.6.2 The effects of ICV infusion of HHPD-41 on food intake and bodyweight

The ICV infusion of HHPD-41, at the onset of the dark phase, significantly increased food intake 1 hour post infusion in Siberian hamsters [0-1h; saline, 0.36 ± 0.07 g; HHPD-41 $5\mu\text{g}$, 0.99 ± 0.22 g $p < 0.05$ vs. saline; TLQP-21 $5\mu\text{g}$, 0.46 ± 0.12 g $p < \text{ns}$ vs. saline] (see Figure 3.6.2. A). However, this effect did not persist beyond this time point, where treated animals consistently ate less than saline treated animals (see Figure 3.6.2. B-D). There was a significant suppressive effect of HHPD-41 at 6-24 hours [6-24h; saline, 10.19 ± 1.92 g; HHPD-41 $5\mu\text{g}$, 5.09 ± 1.15 g; TLQP-21 $5\mu\text{g}$, 5.30 ± 1.05 g] (one way ANOVA $F = 4.09$, $p < 0.05$) (see Figure 3.6.2. E). When the data for the entire 24 hour period post infusion was aggregated, there was a significant suppressive effect of HHPD-41, was once more apparent [0-24h; saline, 13.58 ± 2.32 g; HHPD-41 $5\mu\text{g}$, 8.91 ± 1.03 g; TLQP-21 $5\mu\text{g}$, 8.03 ± 0.80 g] (one way ANOVA $F = 7.78$, $p < 0.05$) (see Figure 3.6.2. F). This was also true for TLQP-21 (one way ANOVA $F = 8.45$, $p < 0.04$) (see Figure 3.6.2. F). However, food intake from the hopper 24 hours post infusion in HHPD-41 treated Siberian hamsters was akin to that of controls (24-48 h; saline 3.99 ± 0.33 g; HHPD-41 3.48 ± 0.47 g; TLQP-21 3.75 ± 0.21 g; $p = 0.48$). The ICV infusion of HHPD-41 at the onset of the dark phase had no effect on body weight (one way ANOVA $F = 2.68$, $p = 0.64$) (see Figure 3.6.2. G).

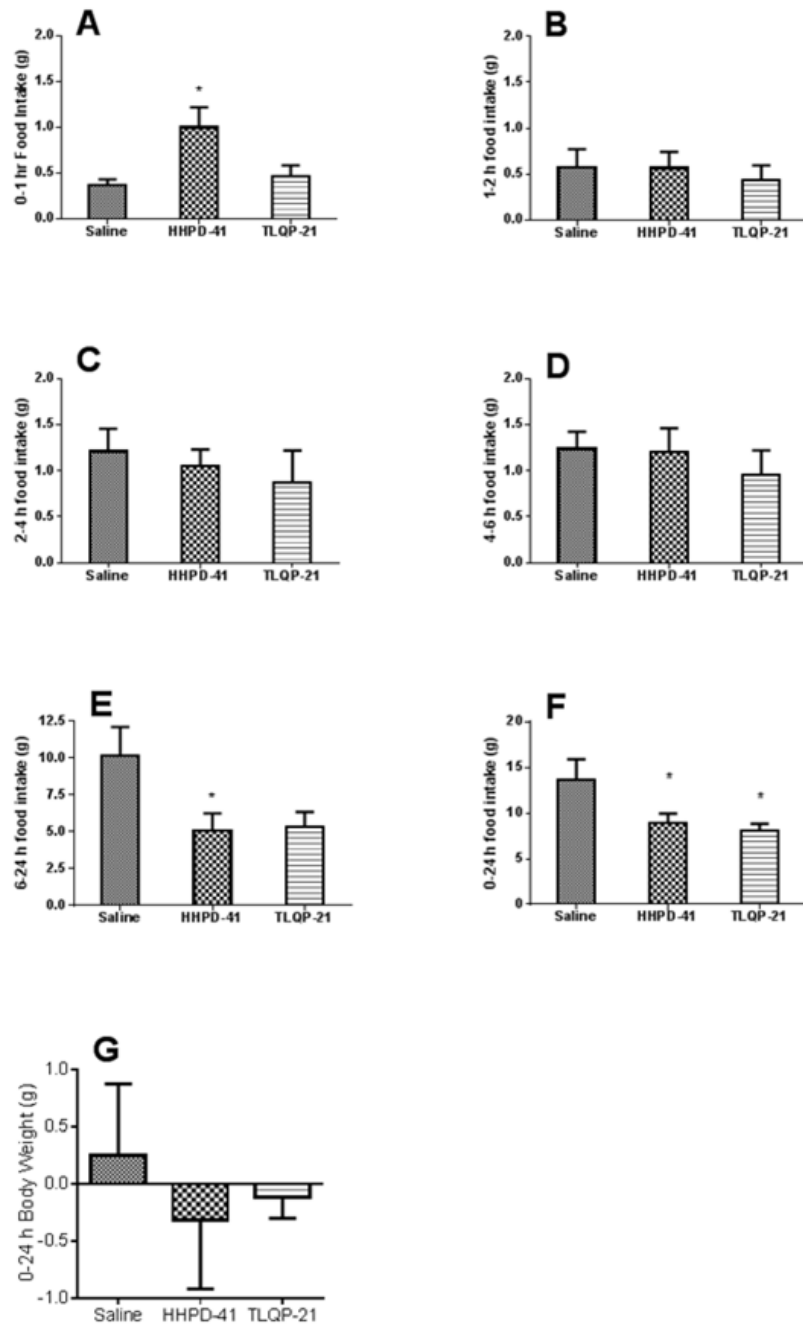


Figure 3.6.2: **Effects of acute ICV infusion of the VGF derived peptides HHPD-41 and TLQP-21 on food intake.** *Ad libitum* fed male Siberian hamsters received a single 1 μ l ICV infusion of either saline, HHPD-41 or TLQP-21 (5 μ g) in a pseudorandom order so that each animal acted as its own control. Food intake was measured 0-1 h (A), 1-2 h (B), 2-4 h (C), 4-6 h (D), 6-24 h (E) and 0-24 h (F) post infusion. Body weight was measured 24 hours post infusion (G). Bars are expressed as mean + SEM. Significance values are as indicated: *, p < 0.05 (n =8).

3.6.3 c-Fos

Immunohistochemistry for *c-fos*, a marker of neuronal activation, revealed HHPD-41 and TLQP-21 increased FOS immunoreactivity in the arcuate nucleus (ARC), paraventricular nucleus (PVN) (see Figure 3.6.3) and ventromedial hypothalamic nucleus (VMN) when compared to saline treated controls. Furthermore *c-fos* is increased in the area referred to as the dorsomedial posterior ARC (dmpARC) (Morgan et al., 2006). However, there was no discernible difference following infusion of HHPD-41 or TLQP-21.

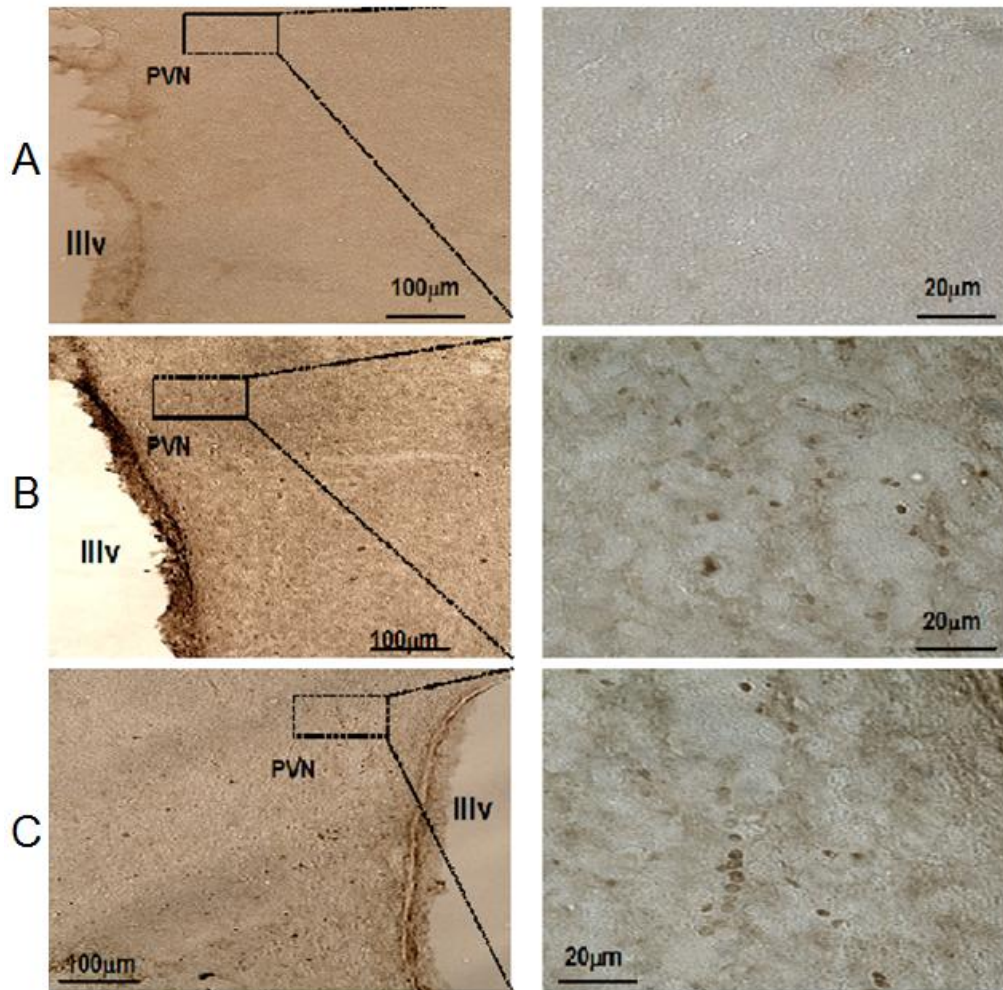


Figure 3.6.3: **Neuronal activation, indicated by *c-fos* expression, in the PVN of Siberian hamsters treated with saline (A), HHPD-41 (B) or TLQP-21 (C).** Immunohistochemistry on perfused LD Siberian hamster brain sections with a *c-Fos* antibody (dark brown) in the region of the PVN. Expression was increased in Siberian hamsters treated with the VGF derived peptides HHPD-41 and TLQP-21 versus saline control. However, no discernible difference in expression was observed following infusion of HHPD-41 or TLQP-21. Scale bars (100 and 20µm respectively).

3.7 DISCUSSION

VGF was first implicated in the regulation of energy homeostasis through the target deletion of VGF gene in mice (Hahm et al., 1999). These mice were lean, hypermetabolic, hyperactive and had altered hypothalamic peptides in the arcuate nucleus, suggesting an anabolic role for VGF (Hahm et al., 1999). However studies following the administration of VGF derived peptides TLQP-21 in mice and Siberian hamsters demonstrated a general catabolic effect (Bartolomucci et al., 2006; Jethwa et al., 2007) – TLQP-21 decreased food intake in Siberian hamsters and prevented DIO in mice by increasing resting energy expenditure. Thus to further characterise the role of VGF derived peptides in the regulation of energy homeostasis the studies in this chapter investigated the acute action of HHPD-41. This peptide is the product of cleavage of TLQP-62, the most abundant of the VGF derived peptides, which yields TLQP-21 and HHPD-41 (Bartolomucci et al., 2007). The principal findings of the studies presented in this chapter were that single infusions of HHPD-41 in the Siberian hamster significantly increased food intake 0-1 hour post infusion in a dose dependent manner, whilst decreasing food intake overall 6-24 hours post infusion. This, however, did not affect bodyweight and nor did it effect behaviour. There was observed increased c-Fos immunoreactivity in the arcuate nucleus (ARC), paraventricular nucleus (PVN), ventromedial nucleus (VMN) and dorsomedial posterior arcuate nucleus (dmpARC) following treatment with the VGF derived peptides HHPD-41 and TLQP-21. There was, however, no discernible difference between the activation of c-Fos in the aforementioned nuclei and peptide infusion.

The initial (0-1hr) effects on food intake following HHPD-41 infusion opposed the effects of acute TLQP-21 infusion, which dose dependently decreased food intake (Jethwa et al., 2007). However, food intake was reduced 6-24hrs in Siberian hamsters post infusion of HHPD-41, akin to the reduction observed following TLQP-21 infusion. In the Jethwa et al., (2007), study chronic infusion of TLQP-21 produced a sustained and additive reduction in food intake (56%

compared to controls) so that body weight was reduced. Jethwa et al., (2007), reported that decreased food intake was not a reflection in a decrease in the number or frequency of meals but by a decrease in food intake per feeding bout, inferring a more rapid achievement of the state of satiation. A similar effect of HHPD-41 was observed in the studies reported in this chapter. The increased food intake induced by HHPD-41 was not a reflection of increased time spent investigating the test meal 1 hour post infusion. However, given that food intake during this initial period is increased, the studies presented in this chapter suggest that food intake per feeding bout was likely to be increased.

The data presented in this chapter, along with data published by Toshinai et al., (2010), suggests the VGF derived peptides have opposing roles in food intake. Toshinai et al., (2010) demonstrated that in rats NERP-2, an N terminal VGF derived peptide, colocalises with the orexins, which stimulate feeding behaviour and enhance energy expenditure via stimulation of the sympathetic nerve, in the LHA. ICV infusion of NERP-2 increased food intake in rats. Much like HHPD-41, NERP-2 dose dependently increased food intake 1 hour post ICV infusion (Toshinai et al., 2010). Treatment with an anti-NERP-2 immunoglobulin G (IgG) decreased food intake (Toshinai et al., 2010). In addition, NERP-2 increased body temperature, oxygen consumption and locomotor activity in rats, similar to the results of Bartolomucci et al., (2006) where ICV infusion of TLQP-21 increased resting energy expenditure and rectal temperature in mice. Furthermore, NERP-2 did not increase food intake or locomotor activity in orexin-deficient mice (Toshinai et al., 2010). Much like TLQP-21 in Siberian hamsters, injection of NERP-2 i.p. in rats did not affect food intake.

Similar to HHPD-41 and NERP-2, NPY is an orexigenic neuropeptide, produced in the ARC of the hypothalamus. Applied centrally, NPY stimulates food intake in rats and mice (Clark et al., 1984; Morley et al., 1987). Furthermore, NPY gene expression increases with food deprivation in rats and in Siberian hamsters

(Bradey et al., 1990; Mercer et al., 2000), similar to VGF mRNA in the mouse and rat (Hahm et al., 1999; Toshinai et al., 2010). ICV infusion of NPY in Siberian hamsters significantly increases food intake 30 minutes post injection, an effect which does not persist beyond 2 hours post infusion (Boss-Williams and Bartness, 1996). A similar initial effect is seen in the HHPD-41 studies presented in this chapter. Similarly AgRP, an endogenous antagonist of the MC3/4R, is up-regulated in response to fasting in the Siberian hamster (Mercer et al., 2000). Whilst ICV infusion of AgRP significantly increased food intake, 1 hour post infusion (Day and Bartness, 2004); a similar effect has been observed in rats and mice (Hagan et al., 2000; Marsh et al., 1999). The studies presented in this chapter identify HHPD-41 as a novel peptide involved in the hypothalamic regulation of food intake.

The studies reported in this chapter also demonstrated infusion of HHPD-41 in the Siberian hamster did not affect body weight significantly. ICV infusion of TLQP-21 reduced body weight in the Siberian hamsters (Jethwa et al., 2007), while body weight gain was attenuated in mice fed a HFD receiving ICV infusions of TLQP-21 (Bartolomucci et al., 2006). The results presented in this chapter suggest that the initial increase in food intake (0-1hr) offsets the subsequent decrease (6-24hrs), and given that food intake is normalised 24-48 hours post infusion, the changes are not substantial enough to bring out a significant change in body weight. Furthermore, infusion of the VGF derived peptide HHPD-41 does not significantly alter behaviour in the Siberian hamster 1 hour post infusion, despite significant increases in food intake. A similar result was observed by Jethwa et al., (2007) following ICV infusion of TLQP-21; despite significantly reduced food intake, there was no significant difference in behaviour.

The rapid and transient induction of the immediate early gene c-Fos in response to diverse pharmacological and physiological stimuli can be utilised

to produce high-resolution maps of cellular activation in the CNS (Sundquist & Nisenbaum 2005). Hahm et al., (1999), demonstrated an increase in VGF mRNA in the ARC of fasted mice. Whilst Toshinai et al., (2010) demonstrated that vgf mRNA levels are up-regulated in the rat LHA upon food deprivation; post-feeding these levels return to a basal level of expression (Toshinai et al., 2010). The studies presented in this chapter demonstrated HHPD-41 and TLQP-21 increased c-Fos immunoreactivity in the ARC, PVN, dmpARC and VMN in comparison to saline controls, areas of the brain whose involvement in food intake has been established (Olszewski et al., 2009). However, there was no discernible difference following infusion of the two VGF derived peptides. From this, the results presented in this chapter infer that VGF and its derived peptides have similar sites of action within the brain. However, given their opposing initial (0-1hr) effect on food intake, this further supports the hypothesis that VGF derived peptides have different receptors/mechanisms of action within hypothalamic nuclei.

Previously TLQP-21 has been shown to bind to adipocyte membranes in a saturable manner (Possenti et al., 2012), and atomic force microscopy of living cells revealed the existence of a single class of binding sites for TLQP-21 (Cassina et al., 2013). Taken together, these results suggested a cell surface receptor for TLQP-21. Recently, however, two possible receptors have been identified for the VGF derived peptide TLQP-21. Chen et al., (2013) identified gC1qR as the receptor for TLQP-21. TLQP-21 activated rat macrophages through gC1qR, and activated macrophages caused mechanical hypersensitivity in rats. gC1qR protein was expressed by both brain and spinal cord derived microglia (Chen et al., 2013). This receptor is indispensable for adipogenesis and insulin signalling (Kim et al., 2009). Furthermore, obese mice fed on a high fat diet (HFD) showed increased density of TLQP-21 binding in adipose tissues (Cassina et al., 2013). However in their experimental model neither TLQP-62 nor LQEQ-19 elicited a response, both of which had been previously implicated in pain processing (Moss et al., 2008 and Riedl et al.,

2009). This further supports the hypothesis of different receptors for the VGF derived peptides. Hannedouche et al., (2013) reported the complement receptor C3AR1 as a receptor for TLQP-21. The measurement of a G protein-coupled receptor (GPCR), namely the complement C3a receptor-1 (C3AR1), mediated activity for TLQP-21 in two different rodent cell lines (Hannedouche et al., 2013). C3AR1 was originally thought to be restricted to the innate immune response, its role limited to the complement cascade. However, it has subsequently been shown to have a role in cancer (Opstal-van Winden et al., 2012), neurogenesis (Klos et al., 2009) and hormone release from the pituitary gland (Francis et al., 2003). However, *C3AR1*^{-/-} mice are transiently resistant to diet-induced obesity and are protected against HFD-induced insulin resistance (Mamane et al., 2009).

Adiponectin, an adipocyte-derived hormone, regulates glucose and lipid metabolism and binds to two different seven-transmembrane domain receptors, namely AdipoR1 and AdipoR2 (Bjursell et al., 2007). Knockout mouse models indicate that the receptors, whilst both involved in energy metabolism, have opposing effects – *AdipoR1*^{-/-} display increased adiposity, reduced glucose tolerance, locomotor activity and energy expenditure, while *AdipoR2*^{-/-} were lean and resistant to diet induced obesity, with increased locomotor activity and energy expenditure (Bjursell et al., 2007). Given the initial opposing roles of the VGF derived peptides in food intake in the Siberian hamster, and the recent data by Chen et al., (2013) and Hannedouche et al., (2013), which identify two different receptors for TLQP-21 which fail to respond to other VGF-derived peptides, the studies of this chapter suggest a similar scenario. Taken with the results presented in this chapter, the VGF derived peptides, while possessing similar sites of action (albeit with opposing initial functions) possibly have different receptors. The proposed site-specific action of VGF derived peptides may also be time-specific. Sadari et al., (2014) reported that VGF expression in the ARC depends on the nutritional status of the animal. Food deprivation induces VGF expression in the NPY neurones, while VGF expression

is increased in POMC neurones in ad libitum fed and fasted-refed animals. However, there is no data available indicating the peptide ratio within these neurones under different feeding conditions. It is proposed that HHPD-41 peptide expression is increased in the NPY/AgRP neurones of the ARC, initiating food intake. The VGF derived peptide HHPD-41 may be rapidly 'turned over' or has a relatively short half life.

Tschop et al., (2001) implicated ghrelin in the regulation of food intake and energy homeostasis in mice and rats. Ghrelin increases pre-prandial and decreases post-prandial (Kolk et al., 2007), akin to VGF expression in the hypothalamus (Hahm et al., 1999; Saderi et al., 2014). The effects of gherlin are mediated by the hypothalamus; ghrelin attenuates leptin-induced reduction in food intake and subsequently body weight by inducing the expression of the orexigenic NPY and AgRP and inhibiting POMC neurones. Similar to ghrelin, HHPD-41 may play a role in meal initiation. The rapid increase in food intake 1 hour post infusion of HHPD-41, which does not persist, is characteristic of an appetite-stimulatory signal. The ghrelin gene also encodes obestatin, which has opposing effects on food intake (Zhang et al., 2005). Asakawa et al., (2005) demonstrated that ghrelin stimulated gastric emptying in mice, a finding which was substantiated in humans (Paik et al., 2004). VGF also regulates gastric emptying however, ICV infusion of TLQP-21 significantly decreased its rate in rats (Severini et al., 2009).

The data presented in this chapter, in conjunction with the Toshinai et al., (2010) data further supports the hypothesis that VGF and its derived peptides have opposing actions on food intake. Furthermore it suggests that VGF is a modulator/amplifier of the metabolic state of the animal – NPY neurones, which are challenged by energy depletion, increase VGF gene expression, possibly favouring the orexigenic peptides NERP-2 and HHPD-41. While POMC neurones, which are active when the energy homeostasis is positive, increase

VGF gene expression (in ad libitum and re-fed animals), favouring the catabolic peptide TLQP-21. Deficiency in prohormone convertase 1/3, which plays a pivotal role in the activation of biologically inactive hormones and cleaves the VGF pro-peptide, has been linked to monogenic forms of obesity (Bandsma et al., 2013). Patients with the deficiency suffer from congenital severe diarrhoea, association with malabsorption, which improves with age, at which point, hyperphagia and excessive weight gain (BMI > 97th percentile) becomes the predominant phenotype (Bandsma et al., 2013). However, given the battery of hormones prohormone convertases act upon, including GLP-1, it is impossible to attribute the effects of this complex phenotype to one hormonal deficiency.

3.8 CONCLUSION

The identification of HHPD-41 as a peptide involved in the hypothalamic regulation of feeding provides further insight into the neuronal network underlying the regulation of energy homeostasis. ICV infusion of the VGF derived peptide HHPD-41 at the onset of the dark phase dose-dependently increased food intake. This effect occurred within 1 hour post infusion compared to saline treated hamsters and was similar to ICV infusion of NERP-2, an N terminal VGF derived peptide, in rats. However, this effect did not persist beyond this time point, where treated animals consistently ate significantly less than saline controls (6-24 hrs). Behaviour and body weight remained unchanged by HHPD-41 infusion. The differences between the observations in the VGF^{-/-} mouse and the administration of TLQP-21 and HHPD-41 appear to be a result of the opposing effects of the VGF derived peptides. Immunohistochemistry studies revealed that HHPD-41 and TLQP-21 increased c-Fos activity in the Arc, PVN and VMN, as well as the dmPFC and DMN, areas of the brain implicated in the regulation of food intake. However, there is no discernible difference in the site of action following infusion of HHPD-41 or TLQP-21 from which we infer the VGF derived peptides TLQP-21 and HHPD-41 have different receptors.

**4 Chapter 4 – CENTRAL OVER-EXPRESSION OF VGF USING
A RECOMBINANT ADENO-ASSOCIATED VIRUS
INCREASES FOOD INTAKE AND ENERGY EXPENDITURE
IN THE SIBERIAN HAMSTER AND MOUSE**

4.1 INTRODUCTION

Viruses represent a highly evolved natural vector for the transfer of foreign DNA into cells (Kay et al., 2001). Adeno-associated virus (AAV) is a human parovirus, initially discovered as a contaminant in an adenovirus preparation (Atchison and Hammon, 1965). It has emerged as an attractive vector system for gene therapy for its potential to persistently express the transgene following integration (Ren et al., 2010). Furthermore, AAV is a non-pathogenic virus able to transduce a variety of host cells and tissues (Gao et al., 2005). This is without severe immune responses (Mandel et al., 2006). The AAV capsid is responsible for cell binding, internalization and trafficking within the target tissue or cell (Van Vliet et al., 2008); AAV is classified on the basis of its viral capsid and there are several natural serotypes, pseudotyped vectors and chimeric capsids currently used in gene transfer studies. For example, AAV-1 and -5 have high transduction efficiency in skeletal muscle, retina and pancreatic islets, as well as the liver (Chang et al., 2003; Chiorini et al., 1999; Loiler et al., 2003). However, of the serotypes, AAV-2 is the most studied (Wu et al., 2006). AAV-2 vectors have been delivered to many different organs, for example, the CNS, liver, lung and muscle by *in vivo* administration and have been shown to efficiently transduce non-dividing cells (Miao et al., 2000). rAAV-2 has been shown to transduce neuronal tissues and cells in the rat (Zhang et al., 2009), SH-SY5Y cells and the mouse striatum (Ren et al., 2010). rAAV-2 is currently in use for the treatment of Parkinson's disease and inherited diseases such as Batten's and Canavan's disease (Mingozzi and High, 2011). Clinical trials using rAAV for the treatment of cystic fibrosis and muscular dystrophy are currently on-going, with early evidence of gene transfer and expression of human clotting factor IX in haemophilia B patients (Patel et al., 2014).

4.1.1 rAAV and energy homeostasis

In order to study the role of neuropeptides in the regulation of energy homeostasis numerous studies have utilised rAAV expressing a gene of interest compared to controls injected with rAAV encoding enhanced green fluorescent

protein (eGFP). In separate experiments, rAAV over-expression of AgRP and NPY in the PVN and LHA increase food intake and body weight gain (see Table 4.1.1). Furthermore, AAV-mediated transfer of the leptin receptor improves the obese phenotype of Koletsky (f/f) rats, which have a gene mutation in the leptin receptor (OB-Rb) (Keen-Rhinehart et al., 2005). rAAV-2 was utilised to knockdown the MC4R in the PVN in rats resulting in high fat diet induced hyperphagia and obesity (Garza et al., 2008). rAAV has been previously used to over-express the AgRP gene in Siberian hamsters, resulting in a significant increase in food take and body weight, in combination with a decrease in energy expenditure (Jethwa et al., 2010). The use of AAV is therefore an effective strategy for manipulating gene expression in nonstandard laboratory species where the generation of transgenic lines is not feasible (Lim et al., 2004; Ross et al., 2009). rAAV vectors transduce more cells than lentiviral (LV) vectors in the rodent hypothalamus and amygdala (de Backer et al., 2010).

Day 40/48	PVN-AgRP	PVN-NPY	LHA-AgRP	LHA-NPY
Body weight gain	↑ 80%	↑ 67%	↑ 80%	↑ 127%
% Fat	↑	↑	↑	↑
Food Intake	↑	↑ L	↑	↑ L
Meal size	↑	-	↑	↑
Meal frequency	↑ L	-	-	-
Body temperature	↓ D	↓ D	-	↓ D
Locomotor activity	↓ D	↓ D	-	↓ D

Table 4.1.1: **Comparison of the feeding and metabolic parameters affected by over-expression of AgRP and NPY in the PVN and LHA respectively.** ↑ increased by over-expression; ↓ decreased by over-expression. % increase in body weight compared to controls at the end of the experimental period (40/48 days). L light phase; D dark phase. Adapted from de Backer et al., 2011.

4.2 THE VIRAL 2A PEPTIDE; A SUITABLE ALTERNATIVE TO THE INTERNAL RIBOSOME ENTRY SITE (ires)

The use of transgenic animals is increasing in biomedical research – over-expression or silencing is accompanied by the expression of a co-transgene in the form of a reporter, often fluorescent in nature. Previous methods relied upon a mixture of AAV-transgene and AAV-GFP (Gardiner et al., 2005). The current method for bicistronic expression vectors utilises the internal ribosomal entry site (ires) (Boender et al., 2014). Isolated from the encephalomyocarditis virus (EMCV), the ires has been extensively used to link two genes transcribed from a single promoter within recombinant viral vectors (Martinez-Salas, 1999). Therefore the ires permits the production of multiple proteins from a single mRNA transcript (Jang et al., 1988). Their efficiency, however, varies in different tissues (Furler et al., 2001). Furthermore,

- The expression of the cistron downstream of the ires sequence is often reduced and therefore expression of transgenes is not equivalent (Mizuguchi et al., 2000)
- They are relatively large (up to 1.5Kb) (Hellen and Sarnow, 2001) and are therefore limiting in low insert capacity vectors

Due to the relatively small size of the AAV genome, which is approximately 4.7Kb, its use is limited to smaller gene sequences, as increases beyond this negatively affect packing and subsequently viral titre (Sun et al., 2003). However, a number of genes, including VGF, are larger than this hence, more recently, viral 2A peptides have emerged as an alternative to ires sequences in multicistronic vector strategies (Trichas et al., 2008). Indeed, similar to the ires, they were identified in picornaviruses (Martin et al., 2006). In such a virus, multiple proteins are derived from a large polyprotein encoded by a single open reading frame. Whilst dependent on their viral original, 2A peptides are relatively short (circa 20 amino acids) and contain the consensus motif Asp-Val/Ile-Glu-X-Asn-Pro-Gly-Pro (Ibrahimi et al., 2009). The peptides act co-translationally, by preventing the formation of a normal peptide bond between

the glycine and proline residue, resulting in ribosomal skipping (Donnelly et al., 2001) and therefore cleavage of the polypeptide. Efficiency of the viral 2A peptide has been demonstrated by its insertion between two reporter genes (Ryan and Drew, 1994) and in a wide range of eukaryotic cells from yeast to mammals (de Felipe and Ryan, 2004). Subsequently the viral 2A peptide was demonstrated to function in the rat brain, in combination with rAAV without cytotoxic effects and across several generations, without attenuation of expression levels (Furler et al., 2001). The advantages of the viral 2A peptide are 3 fold:

- They are relatively small
- They are more reliable than the ires (Chan et al., 2011)
- They lead to the expression of multiple cistrons at equimolar levels (Trichas et al., 2008)

4.3 AIMS AND OBJECTIVE

A possible explanation for the differences between the functional studies of VGF derived peptides (Bartolomucci et al., 2006; Jethwa et al., 2007) and the VGF^{-/-} null mouse (Hahm et al., 1999), maybe a consequence of global deletion of the gene during the course of development and subsequently in the adult. Alternatively, deletion of several encoded bioactive peptides, with opposing effects (as demonstrated in chapter 3), may account for the phenotype of the VGF^{-/-} null mouse. VGF is expressed and differentially processed in a number of neuronal and endocrine tissues, therefore extrapolating the findings from the VGF^{-/-} null mouse is fraught with difficulties; previous findings may not be associated with loss of function in the brain. Thus the aim of these studies was to determine the effects of VGF on energy homeostasis following chronic over-expression of the gene (via a rAAV) in the hypothalamus of Siberian hamsters (in LD and SD) and mice (fed a normal and HFD). The studies also assessed the feasibility of a viral 2A peptide within a nonstandard laboratory species.

4.4 METHODS

4.4.1 Preparation of AAV

The plasmid pAAV-CBA-AgRP-ires-eGFP was a kind gift from Dr Perry Barrett (University of Aberdeen, UK) from which viral particles were synthesised to over-express AgRP mRNA and enhanced green fluorescent protein (eGFP) in a previous study conducted by Jethwa et al. (2010). To construct the plasmid pAAV-CBA-VGF-2a-eGFP-WPRE, from which viral articles were synthesised to over-express VGF and eGFP, the full length mouse VGF cDNA was isolated and inserted into the pSC-B-AMP/KAN cloning vector (a kind gift from Dr Perry Barrett, StrataClone™ Blunt PCR Cloning System, Agilent Technologies, UK). The CBA-CMV-IE promoter was chosen as it is a strong and constitutively active promoter (Kobelt et al., 2010) and had been utilised successfully for AgRP over-expression in the hypothalamus of Siberian hamsters (Jethwa et al., 2010). Following restriction enzyme (RE) digestion to confirm presence of VGF cDNA and sequencing to confirm correct orientation of the cDNA sequence, the VGF cDNA sequence was amplified by PCR. In this reaction, however, the forward and reverse primers, designed to amplify the VGF cDNA sequence contained the following modifications:

- A Kozak sequence was added to the forward primer to ensure the initiation of translation
- A viral 2A sequence was added to the reverse primer
- A point mutation was introduced in the reverse primer to remove the stop codon from the VGF cDNA.
- Restriction enzyme (RE) sites were added to both primers, along with 3 additional nucleotides, to aid recognition by the REs and for future subcloning.

The Kozak sequence (5'-GCCGCCACCATATGG-3' underlined bases denote start codon) emerged as the consensus sequence for initiation of translation in

vertebrates (Kozak, 1987) and has subsequently been shown to significantly increase the desired expression from constructs (Olafsfottir et al., 2008).

Viral 2A sequences have the benefit of ensuring a 1:1 ratio between transgene and reporter gene, in this case eGFP, and are considerably smaller than the internal ribosome entry site (IRES) sequences (Trichas et al., 2008). Due to the packaging constraints of AAV, this would theoretically improve viral titre. By removing the stop codon from the VGF cDNA, transcription and subsequent translation would continue and not prematurely end. Given the large sequence (VGF cDNA was circa 2.2Kb) unique RE sites were added to the primers to aid the subsequent subcloning.

The primer sequences were therefore as follows:

Forward CCCGGAAGCTTACCATGAAAACCTTCACGTTGCCGGCATCC
(5' – 3')

Reverse GGGCCCTGGCCAGGTTCCGGAGCCACGAACTTCTCTGTAAAGCA
(5' – 3') AGCAGGAGACGTGGAAGAAAACCCCGTCCCGAGCACGTGCTGCTG
 CACCGCCCG

The resultant PCR product, which was subject to agarose gel electrophoresis to confirm size and sequencing to ensure no point mutations had been introduced during the cloning, was subsequently digested and subcloned into pAAV-CBA-AgRP-IRES-eGFP-WPRE, excising the AgRP-IRES in the process. The resultant plasmid was designated pAAV-CBA-VGF-2a-eGFP-WPRE (see Figure 4.4.1) after RE digestion and sequencing.

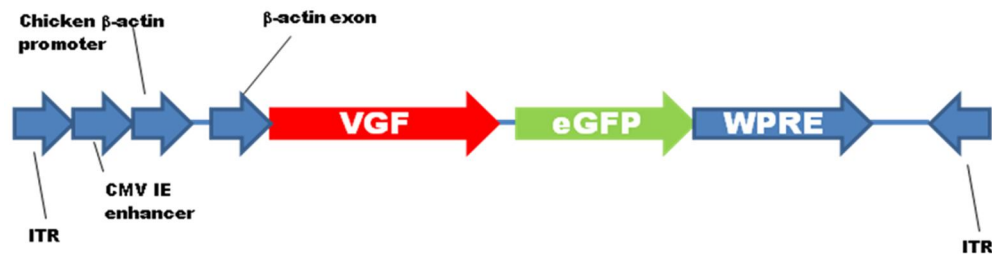


Figure 4.4.1: A schematic of the pAAV-CBA-VGF-2a-eGFP-WPRE. The backbone of the construct remained unchanged from that used to over-express AgRP in the hypothalamus of Siberian hamsters (Jethwa et al., 2010). The AgRP-ires sequence was excised and replaced by VGF cDNA and a viral 2A peptide for the bicistronic expression of VGF and eGFP. ITR – internal tandem repeat, CMV\IE – cytomegalovirus intermediate early promoter, chicken β-actin promoter, VGF containing viral 2A sequence, eGFP – enhanced green fluorescent protein, WPRE – Woodchuck Hepatitis virus post-transcriptional regulatory element.

From pAAV-CBA-VGF-2a-eGFP-WPRE, the rAAV vector was generated by VectorBiolabs, USA. Briefly, the AAV viral particles were produced through co-transfecting HEK cells with pAAV-CBA-VGF-2a-eGFP-WPRE, plus two other “helper” plasmids. 48 hours post transfection, cell pellets were harvested, and viruses were released through three cycles of freeze/thaw, at -80°C and $+37^{\circ}\text{C}$ respectively. Viruses were purified through caesium chloride (CsCl)-gradient ultra-centrifugation, followed by desalting. Viral titer (GC/ml - genome copies/ml) was determined through real-time PCR. The titres obtained were 7.2×10^{12} gc/ml for pAAV-CBA-VGF-2a-eGFP-WPRE and 1×10^{13} gc/ml for AAV-GFP, which expresses GFP under the control of a CMV promoter.

4.4.2 The SH-SY5Y cell line

Details of the SH-SY5Y cell line, can be found in section 5.6.1.1 along with differentiation (see section 5.6.1.1) and transfection (5.6.1.11) protocols.

4.4.3 Typhoon Trio+

Details of the Typhoon Trio+ can be found in section 5.6.1.12.

4.4.4 ImageQuant

Details of the ImageQuant software can be found in section 5.6.1.13.

4.4.5 Animals

Details of the UK Animals (Scientific Procedures) Act 1986 and Project and Personal Licenses can be found in section 2.5.

4.4.5.1 *Siberian hamsters*

Details of the experimental colony of Siberian hamsters can be found in section 2.5.1.

4.4.5.2 *C57Bl/6J Mice*

Details of the experimental mice can be found in section 2.5.2.

4.4.6 Viral infusion

Anaesthesia was induced with 3.5% isoflurane in a N₂O:O₂ mixture and maintained during surgery with 1.7-2.0% isoflurane to ensure complete inhibition of hindpaw reflex, as well as the blink reflex. While anaesthetised (prior to commencement of surgery) animals received a subcutaneous (s.c) injection of carprofen (Rimadyl 50mg/kg) to maintain analgesia. Animals were placed in a stereotaxic frame (David-Kopf Instruments, supplied by Clark electromedical Instruments, Reading, UK) with the incisor bar positioned level with the interaural line. Using the sutures of confluence (bregma) as a landmark, a small hole was drilled on midline. The dura mater was pierced just lateral to the mid-sagittal sinus, which was deflected as a drawn glass capillary

microinjector (30 μ m tip diameter) was lowered into the correct location. Using a Nanolitre injection system (WPI, Stevenage, UK), 200nl of the viral vector was infused bilaterally directed towards the PVN (anteroposterior + 0.03, mediolateral \pm 0.03, dorsoventral -0.58) over 2 minutes. After infusion, the glass microinjector was kept in place for an additional 5 minutes to allow for diffusion and prevention of backflow through the cannula track. The incision was sealed using Michel clips and glue. The surgically prepared animals were allowed to recover for seven days and regularly handled to habituate the animals and minimise stress later. Additionally animals received daily s.c. infusions of analgesia (Rimadyl Pfizer, Kent, UK 50mg/kg), were weighed and provided with a palatable diet consisting of soaked mash pellets.

4.4.7 Comprehensive Laboratory Animal Monitoring System (CLAMS)

Multiple respiratory and feeding behaviour parameters were measured using a Comprehensive Laboratory Animal Monitoring System (CLAMS, Linton Instrumentation, Linton, UK and Columbus Instruments, Columbus, OH, USA). This is an open-circuit calorimeter using eight mouse chambers, where the animals were individually housed with food hoppers (chow was ground down into a rough powder) in the centre of each cage and dropper style water bottles. Metabolic parameters measured included oxygen consumption (VO_2) and carbon dioxide production (VCO_2), such that the respiratory exchange ratio (RER) could be calculated. Feeding behaviour parameters measured included the timing and duration of feeding bouts, food intake for each bout (meal size) and total food intake per unit of time. Locomotor activity was also measured using two sets of infrared beams traversing each cage, which measured vertical and linear movement. The system was operated with an air intake of 0.6 litre/minute for each chamber, and an extracted outflow of 0.4 litre/minute. All measurements were taken at an ambient temperature of 21-22°C. Animals were placed in the system for 48 hours. The first 24 hours allowed the animals to habituate; the latter 24 hours were used for subsequent analysis presented in this thesis. Measurements were recorded every minute over 9 minute

epochs (8 chambers and 1 reference measurement) and meal sizes were noted when in excess of 0.02g. All data was collected using the OxyMac Windows software v4.0 or v4.2 (Columbus Instruments, OH). Excessive moisture from the chambers was removed by calcium carbonate, which was contained within a muslin bag, placed below the grid flooring and therefore out of reach of the animals.

4.4.8 Dissection

Under terminal anaesthesia, administered via intraperitoneal (i.p.) injection of pentobarbital sodium (Euthatal, Rhone Merieux, Harlow, UK), blood was collected by cardiac puncture and stored in EDTA tubes. Samples were stored on ice until centrifugation at 30,000 rpm at 4°C for 10 minutes. Plasma was then collected and stored at -80°C. Tissues were collected at room temperature, weighed and immediately placed on a metal block in dry ice. Frozen tissue was stored at -80°C.

4.4.9 Cryostat

The ambient temperature within the cryostat was maintained at least -15°C. The sample for sectioning was placed in OCT to mount upon the stage, olfactory bulbs facing forward, cortex facing upwards. Thickness was set to 50µm to trim the sample, and sectioning began at the emergence of the optic nerve/chiasm and proceeded through to the substantia nigra at a thickness of 20µm. Every 5 sections (i.e. 100µm), a 50µm section was taken. Slides were left to air dry and subsequently frozen at -20°C.

4.4.10 *In situ* hybridisation

In situ hybridisation allows for the precise localisation of a specific segment of nucleic acid within a histological section – detection is via a riboprobe. In the absence of a commercially available antibody for VGF, or one that detects its derived peptides, *in situ* hybridisation was utilised to ensure viral over-

expression of the VGF gene. A riboprobe for eGFP was also generated as a control. This protocol was adapted from Sweetman et al., (2008).

4.4.10.1 Generation of riboprobes

Riboprobes were generated from the StrataClone Bunt PCR Cloning Vector pSC-B-amp/kan, which contained the VGF cDNA. Utilising the T7 binding site, anti-sense riboprobes were generated, along with anti-sense riboprobes for eGFP from SLAX13-eGFP (a kind gift from Dr Dylan Sweetman, University of Nottingham, UK).

Briefly, 10µg of plasmid DNA was linearised with an appropriate RE (*EcoRV* or *NcoI* respectively) and buffer at 37°C overnight to ensure complete digestion (as described in section 2.3.8). Linearised DNA was purified using phenol:chloroform extraction (as described in section 2.2.2) and 1µg of purified DNA was transcribed using T7 RNA polymerase. The reaction contained digoxigenin-(DIG)-11-deoxyuridine triphosphate (dUTP) as a nonradioactive label of DNA (ratio of 35% with UTP). This moiety can subsequently be detected. The reaction was subsequently purified using a G50 column and the riboprobes were diluted in hybridisation buffer and stored at -20°C.

4.4.10.2 Detection of mRNA

Sections were incubated in 4% paraformaldehyde (PFA) overnight at 4°C, before dehydration in 50% methanol/PBS-Tween20 (PBSTw) and 100% methanol. Sections were then stored at -20°C. Sections were subsequently rehydrated in a decreasing concentration of methanol/PBSTw (75, 50 and 25%) before washing in PBSTw.

Sections were treated with proteinase K (10µg/ml) for 30 minutes at room temperature and rinsed twice in PBSTw before fixing in 4% PFA/0.1%

glutaldehyde for 20 minutes at room temperature. Sections were then washed in PBSTw for 5 minutes before pre-hybridisation, in 1:1 PBSTw: hybridisation (hyb) buffer and in hyb buffer. Sections were then incubated in fresh hyb buffer at 65°C for 6 hours. Sections were then placed in a humidity chamber with riboprobe (pre-warmed to 65°C) overnight at 65°C.

Post hybridisation the sections were rinsed and subsequently washed in hyb buffer at 65°C for 10 minutes before washing twice in wash buffer at 65°C for 30 minutes. Sections were then washed in 1:1 washing buffer: maleic acid buffer containing Tween-20 (MABT), before rinsing in MABT and washing twice in MABT at room temperature.

The MABT was then replaced with MABT/2% Roche blocking agent for 1 hour at room temperature, before being replaced with blocking solution for 1 hour. Subsequently the blocking solution was replaced with blocking solution containing a 1:2000 dilution of anti-DIG-AP fragments and incubated overnight, with rocking, at 4°C.

Sections were subsequently washed thrice in MABT for 1 hour, and then washed in MABT overnight at 4°C.

For the colour reaction, sections were first incubated in 1-methyl-5-thiotetrazole (NMTT) for 10 minutes at room temperature, which was subsequently replaced with NMTT with 9µl NBT and 7µl/ml indoxyl-nitroblue tetrazolium (BCIP). During the reaction, sections were protected from the light. The colour reaction proceeded until the section was stained, washed twice in 5xTBSTw for 10 minutes at room temperature and washed overnight at 4°C in

5xTBSTw. The colour reaction was repeated the following day, to intensify signal and reduce background.

4.4.11 Statistics

GenStat (14th Edition, VSN International, London, UK) was used to determine the sample size for the *in vivo* experimentation. The software calculates the power (probability of detection) and the replication (sample size) required to detect an effect of treatment (see section 3.5.8).

Descriptive statistics (means and standard error mean (SEM)) were generated using PRISM (Prism 6.0, GraphPad, San Diego, CA). Body weight and home cage food intake data were analysed using two-factor analysis of variance (ANOVA) with repeated measures and Bonferroni tests for post-hoc comparisons (GraphPad Prism, version 6.0, GraphPad Software Inc, San Diego, CA, USA). Two-way (time x group) ANOVA was also used to analyse data obtained from the CLAMS apparatus including values for oxygen consumption (VO_2), carbon dioxide production (VCO_2), heat, respiratory exchange ratio (RER) and locomotor activity. Meal frequency and food intake in the CLAMS were calculated in 4 hour epochs and similarly analysed. Data on organ weights at the end of the study were compared using Student's unpaired T test. $p < 0.05$ was considered statistically significant.

4.5 EXPERIMENTAL DESIGN

4.5.1 Siberian hamsters

4.5.1.1 *Study 1: The effects of VGF over-expression in the hypothalamus of Siberian hamsters*

Male Siberian hamsters (n = 32) received either a bilateral infusion of AAV-GFP (n = 16) or AAV-VGF (n = 16) directed at the PVN and were placed in the CLAMS at 1, 2, 4, 8 and 12 weeks post viral infusion. Hamsters were culled 1, 2, 4 or 12 weeks post infusion (n = 4 per treatment, therefore n = 8 per time point).

4.5.1.2 *Study 2: The effects of VGF over-expression in the hypothalamus of Siberian hamsters transferred to SD*

In a separate study, male Siberian hamsters (n = 12) received either a bilateral infusion of AAV-GFP (n = 6) or AAV-VGF (n = 5) directed at the PVN. Hamsters were maintained under LD for 12 weeks before transfer to SD for 20 weeks. Siberian hamsters were transferred to designated SD cabinets (8 hours light: 16 hours dark, lights off at 11:00) and placed in the CLAMS 1, 2, 8, 12 and 20 weeks post transfer to SD. The CLAMS room was maintained at SD (8 hours light: 16 hours dark, lights off at 11:00) akin to the SD cabinets. Hamsters were culled at the end of the study.

4.5.2 Mice

4.5.2.1 *Study 3: The effects of VGF over-expression in the hypothalamus of mice*

Male mice (n = 32) received either a bilateral infusion of AAV-GFP (n = 16) or AAV-VGF (n = 16) directed at the PVN and placed in the CLAMS at 1, 4, 8, 12 and 16 weeks post infusion. Mice were culled at 1, 4, 8 or 16 weeks post infusion (n = 4 per treatment, therefore n = 8 per time point).

4.5.2.2 Study 4: The effects of VGF over-expression in the hypothalamus of the mice transferred to a HFD

In a separate study, male mice (n = 12) received either a bilateral infusion of AAV-GFP (n = 5) or AAV-VGF (n = 6) directed at the PVN and were maintained on normal lab chow for 12 weeks before transfer to a high fat diet for 16 weeks. Mice were placed in the CLAMS at 1, 2, 8 and 16 weeks post transfer to HFD. Mice were culled at the end of the study.

4.6 RESULTS

4.6.1 Construct expression in SH-SY5Y cells

4.6.1.1 Transfection of the SH-SY5Y cell line with pAAV-CBA-VGF-2A-eGFP-WPRE significantly increased eGFP expression

In response to retinoic acid (RA) the SH-SY5Y cell line yielded a homogenous population of cells with a neuronal morphology (see section 5.7.1.2 Chapter 5). To test the viability of the bicistronic construct prior to viral packaging, the SH-SY5Y cell line was transfected with pAAV-CBA-VGF-2a-eGFP-WPRE. GFP expression was widespread 72 hours post transfection (see Figure 4.6.1.1 A). Treatment of the transfected SH-SY5Y cells with 10 μ M RA induced differentiation (see Figure 5.7.1.2 Chapter 5), at which point GFP expression expanded beyond the cell body and extended to the axons/neurites (see Figure 4.6.1.1 B). The increase in GFP expression was similar to that observed following transfection of the SH-SY5Y cell line with the control constructs, pZsGreen1-N1 (see section 5.6.1.11) and pCMVCBG992AmRFP (see section 5.6.2.1), used for studies on the VGF promoter (see Figure 4.6.1.1 C and D).

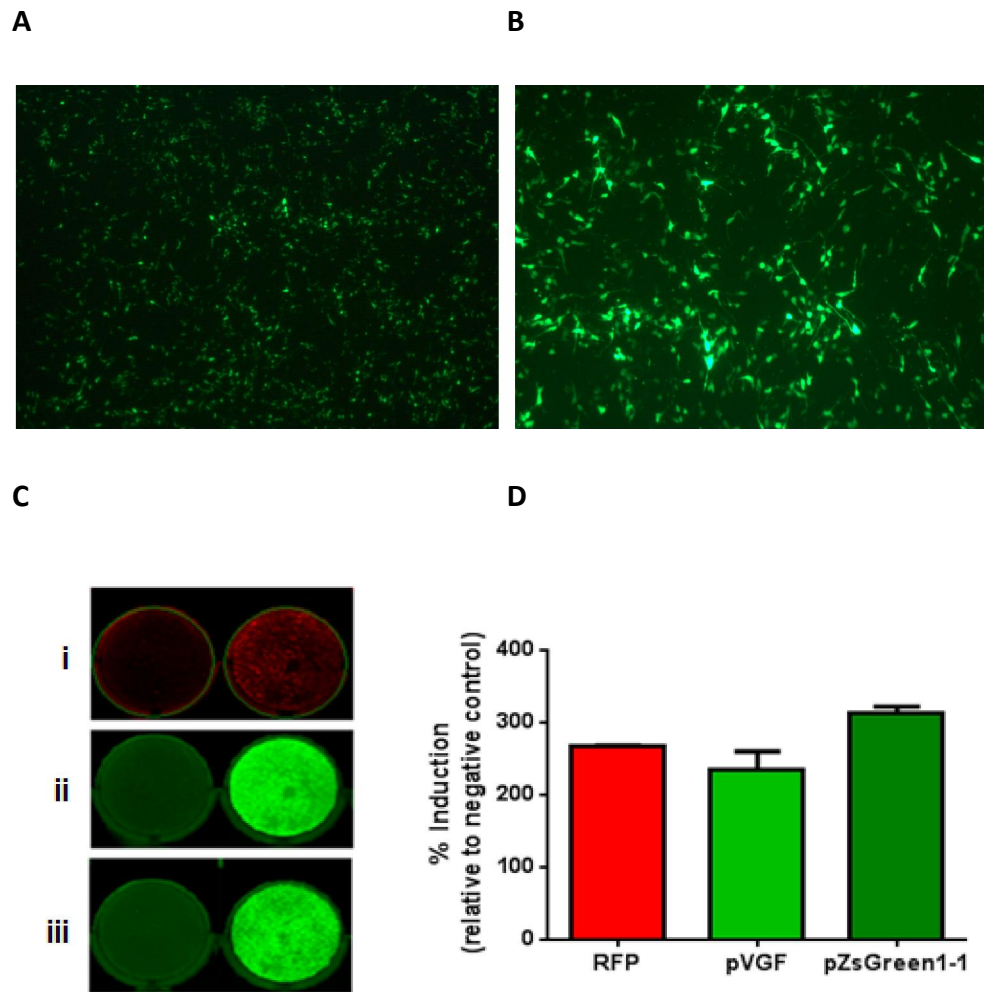


Figure 4.6.1.1: **eGFP expression in SH-SY5Y cells following transfection with pAAV-CBA-VGF-2A-eGFP-WPRE.** SH-SY5Y cells were transfected with pAAV-CBA-VGF-2A-eGFP-WPRE. The cells were visualised by Leica DF420C microscope 72 or 120 hours post transfection for eGFP expression. A – 72 hours post transfection and B – 120 hours post differentiation (192 hours post transfection). Treatment of transfected cells with retinoic acid (RA) resulted in neurite growth. These neuronal projections also expressed eGFP. C – SH-SY5Y cells transfected with pCMVCBG992AmRFP (i), pAAV-CBA-VGF-2A-eGFP-WPRE (ii) and pZsGreen1-N1 (iii). D – SH-SY5Y cells transfected with the pAAV-CBA-VGF-2A-eGFP-WPRE construct displayed a similar percentage increase in GFP, compared to cells transfected with pCMVCBG992AmRFP and pZsGreen1-N1. Values are group mean + SEM (n =3).

4.6.1.2 Transfection of the SH-SY5Y cell line with pAAV-CBA-VGF-2a-eGFP-WPRE significantly increased VGF mRNA

The increase in eGFP was associated with an increase in VGF expression following transfection of pAAV-CBA-VGF-2A-eGFP-WPRE. There was a significant increase in VGF mRNA (20-fold) 72 hours post transfection, compared to controls transfected with pZsGreen1-N1 (see Figure 4.6.1.2).

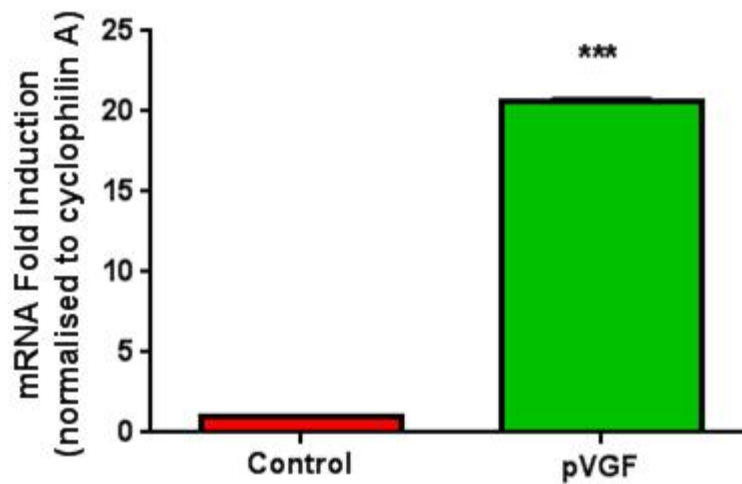


Figure 4.6.1.2: SH-SY5Y cells transfected with pAAV-CBA-VGF-2A-eGFP-WPRE results in significantly increased VGF mRNA expression. SH-SY5Y cells transfected with pAAV-CBA-VGF-2a-eGFP-WPRE demonstrate a 20-fold increase in VGF mRNA 72 hours post transfection when compared to transfected (pZsGreen1-N1) controls. Values are group mean + SEM. Significance values are indicated: *** $p < 0.0001$ vs. control ($n = 3$).

4.6.1.3 AAV-VGF infection of SH-SY5Y cells significantly increased eGFP expression

eGFP expression was significantly increased in undifferentiated SH-SY5Y cells infected with AAV-CBA-VGF-2A-eGFP-WPRE (AAV-VGF) when compared to control cells transfected with pCMVCBG992AmRFP. This effect was dependent on the multiplicity of infection (MOI); as MOI increased, the level of GFP expression increased (see Figure 4.6.1.3).

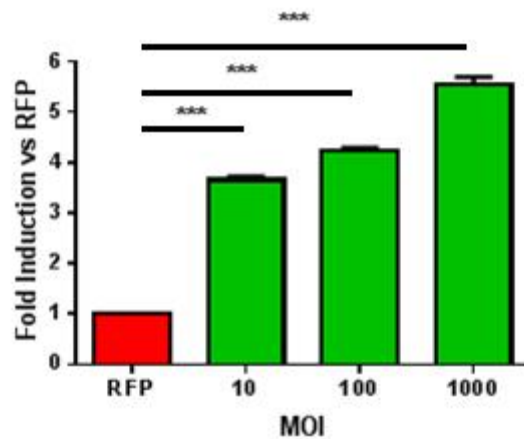


Figure 4.6.1.3: **Increased MOI increases eGFP expression in SH-SY5Y cells.** Undifferentiated SH-SY5Y cells were transfected with pCMVCBG992AmRFP or infected with AAV-VGF with an increasing MOI. 72 hours post transfection/infected, the cells were differentiated by treatment with 10 μ M RA for 120 hours (see section 5.7.1.2). Fluorescence was then quantified using the Typhoon Trio+ and associated software. Values are group mean + SEM. Significance values are as indicated: *** p < 0.001 vs. control (n =3).

4.6.2 Study 1: The effects of VGF over-expression in the hypothalamus of Siberian hamsters

4.6.2.1 *Over-expression of VGF mRNA significantly increased food intake, but bodyweight remained constant*

Infusion of AAV (control or treatment) into the hypothalamus resulted in a small transient decrease in body weight in both control and treated animals (see Figure 4.6.2.1 A). However by week 5 there was an increase in the body weights of the Siberian hamsters receiving the AAV-GFP vector, resulting in a significant divergence from the group treated with the AAV-VGF vector (treatment vs. time interaction $F = 5.037$, $p < 0.0001$). By 12 weeks post-infusion, body weights had increased 12.6% relative to pre-surgical body weights in the AAV-GFP group, compared to an increase of just 1% in the AAV-VGF treated group (unpaired T test, $p < 0.05$) (see Figure 4.6.2.1 A).

Although body weights were lower in the AAV-VGF treated group (compared to controls) at the end of the study, this was not due to food intake, since there was a significant increase in daily food intake in the home cage in the AAV-VGF group (effect of treatment $F = 14.90$, $p < 0.01$), as well as an increase in food intake per gram body weight (effect of treatment $F = 8.983$, $p < 0.05$) (see Figure 4.6.2.1 B and C respectively). There was also a significant increase in cumulative food intake (effect of treatment $F = 3.624$, $p < 0.05$) and cumulative food intake per gram body weight (treatment vs. time interaction $F = 10.91$, $p < 0.0001$) (see Figure 4.6.2.1 D and E). The change in daily food intake could be attributed to the increase in meal duration at 2 weeks post infusion in the AAV-VGF treated group compared to AAV-GFP controls (treatment vs. time interaction: $F = 5.579$, $p < 0.001$), as meal frequency was unaffected (see Figure 4.6.2.2). There was no difference in meal duration at weeks 4 ($p > 0.05$), but by 12 weeks post infusion a significant increase in meal duration was again observed (effect of treatment, $F = 7.348$, $p < 0.05$) (see Figure 4.6.2.1 F (i)).

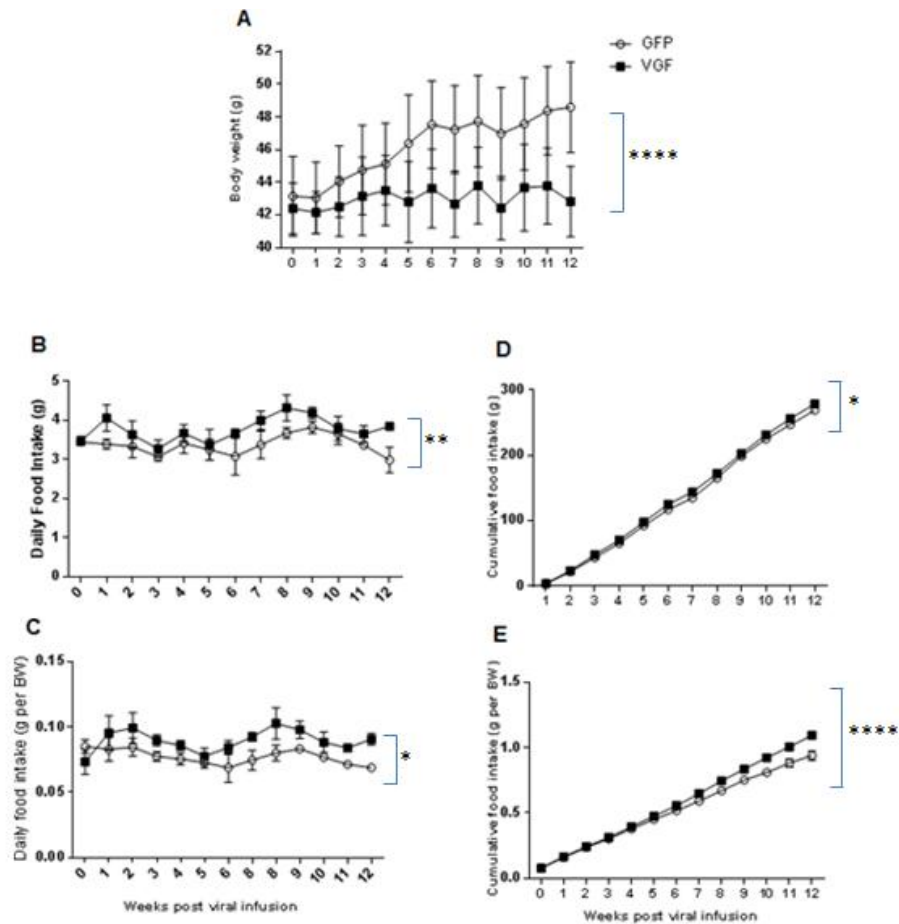


Figure 4.6.2.1: **Over-expression of VGF mRNA in the hypothalamus of Siberian hamsters significantly increased food intake, while body weight was significantly reduced.** Body weight (A), daily food intake (B), daily food intake per gram body weight (C), cumulative food intake (D) and cumulative food intake per gram body weight (E) of adult male Siberian hamsters receiving bilateral injections of 200 nl of either AAV-GFP (as a control, open circles) or AAV-VGF (black squares) in the PVN at a concentration of 7.2×10^{12} gc/ml for AAV-VGF and 1×10^{13} gc/ml for AAV-GFP ($n = 4$ per group). Siberian hamsters were maintained under LD and placed in metabolic cages for 48 hrs at 1, 2, 4, 8 and 12 weeks post viral infusion. Values are group mean \pm SEM ($n = 4$). Significance values are as indicated: * $p < 0.05$, ** $p < 0.01$, **** $p < 0.0001$ (vs. control).

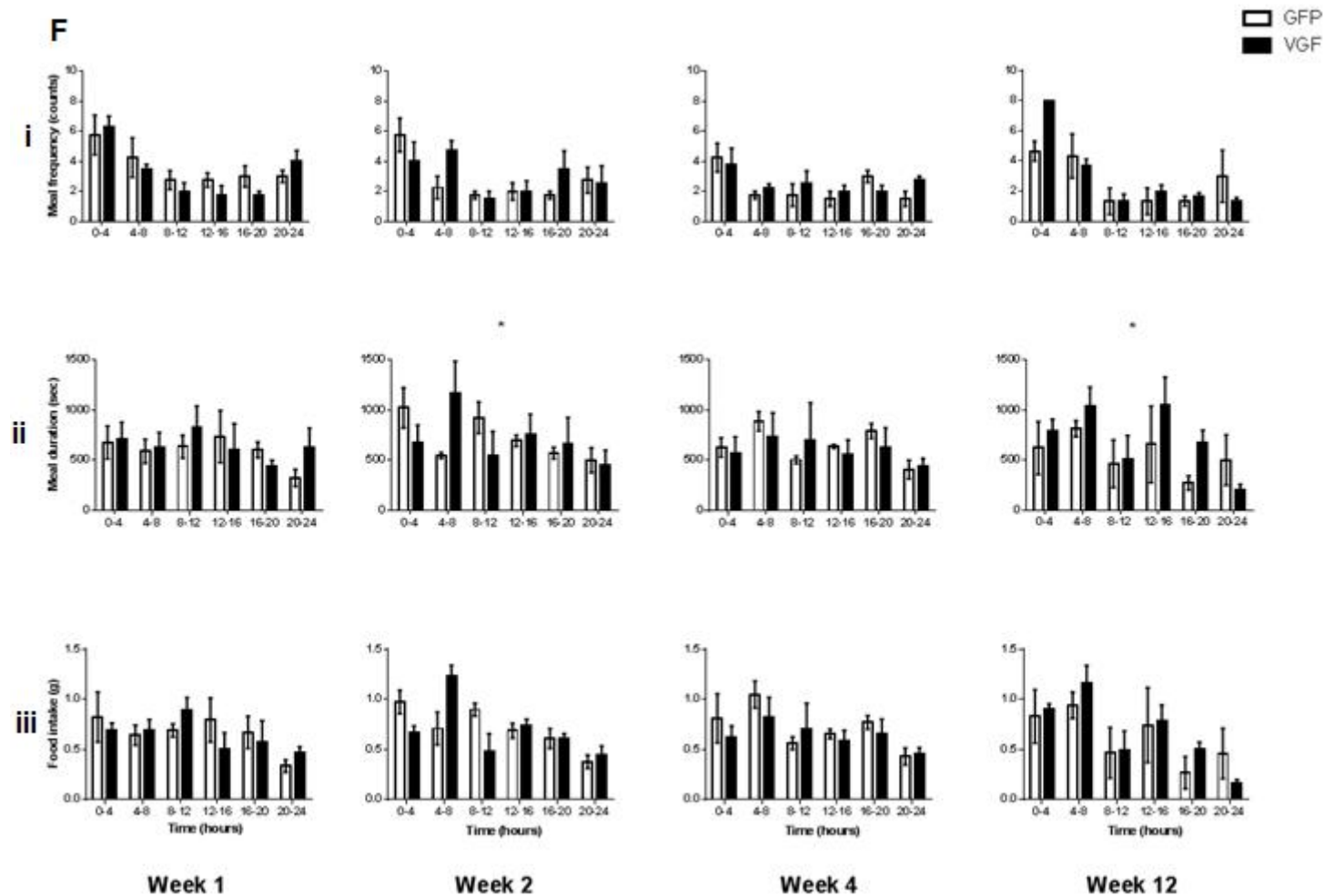
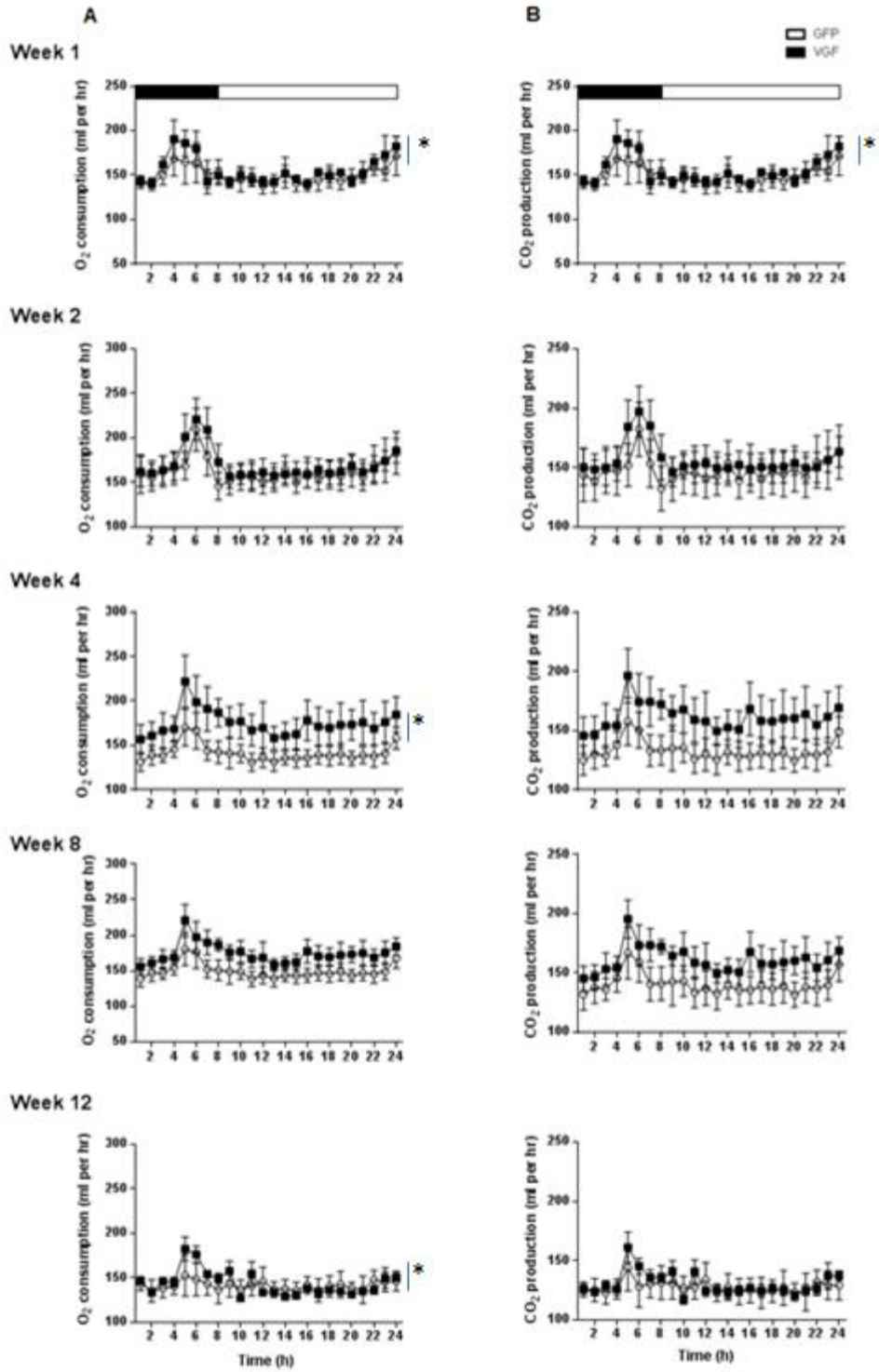


Figure 4.6.2.1 F: **Over-expression of VGF mRNA in the hypothalamus of Siberian hamsters significantly affected feeding behaviour.** 24 hr profiles for meal frequency (i), meal duration (ii) and food intake (iii) of Siberian hamsters in metabolic cages during long day exposure 1, 2, 4, and 12 weeks post viral infusion. Week 8 data was not collected due to an instrument fault. Siberian hamsters received either the control AAV-GFP vector (open bars) or the AAV-VGF vector (black bars). Values are group mean \pm SEM. Significance values are as indicated: * $p < 0.05$ vs. control ($n = 4$).

4.6.2.2 Over-expression of VGF mRNA significantly increased oxygen consumption

Oxygen consumption was significantly increased at 1, 4, and 12 weeks post infusion (see Figure 4.6.2.2 A) in the AAV-VGF group compared to AAV-GFP control group (treatment vs. time interaction: week 1 $F = 1.630$, $p < 0.05$; week 4; $F(23, 138) = 1.598$, $p < 0.05$; week 12; $F = 2.573$, $p < 0.001$). At 2 and 8 weeks the effect on oxygen consumption fails to reach significance although at both time points there was an observable increase (see Figure 4.6.2.2 A). Carbon dioxide production was significantly increased at 1 week post infusion (treatment vs. time interaction $F = 1.845$, $p < 0.05$) (see Figure 4.6.2.2 B). However there was no significant difference observed at any other time point. Respiratory exchange ratio (RER) did not change at any time point until 12 weeks post infusion where it was increased in the AAV-VGF treated group (treatment vs. time interaction $F = 1.910$ $p < 0.01$) (see Figure 4.6.2.2 C). No change in activity was observed (see Figure 4.6.2.2 D).



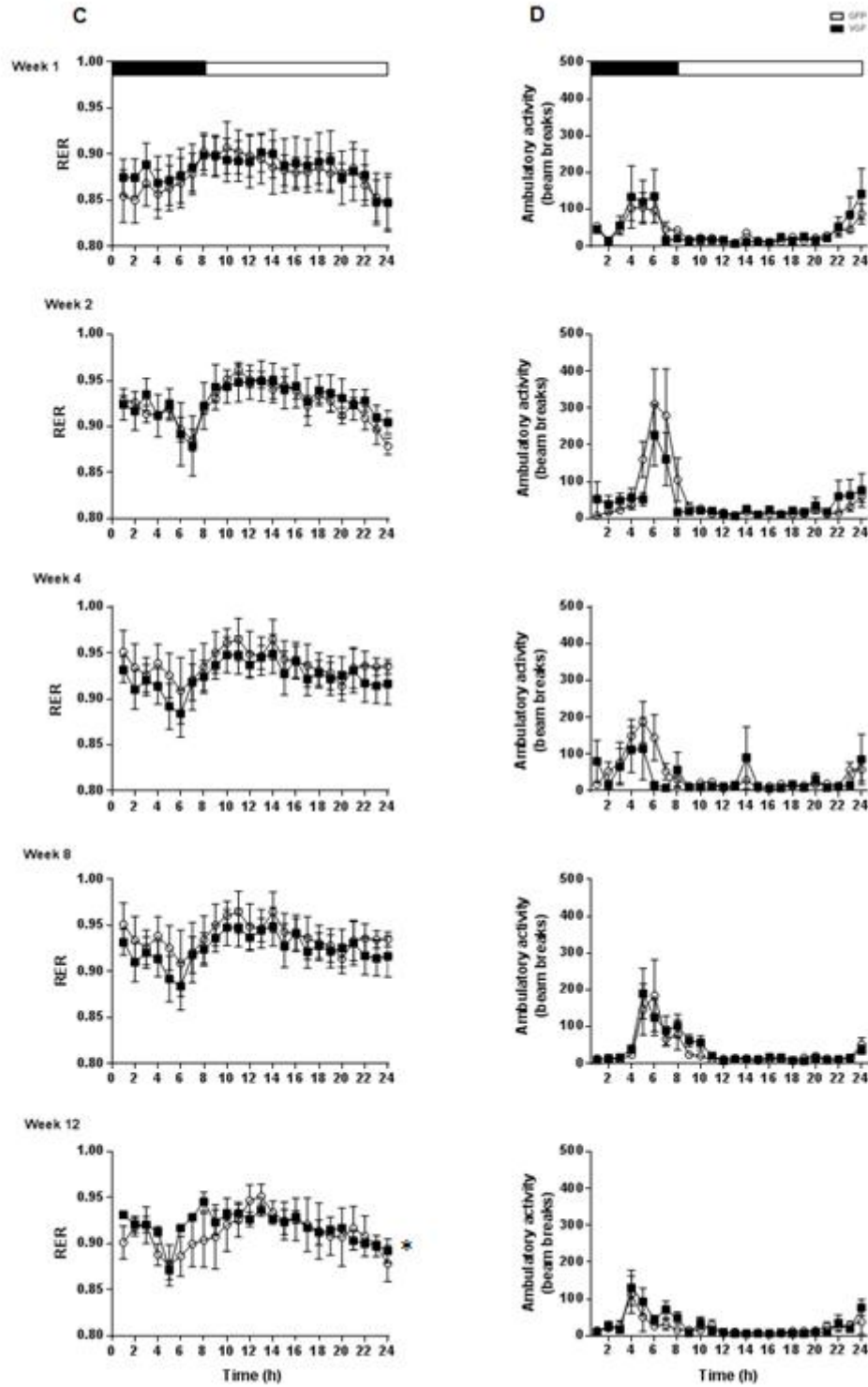


Figure 4.6.2.3: The metabolic parameters of Siberian hamsters over-expressing VGF mRNA in the hypothalamus was significantly altered. 24 hour profiles for oxygen consumption (A) and carbon dioxide production (B) and RER (C) and activity (D) of Siberian hamsters in CLAMS during long day exposure 1, 2, 4, 8 and 12 weeks post viral infusion. Siberian hamsters received either the control GFP vector (open circles) or the VGF-GFP vector (black squares). Solid

bar indicates the dark phase (8:16 light cycle). Values are group mean \pm SEM (n =4). Significance values are as indicated: * p < 0.05 vs. control.

4.6.2.3 *Over-expression of VGF mRNA results in an increase in brown adipose tissue*

Despite the significant difference in body weight, there was no significant effect of AAV-VGF treatment on liver, epididymal or subcutaneous fat or gastrocnemius muscle weights. However, BAT weight was significantly increased in the AAV-VGF treated group (unpaired T-test, p < 0.05 vs. GFP controls).

	Liver (mg per g BW)	Epididymal fat pad (mg per g BW)	Brown adipose tissue (mg per g BW)	Subcutaneous fat (mg per g BW)	Gastrocnemius muscle (mg per g BW)
GFP (n = 4)	36.1 \pm 1.90	23.6 \pm 1.61	2.9 \pm 0.23	24.4 \pm 3.39	1.3 \pm 0.21
VGF (n = 4)	38.0 \pm 3.69	22.8 \pm 0.49	4.6 \pm 0.42 *	17.4 \pm 3.48	1.6 \pm 0.21

Table 4.6.2.4: **Over-expression of VGF mRNA in the hypothalamus of Siberian hamsters, maintained in LD, resulted in significantly increased BAT weight.** Mean (\pm SEM) mean wet tissue weight (mg per gram body weight) in Siberian hamsters administered with AAV-GFP or AAV-VGF bilaterally directed towards the PVN at the end of the study (week 12). * p < 0.05 vs. GFP (n = 4 per group).

4.6.3 Study 2: The effects of VGF over-expression in the hypothalamus of Siberian hamsters transferred to SD

As expected the Siberian hamsters showed a clear progressive loss of body weight over the 20 weeks of SD exposure (effect of time: $F = 7.433$, $p < 0.0001$) (see Figure 4.6.3.1 A) and this loss of body weight was associated with a moult to a white winter pelage (see Table 4.6.3). The degree of loss of body weight in the responsive Siberian hamsters was similar in both groups (13.3 and 17.8% respectively) (see Table 4.6.3). At the end of the study there was a significant difference in the weight of the epididymal fat pads (GFP: 14.8 ± 0.9 mg per g BW; VGF: 10.9 ± 0.7 mg per g BW; $p < 0.05$ vs. GFP controls) (see Table 4.6.3). Three Siberian hamsters (two from the GFP group, one from the VGF group) failed to respond to photoperiod, which was characterised by maintenance of body weight, a failure to develop the winter coat and an increased paired testes weight at the end of the study. These animals were excluded from the analysis as they failed to respond to the SD photoperiod.

	Body weight (g)	Change in BW under SD (%)	Pelage (1-4)	Paired testes weight (mg per BW)	Epididymal fat pad (mg per BW)
GFP (n =4)	38.3 ± 1.06	13.34 ± 2.43	1.25 ± 0.25	6.76 ± 1.35	14.81 ± 0.9
VGF (n =4)	37.1 ± 0.82	17.79 ± 2.58	1	6.09 ± 0.71	$10.9 \pm 0.7^*$

Table 4.6.3: **Over-expression of VGF mRNA in the hypothalamus of Siberian hamsters, switched to short day (SD) photoperiod, resulted in a significant decrease in epididymal fat pad.** Mean \pm SEM changes in body weight after exposure to SD and mean wet tissue weights (and pelage scores) at the end of the study. * $p < 0.05$ vs. GFP treated group (n = 4 per group).

4.6.3.1 Over-expression of VGF mRNA in SD has no effect on body weight, however food intake was significantly increased

Body weight was unaffected by treatment in the Siberian hamsters exposed to SD photoperiod (body weight, GFP: 38.3 ± 1.1 ; VGF: 37.1 ± 0.82 g; $p = \text{n.s}$) (see Figure 4.6.3.1 A). Daily food intake and daily food intake per gram body weight were not significantly affected in the AAV-VGF treatment group (treatment vs. time interaction $F = 0.8314$, $p = 0.67$; and $F = 0.9071$, $p = 0.58$ respectively) (see Figure 4.5.3.1 B and C). However there was a trend for an increase in cumulative food intake (treatment vs. time interaction $F = 1.557$, $p = 0.08$) and a significant increase in cumulative food intake per gram body weight (treatment vs. time interaction $F = 3.427$, $p < 0.0001$) (see Figure 4.6.3.1 D and E). Again this could be attributed to an increase in meal duration in the AAV-VGF treated group compared to AAV-GFP controls at 1 and 20 weeks post transfer to SD (treatment vs. time interaction 1 week: $F = 3.745$, $p < 0.05$; 20 weeks: $F = 4.400$, $p < 0.02$) (see Figure 4.6.3.1 F). There was no difference in meal frequency or food intake in CLAMS ($p > 0.05$).

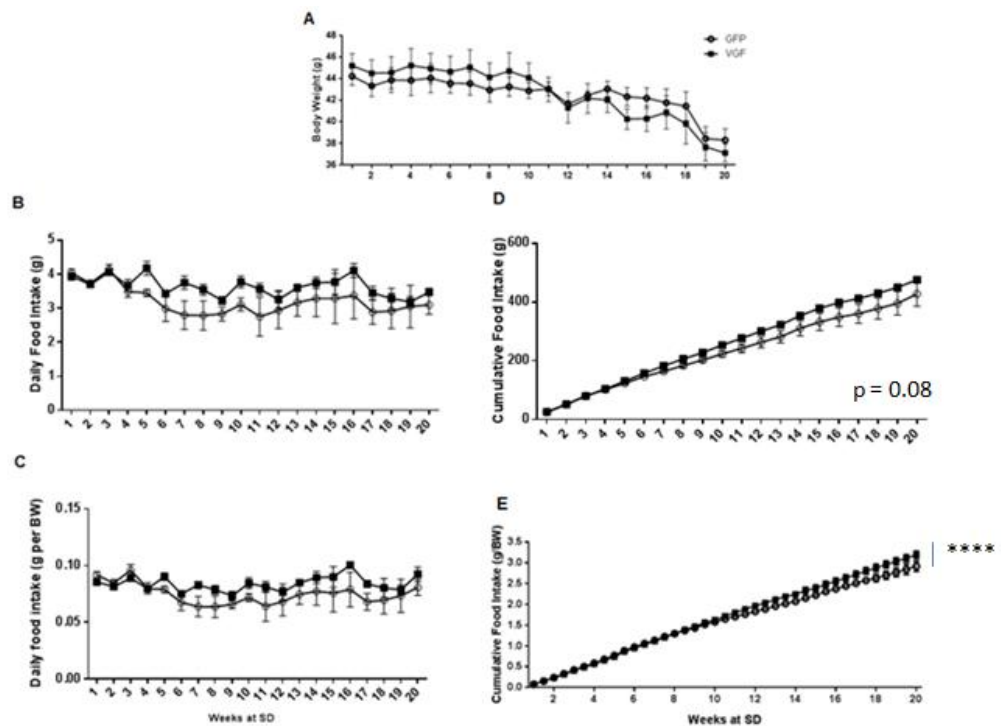


Figure 4.6.3.1: **Despite no differences in body weight of Siberian hamsters over-expressing VGF mRNA within the hypothalamus, cumulative food intake was significantly increased.** Body weight (A), daily food intake (B), daily food intake per gram body weight (C), cumulative food intake (D) and cumulative food intake per gram body weight (E) of adult male Siberian hamsters receiving bilateral injections of 200nl of either AAV-GFP (as a control, open circles) or AAV-VGF (black squares) in the PVN at a concentration of 1×10^{13} gc/ml for AAV-GFP and 7.2×10^{12} gc/ml for AAV-VGF ($n = 4$ per group). Siberian hamsters were maintained under SD. Values are group means (\pm SEM). Significance values are as indicated: **** $p < 0.0001$ vs. control.

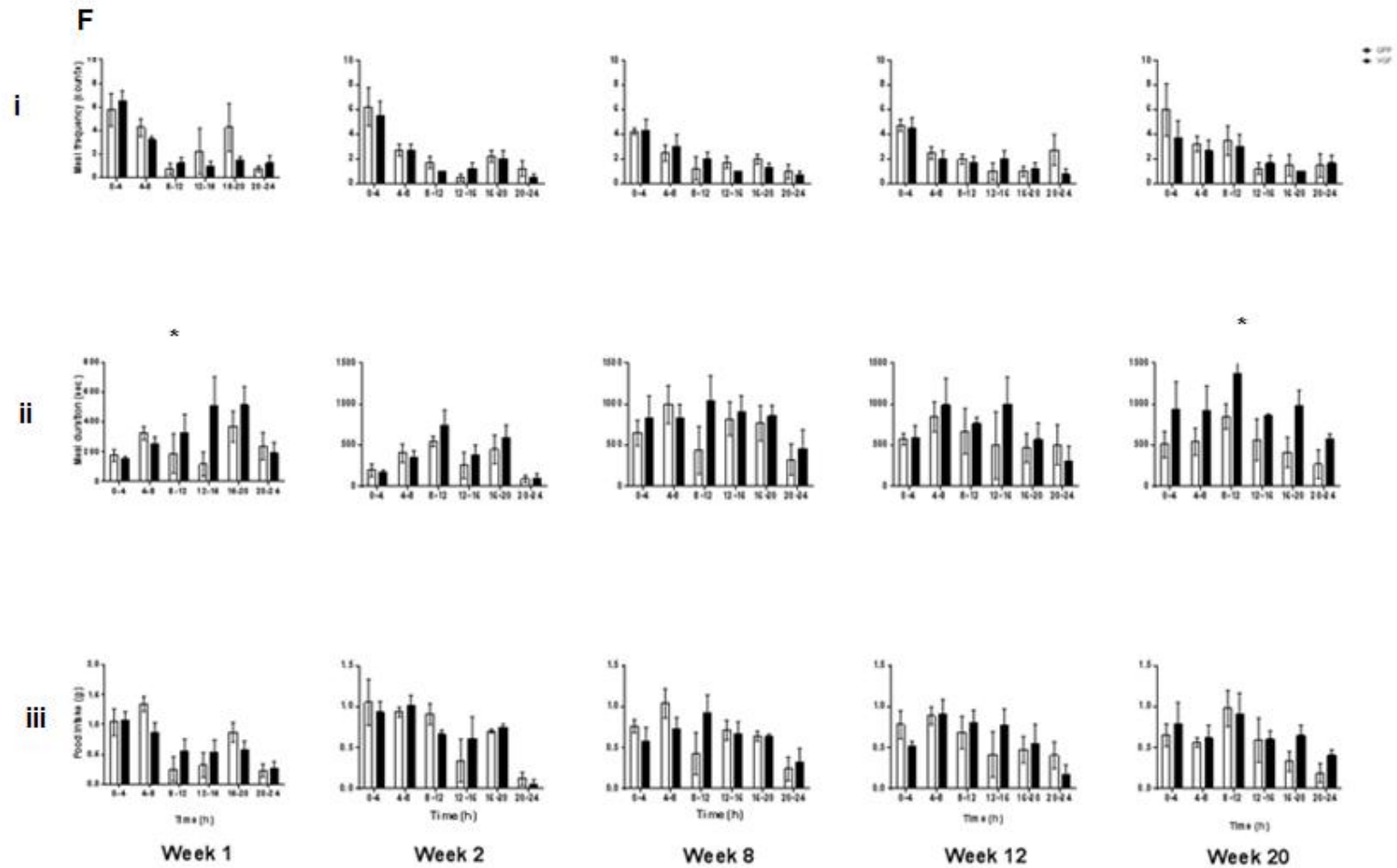
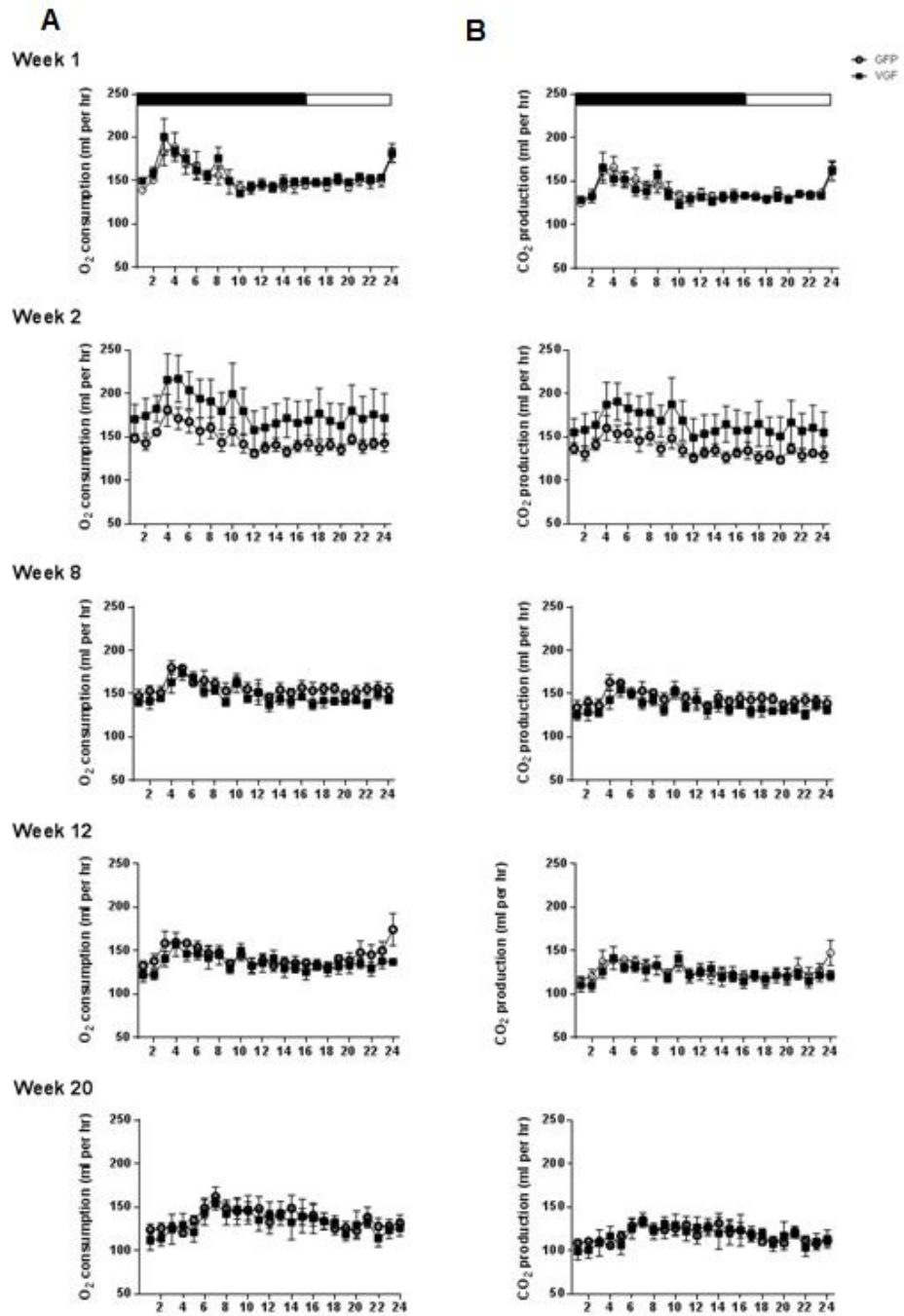


Figure 4.6.3.1 F: **Over-expression of VGF mRNA in the hypothalamus of Siberian hamsters significantly affected feeding behaviour.** 24 hour profiles for meal frequency (i), meal duration (ii) and food intake (iii) of Siberian hamsters in metabolic cages during short day exposure 1, 2, 8, 12 and 20 weeks post transfer to SD. Siberian hamsters received either the control GFP vector (open bars) or the VGF-GFP vector (black bars). Values are group mean, (n = 4 per group; \pm SEM). Significance values are as indicated: * p < 0.05.

4.6.3.2 Over-expression of VGF mRNA increased oxygen consumption and carbon dioxide production, RER was significantly increased

There was an increase in both oxygen consumption and carbon dioxide production in the VGF group over the 20 weeks post transfer to SD (see Figure 4.6.3.3), but this failed to reach significance. At 8 and 12 weeks post transfer, a significant increase in RER was observed in the AAV-VGF treated group compared to AAV-GFP controls (effect of treatment; 8 weeks: $F = 1.756$, $p < 0.05$; 12 weeks: $F = 5.644$, $p < 0.05$) (see Figure 4.6.3.2).



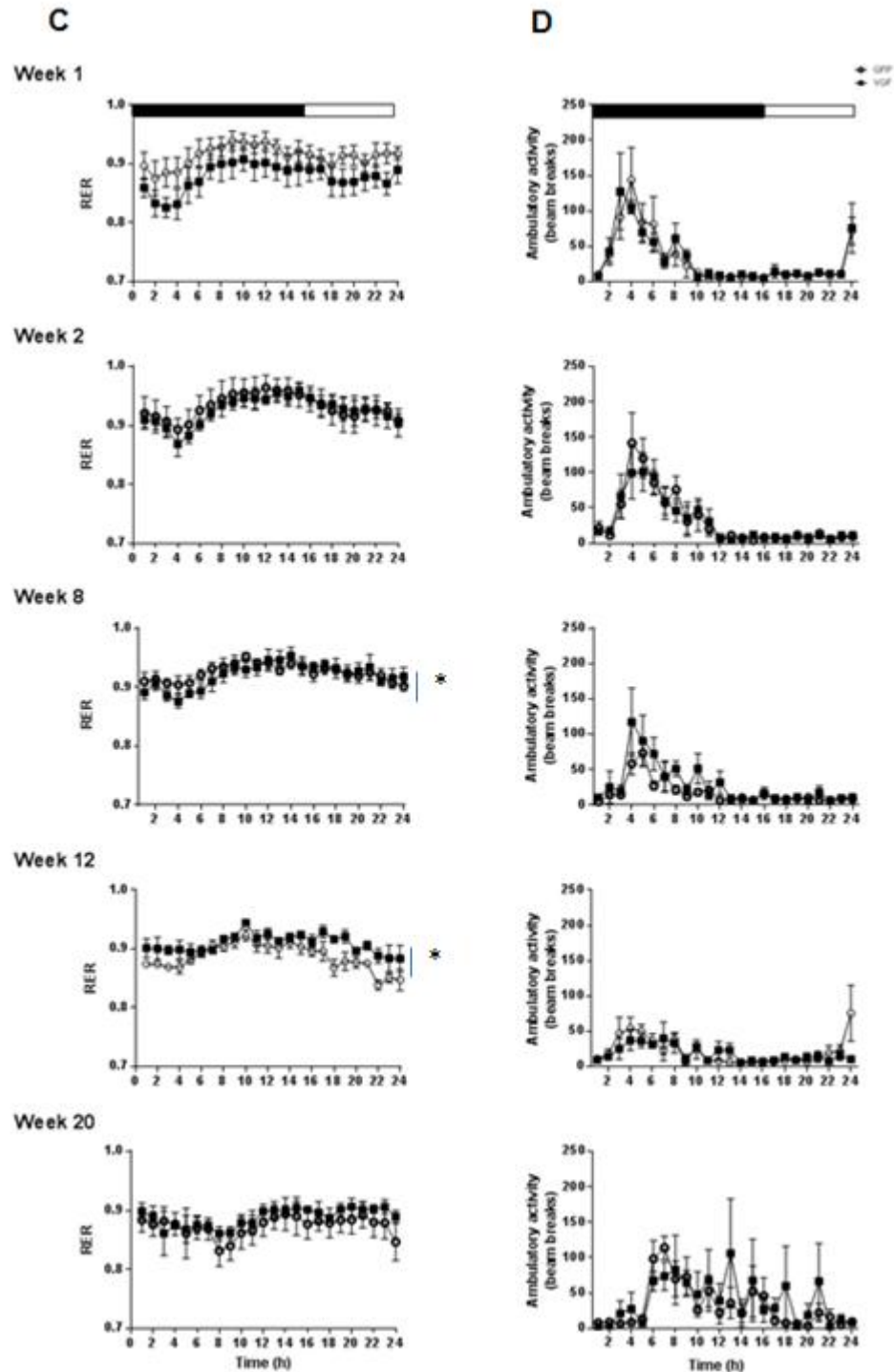


Figure 4.6.3.2: **The metabolic parameters of Siberian hamsters over-expressing VGF mRNA in the hypothalamus was altered.** 24 hour profiles for oxygen consumption (A), carbon dioxide production (B), RER (C) and activity (D) of Siberian hamsters in CLAMS 1, 2, 8, 12 and 20 weeks post transfer to short days (SD). Siberian hamsters received either the control GFP vector (open circles) or the VGF-GFP vector (black squares). Values are group mean ($n = 4, \pm$

SEM). Solid bar indicates the dark phase (16:8 dark: light cycle). Significance values are as indicated: * $p < 0.05$ (vs. control).

4.6.3.3 eGFP expression in the hypothalamus of Siberian hamsters was widespread

Post-mortem analysis of eGFP by fluorescence microscopy revealed widespread expression of eGFP at the end of the study (approximately 32 weeks post infusion) in the hypothalamus and along the cannula infusion tract. GFP expression was observed in all treated and control Siberian hamsters (see Figure 4.6.3.3 A). More specifically, eGFP expression was apparent along the third ventricle (3V), suprachiasmatic nucleus (SCN), LHA, the anterior hypothalamic nucleus, PVN, ARC, VMH and DMN as well as the dmpARC (see Figure 4.6.3.3 B).

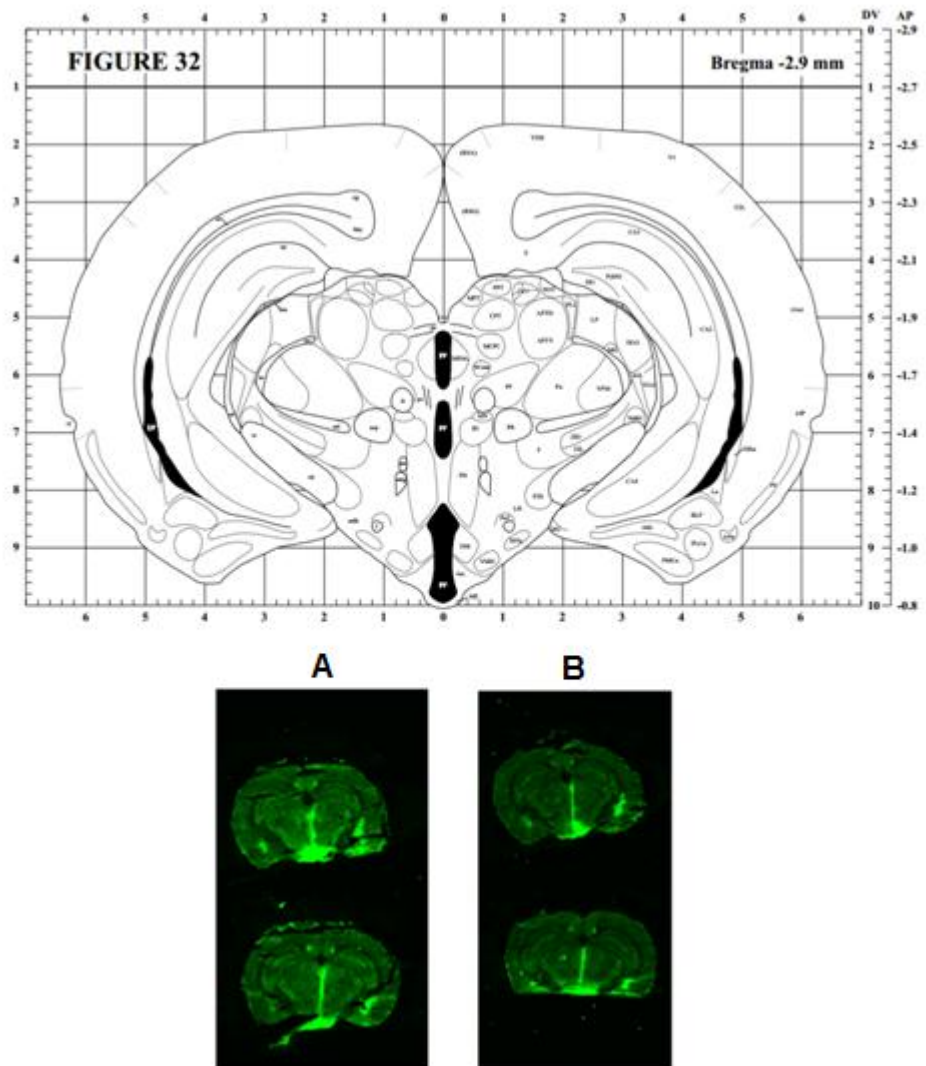


Figure 4.6.3.3 A: **eGFP expression in the hypothalamus of Siberian hamsters.** Examples of the distribution of GFP within the hypothalamus of Siberian hamsters receiving the control vector (A) or the VGF over-expression vector (B).

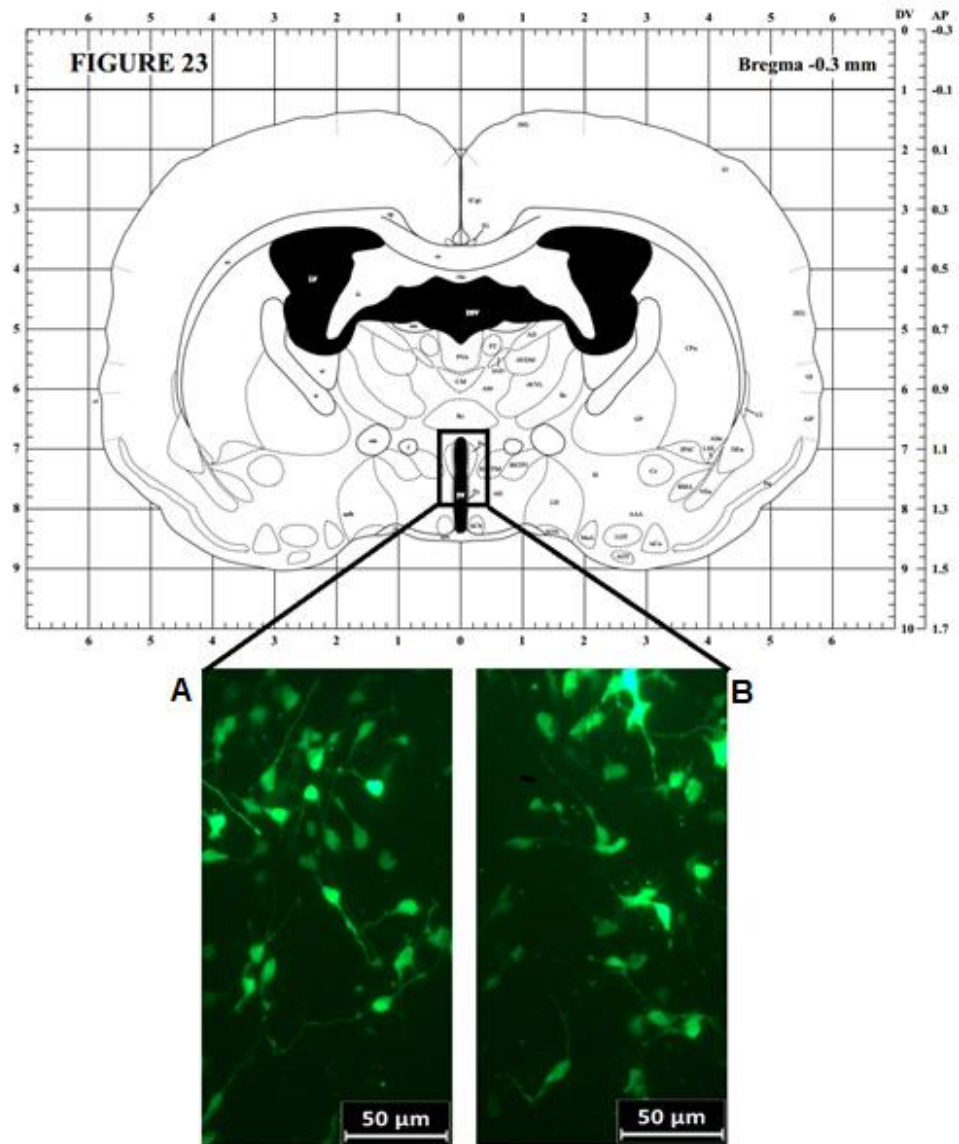


Figure 4.6.3.3 B: **eGFP expression in the PVN of Siberian hamsters.** Examples of the widespread transfection of the cell soma in the region of the PVN. A – AAV-GFP, B – AAV-VGF. Scale bar = 50μm (Adapted from Morin and Wood, 2001).

4.6.3.4 VGF mRNA expression was higher in Siberian hamsters receiving the over-expression vector

To confirm the over-expression by the AAV-VGF vector, VGF mRNA was determined. All Siberian hamsters receiving the VGF vector demonstrated VGF expression that corresponded to the eGFP expression observed by fluorescence microscopy. Although VGF expression was observed in those receiving the control vector, the levels were very low (see Figure 4.6.3.4). Similar to the eGFP expression, VGF expression was apparent along the 3V, SCN, LHA, the anterior hypothalamic nucleus, PVN, ARC, VMH and DMN and dmpARC (see Figure 4.6.3.4).

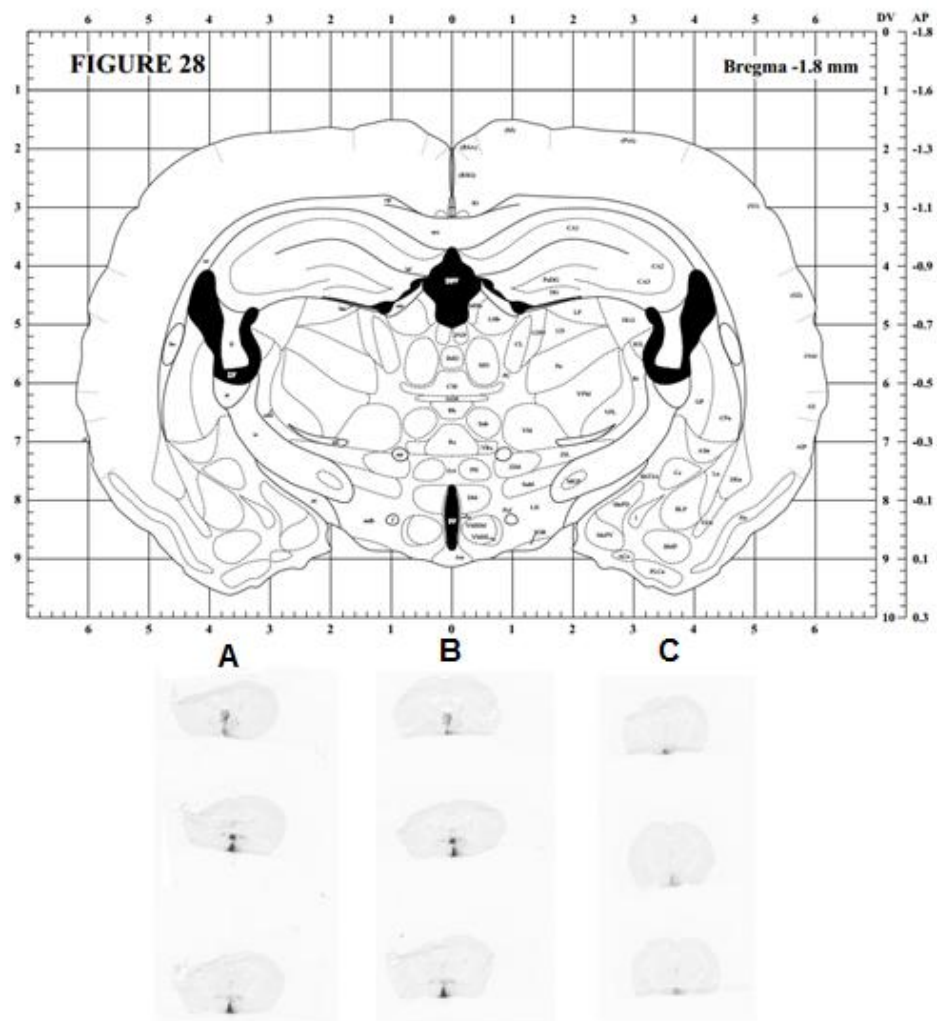


Figure 4.6.3.4: **Examples of the distribution of eGFP and VGF mRNA in the Siberian hamster following SD exposure.** Corresponding in situ hybridisation of eGFP (A) and VGF (B) mRNA in Siberian hamsters infused with the AAV-VGF vector. The AAV-GFP infused control group demonstrated much lower levels of VGF mRNA (C). Expression of both vectors was highest in the arcuate nucleus, with additional expression in the PVN and LHA in Siberian hamsters receiving the AAV-VGF vector (adapted from Morin and Wood, 2001).

4.6.4 Study 3: The effects of VGF over-expression in the hypothalamus of the mouse

4.6.4.1 *Over-expression of VGF mRNA significantly affects food intake and body weight*

Infusion of AAV (GFP control or VGF treatment) into the hypothalamus of mice resulted in a small transient decrease in body weight (see Figure 4.6.4.1 A). However by week 6 there was a greater increase in the body weight of mice receiving the GFP vector, resulting in a significant divergence from the group treated with the VGF vector (treatment vs. time interaction $F = 1.890$, $p < 0.05$) (see Figure 4.6.4.1 A).

Although body weight was lower in the AAV-VGF treated group (compared to controls) there was a trend towards an increase in daily food intake in the home cage (both total and per gram body weight) (treatment vs. time interaction $F = 1.541$, $p = 0.1$ and $F = 1.625$, $p = 0.08$ respectively) (see Figure 4.6.4.1 B and C). As a result there was a significant increase in cumulative food intake (treatment vs. time interaction $F = 3.442$, $p < 0.0001$) and cumulative food intake per gram body weight (treatment vs. time interaction $F = 3.340$, $p < 0.001$) (see Figure 4.6.4.1 D and E). Meal duration at 12 and 16 weeks post infusion tended to be increased in the AAV-VGF group compared to AAV-GFP treated controls (treatment vs. time interaction $F = 2.354$, $p < 0.1$ and $F = 3.242$, $p < 0.05$ respectively), whereas meal frequency was unaffected (see Figure 4.6.4.1 F).

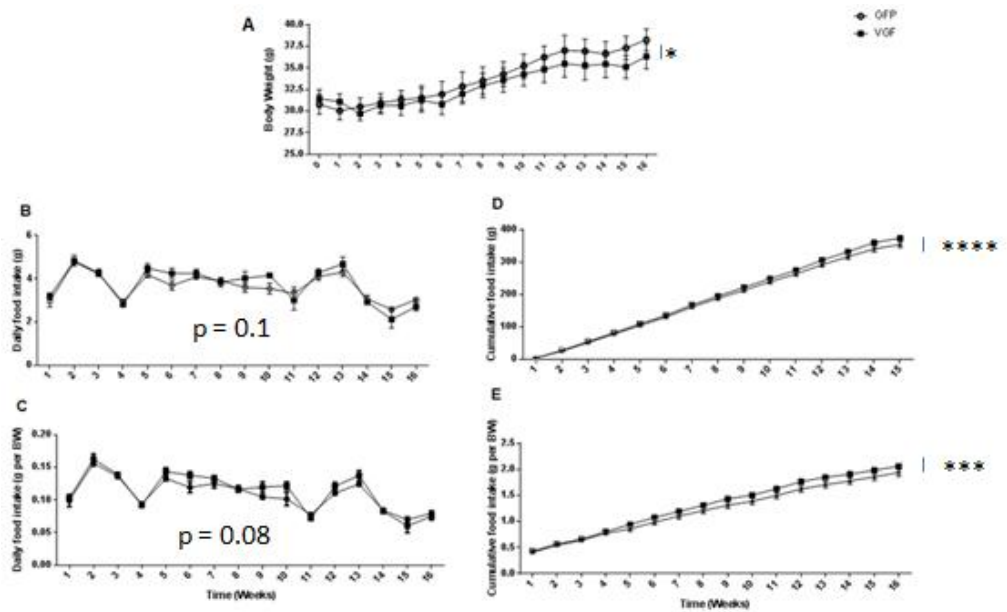


Figure 4.6.4.1: **Despite significantly increased food intake in mice over-expressing VGF mRNA within the hypothalamus, body weight was reduced.** Body weight (A), daily food intake (B), daily food intake per gram body weight (C), cumulative food intake (D) and cumulative food intake per gram body weight (E) of adult male mice receiving bilateral injections of 200nl of either AAV-GFP (as a control, open circles) or AAV-VGF (black squares) at a concentration of 7.2×10^{12} gc/ml for AAV-VGF and 1×10^{13} gc/ml for AAV-GFP (n = 4 per group). Values are group means \pm SEM. Significance values are as indicated: * $p < 0.05$, *** $p < 0.001$, **** $p < 0.0001$ (vs. control).

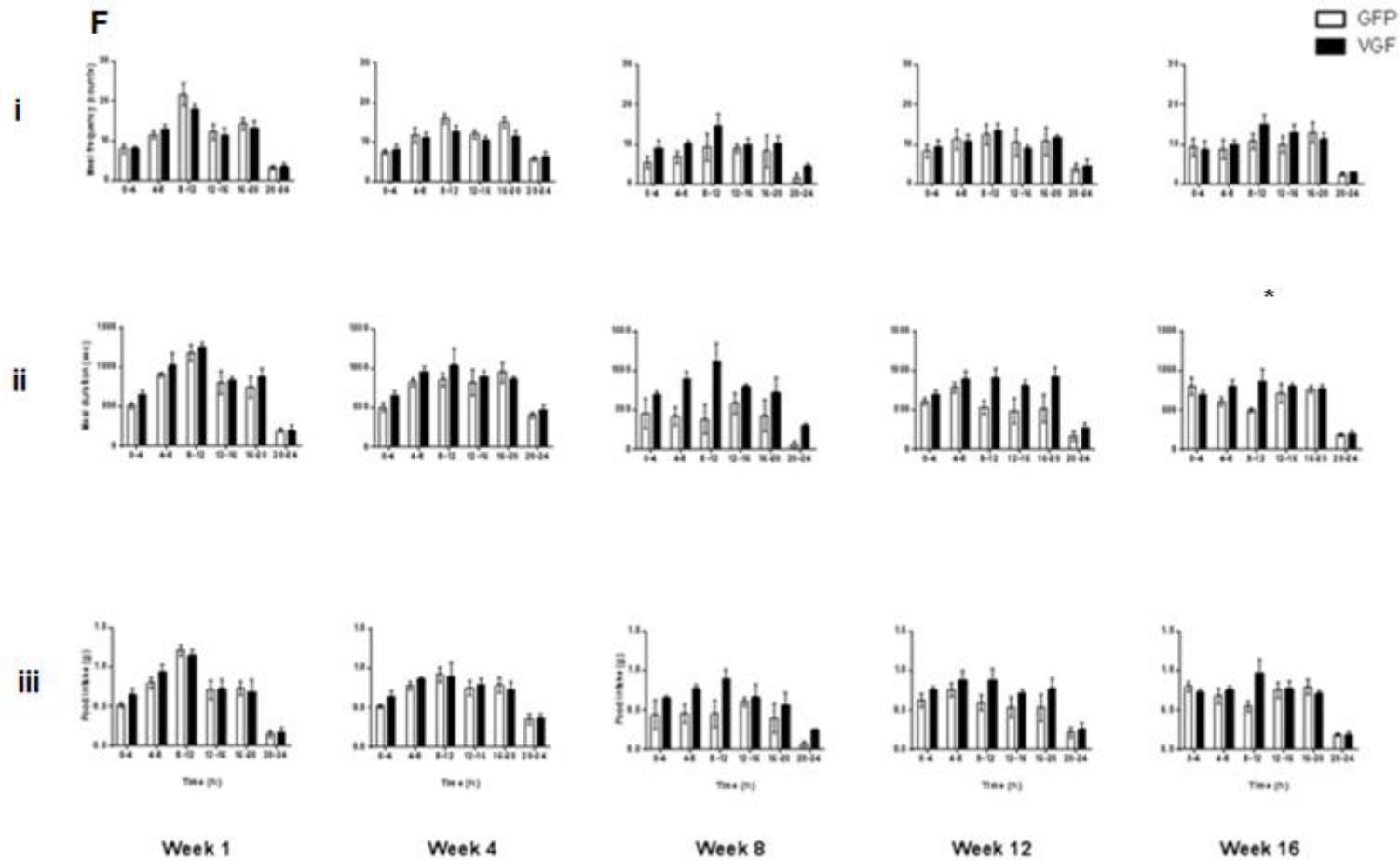
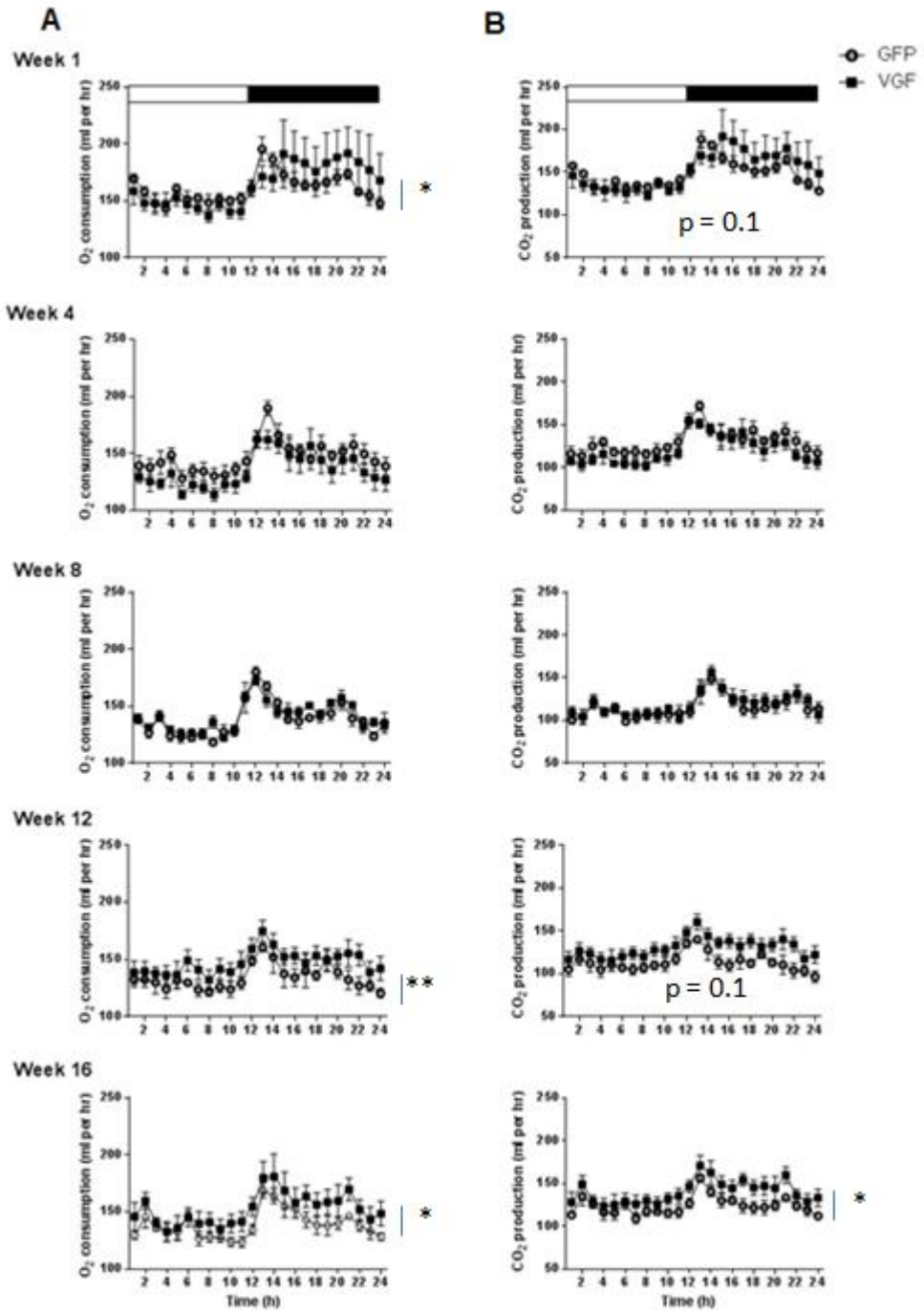


Figure 4.6.4.1 F: **Over-expression of VGF mRNA in the hypothalamus of mice significantly affected feeding behaviour.** 24 hr profiles for meal frequency (i), meal duration (ii) and food intake (iii) of mice in metabolic cages 1, 4, 8, 12 and 16 weeks post viral infusion. Mice received either the control GFP vector (open bars) or the AAV-VGF vector (black bars). Values are group mean \pm SEM (n = 4 per group). Significance values are as indicated: * p < 0.05 (vs. control).

4.6.4.2 Over-expression of VGF mRNA significantly increased oxygen consumption

Oxygen consumption was significantly increased in the dark phase 1 week post infusion in the AAV-VGF treated group compared to AAV-GFP controls (treatment vs. time interaction $F = 1.983$, $p < 0.05$) (see Figure 4.6.4.2 A). This was despite significantly reduced activity in the AAV-VGF treated group compared to controls (treatment vs. time interaction $F = 1.796$, $p < 0.05$) (see Figure 4.6.4.2 D). At 12 and 16 weeks, oxygen consumption was significantly increased in the AAV-VGF treated group for most of the 24 hour period (treatment vs. time interaction $F = 2.275$, $p < 0.01$; $F = 0.2147$, $p < 0.05$), but there were no significant differences at 4 and 8 weeks (see Figure 4.6.4.2 A). At 16 weeks post infusion carbon dioxide production was significantly increased in the AAV-VGF treated group (treatment vs. time interaction $F = 1.796$, $p < 0.05$). Similarly, there was a trend for an increase in carbon dioxide production (treatment vs. time interaction $F = 1.648$, $p = 0.10$; $F = 0.7812$, $p = 0.10$), 1 and 12 weeks post infusion, but no differences at 4 and 8 weeks post infusion (see Figure 4.6.4.2 B). RER was significantly increased in the AAV-VGF treated group 8 weeks post infusion (treatment vs. time interaction $F = 2.790$, $p < 0.01$). There was also a trend for an increase in RER in the AAV-VGF treated group at 1 and 16 weeks post infusion (treatment vs. time interaction: $F = 1.823$, $p = 0.07$; $F = 1.242$, $p = 0.07$), but no differences at 4 and 12 weeks (see Figure 4.6.4.2 C). Activity was unaffected at all other times points (see Figure 4.6.4.2 D).



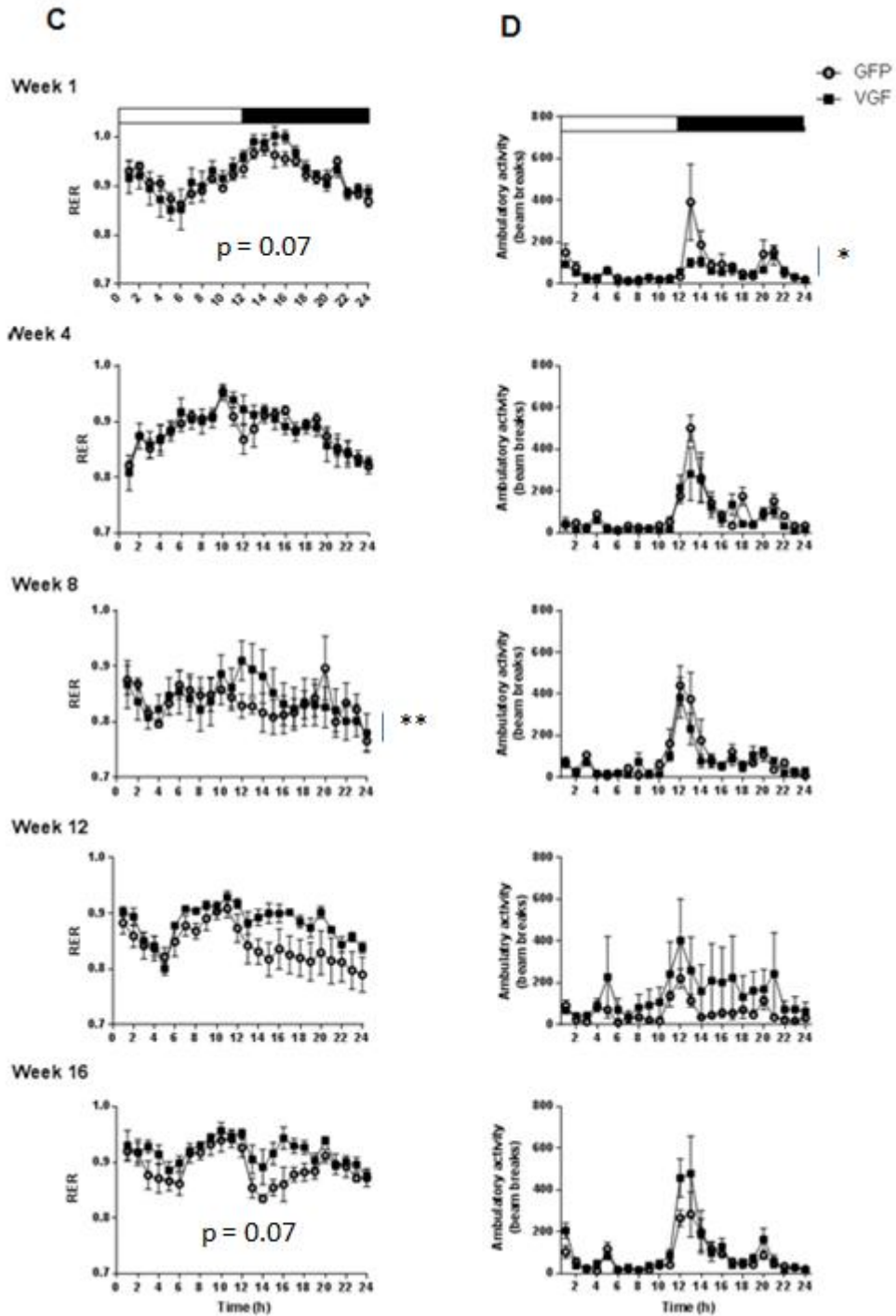


Figure 4.6.4.2: **The metabolic parameters of mice over-expressing VGF mRNA in the hypothalamus were significantly altered.** 24 hr profiles for oxygen consumption (A), carbon dioxide production (B), RER (C) and activity (D) of mice in metabolic cages 1, 4, 8, 12 and 16 weeks post viral infusion. Mice received either the control GFP vector (open circles) or the VGF-GFP vector (black squares). Values are group means \pm SEM, $n = 4$ per group. Solid bar indicates

the dark phase (12:12 light cycle). Significance values are as indicated: * $p < 0.05$, ** $p < 0.01$ (vs. control).

4.6.4.3 Over-expression of VGF mRNA significantly affected the epididymal fat weight

Despite the lack of a positive effect on body weight, there was a significant effect on the mass per gram body weight of the epididymal fat pad between the groups. Initially (by week 4) the epididymal fat pad was significantly increased (unpaired T Test, $p < 0.05$) in the AAV-VGF treated mice (Table 4.6.4.3 A). However, by week 16, the mice which received AAV-VGF, had significantly reduced epididymal fat mass (unpaired T Test, $p < 0.05$) (see Table 4.6.4.3 B).

Table A – Week 4	Liver (mg per g BW)	Epididymal fat pad (mg per g BW)	Brown adipose tissue (mg per g BW)	Subcutaneous fat (mg per g BW)
GFP (n = 4)	38.2 ± 3.40	16.3 ± 3.12	3.3 ± 1.4	6.4 ± 0.98
VGF (n = 4)	31.7 ± 4.81	25.3 ± 1.91 *	1.5 ± 0.32	5.5 ± 0.19

Table B – Week 16	Liver (mg per g BW)	Epididymal fat pad (mg per g BW)	Brown adipose tissue (mg per g BW)	Subcutaneous fat (mg per g BW)
GFP (n =4)	32.9 ± 2.94	53.8 ± 4.8	6.6 ± 1.23	8.2 ± 2.79
VGF (n =4)	35.9 ± 2.85	30.6 ± 9.02 *	6.0 ± 2.58	7.9 ± 0.18

Table 4.6.4.3: **Over-expression of VGF mRNA in the hypothalamus of mice resulted in differential fat mass.** The significant increases in food intake in mice

which over-express VGF mRNA within the hypothalamus resulted in differential fat mass. Initially, there was a significant increase in epididymal fat pad weight in mice which over-expressed VGF mRNA within the hypothalamus (A). However, by 16 weeks post infusion, epididymal fat mass was significantly reduced in the VGF group. Group mean (\pm SEM) tissue weights at the end of the study, 16 weeks post viral infusion. All weights are wet mass per gram body weight. * $p < 0.05$ vs. GFP (n = 4 per group).

4.6.5 Study 4: The effects of VGF over-expression in the hypothalamus of mice transferred to a HFD

4.6.5.1 Over-expression of VGF mRNA significantly increased body weight but food intake was unaffected

As expected, the mice showed a clear and progressive increase in body weight over the 16 weeks of exposure to HFD. The degree of body weight gain in the mice was more significant in the AAV-VGF treated group (200% for VGF vs 177% for GFP, unpaired T test $p < 0.01$) (see Figure 4.6.5.1 A). Despite this effect on body weight, there was no significant effect on the mass per gram body weight for the liver or epididymal and subcutaneous fat. However, there was a trend towards increased BAT weight in the VGF group (GFP: 10.6 ± 1.65 mg; VGF: 14.0 ± 1.41 mg per g BW; $p = 0.09$).

	Liver (mg per g BW)	Epididymal fat pad (mg per g BW)	Brown adipose tissue (mg per g BW)	Subcutaneous fat (mg per g BW)
GFP (n =5)	55.0 ± 4.99	48.1 ± 5.79	10.6 ± 1.65	20.0 ± 5.01
VGF (n =6)	56.71 ± 4.65	56.0 ± 4.52	14.0 ± 1.41	21.4 ± 3.43

Table 4.6.5.1 – **Despite the significant increase in body weight, VGF over-expression had no significant affect on fat depots.** Mean (\pm SEM) tissue weight at the end of the study, 16 weeks post transfer to HFD. All weights are wet mass per gram body weight.

There was a significant increase in daily food intake and cumulative food intake in the AAV-VGF treated group (treatment vs. time interaction $F = 3.623$, $p < 0.0001$ and $F = 7.117$, $p < 0.0001$) (see Figure 4.6.5.1 B and D). However, daily food intake per gram body weight and cumulative food intake per gram body weight were unaffected (treatment vs. time interaction $F = 0.6545$, $p = 0.82$ and

F = 0.28, p = 0.99 respectively) (see Figure 4.6.5.1 C and E), as were meal frequency, duration and food intake in the CLAMS (see Figure 4.6.5.1 F).

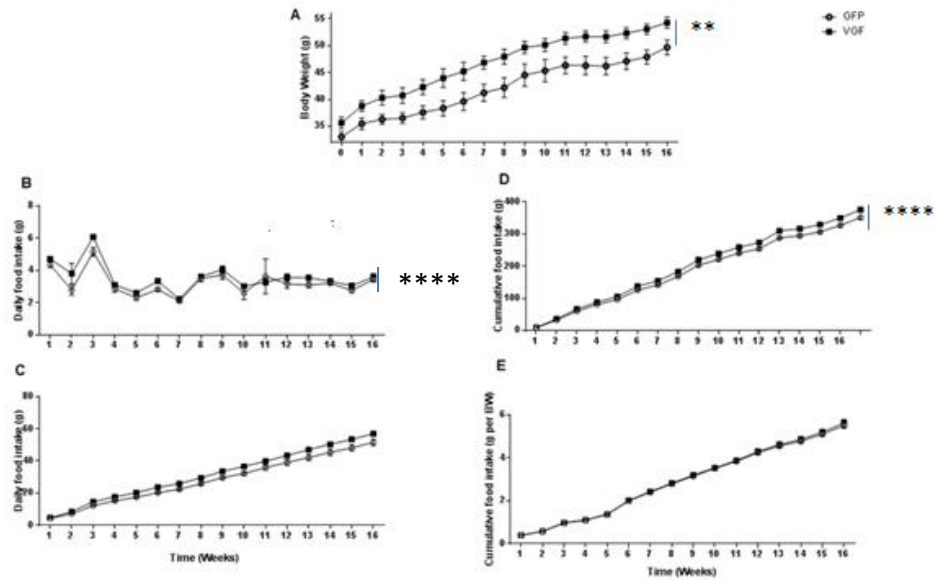


Figure 4.6.5.1: The over-expression of VGF mRNA in the hypothalamus of mice fed a high fat diet (HFD) resulted in significantly increased body weight but unaltered food intake. Body weight (A), daily food intake (B), daily food intake per gram body weight (C), cumulative food intake (D) and cumulative food intake per gram body weight (E) of adult male mice receiving bilateral injections of 200 nl of either AAV-GFP (as a control, open circles) or AAV-VGF (black squares) at a concentration of 7.2×10^{12} gc/ml for AAV-VGF and 1×10^{13} gc/ml for AAV-GFP (n = 5/6 per group) fed a HFD. Values are group means (\pm SEM). ** p < 0.01, **** p < 0.0001 (vs.control).

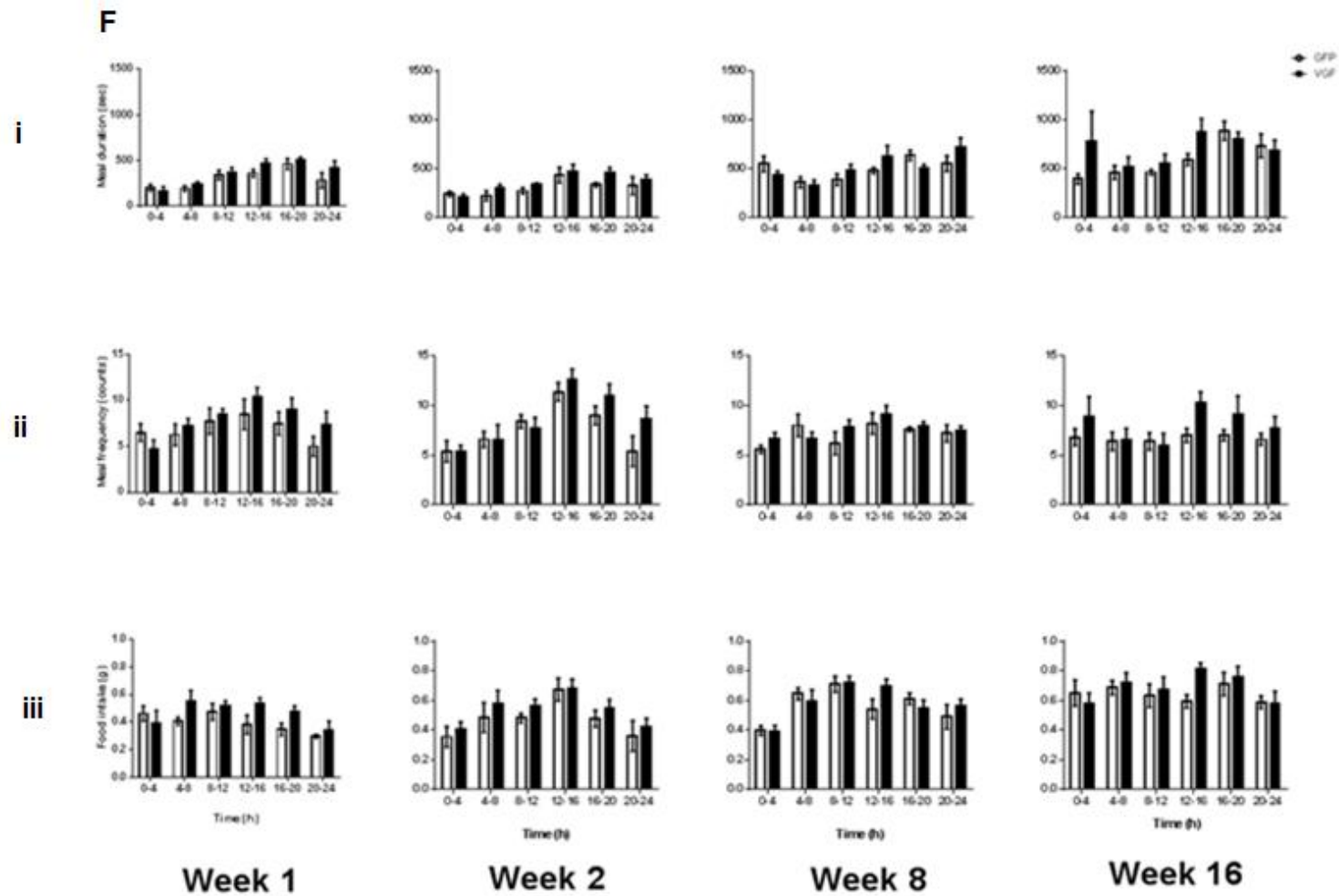
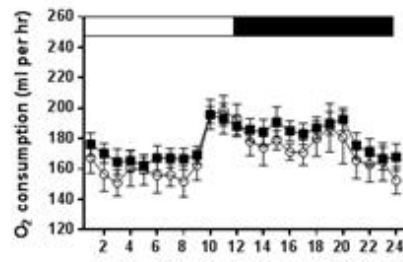


Figure 4.6.5.1 F: **Over-expression of VGF mRNA in the hypothalamus of mice significantly affected feeding behaviour.** 24 hour profiles for meal duration (i), meal frequency (ii) and food intake (iii) of mice in metabolic cages 1, 4, 8 and 16 weeks post transfer to a HFD. Mice received either the control GFP vector (open bars) or the VGF vector (black bars). Values are group mean \pm SEM, n = 5/6 per group.

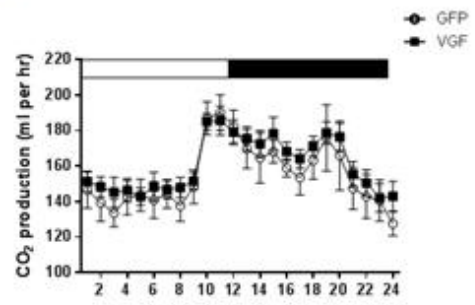
4.6.5.2 Over-expression of VGF mRNA significantly increased RER

There was a trend towards increased oxygen consumption in the AAV-VGF treated group 1 week post transfer to HFD (treatment vs. time interaction $F = 1.676$, $p = 0.09$). This was despite a trend towards decreased activity in the VGF group in week 1 (treatment vs. time interaction $F = 1.445$, $p = 0.09$). However, at 2, 8 and 16 weeks post transfer to a HFD there was no effect on oxygen consumption, carbon dioxide production or activity. There was, however, a significant increase in RER in the VGF group, 8 and 16 weeks post transfer to a HFD (week 8: effect of treatment $F = 13.45$, $p < 0.01$; week 16: treatment vs. time interaction $F = 2.062$, $p < 0.01$) (see Figure 4.6.5.3), but no differences at 1 and 2 weeks.

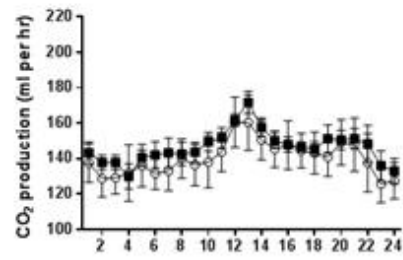
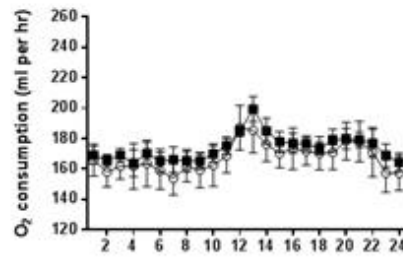
A
Week 1



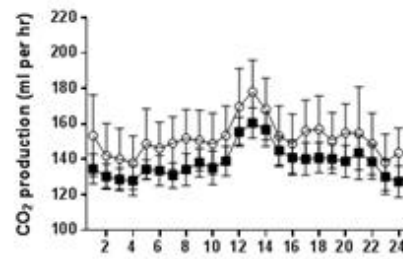
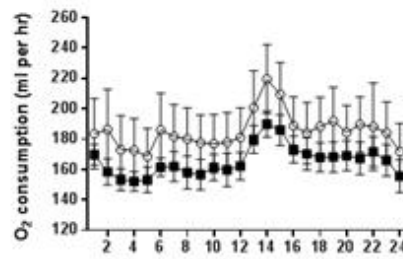
B



Week 2



Week 8



Week 16

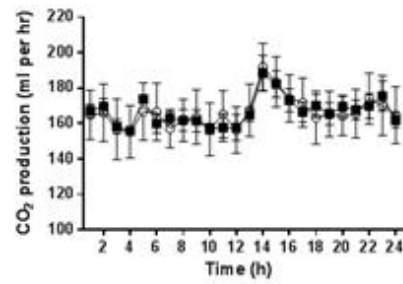
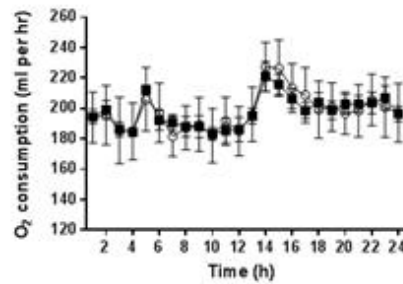


Figure 4.6.5.2: **The metabolic parameters of mice over-expressing VGF mRNA in the hypothalamus was significantly altered 8 weeks post exposure to HFD.** 24 hr profiles for oxygen consumption (A), carbon dioxide production (B), and RER (C) and activity (D) of mice in metabolic cages 1, 2, 8 and 16 weeks post transfer to HFD. Mice received either the control GFP vector (open circles) or the VGF vector (black squares). Values are group mean \pm SEM, n = 5/6 per group. Solid bar indicates the dark phase (12:12 light cycle).

4.6.5.3 Hypothalamic expression of eGFP is similar to Siberian hamsters

Post-mortem analysis of eGFP by fluorescence microscopy revealed widespread expression of eGFP in the hypothalamus and along the cannula infusion tract at the end of the study (approximately 28 weeks post infusion). eGFP expression was observed in all treated and control mice. More specifically, eGFP expression was apparent along the 3V, SCN, the LHA, the anterior hypothalamic nucleus, PVN, ARC, VMH and DMN.

4.6.5.4 In situ hybridisation revealed similar expression to Siberian hamsters

VGF mRNA was determined to confirm the over-expression by the VGF-eGFP vector. All mice receiving the VGF vector demonstrated VGF expression that corresponded to eGFP expression observed by fluorescence microscopy. Although VGF expression was observed in those receiving the control vector, the levels observed were very low. Similar to the eGFP expression, VGF mRNA expression was apparent along the 3V, SCN, LHA, the anterior hypothalamic nucleus, PVN, ARC, VMH and DMN, similar to the results in Siberian hamsters.

4.7 DISCUSSION

To further elucidate the role of VGF in the hypothalamus of Siberian hamsters and mice, VGF mRNA and eGFP were over expressed using a rAAV vector utilising the viral 2A sequence for bicistronic gene expression. The over-expression of VGF in the hypothalamus resulted in reduced body weight gain. Surprisingly, this reduction in body weight was associated with increased food intake and energy expenditure. These effects were attenuated in disrupted models of energy regulation; food intake and energy expenditure were more akin to control Siberian hamsters post transfer SD and mice fed a HFD. The studies presented in this chapter support the notion that global ablation of the VGF gene during the course of development resulted in an errant phenotype. Previous studies have demonstrated that chronic infusion of AgRP increased food intake and decreased oxygen consumption and the capacity of BAT to expend energy (Small et al., 2003), while over-expression resulted in significantly increased food intake, body weight and reduced energy expenditure (see Table 4.1; de Backer et al., 2011). The studies presented in this chapter are more analogous to CART, which has orexigenic and anorectic effects (Dhillon et al., 2002; Kristensen et al., 1998) dependent upon its site of hypothalamic injection (Murphy, 2006). Similarly to VGF over-expression, the over-expression of CART in the ARC of rats resulted in increased cumulative food intake (Kong et al., 2003) a result of increased thermogenic response in BAT.

The studies presented in this chapter demonstrate, for the first time, the effectiveness of the viral 2A sequence *in vivo* in a non-standard laboratory species. The results indicated no adverse effects of the viral 2A peptide and that the 2A peptide mediates co-translational 'cleavage' in the hypothalamus in Siberian hamsters akin to that in other animal models (Trichas et al., 2008). These studies further established the viral 2A peptide as a viable alternative to ires sequences for bicistronic gene expression. It is also clear that gene transfection using a rAAV vector is a highly effective technique for manipulating

gene function *in vivo*, specifically in the hypothalamus of standard and nonstandard laboratory species, and can have profound effects on both physiology and behaviour. rAAV was previously shown to be a highly effective vector for gene transfection by Jethwa et al., (2010), where the over-expression of AgRP in Siberian hamsters resulted in a substantial and prolonged increase in body weight, as a result of increased food intake. The results presented in this chapter have further substantiated it as a viable option for over-expression studies. A previous limiting factor of AAV was the size of 'foreign' DNA which could effectively be packaged – the AAV genome is 4.7Kb - and any construct greater than this subsequently reduced viral titre, affecting over-expression of the transgene (Grieger and Samulski, 2005). However, other larger vectors, such as lentiviruses (LVs), do not transduce the hypothalamus adequately (de Backer et al., 2010). The implementation of the viral 2A peptide (circa 60 bases) is favourable given the size of the ires alternative (up to 1.5Kb) as a way of reducing vector size and therefore improving efficiency of transfection and subsequently viral titre. Furthermore, the viral 2A peptide is more reliable than the ires (as demonstrated recently by Payne et al., 2013).

Thus the studies reported in this chapter were able to use rAAV as a transfection system which consisted of the large VGF gene and eGFP for visualisation. The studies conducted in this chapter demonstrate that over-expression of VGF mRNA produces a complex, yet similar, phenotype in Siberian hamsters and mice. In the Siberian hamster in LD, over-expression of VGF mRNA resulted in a reduction in body weight (compared to GFP controls), possibly due to the increase in oxygen consumption and energy expenditure, which was independent of activity, and despite a significant increase in daily food intake (total and per gram body weight) and cumulative food intake (total and per gram body weight) (all in the home cage). The change in food intake was potentially a consequence of increased meal duration as demonstrated in the CLAMS. The hypothesis therefore is that the changes in body weight are dependent upon the increased energy expenditure observed in the VGF

treated group, but independent of activity, while the increases in food intake may be a compensatory mechanism to limit weight loss. The studies in mice demonstrated that over-expression of VGF mRNA in the hypothalamus resulted in similar effects as those observed in Siberian hamsters. Body weight was significantly reduced in the VGF treated group (compared to controls), possibly due to an increase in oxygen consumption and energy expenditure independent of activity, and despite a trend towards increased daily food intake (total and per gram body weight) and a significant increase in cumulative food intake (total and per gram body weight). Once again, the change in food intake was a likely consequence of increased meal duration demonstrated in CLAMS. However, over-expression of VGF mRNA has differing effects on the fat pads of Siberian hamsters and mice. In the Siberian hamster, BAT weight was significantly increased, while in the mouse, epididymal fat mass in the VGF treated group was significantly reduced (after an initial increase).

Over-expression of VGF mRNA in the hypothalamus did not prevent the transition to the seasonal catabolic state of Siberian hamsters transferred to short day photoperiod, despite a trend for an increase in cumulative food intake (total) and significantly increased cumulative food intake (per gram body weight). However, the epididymal fat pad (per gram body weight) was significantly reduced in the VGF treated group. In mice transferred to a HFD, body weight was significantly increased in the VGF treated group; whilst there was no effect on daily or cumulative food intake (per gram body weight). Daily and cumulative food intake (total), however, were significantly increased. Whilst there was a trend towards an increase in BAT weight (per gram body weight) in the VGF treated group.

4.7.1 The timecourse studies in the Siberian hamster and C57Bl/6J mouse

The increase in food intake may reflect a number of different responses to increased VGF mRNA. The increases in food intake (as observed in the home

cake) may be a result of the observed increases in metabolic parameters in CLAMS, which are independent of activity and therefore an autonomic response designed to maintain energy stores. Alternatively, energy expenditure may increase as a consequence of increased food intake, a process known as diet-induced thermogenesis (Westerterp, 2004). In the Siberian hamster, increases in food intake are parallel with increases in energy expenditure. While in the mouse increases in food intake are apparent before the increases in energy expenditure. This results in an initial significant increase in epididymal fat (per gram body weight) before a long term reduction was apparent (Table 4.6.4.3).

In response to cold exposure, mice increase metabolic rate and activate BAT (Ravussin et al., 2014). Watson et al., (2009) demonstrated that VGF^{-/-} mice display reduced accumulation of fat, along with an up-regulation of uncoupling proteins (UCPs) in BAT. However, despite this up-regulation, VGF^{-/-} mice were cold intolerant. BAT contains an abundance of mitochondria, which uniquely express UCP-1 which dissipates the proton gradient of the inner mitochondrial membrane that is formed as a result of oxidative phosphorylation, resulting in heat production (Schulz and Tseng, 2013). This process is known as non-shivering/adaptive thermogenesis. In the mouse, the absence of UCP-1 was associated with increased body weight (Feldmann et al., 2009; Lowell et al., 1993), while surgical denervation or excision of BAT in mice resulted in increased body weight (Dulloo and Miller, 1984). BAT metabolism is accompanied by specific cerebral activation, including the thalamus (Orava et al., 2014). Furthermore, BAT has a rich sympathetic nerve and vascular supply (Rosenbaum and Leibel, 2010); its activation is dependent on thyroid hormone receptors (TRs) (Alkemade, 2010) and adrenoreceptors (Chernogubova et al., 2005). Recent studies have suggested a role for BAT in humans (Cypess et al., 2009; Ouellet et al., 2012); functional BAT's metabolic activity was reduced in the obese (Nedergaard et al., 2007), while activation of BAT increased whole-body energy expenditure; a direct consequence of increased oxidation of

glucose and fatty acids (Bartelt et al., 2011; Cannon and Nedergaard, 2004). The increased energy expenditure in Siberian hamsters and mice as a result of over-expression of VGF was not a consequence of increased locomoter activity. Over-expression did, however, result in significantly increased BAT weight in the Siberian hamster. Despite significantly increased food intake, there was no significant effect on the epididymal or subcutaneous fat pads. When rodents are placed in a cold environment, their body temperature is acutely defended by shivering thermogenesis via muscle contractions (van der Lans et al., 2013). Prolonged exposure results in a decrease in shivering, however energy expenditure remains elevated; in rodents this was attributed to increased BAT (Nedergaard et al., 2001). A recent study (van der Lans et al., 2013) demonstrated a similar finding in humans. These studies suggest (as a working hypothesis) that the over-expression of VGF in the hypothalamus of Siberian hamsters activates BAT, the result of which is an increase in food intake to maintain body weight. Kong et al., (2003) demonstrated the over-expression of CART in the ARC of rats resulted in increased cumulative food intake due to an increased thermogenic response in BAT; a similar phenotype of that of the Siberian hamster presented in this chapter.

However, the over-expression of VGF mRNA in mice did not significantly affect BAT. Indeed, increases in food intake were seen before increases in energy expenditure in the mouse, so that epididymal fat was significantly increased at 4 weeks post infusion in the studies reported in this chapter. Previous studies have demonstrated an increased in epididymal fat pad weight in response to increased food intake (Sousa-Ferreira et al., 2011). Long term over-expression of VGF mRNA, however, resulted in a significantly increase in energy expenditure and a significant reduction in epididymal fat. Previous studies have demonstrated a reduction in epididymal fat pad weight as a consequence of increased metabolic rate (Adams et al., 2006). An increase in BAT would result in a more metabolically active animal; similarly, a reduction in epididymal fat is associated with metabolic recovery (Takada et al., 2008). The mechanistic

difference of increased energy expenditure was akin to the catabolic difference exerted by the TLQP-21 peptide in mice (Bartolomucci et al., 2006) and Siberian hamsters (Jethwa et al., 2007). ICV TLQP-21 infusion in Siberian hamsters did not affect oxygen consumption, carbon dioxide production, RER or activity (Jethwa et al., 2007). TLQP-21 did, however, have a profound catabolic effect reducing food intake and meal size (Jethwa et al., 2007). TLQP-21 infusion in mice increased resting energy expenditure (Bartolomucci et al., 2006).

In support of this mechanistic difference, the increased energy expenditure displayed by mice as a result of ICV infusion of TLQP-21, was not accompanied by increased gene expression of β 3-AR or UCP-1 in BAT (Bartolomucci et al., 2006). Therefore it was inferred that activation of BAT thermogenesis was not the primary mediator of the effects observed. However, an increase in UCP-1 gene expression was observed in WAT, as well as β 3-AR and PPAR- δ gene expression (Bartolomucci et al., 2007). This 'beige-ing' of WAT, to become more BAT-like, could be responsible for alterations in energy expenditure. Furthermore, NERP-2, an N terminal VGF derived peptide, was shown to colocalise with the orexins, a family of neuropeptides that induce feeding behaviour and increase energy expenditure via stimulation of sympathetic nerve activity in the LHA. Indeed, ICV infusion of NERP-2 increases food intake and energy expenditure in rats via the orexin system (Toshnai et al., 2010). Mice which over-express orexin are resistant to diet induced obesity as a result of increased energy expenditure despite significantly increased daily food intake (Funato et al., 2009).

VGF mRNA co-localised with POMC in the fed state, and NPY in the fasted state (Hahm et al., 2002; Saderi et al., 2014). This is a remarkable characteristic – NPY neurones which are challenged by energy depletion, express VGF during fasting, while POMC neurones, which are active when energy balance is positive, express VGF in ad libitum fed animals, as well as those refed following

a fast. The recently published Saderi et al., (2014) data suggested that VGF was expressed within the NPY/POMC neurones of the hypothalamus in response to metabolic condition and whichever the more active neurones, the higher level of VGF. A similar analogy can be drawn from the response of VGF following salt loading in the PVN (Mahata et al., 1993) and light stimulation in the SCN (Wisor and Takahashi, 1997). Here over-expression of VGF mRNA in the Siberian hamster and mouse resulted in increased food intake. As VGF is expressed under all conditions in the POMC neurones (Saderi et al., 2014) – increases in expression may be less consequential. It is therefore postulated this may account for the increased food intake demonstrated by the Siberian hamsters and mice respectively. These studies may highlight the inherent evolutionary bias towards increased food intake in the energy homeostasis system. The ability to defend body fat in times of food deprivation is greater than the need to protect against weight gain (Schwartz et al., 2003).

The findings of the studies presented in this chapter and those of Bartolomucci et al., 2006 and Jethwa et al., 2007, which utilised the VGF derived peptide TLQP-21, however, are in stark contrast with the VGF^{-/-} mouse, which was hypermetabolic and hyperactive (Hahm et al., 1999). The complex phenotype produced by the VGF^{-/-} (Hahm et al., 1999) is a likely consequence of global ablation of the gene and its derived peptides during development, as well as in the adult. Hahm et al., (1999) postulated that an increase in VGF expression in the hypothalamus of mice would increase food intake and body weight, while energy expenditure would decrease, resulting in an obese phenotype. These studies demonstrate while over-expression of VGF mRNA in the hypothalamus of mice increased food intake, body weight is reduced as a result of increased energy expenditure.

4.7.2 VGF over-expression in disrupted models of energy homeostasis

In the SD study, daily food intake (total and per gram body weight) and energy expenditure were unaffected by the over-expression of VGF mRNA – its effects were therefore reduced in SD. There was, however, a trend for an increase in cumulative food intake (total) and a significant increase in cumulative food intake (per gram bodyweight). Despite these increases the long term seasonal regulation of body weight persisted in the Siberian hamster. The 20 week exposure to SD resulted in a reduction in body weight, the development of the white winter pelage and a reduction in paired testes weight. The degree of body weight loss, in response to photoperiod, was similar between the VGF treated and GFP control groups; weight loss was unaffected by treatment. This further supports the hypothesis that the response to photoperiod is a distinct neuroendocrine process (Jethwa and Ebling, 2008). Three Siberian hamsters failed to respond to SD, however, this was not associated with treatment as two of the Siberian hamsters which failed to respond received the GFP vector. A failure to respond to SD has been noted in Siberian hamsters in our colony (Jethwa et al., 2010) and in others (Freeman and Goldman, 1997).

Previous research has demonstrated the reduction in body weight is a reflection of reduced caloric intake (Knopper and Boily, 2000), while other groups hypothesise increased energy expenditure is response for the development of the SD phenotype (Wade and Bartness, 1984). Warner et al., (2010), demonstrated an initial, transient increase in oxygen consumption, heat production and locomotor activity in response to SD, with a subsequent decrease in caloric intake. This supports their hypothesis that energy expenditure underlies the initial phase of weight loss in the Siberian hamster in response to SD photoperiod. These studies demonstrated that VGF mRNA significantly increased food intake. In a similar study, conducted by Jethwa et al., (2010), over-expression of AgRP increased food intake and decreased energy expenditure in the Siberian hamster, effects which did not block the

seasonal catabolic response. Furthermore, several studies have failed to identify gene expression changes in the major homeostatic genes in the hypothalamus, namely NPY, AgRP, POMC, CART, orexin and thyrotropin-releasing hormone (Ebling et al., 1998; Mercer et al., 1995; Mercer et al., 2000, Rousseau et al., 2002). Taken in combination with the findings presented in this chapter these studies provide further evidence indicating that seasonal cycles of weight loss are not simply effected by a readjustment of the homeostatic mechanisms.

Barrett et al., 2005 demonstrated an up-regulation of VGF mRNA in the dmPAC, a major site of gene expression change in response to photoperiod, in Siberian hamsters. However, expression across the remainder of the ARC, is lower in SD (Barrett et al., 2005). As an adaptation to survive winter, the Siberian hamster undergoes physiological and behavioural adaptations, including the increased capacity for thermogenesis. Furthermore, the thermogenic capacity of BAT is increased in the Syrian hamster exposed to SD (McElroy et al., 1986) – interscapular BAT pads from SD hamsters were 53% heavier and contained comparably more protein and DNA. Demas et al., (2002) demonstrated that there was an increase in UCP-1 and PPAR- γ in Siberian hamsters in SD, as well as an increase in lipid mobilisation and utilisation, suggesting BAT is more active. This may explain why the effects of VGF mRNA over-expression are attenuated in SD. Indeed, BAT is no longer significantly increased. However epididymal fat was significantly reduced – a possible consequence of initial increases in energy expenditure.

A recent study of prohormone convertases 1 (PC1/3) and 2 (PC2) gene expression in the hypothalamus of Siberian hamsters found that SD induced PC2 within the ARC. The results indicate that a major part of neuroendocrine body weight control in seasonal adaptation may be affected by post-translational processing mediated by these enzymes (Helwig et al., 2006).

Furthermore, starvation in rats results in decreased PC1 and PC2 gene and protein expression in the PVN, which is reversed by exogenous leptin administration (Sanchez et al., 2004). The VGF pro-polypeptide undergoes endoproteolytic processing by the PCs – alterations in their expression may favour one or more of the VGF derived peptides, which may result in alterations in food intake and/or energy expenditure. The studies presented in chapter 3 demonstrated the initial opposing roles of the VGF derived peptides, HHPD-41 and TLQP-21 following ICV infusion. Bartolomucci et al., (2006) and Toshinai et al., (2010) have shown that TLQP-21 increases resting energy expenditure in mice and NERP-2 increases food intake and energy expenditure in rats, respectively. It is therefore possible that the panel of VGF derived peptides alters with photoperiod, producing differential effects.

The post mortem analysis of fluorescence emitted by eGFP and of *in situ* hybridisation for VGF mRNA performed 32 weeks post infusion of viral vectors revealed a high number of cells, over a large area of the brain, expressed the vectors. Despite the bilateral infusion of 200nl and a micropipette tip of 30µm, it was apparent that cells up to 300-400µm expressed the vector. Cells more dorsal in the brain adjacent to the tract of the micropipette also expressed the vectors. Higher lateral expression was noted in some of the animals, a reflection of a technical issue with the infusion of viral vectors at low volumes through small diameters. Nevertheless, the widespread expression of GFP (and VGF mRNA as confirmed by *in situ* hybridisation), induced a significant increase in food intake and energy expenditure in Siberian hamsters. The strategy was to target the infusion of the vector at the ARC because it was a demonstrated site of expression within the hypothalamus. The studies presented in this chapter have demonstrated an increase in VGF mRNA in the ARC, dmpARC, PVN, the LHA, VMN, DMN and the area surrounding the third ventricle, as well as along the infusion tract.

Similar to the findings in Siberian hamsters transferred to SD, C57Bl/6J mice fed a HFD develop obesity. The over-expression of VGF mRNA resulted in significantly increased body weight. As a result, daily and cumulative food intakes (total) were significantly increased. However, the previously observed increases in daily and cumulative food intakes per gram body weight were no longer apparent. This is a possible effect of the increased palatability of the HFD. At the latter time points, RER was significantly increased in mice which over-expressed VGF mRNA, however this may have been a consequence of their increased body weight compared to controls. There was no significant effect on tissue weights, however there was a trend for an increase in BAT in the VGF group.

Recent studies have found that mice fed a HFD increased norepinephrine-induced thermogenesis, an effect which was not observed in UCP-1^{-/-} mice (Feldmann et al., 2009). If the working hypothesis is true (VGF activates BAT) the capacity for increased thermogenesis will be reduced as a result of exposure to HFD, similar to the Siberian hamsters in SD. This hypothesis is further supported by Watson et al., (2009) who demonstrated VGF^{-/-} mice were cold intolerant. It has been previously demonstrated that VGF mRNA increases in the hypothalamus in response to fasting and these increases are normalised by leptin delivery (Hahm et al., 1999). Lin et al., 2010 demonstrated mice switched to a HFD maintain energy intake for 4 weeks, parallel to controls fed a standard diet. By week 8, the HFD group began a gradual increase in energy intake, which increased further at 15 weeks. This corresponded to the ability of mice to respond to leptin; 1 week post transfer to a HFD, the mice retained the ability to respond to exogenous leptin delivery. However, by week 8, exogenous leptin did not affect food intake or body weight. By week 19, ICV infusion of 0.1µg leptin demonstrated no significant effect on food intake or body weight on mice fed a HFD (Lin et al., 2010). It is therefore possible that mice fed a HFD lose the ability to respond to VGF due to alternations in the leptin signalling pathway.

Similar to the Siberian hamster study, the post mortem analysis of fluorescence emitted by eGFP and of immunoreactivity performed 32 weeks post infusion of viral vectors revealed a high number of cells, over a large area of the brain, expressed the vectors in mice.

4.8 CONCLUSION

In conclusion, the over-expression of VGF in the hypothalamus produced a reduced body weight phenotype, as significant increases in food intake are offset by significant increases in energy expenditure. However, when energy homeostasis is challenged by photoperiod or diet, the effects of VGF mRNA over-expression are diminished, possibly due to alterations in BAT activity. This supports the hypothesis that the VGF gene has opposing effects on energy homeostasis and that global ablation of the VGF gene during the course of development resulted in an errant phenotype.

5 Chapter 5 – THYROID HORMONE (T3), IN VITRO, REPRESSES VGF ENDOGENOUS EXPRESSION AND PROMOTER ACTIVITY; A NOVEL, POSSIBLE MECHANISM FOR THE SEASONAL REGULATION OF APPETITE

5.1 THE HYPOTHALAMUS-PITUITARY-THYROID (HPT) AXIS

The hypothalamic-pituitary-thyroid (HPT) axis is paramount in the control of metabolic processes in vertebrate organisms (Costa-e-Sousa and Hollenberg, 2012). The HPT axis is regulated by the secretion of thyrotropin-releasing hormone (TRH), a tripeptide produced by the PVN (Lechan and Fekete. 2004), which travels across the ME to stimulate the release of thyroid-stimulating hormone (TSH) from the anterior pituitary into the circulation (Bianco and Kim, 2006). TSH stimulates the release of thyroid hormones (THs) from the thyroid gland. Although there is evidence for the non-genomic actions of TH (Davis et al., 2008), many of the effects of TH are mediated by the genomic pathway which requires the activation of thyroid hormone receptors (TRs) (Senese et al., 2014). TRs belong to a nuclear receptor (NR) superfamily, which include retinoic acid (RAR) and vitamin D (VDR) receptors, as well as peroxisomal proliferator receptors (PPARs) (Yen et al., 2006), and regulate energy homeostasis (Barker, 1951; Silva, 1995). The biologically active form of TH, 3,5,3'-triiodothyronine (T3), stimulates basal metabolic rate (Decherf et al., 2010), energy expenditure in peripheral tissues (Kim, 2008) and energy homeostasis in the brain (Herwig et al., 2009). Lopez et al., (2010), demonstrated increases in metabolic rate induced by TH involved the inhibition of AMP-activated protein kinase (AMPK) in the hypothalamus, resulting in heat production in BAT via the sympathetic nervous system. In support of this, in humans, hyperthyroidism results in increased catabolism and therefore weight loss, while hypothyroidism results in weight gain (Silva, 1995). Along with its precursor, thyroxine (T4), THs influence gene expression in virtually every vertebrate tissue via TRs with specific target gene promoters, enhancing or repressing transcription (Bianco and Kim, 2006).

The activation and deactivation of the THs is via the iodothyronine deiodinases, of which there are three types – these enzymes regulate TH via the removal of specific moieties from the precursor molecule, T4 (Bianco and Kim, 2006). The enzymatic conversion of T4 into the biologically active T3 is governed by

deiodinase 2 (DIO2). Whereas deiodinase 3 (DIO3) converts T4 to the inactive reverse T3 and thereby converts T3 to an inactive form (Ebling, 2014). DIO1 activates or inactivates T4 on an equimolar basis (Bianco and Kim, 2006) as it can function as an outer or inner ring deiodinase (Maia et al., 2011). In the Siberian hamster, there is high gene expression of DIO2 in LD and relatively low DIO3 expression. Exposure of Siberian hamsters to SD reverses gene expression – DIO2 is reduced, while DIO3 is up-regulated (Barrett et al., 2007; Watanabe et al., 2004). These patterns of expression have also been noted in photoperiodic species of rat (Ross et al., 2011) and mice (Ono et al., 2008). The availability of T3 to the hypothalamus in the Siberian hamster is therefore controlled by the expression of DIO2 and DIO3 within cells which line the third ventricle (tanycytes) (Herwig et al., 2013). It has been postulated that more than 75% of nuclear T3 in the brain is derived from this conversion – therefore the expression and activity of these enzymes is key to determining availability within the hypothalamus (Hazlerigg and Loudon, 2008). The enzymatic profiles suggest that T3 availability is reduced in response to SD photoperiod.

In a study conducted by Barrett et al., (2007), where Siberian hamsters maintained in LD were microimplanted with 10µg of T3, estimated to release 100pg of T3 per day, the changes associated with exposure to SD (reduction in food intake, decreased body weight as a result of decreases in intra-abdominal fat depots and testicular regression) were completely prevented. Furthermore, systemic administration of T3 blocked testicular regression in Siberian hamsters (Freeman et al., 2007). Siberian hamsters maintained in SD, which received intrahypothalamic T3 implants, underwent an anabolic response, akin to control animals transferred to LD (Murphy et al., 2012). Furthermore, Siberian hamsters with the intrahypothalamic T3 implants did not display torpor bouts in SD (Murphy et al., 2012). T3 acts on the hypothalamic neurones of the ARC and PVN as a short-term signal of energy deficit imposed by starvation (Boelen et al., 2008; Coppola et al., 2007; Fekete and Lechan, 2007; Lechan and Fekete, 2006). These studies demonstrate the important role of

thyroid hormone availability in the regulation of seasonal energy metabolism in the Siberian hamster (Ebling, 2014). VGF mRNA expression is greater in the dorsomedial posterior arcuate nucleus (dmpARC) in Siberian hamsters in response to short photoperiod (Barrett et al., 2005) however expression across the remainder of the ARC is greater in LD (Jethwa et al., 2007). It has been hypothesized that hypothalamic thyroid hormone availability plays a key role in the seasonal regulation of appetite and body weight, since a reduction in local availability of T3, implicated by the changes in gene expression of the DIO enzymes, in SD results in hypophagia and weight loss (Murphy et al., 2012).

5.2 THYROID HORMONE RECEPTOR (TR)

TH receptors (TRs) are transcription factors, which are ligand-regulated, binding TH, as well as specific DNA-sequences known as thyroid hormone response elements (TREs), which are located within the promoter regions of target genes (Yen et al., 2006). Similar to other NRs, TRs contain two 'zinc finger' motifs and a carboxy-terminal ligand binding domain, functionally important for heterodimerisation with the retinoid X receptor (RXR) (Yen et al., 2006). The ligand binding domain's structure indicates upon binding, ligands induce a conformational structural change which favours the dissociation of suppressors and the recruitment of activators (Cheung et al., 2010). A subset of NRs, which includes TR and RAR, regulate transcription in the presence or absence of ligand binding (Glass and Rosenfeld, 2000). TRs are derived from two genes on different chromosomes (Cheung, 2000) – TR α and TR β . TR α produces two proteins, TR α -1 and c-erbA α -2, the latter of which is unable to bind TH and therefore prevents TR-mediated transcription. TR β also produces two proteins, TR β -1 and TR β -2 (Yen et al., 2006), which bind T3 with high affinity and mediate TH-regulated transcription. Glass (1994), proposed that the ability of TRs to bind to, and therefore regulate transcription of, a number of DNA sequences is a consequence of their likely heterodimerisation with RXRs, which have the ability to heterodimerise with other NRs, for example VDRs. Furthermore, heterodimerisation increases binding of TRs to TREs, the

responsiveness of TR to T3 and the transcriptional activation (Zhang and Kahl, 1993).

5.3 THYROID HORMONE RESPONSE ELEMENT (TRE)

The consensus TRE sequence as proposed by Wu et al., (2000) is AGGTCA, often arranged as directed repeats (Brent et al., 1992). de Luca (1991) identified the TRE, AP-1 and vitamin D response element (VDRE) as working in combination with the retinoic acid response element (RARE). TRs were previously found and characterised in the SH-SY5Y cell line (Goya and Timiras, 1991).

TREs can positively or negatively regulate transcription (Decherf et al., 2013); 3 separate TRE half sites have been identified in the *Trh* promoter, which act in combination repressing gene expression (Satoh et al., 1996). Energy homeostasis requires the co-ordination of activity of distinct hypothalamic nuclei, which dictate food intake and energy expenditure. α MSH and its receptor MC4R is a key component of these processes (Gauthier et al., 2001) – mutations in the human receptor are associated with obesity and mice lacking the MC4R gene are also obese. Furthermore, adeno-associated virus-mediated knockdown of the MC4R in the PVN of the hypothalamus promotes high-fat diet-induced hyperphagia and obesity (Garza et al., 2008). Another component of these processes is T3, a determinant of metabolic rate (Silva, 1995). Mutation of the TRE within the promoter region of MC4R increases promoter activity and results in the loss of T3 dependent repression of gene expression. The sequence occurs in the proximal region of the promoter, in close proximity to a CAAT box (Lubrano-Bertheliet et al., 2003), evidence for a role for TRs in the transcriptional machinery/regulation of the MC4R gene by T3 (Decherf et al., 2010). Increased T3 reduces hypothalamic sensitivity to AgRP signalling and other MC4R ligands (Decherf et al., 2010), while repression of the MC4R would stimulate orexigenic pathways through NPY signalling (Coppola et al., 2007; Ishii et al., 2003). Furthermore, MC4R mRNA levels in the ARC and VMH of

Siberian hamsters are significantly affected by photoperiod – expression in LD is lower than that in SD (Ellis et al., 2008), where DIO2 expression is higher, reducing the hypothalamic availability of T3, reducing gene suppression.

5.4 VITAMIN D (1,25-DIHYDROXYVITAMIN D₃ (1,25D₃))

Vitamin D and its activated metabolite 1,25-dihydroxyvitamin D₃ (1,25D₃) is essential for normal insulin secretion from the rat pancreas (Kadowaki and Normal, 1984); deficiency in vitamin D results in the inhibition of pancreatic secretion of insulin (Norman et al., 1980). Replacement therapy with the active metabolite 1,25D₃ reverses impaired glucose tolerance. 1,25D₃ exerts its effects as a ligand for the VDR (Nuclear Receptors Nomenclature Committee); a nuclear hormone receptor that regulates gene expression as a vitamin D dependent transcription factor. Like T3, its action is exerted by binding, preferentially as a heterodimer with the RXR, to a specific sequence – the vitamin D response element (VDRE) (Calle et al., 2008). The VDRE consists of two direct and imperfect repeats of six nucleotides separated by three nucleotides (Calle et al., 2008). Whilst the VDR occupies the 3' site, RXR binds to the 5' site (Haussler et al., 1998). There are two consensus VDRE sequences 5'GGGTCANNGGGGCA3' (Maestro et al., 2003) and 5'PuGGTCANNPuTTCA3'(Colnot et al., 1995). Interestingly, Takeda et al., (1994) demonstrated the formation of a complex between VDRE, the active metabolite 1,25D₃, RA and T3.

5.5 AIMS AND OBJECTIVES

Tissue-specific expression of the *vgf* gene is controlled by the elements outlined in section 1.4.1, in combination with as yet unidentified elements (Levi et al., 2004). VGF mRNA expression is altered by photoperiod in Siberian hamsters, with increased levels observed in the SD in the *dmpARC* (Barrett et al., 2005). However, expression in the remainder of the ARC was higher in LD (Barrett et al., 2005; Jethwa et al., 2007). It has recently been postulated that

hypothalamic thyroid hormone availability plays a key role in the seasonal regulation of appetite and bodyweight, since a reduction in the local availability of T3 in SD results in hypophagia and weight loss (Murphy et al., 2012). A heterodimer of TR, RAR, is also significantly reduced in SD, along with components of its signalling pathway, namely cellular retinol binding protein 1 (CRBP-1) and cellular retinoic acid binding protein 2 (CRABP-2) (Ross et al., 2005). Furthermore RALDH-1, which is responsible for the local conversion of retinol to retinoic acid, is decreased in the ARC in response to SD in the rat (Shearer et al., 2012). Therefore, using the SH-SY5Y cell line as an *in vitro* model, the studies presented in this chapter investigated the effect of T3 on endogenous VGF expression and the VGF promoter as a mechanism for the observed decrease in VGF expression in SD in the hypothalamus as a possible mechanism for the seasonal regulation of appetite. Having identified a VDRE within the VGF promoter the studies also investigated whether 1,25D3, the active metabolite of vitamin D, alters VGF expression.

5.6 MATERIALS AND METHODS

5.6.1 Cell Culture

5.6.1.1 *The SH-SY5Y cell line*

The SH-SY5Y cell line is a thrice cloned subline of the neuroblastoma cell line SK-N-SH established in 1970 from a metastatic bone tumour (Biebdler et al., 1973; Hattangady and Rajadhysksha, 2009). The SK-N-SH cell line is comprised of two morphologically and biochemically distinct phenotypes: neuroblastic (N-type), which can undergo differentiation, and substrate adherent (S-type) (Ross et al., 1983). Whilst the SH-SY5Y cell line contains a low proportion of S-type cells, upon differentiation this subtype does not undergo differentiation (Encinas et al., 2000) and continues to proliferate outgrowing the N-type cells, which stop proliferating in the presence of a differentiation reagent. Therefore long term treatments with differentiation media does not result in homogeneously neuronal cell populations (Encinas et al., 2000). Previous reports have indicated that NGF treatment of the SH-SY5Y cell line results in a change in the proliferation (LoPresti et al., 1992; Simpson et al., 2001) and differentiation properties (Lavenius et al., 1995; Poluha et al., 1995) of the neuroblastoma cells. While sequential exposure to retinoic acid and neurotrophins yields a homogenous population of differentiated cells (Encinas et al., 2000). Therefore this cell line is suitable for the experiments in this chapter. The PC12 cell line was considered unsuitable as NGF is commonly used to differentiate this cell line, which results in the induction of VGF. The human neuroblastoma cell line SH-SY5Y cell line (a kind gift from Dr Perry Barrett, University of Aberdeen, UK) was cultured in Dubecco's modified Eagle's medium/nutrient mixture F-12 Ham (Sigma, UK), supplemented with 10% fetal bovine serum (Sigma, UK) and 100units/litre penicillin and 100mg/litre streptomycin (Sigma, UK). Cells were routinely split 1:3 with 0.05% trypsin (Sigma, UK), twice a week and were incubated at 37°C, 5% CO₂. The cells were cultured for a maximum of 20 passages.

5.6.1.2 Differentiation

NGF is routinely used to differentiate the PC12 cell line and induce VGF gene expression (Canu et al., 1997; Das et al., 2004). However, the differentiation medium required for the SH-SY5Y cell line has not been readily defined. Previous studies had demonstrated differentiation of the SH-SY5Y cell line with retinoic acid (RA) (Cheung et al., 2009; Pahlman et al., 1984), phorbol esters such as 12-O-tetradecanoyl-phorbol-13-acetate (TPA) (Pahlman et al., 1983; Pahlman et al., 1981) and growth factors, namely IGF-1 and BDNF (Encinas et al., 2000; Ivankovic-Diki et al., 2000; Kim et al., 1997). To induce differentiation, cells were treated with 10 μ M all-trans-RA (Sigma, UK). The medium was changed every 48 hours. After 5 days, medium was withdrawn and replaced with medium containing NGF (50ng/ml, Promega, UK). Cell cultures were then maintained for a further 5 days. The length of the neurites, a marker of differentiation, was calculated using ImagePro software, which was calibrated using a haemocytometer, and a differentiated cell was defined as a cell with a neurite length greater than the length of the cell body. Differentiation was also associated with increased growth associated protein-43 (GAP43), involved in neurite formation, regeneration and plasticity; microtubule-associated protein-2 (Map2), which stabilises microtubules; and Tau, which also stabilises neuronal microtubules.

5.6.1.3 Adhesion

Ivankovic-Diki et al., (2000) demonstrated that adhesion and expression of several growth factor receptors was required in order for the SH-SY5Y cell line to differentiate. In order to determine which matrix would support neurite outgrowth, SH-SY5Y cells were plated in uncoated 6 well plates (plastic, control) or plates coated with 10 μ g/ml collagen (Sigma, UK) or 0.01% poly-L-lysine (Sigma, UK). Pictures were taken 24, 48, 72, 96 and 120 hours post differentiation to determine neurite length.

5.6.1.4 Endogenous expression

For the measurement of endogenous VGF gene expression, cells were seeded in a 6-well plate, at a density of 5×10^4 cells per well and cultured 24 hours before experimentation. Cells were treated with $10 \mu\text{M}$ RA (Sigma, UK), 50 ng/ml NGF, 10 nM T3 (Sigma, UK) and 10 nM 1,25D3 (Sigma, UK) diluted as per manufacturer's instructions.

5.6.1.5 RNA extraction

RNA was extracted from cells using the Roche High Pure Isolation Kit (Roche Life Science, UK). Briefly, cells were resuspended in $200 \mu\text{l}$ RNase free PBS. $400 \mu\text{l}$ of lysis-binding buffer was added to the cell suspension and vortexed for 15 seconds. The sample was added to the upper reservoir of the filter tube and centrifuged at $8000 \times g$ for 15 seconds. The flow-through liquid was discarded and a 1/10 dilution of DNase I/incubation buffer was added to the reservoir and incubated at room temperature for 15 minutes. After three subsequent wash and centrifugation steps with buffers I and II at $8000 \times g$ for 15 seconds, RNA was eluted from the column in a volume of $50 \mu\text{l}$ via centrifugation at $8000 \times g$ for 1 minute. RNA was stored at -80°C .

5.6.1.6 Generation of first strand complimentary DNA

First strand complimentary DNA (cDNA) was obtained from total RNA by means of reverse transcriptase (Transcriptor First Strand cDNA Synthesis Kit, Roche, UK) using random primers. Briefly, $1 \mu\text{g}$ total RNA was combined with $60 \mu\text{M}$ random hexamer primers. The template-primer mixture was denatured for 10 minutes at 65°C . The remaining components of the reaction were then added following cooling on ice: $4 \mu\text{l}$ reaction buffer, $0.5 \mu\text{l}$ protector RNase inhibitor (20 U), $2 \mu\text{l}$ deoxynucleotide mix (1 mM each) and $0.5 \mu\text{l}$ transcriptor reverse transcriptase (10 U). The reagents are mixed and the reaction incubated for 10 mins at 25°C , 30 minutes at 55°C , 5 minutes at 85°C , then cooled at 4°C . The cDNA was stored at -20°C .

5.6.1.7 Oligonucleotide primer design

Primers were designed from database sequences. Sequence data was input into Primer3 in FASTA format and primers were designed using the default criteria (Primer size; 18-27bp, Melting temperature 55-62°C, Amplicon size 50-150bp) and obtained from Sigma, UK. Primer tube was centrifuged prior to opening to prevent loss of pellet. All primers were high-purity salt free and synthesised at a concentration of 0.01µM. All oligonucleotide primer pairs were assessed by endpoint PCR to ensure a single amplicon of the expected size was produced. The primer sequences were therefore as follows:

	Forward	AAGTCCCTTGCCATCCTAAA
	(5' – 3')	
B-actin		
	Reverse	ATGCTATCACCTCCCCTGTG
	(5' – 3')	
	Forward	CCCTCTGTGTAGTGGCCTTT
	(5' – 3')	
B-tubulin		
	Reverse	CCAGACAACCTTTGTATTTGGTCA
	(5' – 3')	
	Forward	GACCCTCCTCTCCACCTCTC
	(5' – 3')	
VGF		
	Reverse	ACCGGCTCTTTATGCTCAGA
	(5' – 3')	

	Forward	AGTGAGCAGCGAGCAGAA
	(5' – 3')	
GAP-43	Reverse	GTTGCGGCCTATGAGCTT
	(5' – 3')	
	Forward	CATGGGTCA CAGGGCACCTATTC
	(5' – 3')	
Map-2	Reverse	GGTGGAGAAGGAGGCAGATTAGCTG
	(5' – 3')	
	Forward	GCGGCAGTGTGCATATAGTCTACA
	(5' – 3')	
Tau	Reverse	GGAAGGTCAGCTTGTGGGTTTCAA
	(5' – 3')	
	Forward	TCCTGCTTTCAAGAATTATTCC
	(5' – 3')	
Cyclophilin A	Reverse	ATTCGAGTTGTACAGTCAGC
	(5' – 3')	

5.6.1.8 Polymerase chain reaction

The polymerase chain reaction (PCR) allows for the amplification of a target sequence specific to a gene of interest. The technique can be utilised to obtain semi-quantitative (End-Point) or quantitative gene expression data. For each PCR cycle, cDNA strands were denatured at 94°C. The temperature was subsequently reduced to 55 – 65°C to allow for primer annealing. Subsequently

the temperature of the reaction was raised to 72°C to allow for the extension of the primer to form the desired amplicon. This was repeated for a maximum of 35 cycles (for End-Point PCR).

5.6.1.9 Quantitative PCR

This technique permits the relative quantification of specific DNA or RNA sequences from samples and therefore allows for the assessment of gene expression. The reaction is performed with SYBR green optimised for the LightCycler 480 (Roche Life Science, UK). SYBR green is a dye which fluoresces only when bound to double stranded DNA (dsDNA). This fluorescence is proportional to the amount of the target sequence, which permits the quantification of PCR products. Reactions were performed in triplicate using 5µl cDNA in SYBR Master Mix 1 (Roche, UK), with a final concentration of 0.25µM primers, in a total volume of 15µl. Cycling parameters were an initial 95°C for 5 minutes, followed by 40 cycles of 95°C/10 seconds, 55°C/10 seconds and 72°C/30 seconds. All reactions were run on a 384 well plate on the aforementioned instrument as per manufacturer's instructions. Quantitative data was generated by comparing samples to a series of known dilutions of pooled cDNA.

5.6.1.10 Data normalisation

Quantitative PCR data was normalised by the use of internal reference genes. Ct values were normalised to the housekeeping gene, cyclophilin A, chosen as it was the most stable reference gene under the experimental conditions. B-actin and β-tubulin were also considered, however, their expression, whilst stable in undifferentiated cells, was increased in response to treatment with RA.

5.6.1.11 Transfection

Under standard conditions mammalian cells will take up and express DNA with low efficiency due to the largely impenetrable lipid bilayer of the cell membrane, which inhibits the entry of charged molecules. Transfection allows the delivery of DNA (RNA, proteins and macromolecules) into eukaryotic cells and can be utilised to study gene regulation (as well as protein expression and function). FuGENE HD transfection reagent (Roche Life Science, UK) is a “next generation” transfection reagent which is free of animal- or human-derived components, stable at room temperature, and sterile (0.1µm) filtered. It offers “excellent” transfection efficiency for many cell lines that are not transfected well by other reagents such as HeLa, PC-3 and SH-SY5Y. Briefly, cells were plated in 24 well plates the day before transfection. On the day of transfection, media was removed and replaced with low serum media, without antibiotics, as these were found to impede the transfection. 16µg plasmid DNA was added to 800µl OptiMEM I reduced serum media (transfection media, Sigma, UK), to give a concentration of 20µg/ml. 6µl of transfection reagent was added to 100µl of transfection media (which contained 2µg/100µl DNA) and mixed by pipetting. 10µl was added to the cells after 15 minutes incubation at room temperature. The cells were subsequently incubated for 72 hours prior to assessment of transfection efficiency using the Typhoon Trio+ Imaging Suite (GE Healthcare Life Sciences, UK) and subsequent experimentation. A positive control, pZsGreen1-N1 (Clontech, USA) in which ZsGreen1 was expressed under the control of a CMV promoter, and a negative control, in which mRFP was expressed in a promoterless vector, were performed alongside each transfection in the SH-SY5Y cell line.

5.6.1.12 Typhoon Trio+

The Typhoon Trio+ instrument is a variable-mode imager that produces digital images of radioactive, fluorescent or chemiluminescent samples. Briefly, a fluorescent/chemiluminescent sample is placed onto the glass plate of the instrument. Using the associated scanner control software, parameters

(excitation/emission filter, sensitivity, focal plane) are selected which are appropriate for the sample type. The sample containing the fluorophore emits light in the following way: when the green laser (532nm) or the red laser (633nm) illuminates each one-pixel section of a fluorescent sample, the fluorochrome emits light with a characteristic spectrum. The optical system collects the emitted light and directs it through the selected emission filter. Each filter allows only the emitted light within the filter's bandwidth to pass through the designated photomultiplier tube (PMT). The PMT converts the light to an electric current, which varies with the intensity of the light collected by the PMT.

5.6.1.13 ImageQuant

The ImageQuant software (GE Life Sciences, UK) was used to convert the analog signal to a digital file – mapping the information to the appropriate pixel location on the monitor to produce an accurate image of the original sample. The software was used to quantify the variations in the signal as the level of signal is proportional to the amount of fluorescence present in the sample.

5.6.1.14 Statistics

All data is reported as means \pm standard error of the mean (SEM), while comparisons between multiple groups were performed using analysis of variance (ANOVA). Significance was accepted as $p < 0.05$. All statistical analyses were performed using GraphPad Prism 6.0.

5.6.2 Cloning

5.6.2.1 Development of a reporter construct

pZsGreen1-1 (Clontech Laboratories, USA) is a promoterless vector that can be used to monitor transcription from different promoters and enhancers inserted into the multiple cloning site (MCS). However, to test the feasibility of the viral 2A sequence, we excised the ZsGreen1 gene from the aforementioned mammalian expression vector and added the CBG99 luciferase and mRFP from pCR2CBG992AMRFP. Briefly, both plasmids were digested with *Bam*HI and *Not*I and purified via gel extraction (QIAquick gel extraction, QIAGEN, UK). The purified pZsGreen1-1 backbone was then treated with alkaline phosphatase, ligated overnight with the luciferase and fluorescent genes from pCR2CBG992AMRFP and transformed into JM109 cells (Promega, UK). Cultures were then grown overnight, before plating and colony selection. Purified plasmids were subject to restriction enzyme (RE) digestion and sequencing (performed by Source BioScience, UK) to confirm identity. The new reporter construct was designated pCBG992AmRFP. Subsequently a CMV promoter, from pLenti6.4-CMV-C/EBPPA (a kind gift from Prof Michael Lomax, University of Nottingham, UK) was added to the MCS of the pCBG992AmRFP vector to assess function. The aforementioned plasmid was digested, using the previously described strategy, with the REs *Sa*II and *Spe*I (NEB, UK) and the CMV was added to the new vector utilising the *Xho*I and *Spe*I sites in the MCS. This construct was designated pCMVCBG992AmRFP.

5.6.2.2 Development of the promoter constructs

The plasmid designated pVGFCBG992AmRFP (see Figure 5.6.2.2) was constructed consisting of the sequence of the mouse VGF promoter from -1159 to +51, cloned into pCBG992AmRFP between *Nco*I and *Sac*I. The mouse VGF promoter was isolated from genomic DNA, amplified by PCR and inserted into the pGEM-T Easy vector (Promega, UK) for subcloning. The primer sequences were therefore as follows:

Forward A A G G G T G T G G G A G A G T T G G
(5' – 3')

VGF

Reverse G A G G G A T G G A C A G C G G A G
(5' – 3')

Briefly, 50ng of the pGEM-T Easy vector was incubated with the PCR product and 3 Weiss units of T4 DNA Ligase (Promega, UK), overnight at 4°C. Post clean-up (using the QIAquick PCR purification kit, QIAGEN, UK), the ligated vector was transformed, grown, purified and subjected to RE digestion and sequencing to confirm presence of insert. The pGEM-T Easy vector was digested with *SpeI* and *SacI* (NEB, UK) to liberate the VGF promoter fragment and inserted into the reporter construct. Subsequently a 5' deletion of the mouse VGF promoter was produced using the unique site *BglII* in the reporter construct, upstream of the insert, and *MboI*, a RE site contained within the promoter (NEB, UK). The digested plasmid was treated with T4 Ligase (see section 2.3.3). Following growth and purification (see section 2.3.5), agarose gel electrophoresis and sequencing demonstrated the successful deletion of the 5' promoter region (-1159 to -632). The truncated mouse VGF promoter contained within the vector represented the region -631 to +51 and lacked the postulated TRE.

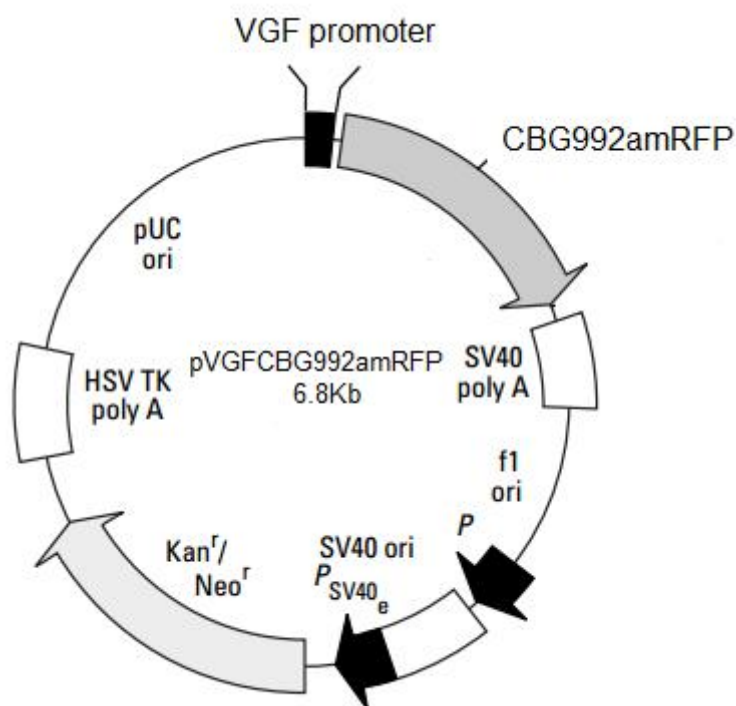


Figure 5.6.2.2: **Plasmid map of pVGFCBG992AmRFP containing 1Kb of the VGF promoter.** The SV40 polyadenylation signal downstream of the reporter genes (CBG99; click beetle luciferase and mRFP; monomeric red fluorescent protein) directs processing of the 3' end of the CBG2AmRFP mRNA. The vector backbone contains an SV40 origin of replication for propagation in E.coli and an f1 origin for single-stranded DNA production. Kan^r/Neo^r denote antibiotic resistant genes driven by an SV40 early promoter. The Herpes simplex virus thymidine kinase (HSV TK) gene provides a polyadenylation signal. Adapted from pZsGreen1-1, Clontech Laboratories, USA.

5.7 RESULTS

5.7.1 Characterisation of the SH-SY5Y cell line

5.7.1.1 Nerve growth factor (NGF) treatment of the SH-SY5Y cell line increased proliferation

Treatment of the SH-SY5Y cell line with NGF resulted in increased cell proliferation (see Figure 5.7.1.1). After 48 hours treatment with NGF, cell number was significantly increased (one way ANOVA $F(1.821, 3.641) = 81.73$, $p = 0.001$ vs. control) at concentrations equal to or greater than 50ng/ml. There were no significant differences between the higher concentrations of NGF. There was no effect of treatment on cellular morphology; neurite outgrowth, a marker of neuronal differentiation, remained stable.

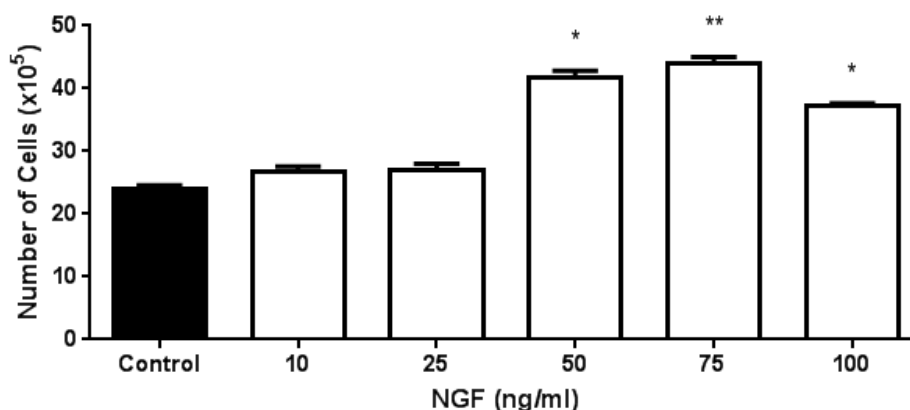


Figure 5.7.1.1: **Treatment of the SH-SY5Y cell line with NGF increased cell proliferation.** SH-SY5Y cells were treated with 10-100ng/ml NGF and cell number was measured 48 hours later. Low concentrations of NGF (≤ 25 ng/ml) had no effect on cell number, but higher concentrations of NGF (≥ 50 ng/ml) significantly increased proliferation in the SH-SY5Y cell line. However there was no dose response effect, as there was no significant difference between the higher doses of NGF treatment. All values are mean + SEM ($n = 6$, * $p < 0.05$, ** $p < 0.01$ vs control).

5.7.1.2 Retinoic acid (RA) treatment of the SH-SY5Y cell line reduces proliferation and increased differentiation

In contrast to the effects of NGF, treatment of the SH-SY5Y cell line with RA for 120 hours reduced cell proliferation (see Figure 5.7.1.2), but only at concentrations equal to or greater than 10 μ M (F (1.231, 2.462) = 260.0, p = 0.001 vs. control). The reduction in cell proliferation was associated with increased differentiation of the SH-SY5Y cell line. Cellular morphology was significantly altered in response to treatment with 10 μ M RA, with neurite outgrowth, a marker of neuronal differentiation, being significantly increased (F (3, 16) = 282.7, p < 0.0001 vs. control) after 2.5 and 5 days of treatment.

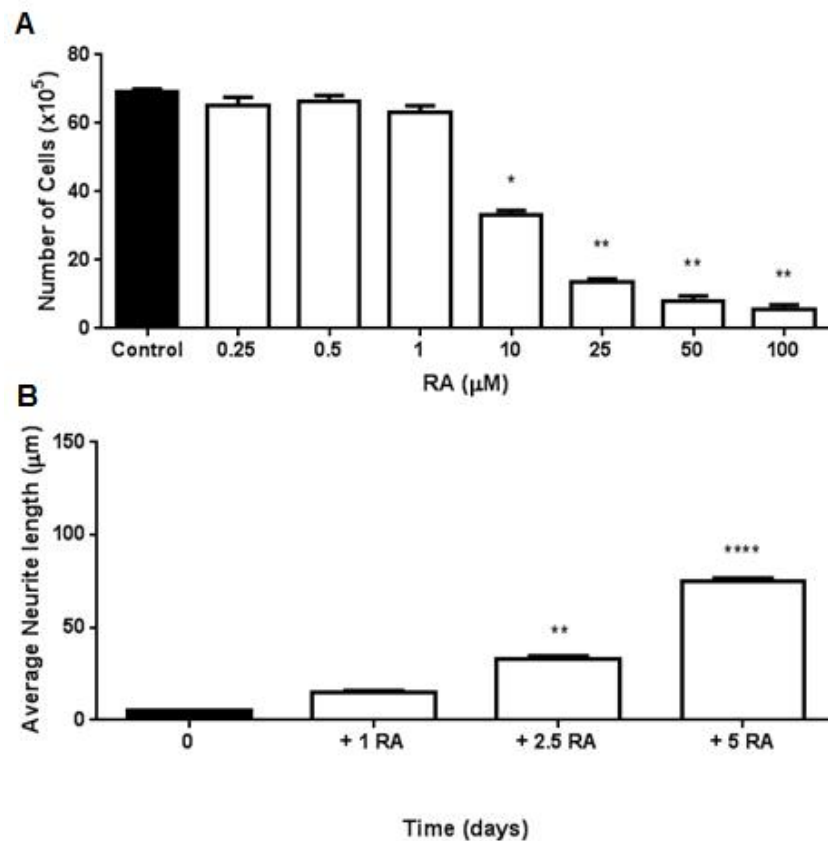


Figure 5.7.1.2: **Treatment of the SH-SY5Y cell line with RA reduced cell proliferation and increased differentiation.** A) RA treatment of the SH-SY5Y cell line significantly decreased cell proliferation at concentrations equal to or greater than 10 μ M (F (1.231, 2.462) = 260.0, p = 0.001). B) 10 μ M RA treatment significantly increased differentiation, increasing neurite outgrowth 2.5 and 5 (but not 1) days post addition to the culture medium (F (3, 16) = 282.7, p < 0.0001). All values are mean + SEM (n = 6, * p < 0.05, ** p < 0.01, **** p < 0.0001 vs control).

5.7.1.3 Long term treatment of the SH-SY5Y cell line with RA resulted in a heterogeneous population of neuronal cells

The SH-SY5Y cell line consisted of two morphologically and biochemically distinct phenotypes; the N-type and S-type (see Figure 5.7.1.3 A arrows). The S-type does not undergo differentiation in response to RA and therefore continued to proliferate (see Figure 5.7.1.3 B)

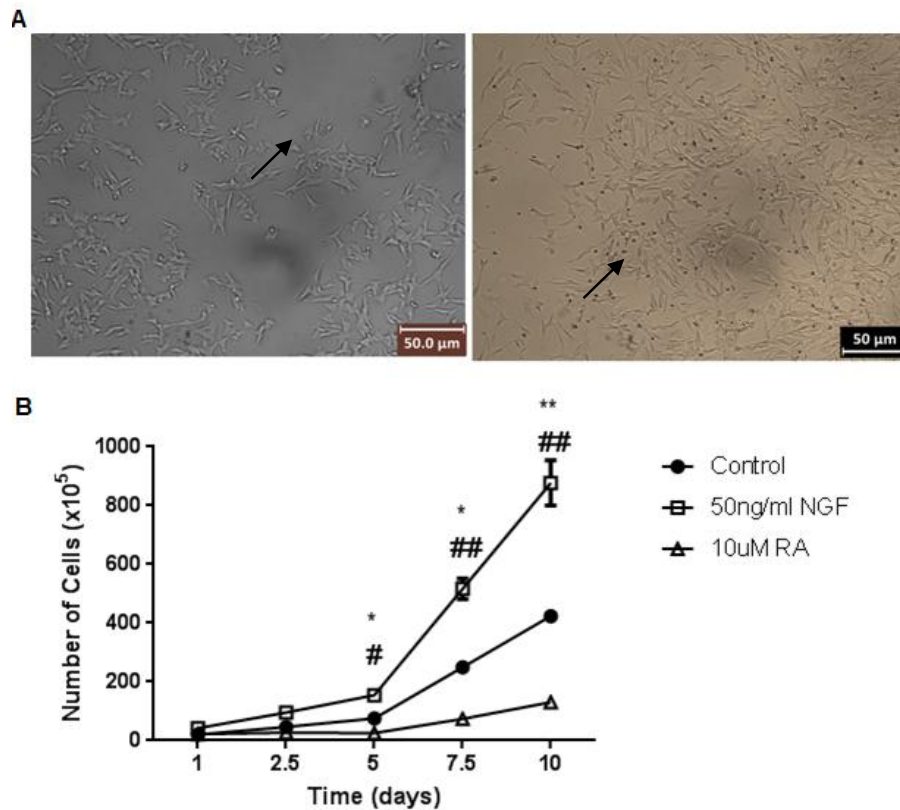


Figure 5.7.1.3: **Long term treatment of the SH-SY5Y cell line with RA resulted in a heterogeneous population of neuronal cells.** A) The proliferation of S-type cells (arrows) in the presence of RA. B) Whilst long term treatment of the SH-SY5Y cell line with RA results in a significant reduction in cell number, continued exposure (post 5 days) results in the proliferation of S-type cells and therefore an increased cell number, representing a heterogeneous culture. All values are mean \pm SEM ($n = 6$, * $p < 0.05$, ** $p < 0.01$ for comparisons between control and treatment, # $p < 0.05$, ## $p < 0.01$ for comparisons between RA and NGF).

5.7.1.4 Exposure of the SH-SY5Y cell line to RA and subsequently NGF resulted in a homogenous population of neuronal cells

Long term exposure of the SH-SY5Y cell line to RA results in a heterogenous population of cells with distinct phenotypes (see Figure 5.7.1.3 A). Treatment

of the RA-differentiated cells with NGF reduced the number of S-type cells, resulting in a more homogenous population of N-type cells (see Figure 5.7.1.4 A). Moreover, treatment with NGF increased the neuronal morphology of the N-type cells as neurite outgrowth was significantly increased in response to NGF ($p < 0.05$, Figure 5.7.1.4 B). Under these conditions, cultures could be maintained for up to 20 days without displaying signs of cell death or reversion from the neuronal phenotype.

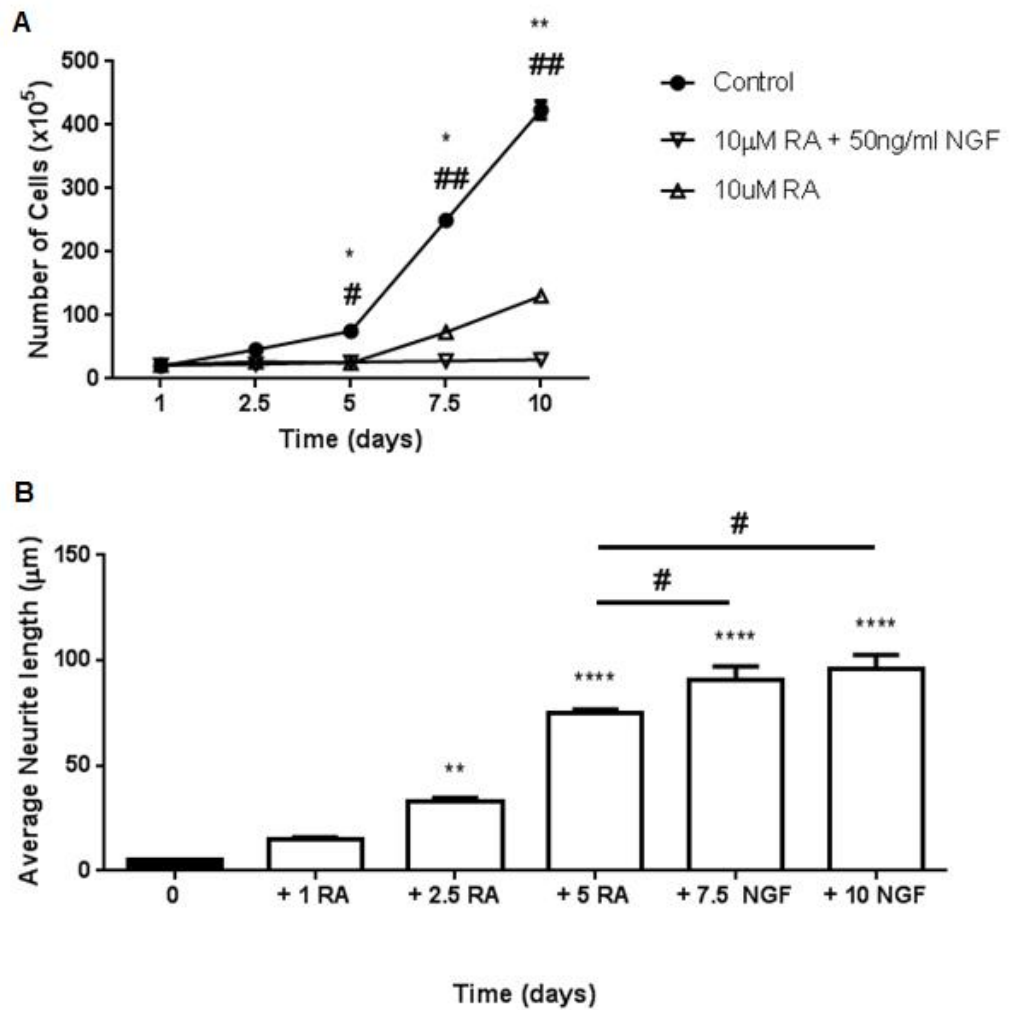


Figure 5.7.1.4: **Treatment of the SH-SY5Y cell line with RA and NGF resulted in a more homogenous population of N-type cells.** Treatment of the SH-SY5Y cell line with 10µM RA for 5 days and subsequently 50ng/ml NGF for 5 days resulted in A) reduced cellular proliferation and B) enhanced differentiation. All values are mean SEM (n = 6), * p < 0.05, ** p < 0.01 for comparisons between control and treatment, # p < 0.05, ## p < 0.01, for comparisons between RA and RA and NGF). For neurite length: n = 6 fields of view per well, treatment n = 3.

5.7.1.5 Collagen increased neurite outgrowth in the SH-SY5Y cell line

Coating of the culture wells with either poly-l-lysine or collagen significantly increased RA-induced neurite outgrowth in the SH-SY5Y cell line ($p < 0.0001$, Figure 5.7.1.5). Neurite outgrowth was significantly greater in collagen coated wells compared to those coated in poly-l-lysine ($p < 0.001$).

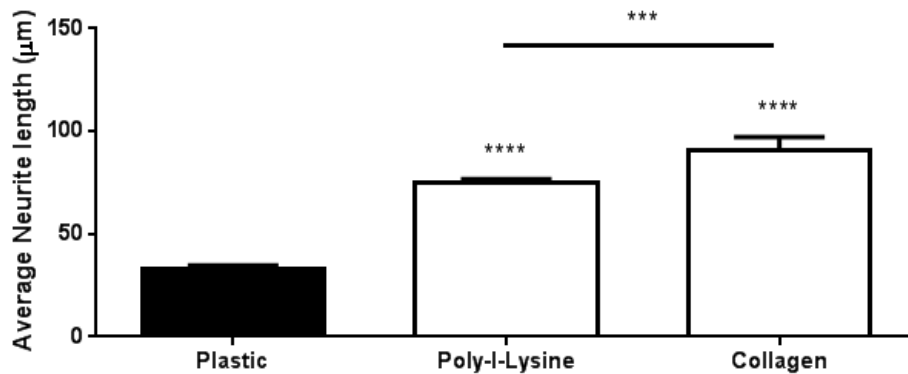


Figure 5.7.1.5: **The effect of extracellular matrices on neurite outgrowth in the differentiated SH-SY5Y cell line.** Adhesion of the SH-SY5Y cell line to plastic, poly-l-lysine or collagen resulted in neurite outgrowth. Neurite length was significantly greater in wells coated with poly-l-lysine and collagen ($p < 0.0001$ vs. control), 5 days post treatment with differentiation media. All values are mean + SEM ($n = 6$ fields of view per well, treatment $n = 3$, *** $p < 0.001$, **** $p < 0.0001$).

5.7.1.6 RA treatment of the SH-SY5Y cell line increased neuronal markers of differentiation

RA treatment of the SH-SY5Y cell line for 5 days significantly increased (all $p < 0.05$) the expression of the neuronal markers of differentiation (see Figure 5.7.1.6).

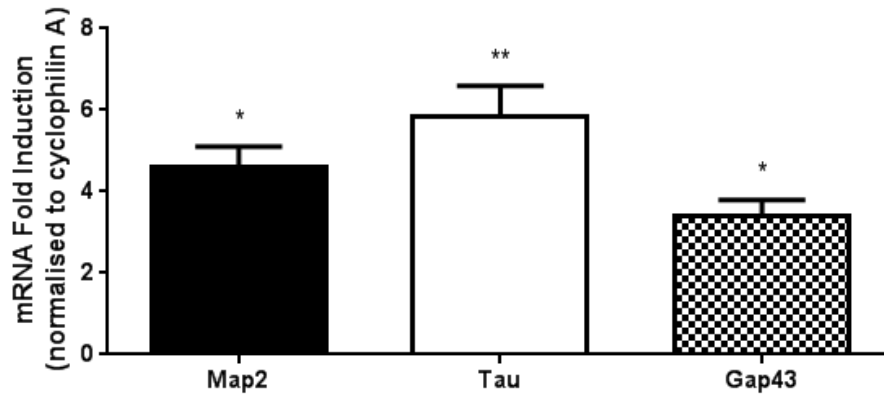


Figure 5.7.1.6: **RA treatment of the SH-SY5Y cell line increased neuronal markers of differentiation.** In response to RA, the SH-SY5Y cell line differentiates – this is associated with a significant increase in Map2, Tau and Gap43, markers of neuronal differentiation. Expression of each mRNA was quantified by RT-PCR, normalised to cyclophilin A mRNA and then compared to the normalised expression in undifferentiated cells. All values are mean + SEM ($n = 6$, * $p < 0.05$, ** $p < 0.01$ for comparisons between control and treatment).

Therefore, having established a rapid and simple procedure to obtain a homogenous neuronal like population of cells from the SH-SY5Y cell line, we sought to further define the response of endogenous VGF expression to RA and NGF.

5.7.2 The response of endogenous VGF expression to RA, NGF, T3 and 1,25D3 treatment of the SH-SY5Y cell line

5.7.2.1 RA and NGF treatment of undifferentiated SH-SY5Y cells significantly increased endogenous VGF expression

Treatment of the SH-SY5Y cell line with 10 μ M RA for 24 and 48 hours significantly increased VGF mRNA ($p < 0.05$), 2- and 4-fold respectively. Over the same time period, VGF mRNA expression was significantly increased 5- and 3-fold ($p < 0.01$ and $p < 0.05$ respectively) in response to treatment with 50ng/ml NGF (see Figure 5.7.2.1). Treatment of differentiated SH-SY5Y cells produced a similar result (see section 5.7.2.2).

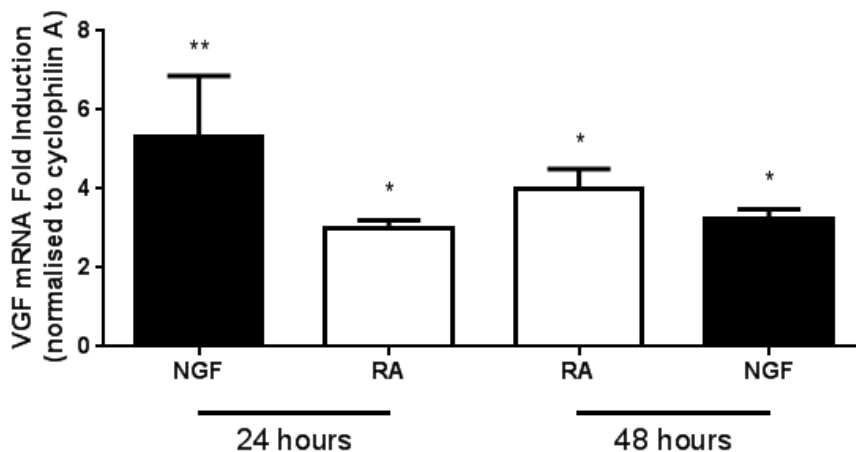


Figure 5.7.2.1: **Endogenous VGF mRNA expression in undifferentiated SH-SY5Y cells was increased by treatment with NGF and RA.** VGF mRNA levels were quantified by RT-PCR, normalised to cyclophilin A mRNA and then compared to the normalised expression in control cells. Both 50ng/ml NGF and 10 μ M RA increased VGF mRNA after 24 and 48 hours of treatment in undifferentiated SH-SY5Y cells. All values are mean + SEM ($n = 6$, * $p < 0.05$, ** $p < 0.01$ for comparisons between control and treatment).

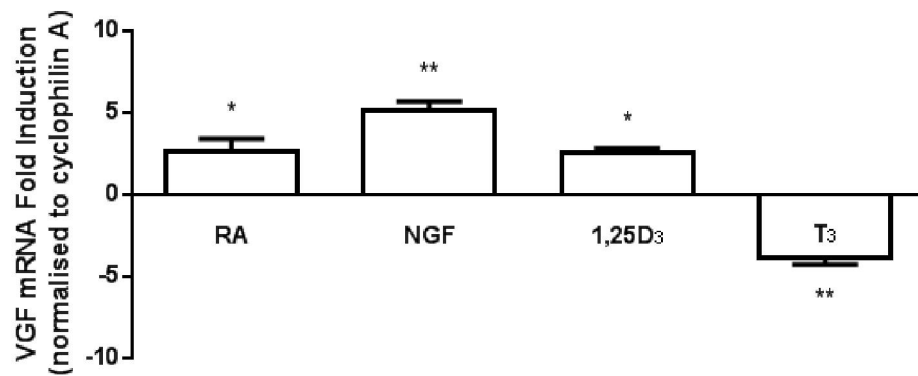
5.7.2.2 T3 treatment of undifferentiated and differentiated SH-SY5Y cells significantly reduced endogenous VGF expression

In contrast to the previously observed stimulatory effects of NGF and RA on VGF mRNA expression in undifferentiated SH-SY5Y cells (see Figure 5.6.2.1), treatment of undifferentiated SH-SY5Y cells with 10nM T3 for 24 hours resulted in a 4-fold reduction in VGF mRNA ($p < 0.01$, Figure 5.7.2.2 A). Similar effects were seen in differentiated SH-SY5Y cells (see Figure 5.7.2.2 B), with endogenous VGF expression being significantly increased in response to 10 μ M RA and 50ng/ml NGF (2- and 10-fold, $p < 0.05$ and $p < 0.01$ vs. control respectively), whereas 10nM T3 reduced VGF mRNA expression 7-fold ($p < 0.01$, Figure 5.7.2.2 B).

5.7.2.3 1,25D3 treatment of undifferentiated and differentiated SH-SY5Y cells significantly increased endogenous VGF expression

In contrast to the previously observed repressive effect of T3 on VGF mRNA expression, treatment of the SH-SY5Y cell line with 10nM 1,25D3 for 24 hours significantly increased VGF mRNA ($p < 0.05$, Figure 5.7.2.2 A) 2.5-fold. Similar effects were seen in differentiated SH-SY5Y cells, with endogenous VGF expression being significantly increased by 10nM 1,25D3 treatment ($p < 0.05$, Figure 5.7.2.2 B).

A



B

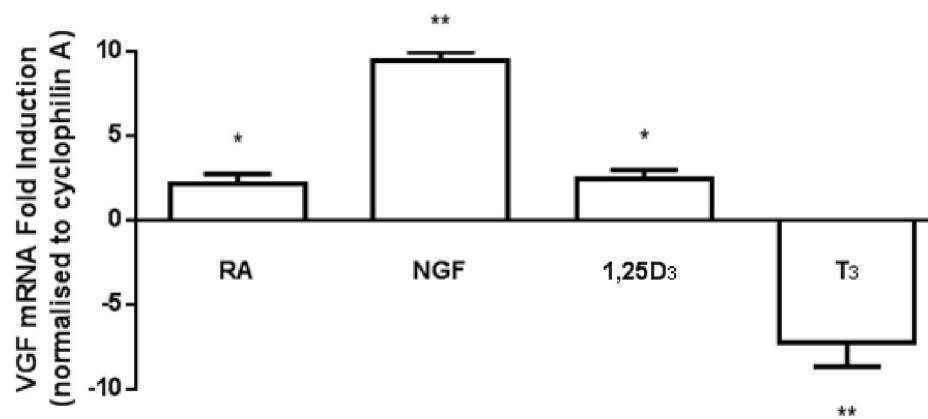


Figure 5.7.2.2: **Treatment of undifferentiated and differentiated SH-SY5Y cells with T3 reduced while 1,25D3 increased endogenous VGF expression.** VGF mRNA levels were quantified by RT-PCR and normalised to cyclophilin A mRNA and then compared to the normalised expression in control cells. A) Treatment of undifferentiated SH-SY5Y cells with 10nM T3 resulted in a significant reduction in VGF mRNA, while treatment with 10nM 1,25D3 significantly increased VGF mRNA expression. B) Treatment of differentiated SH-SY5Y cells with 10nM T3 and 1,25D3 produced a similar result; however the fold change in response to NGF and T3 was greater in differentiated cells. All values are mean \pm SEM (n = 6, * p < 0.05, ** p < 0.01 for comparisons between control and treatment).

5.7.3 The response of the VGF promoter to RA, NGF, T3 and 1,25D3 treatment.

Transfection, using FugeneHD, of the SH-SY5Y cell line with a mammalian expression vector containing 1Kb and 0.5Kb (see Figure 5.7.3 A) of the *vgf* promoter demonstrated higher promoter activity than the promoterless negative control following 72 hours incubation (see Figure 5.7.3 B). However, there was no significant difference in promoter activities when comparing the 1Kb and 0.5Kb VGF promoter constructs.

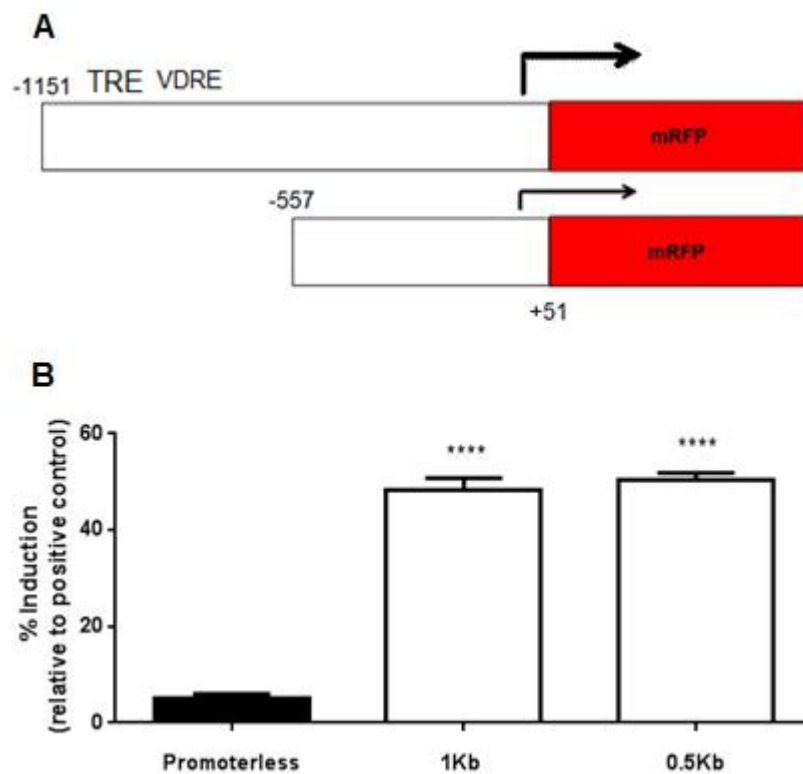


Figure 5.7.3: **The VGF promoter constructs and their promoter activities.** The VGF promoter (1Kb) was cloned into a mammalian expression vector, based on the backbone of pZsGreen1-1 (Clontech), in which the reporter gene was substituted for an mRFP. A subsequent truncated construct (0.5Kb), which lacked the potential TRE and VDRE, was generated via 5' deletion. Promoter activity (fluorescence) was significantly increased in cells transfected with the 1Kb and 0.5Kb VGF promoter constructs, but there was no significant difference between them. Promoter activities are shown relative to the positive control (100%), containing a CMV promoter. All values are mean + SEM (n = 6, **** p < 0.0001 for comparisons between control and treatment).

5.7.3.1 RA and NGF treatment of undifferentiated and differentiated SH-SY5Y cells significantly increased reporter gene expression

At 72 hours post transfection with the 1Kb VGF promoter construct, undifferentiated SH-SY5Y cells were treated with 50ng/ml NGF, which resulted in a rapid and significant increase in VGF promoter activity. However, this increase was transient and there was a subsequent reduction in the promoter activity in response to NGF treatment after 48 hours (two way ANOVA repeated measures treatment vs time interaction $F = 27.94$, $p < 0.0001$). Treatment with 10 μ M RA also resulted in a significant increase in VGF promoter activity, but this was a much slower effect. Initial VGF promoter activity remained constant, until 6 hours post treatment, when promoter activity increased and continued to increase at 24 and 48 hours (treatment vs time interaction $F(12, 36) = 30.91$, $p < 0.001$). A similar effect of RA (treatment vs. time interaction $F = 30.91$, $p < 0.0001$) and NGF (treatment vs. time interaction $F = 36.78$, $p < 0.0001$) treatment on VGF (1Kb) promoter activity was observed in differentiated SH-SY5Y cells.

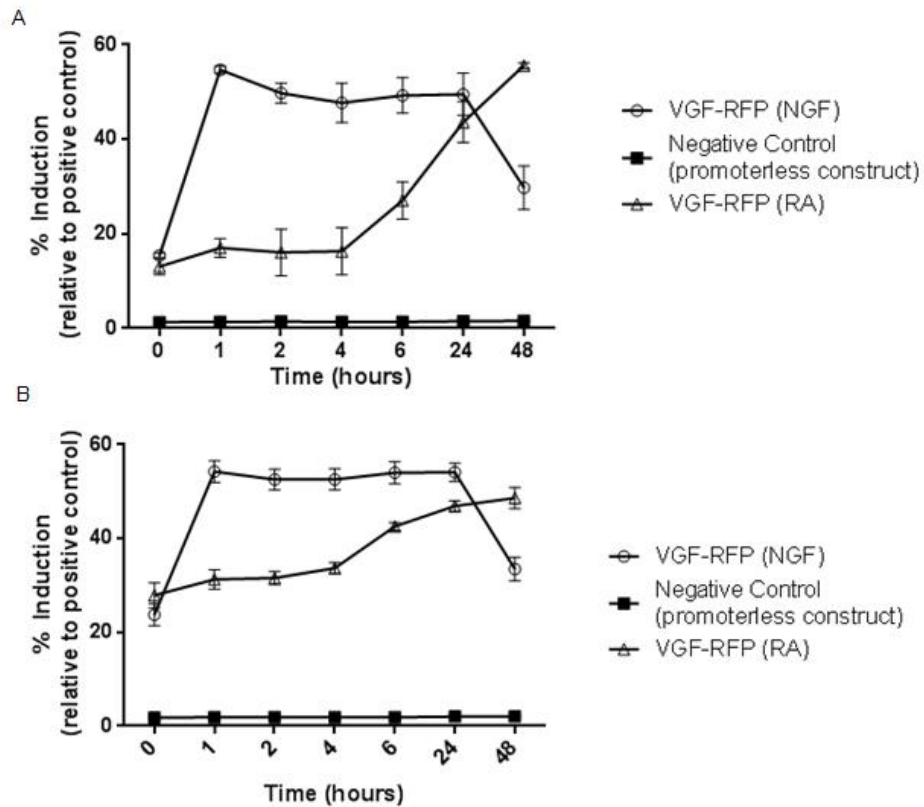


Figure 5.7.3.1: RA and NGF treatment of undifferentiated and differentiated SH-SY5Y cells increased VGF promoter activity. A) Undifferentiated SH-SY5Y cells were transfected with a reporter construct containing 1Kb of the *vgf* promoter. 72 hours post transfection, 50ng/ml NGF rapidly induced reporter gene expression, which was maintained for 24 hours, but there was a subsequent reduction at 48 hours (interaction, $p < 0.0001$). 10 μ M RA treatment of cells resulted in a slower, yet significant, increase in VGF promoter activity, starting 6 hours post treatment (interaction, $p < 0.001$). B) Undifferentiated cells were transfected as previously described in A. 72 hours post transfection, cells were differentiated with 10 μ M RA for 5 days. Differentiated transfected cells were then treated with 10 μ M RA or 50ng/ml NGF for 48 hours. Treatment of differentiated SH-SY5Y cells with NGF ($p < 0.0001$) and RA ($p < 0.0001$) produced a similar effect. Promoter activities are shown relative to the positive control (100%), containing a CMV promoter. All values are mean \pm SEM ($n = 6$).

5.7.3.2 T3 reduced *vgf* promoter activity in undifferentiated and differentiated SH-SY5Y cells

Undifferentiated SH-SY5Y cells were transfected with a reporter construct containing either the 1Kb of the *vgf* promoter, which contains the postulated TRE, or 0.5Kb of the *vgf* promoter, which lacks the postulated TRE. 72 hours post transfection, the undifferentiated cells were treated with 10nM T3, which significantly reduced the 1Kb VGF promoter activity, particularly after 6 and 24hrs treatment (treatment vs. time interaction $F = 86.13$, $p < 0.0001$; Figure 5.6.3.2 A). In contrast, 10nM T3 had no effect on the 0.5Kb *vgf* promoter activity. Similar effects of T3 treatment on the 1Kb (treatment vs. time interaction $F = 201.7$, $p < 0.0001$) and 0.5Kb VGF promoter activities were also observed in differentiated SH-SY5Y cells (see Figure 5.7.3.2 B).

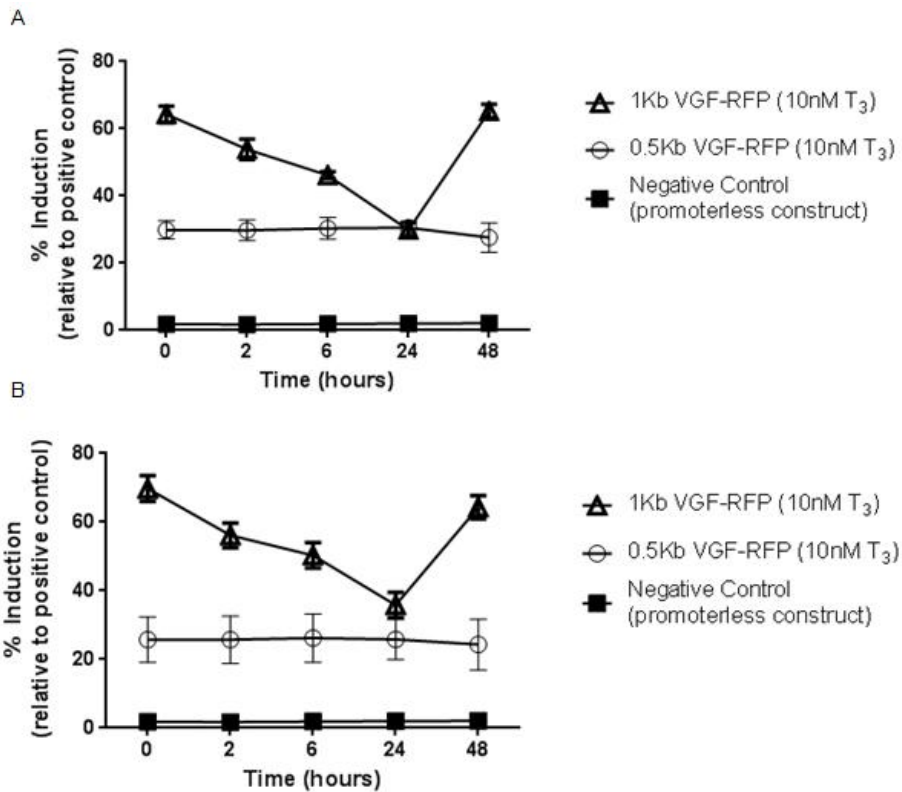


Figure 5.7.3.2: T₃ reduces vgf promoter activity in undifferentiated and differentiated SH-SY5Y cells. A) Undifferentiated SH-SY5Y cells were transfected with a reporter construct containing 1Kb or 0.5Kb of the vgf promoter (containing or lacking the postulated TRE respectively). 72 hours post transfection, undifferentiated cells were treated with 10nM T₃, which significantly reduced reporter gene expression ($p < 0.001$). Removal of the TRE, via 5' deletion, however, blocked the effect of T₃. B) Undifferentiated cells were transfected as previously described in A. 72 hours post transfection, cells were differentiated with 10 μ M RA for 5 days. Differentiated transfected cells were then treated with 10nM T₃ for 48 hours. Treatment of differentiated SH-SY5Y cells with T₃ showed similar effects. Promoter activities are shown relative to the positive control (100%), containing a CMV promoter. All values are mean \pm SEM ($n = 6$).

5.7.3.3 1,25 D3 increased *vgf* promoter activity in undifferentiated and differentiated SH-SY5Y cells

Undifferentiated SH-SY5Y cells were transfected with a reporter construct containing either the 1Kb of the *vgf* promoter, which contains the postulated VDR, or 0.5Kb of the *vgf* promoter, which lacks the postulated VDRE. 72 hours post transfection, the undifferentiated cells were treated with 10nM 1,25D3, which significantly increased the 1Kb VGF promoter activity, particularly after 2 and 6hrs treatment (treatment vs time interaction $F = 14.28$, $p < 0.0001$; Figure 5.6.3.3 A). In contrast, 10nM 1,25D3 had no effect on the 0.5Kb *vgf* promoter activity. Similar effects of 1,25D3 treatment on the 1Kb (treatment vs. time interaction $F = 14.28$, $p < 0.0001$) and 0.5Kb VGF promoter activities were also observed in differentiated SH-SY5Y cells (see Figure 5.7.3.3 B).

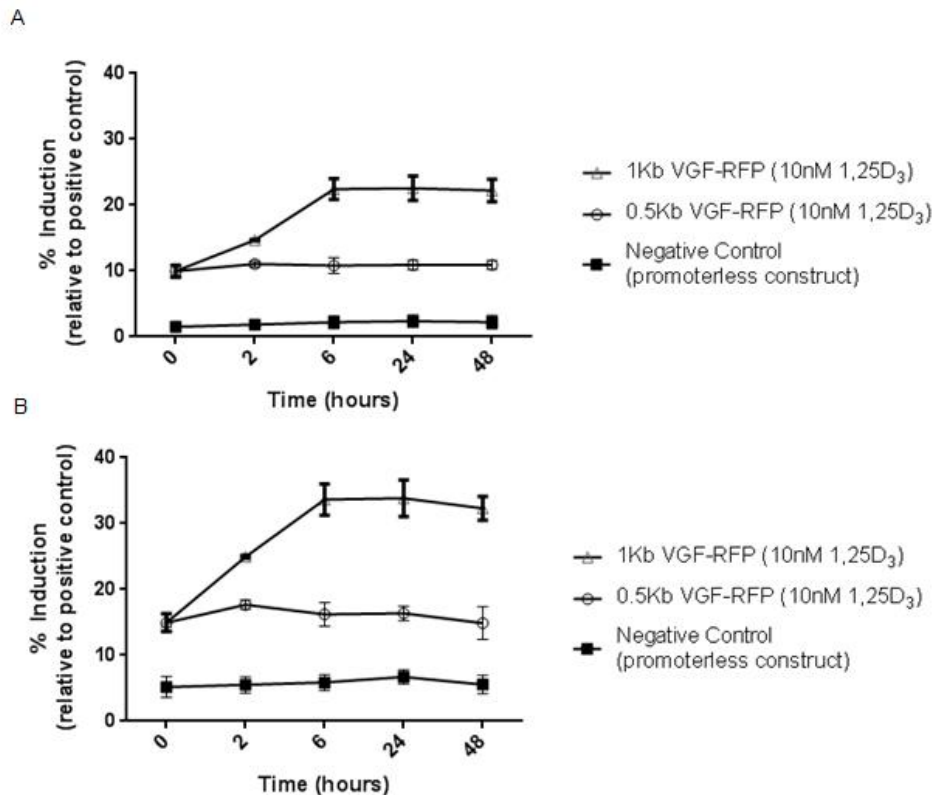


Figure 5.7.3.3: **1,25D₃ increased *vgf* promoter activity in undifferentiated and differentiated SH-SY5Y cells.** A) Undifferentiated SH-SY5Y cells were transfected with a reporter construct containing 1Kb or 0.5Kb of the *vgf* promoter (containing or lacking the postulated VDR respectively). 72 hours post transfection, undifferentiated cells were treated with 10nM 1,25D₃, which significantly reduced reporter gene expression ($p < 0.001$). Removal of the VDR, via 5' deletion, however, blocked the effect of 1,25D₃. B) Undifferentiated cells were transfected as previously described in A. 72 hours post transfection, cells were differentiated with 10 μ M RA for 5 days. Differentiated transfected cells were then treated with 10nM 1,25D₃ for 48 hours. Treatment of differentiated SH-SY5Y cells with vitamin D showed similar effects. Promoter activities are shown relative to the positive control (100%), containing a CMV promoter. All values are mean \pm SEM ($n = 6$).

5.8 DISCUSSION

Tissue-specific expression of the *vgf* gene has been previously described (Canu et al., 1997), however unidentified elements remained (Levi et al., 2004). VGF mRNA expression was reduced in the ARC in response to SD (Barrett et al., 2005). RAR, was also significantly reduced in SD, along with components of its signalling pathway, namely cellular retinol binding protein 1 (CRBP-1) and cellular retinoic acid binding protein 2 (CRABP-2) (Ross et al., 2005). Furthermore RALDH-1, which is responsible for the local conversion of retinol to retinoic acid, was decreased in the ARC in response to SD in the rat (Shearer et al., 2012). Therefore, using the SH-SY5Y cell line as an *in vitro* model, the studies presented in this chapter demonstrated, for the first time, RA increased endogenous VGF mRNA expression and promoter activity. Furthermore a possible TRE was identified within the *vgf* promoter. T3 treatment of the SH-SY5Y reduced endogenous VGF mRNA expression and promoter activity. Removal of the possible TRE from the promoter construct resulted in the loss of T3 dependent repression. These studies propose a possible mechanism for the seasonal regulation of appetite in the Siberian hamster.

The previously used PC12 cell line was considered unsuitable for the studies reported in this chapter as NGF is commonly used to differentiate this cell line, which results in the induction of VGF mRNA (Possenti et al., 1992; Salton et al., 1991). Therefore the first objective was to optimise a method to differentiate the SH-SY5Y cell line into a neuronal model – the differentiation process was required to mimic the intracellular environment of a neuronal cell. During this process of differentiation, the SH-SY5Y cell line stops proliferating, extends long neurites and expresses neuronal specific markers, such as GAP43, Map2 and Tau. Post-differentiation, the SH-SY5Y cell line resembles dopaminergic neurones and can be utilised as a model for neurite outgrowth (Xie et al., 2010). Previous groups have utilised phorbol esters such as 12-O-tetradecanoyl-phorbol-13-acetate (TPA) (Pahlman et al., 1983; Pahlman et al., 1981) and growth factors, namely IGF-1 and BDNF (Ivankovic-Diki et al., 2000; Kim et al.,

1997) to differentiate the SH-SY5Y cell line. However, short term treatment of the SH-SY5Y cell line with RA results in a homogenous population of cells with neuronal morphology (Encinas et al., 2000; Dwane et al., 2013).

De et al., (2005) had previously shown an increase in differentiation in SH-SY5Y cells following NGF treatment, but the studies presented in this chapter demonstrated that NGF increased cell proliferation. De et al., (2005) utilised a sub-cloned, positively selected cell line, possibly accounting for the differing results. The studies presented in this chapter demonstrated, in response to RA, the SH-SY5Y cell body expanded. The cells then developed numerous long neurite processes, greater than the length of the cell body. These processes elongated in a time and RA-dependent manner. RA was not considered cytotoxic, as cell viability did not decrease in response to treatment, and cell numbers did not decrease below starting levels. Previous reports have demonstrated that SH-SY5Y cells are more resistant to cytotoxic compounds in response to RA pre-treatment (Simpson et al., 2001; Tieu et al., 1999).

However, chronic long term exposure of the SH-SY5Y cell line to RA resulted in a heterogeneous population of cells, consisting of the differentiated neuroplastic (N-type) cells and proliferative substrate adherent (S-type) cells. The S-type cells do not undergo differentiation in response to RA, but continued to proliferate and outgrow the differentiated N-type cells. Previous reports had identified BDNF as enhancing the effects of differentiation post treatment with RA (Arcangeli et al., 1999), while Edsio et al., (2003) found a similar effect with NGF. The studies in this chapter demonstrated that treatment of SH-SY5Y cells with NGF post differentiation with RA, resulted in the cessation of proliferation of S-type cells and an enhancement of differentiation of the N-type cells, as measured by the extension of neurites, which significantly increased in length. As long as NGF was supplemented every

48 hours, these cultures could be maintained for 20 days without showing any signs of cell death or reversion from the neuronal phenotype.

Coating the cell culture plates with poly-l-lysine or collagen prevented the loss of N-type cells and resulted in a more homogenous population of cells, as well as inducing greater neurite outgrowth. Indeed Dwane et al., (2013) recently showed that laminin induces the longest and highest number of neurites in SH-SY5Y cells, in comparison to collagen and fibronectin. It is perhaps not surprising that laminin induces greater neurite outgrowth as it is a major glycoprotein present in the extracellular matrix in the developing brain. However, initial experiments with the SH-SY5Y cell line by Dwane et al. (2013), in which laminin was chosen as the matrix for cell adhesion, were not continued beyond 72 hours. The studies presented in this chapter demonstrated that neurite outgrowth continues beyond this time point and is enhanced by the addition of NGF.

To further establish that treatment of the SH-SY5Y cell line with RA resulted in differentiation, the mRNA expression levels of some well known differentiation markers were determined. Differentiated SH-SY5Y cells express higher levels of neuronal specific markers, including Gap43 (Meiri et al., 1986), Tau (Cuende et al., 2008) and Map2 (Li et al., 2000; Pan et al., 2005; Sharma et al., 1999). In the studies presented in this chapter differentiation, as determined by the extension of long neurites, was associated with a significant increase in the mRNA expression of all three gene markers. Indeed this response was a time dependent process following exposure to RA. While the studies presented in this chapter observed an increase in Gap43 5 days post treatment, similar to the findings of Cuende et al., (2008), Dwane et al. (2013) reported that RA treatment of the SH-SY5Y cell line for 72 hours did not increase Gap43 at the protein level. Studies described in this chapter demonstrated a significant increase in Map2 mRNA, observed 2 days post treatment of SH-SY5Y cells with

10 μ M RA. While significant increases in Tau were only observed 5 days post treatment with RA. These studies therefore suggest Map2 as an early marker of differentiation in the SH-SY5Y cell line, while Gap43 and Tau are suitable late markers.

The selection and validation of candidate housekeeping genes is important in gene expression analysis as the technique of RT-PCR has been integral to biological research. Therefore the need for stably expressed housekeeping genes is crucial for reliable and repeatable results; these genes need to be carefully evaluated. B-actin and β -tubulin were initially considered, as their expression was stable in undifferentiated SH-SY5Y cells. However, the differentiation process resulted in an increase in both β -actin and β -tubulin mRNA levels. Therefore cyclophilin A was chosen as the reference gene as it was the most stable gene under the experimental conditions. Data normalisation requires an internal control gene, uniformly expressed during change in environmental/experimental conditions in a given system – these studies identified cyclophilin A as a potential candidate, as well as excluding two more commonly used reference genes.

This protocol will be useful for research groups that are studying neuronal protein-protein interactions, as well as promoter studies, but are unable to utilise/manipulate primary hippocampal neurones. There is a need for an *in vitro* model, which is akin to mature neurones *in vivo*; an ideal solution would be the use of primary cell cultures, from human neuronal crest stem cells; however their use is fraught with ethical concerns and culturing issues (Delfino-Machin et al., 2007). Hence immortalised cell lines are a current suitable alternative. Having characterised the SH-SY5Y cell line, the studies presented in this chapter validated the model utilising NGF, a known inducer of VGF (Canu et al., 1997; Levi et al., 1985).

5.8.1 NGF, RA and 1,25D3: Transcriptional activators of the VGF gene and promoter

Levi et al. (1985) demonstrated VGF mRNA was rapidly induced, to the maximal level, 5 hours after the addition of 250ng/ml NGF to PC12 cultures. The studies conducted in this chapter further characterised the response of VGF mRNA to NGF in the SH-SY5Y model. Endogenous VGF gene expression was significantly increased 24 and 48 hours post treatment of the SH-SY5Y cell line with 50ng/ml NGF. Previous studies, utilising the rat promoter, had demonstrated regulatory elements between -600 and +40 (in relation to the transcriptional start site) responsible for the induction of the gene by NGF (Possenti et al., 1992). The studies reported in this chapter, utilising 1Kb of the *vgf* promoter, demonstrated a rapid (+ 1 hour) increase in promoter activity in response to treatment with NGF in both undifferentiated and differentiated SH-SY5Y cells. These maximal levels of promoter activity were maintained for 24 hours in agreement with previous studies (Levi et al., 1985; Canu et al., 1997).

In the studies presented in this chapter, VGF expression increased in response to RA, – the maximum fold induction was observed 48 hours post treatment. VGF mRNA expression was increased in response to SD in the dmpARC of the Siberian hamster (Barrett et al., 2005). However, expression of VGF mRNA is lower in SD (in comparison to LD) across the remainder of the ARC (Barrett et al., 2005). Components of the retinoic acid signalling pathway – CRBP-1, CRABP-2, RAR and RXR – are all reduced in response to SD in the Siberian hamster (Barrett et al., 2006; Ross et al., 2005). Furthermore, in the photoperiod responsive rat, expression of RALDH-1, which converts retinol to RA, is also reduced in the ARC in SD (Shearer et al., 2010) (see Figure 5.8.2). This is presented as a possible mechanism for the reduction in VGF expression in the ARC in response to SD in the Siberian hamster.

Previous studies have demonstrated RA induced increases in VGF protein expression in SK-N-BE cells 72 hours post treatment (Cerchia et al., 2006). RA has been demonstrated to induce neurogenesis by activating both RAR and PPAR β/δ (Yu et al., 2010). Recently, VGF and its derived peptides have also been implicated in neurogenesis (Thakker-Varia et al., 2014). Thakker-Varia et al., (2014) demonstrated that TLQP-62 enhanced adult hippocampal neurogenesis via generation of early progenitor cells. TLQP-62 significantly increased the number of neural progenitor cells while reducing the number of differentiated Type 3 cells. This effect was confirmed *in vitro* where a scrambled version of the TLQP-62 peptide had no effect.

The studies presented in this chapter also generated data which suggested treatment of the SH-SY5Y cell line with 1,25D3 resulted in a significant increase in endogenous VGF mRNA expression (at levels similar to RA). Furthermore, VGF promoter activity increases in response to treatment of undifferentiated and differentiated cells with 1,25D3. Interestingly, 1,25D3 demonstrated neuroprotective qualities *in vitro* (Brewer et al., 2001; Oermann et al., 2004; Wang et al., 2004), while treatment of the SH-SY5Y cell line with 1,25D3 halted proliferation (previously observed by Celli et al., 1999), akin to the effects of RA. However, long term incubation with 1,25D3 only resulted in a slight trend towards differentiation (Celli et al., 1999). More recently, Agholme et al., (2010) proposed pre-treatment with RA, followed by extracellular matrix gel adhesion, in combination with BDNF, neuregulin β 1, NGF and 1,25D3, resulted in differentiated SH-SY5Y cells with unambiguous resemblance to adult neurones. The results presented in this chapter, in combination with those from Esposito et al., (2008), who suggest receptor tyrosine kinase (RET) activation is a critical step in differentiation, Korecka et al., 2013, who suggest RA induces RET expression in SH-SY5Y cells, and Cerchia et al., (2006), who suggest inhibition of RET in SK-N-BE cells ablates increases in VGF expression, support differentiation-induced expression of the VGF gene.

Furthermore, Maestro et al., (2003) reported a functional VDRE in the human insulin receptor gene promoter, which was induced by 1,25D3 in transfected U-937 human cells. The fold induction by 1,25D3 treatment (approximately 1.8 and 1.6 respectively) was akin to the effect of 1,25D3 treatment of the SH-SY5Y cell line on the *vgf* promoter and endogenous gene expression. Similar to the *vgf* promoter, the VDRE in the human insulin receptor promoter is flanked by AP-1 and AP-2 sites (Calle et al., 2008). Furthermore, nuclear receptor sites for vitamin D are found in the midbrain and hindbrain of Siberian hamsters (Stumpf et al., 1992); VDR distribution suggested a role for vitamin D in the regulation of neuroendocrine and metabolic functions. Indeed, Earthman et al., 2012 proposed a link between obesity and low circulating 25-hydroxyvitamin D concentrations.

5.8.2 T3: A transcriptional repressor of the VGF gene and promoter

T3 represses the MC4R gene via a TRE; while mutation of this sequence abolished the T3 dependent repression (Decherf et al., 2010). Treatment of the SH-SY5Y cell line with 10nM T3 resulted in decreased endogenous VGF gene expression, as well as promoter activity. Repression of promoter activity was nullified via removal of the potential TRE from the promoter construct. TREs have previously been shown to function in combination with RAR/RXR (de Luca, 1991). Cheung et al. (2010) demonstrated that heterodimerisation of the TR with the RXR favours the dissociation of suppressors and the recruitment of activators. Therefore it is hypothesised the inability of TR to heterodimerise with RXR results in the repression of VGF in SD (see Figure 5.8.2).

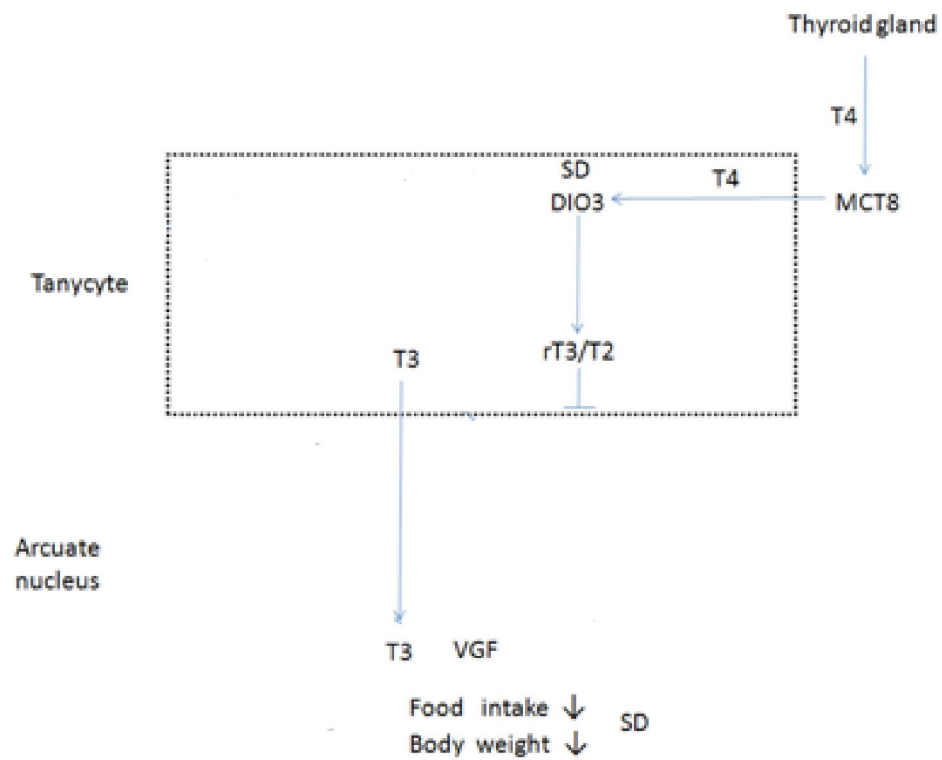
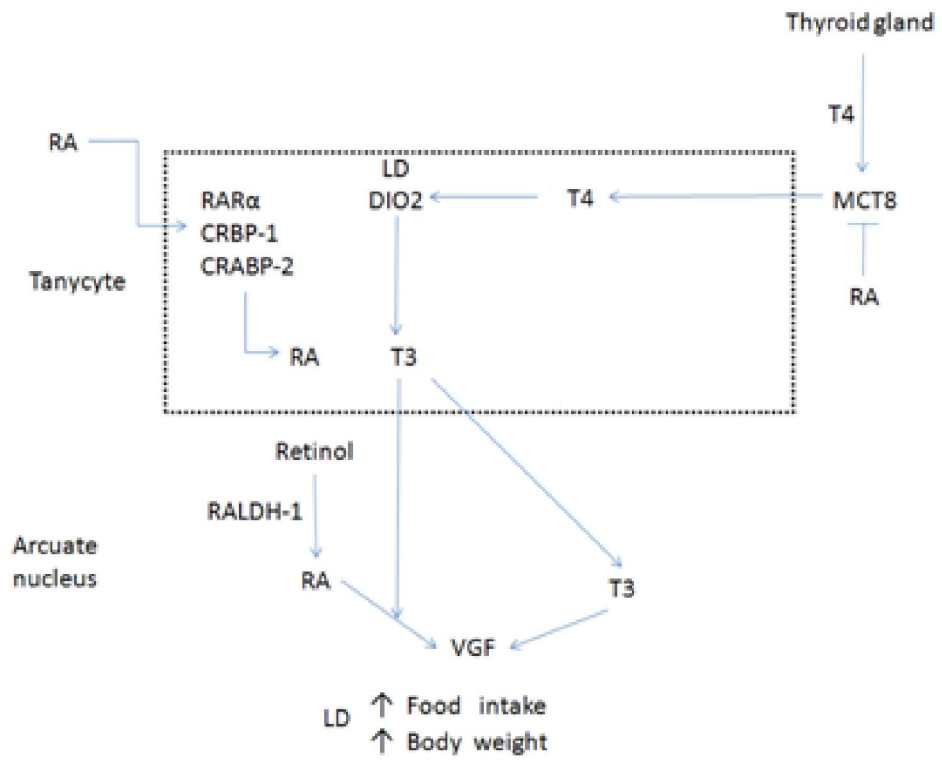


Figure 5.8.2: Schematic of the proposed role of T3 and RA in the hypothalamus of Siberian hamsters as a possible mechanism for the seasonal regulation of appetite. Components of the retinoic acid signalling pathway – CRBP-1, CRABP-2, RAR and RXR – are all reduced in response to SD in the Siberian hamster (Barrett et al., 2006; Ross et al., 2005), while RALDH-1 is reduced in SD in the rat (Shearer et al., 2012). The studies presented in this chapter demonstrate the increased endogenous expression of VGF and promoter activity in response to treatment of the SH-SY5Y cell line. T3 reduced both endogenous expression of VGF and promoter activity, an effect which was nullified by removal of the TRE from the promoter construct. Cheung et al., demonstrated the heterodimerisation of the TR with the RXR favours the dissociation of suppressors and the recruitment of activators. The reduction of RA in SD results in the T3 repression of VGF mRNA in the ARC. Adapted from Ebling, 2014.

There are two further potential mechanisms for the repression of the VGF gene by T3:

1. Silva and Aranda, (2004) demonstrated that T3 inhibited the ras-induced proliferation in neuroblastoma cells and blocked the induction of cyclin D1 expression via the repression of the cyclic AMP response element binding protein (CREB). CREB is a key constituent of the VGF promoter. The cyclic AMP response element (CRE) of the *vgf* promoter is embedded in a 14-bp palindromic sequence – mutations within the CRE sequence abolish NGF and cAMP response (Hawley et al., 1992), while disruption of the palindromic sequence abolishes induction by NGF (Possenti et al., 1992). It was hypothesised by Levi et al., (2004) that VGF expression, in a cell specific manner, requires the combinatorial action of several regulatory complexes, which bind to distinct promoter motifs. This was demonstrated, in relation to the CRE, by D’Arcangelo et al., (1996) where the CCAAT box was shown to be important for the induction of the gene by NGF.
2. In the Siberian hamster in LD, there is a reduction in leptin-induced phosphorylation of signal transducer and activator of transcription-3 (STAT-3) (Tups et al., 2012). Leptin in the hypothalamus binds to its receptor, the ObRb, and activates janus kinase (JAK)-2 tyrosine kinase, resulting in the phosphorylation (activation) of the transcription factor STAT-3 (Benomar et al., 2009). STAT-3 has been shown to control the expression of anorectic and orexigenic neuropeptides (Ahima et al., 2000; Friedman and Halaas, 1998). STAT-3 has also been shown to interact with the CCAAT/enhancer binding protein beta (C/EBP-beta), a binding site (CCAAT box) for which is found in the VGF promoter (Li et al., 1993). The CCAAT box, when mutated, abolishes NGF induction of VGF (D’Arcangelo et al., 1996). T3 decreased STAT-3 phosphorylation in embryonic neural stem cells (Chen et al., 2012). The studies presented in this chapter propose the binding of T3 to its receptor and

subsequently the identified potential TRE reduces VGF endogenous expression and VGF promoter activity in the SH-SY5Y cell line. However, another possible mode of action is via repressing the transcriptional activation of transcription factors such as the STAT-3 C/EBP-beta complex.

In addition hypothyroidism, associated with low levels of T3, stimulates PC-1 and -2 mRNA in the rat hypothalamus and cerebral cortex (Shen et al., 2004). Furthermore, Helwig et al., (2006) demonstrated gene expression of PC-2 was significantly higher in SD in the ARC of Siberian hamsters. Subsequently Shen et al., (2005) demonstrated hyperthyroidism suppresses PC-1 and -2 mRNA. These enzymes are responsible for the processing of the pro-VGF polypeptide (Levi et al., 2004). Therefore it is possible that while VGF mRNA expression is reduced in SD, VGF derived peptides are more abundant in SD. However, this hypothesis does not account for the increase in VGF mRNA in the dmpARC of Siberian hamsters (Barrett et al., 2005). The dmpARC has been proposed as an important integrating centre mediating photoperiodic response, as it is the most responsive of the brain nuclei outside the SCN (Barrett et al., 2005). Considering the published results (Bartolomucci et al., 2006; Jethwa et al., 2007; Toshinai et al., 2010; Saderi et al., 2014), VGF and its derived peptides may be differentially expressed in brain nuclei in response to photoperiod as well as energy homeostasis.

5.9 CONCLUSION

The SH-SY5Y cell line for the study of neuronal VGF gene expression *in vitro* has been validated by the studies reported in this chapter and the response of VGF to NGF and RA has been further characterised. Treatment of the SH-SY5Y cell line with T3 causes a reduction in both endogenous VGF expression and VGF promoter activity, with the effect on promoter activity being lost when a postulated TRE within the VGF promoter was removed. These studies propose possible mechanisms whereby T3 and VGF may interact in the seasonal regulation of appetite. Further work is required *in vivo* to substantiate this proposed mechanism.

6 Chapter 6 – GENERAL DISCUSSION

6.1 SUMMARY

The primary aim of this thesis was to investigate the role and regulation of VGF and its derived peptides in the regulation of energy homeostasis. Previous studies suggested an anabolic role for VGF and its derived peptides; VGF^{-/-} mice were lean, hypermetabolic and hyperactive, with increased food intake per gram body weight (Hahm et al., 1999; Hahm et al., 2002). However, this proposed anabolic role for VGF was not supported by subsequent studies where TLQP-21 increased energy expenditure in mice and reduced food intake in Siberian hamsters (Bartolomucci et al., 2006; Jethwa et al., 2007). Two hypotheses were proposed; i) global ablation of the VGF gene during the course of development resulted in an errant phenotype and ii) VGF derived peptides have opposing roles in the regulation of food intake and energy expenditure.

The studies presented in chapter 3 of this thesis established the initial opposing and time-dependent effects of the VGF derived peptide, HHPD-41, on food intake in the Siberian hamster. The response to ICV infusion of HHPD-41 was a significant and dose dependent increase in food intake (0-1hr), opposing the actions of TLQP-21, which reduced food intake (Jethwa et al., 2007). This, however, was followed by a reduction in food intake (6-24hrs); a similar effect was observed following the ICV infusion of TLQP-21 (see Figure 3.6.2 and Jethwa et al., 2007). Subsequently, in chapter 4, the role of VGF in the regulation of energy balance was further elucidated. Hypothalamic over-expression of VGF mRNA reduced body weight in both the C57Bl/6J mouse and Siberian hamster. Surprisingly, this decrease in body weight was associated with an increase in both food intake and energy expenditure. These effects (on food intake and energy expenditure) were attenuated in disrupted models of energy regulation; food intake and energy expenditure were akin to control Siberian hamsters transferred to SD and in mice fed a HFD. Interestingly, the effects of over-expression do not mirror the peptide studies; a possible result of over-expression of multiple bioactive VGF derived peptides in a non-regulated fashion. Saderi et al., (2014) recently demonstrated expression on

VGF in AgRP/NPY and POMC neurones, which altered in response to the metabolic state of the animal. In addition, for the first time these studies demonstrated the effectiveness of the viral 2A peptide *in vivo* in non-standard laboratory animals. These studies established the viral 2A peptide as an alternative to the ires sequence currently utilised in bicistronic vector strategies and rAAV as a highly effective technique for manipulating gene function *in vivo*. Finally, the studies in chapter 5 investigated the regulation of the VGF gene promoter.. Previous studies identified VGF mRNA was reduced in the ARC and hypothalamus in Siberian hamsters transferred to SD (Barrett et al., 2005), while SD is associated with a reduction in food intake and intra-abdominal fat. The studies in chapter 4 demonstrated that over-expression of VGF mRNA significantly increased food intake in LD and SD. It was found that treatment of the SH-SY5Y cell line with RA increased endogenous VGF gene expression and promoter activity. Interestingly, the components of the RA signalling pathway were reduced in response to SD in the Siberian hamster (Barrett et al., 2006; Ross et al., 2005) and rat (Shearer et al., 2010). Furthermore, a possible TRE was identified in the promoter region of the VGF gene. Treatment of the SH-SY5Y cell line with T3 reduced endogenous VGF gene expression and promoter activity. Removal of the possible TRE from the promoter construct nullified the effect of T3 treatment on *vgf* promoter activity.

6.1.1 The ICV infusion of HHPD-41 demonstrated an initial opposing role of VGF derived peptides in food intake

For the first time these studies observed effects of ICV infusion of HHPD-41 demonstrating it is a novel member of a growing list of neuropeptides in the hypothalamus which regulate feeding and energy expenditure. This finding further supports the role of the VGF gene in the regulation of food intake. Its short term effect (0-1hr) of significantly increased food intake is akin to ICV infusion of NPY in the Siberian hamster (Boss-Williams and Bartness, 1996), which also increased cumulative food intake 0-2hrs post administration.

However, the longer-term effect 6-24 hours was a significant reduction in food intake, a similar effect to TLQP-21 (see figure 3.6.2 and Jethwa et al., 2007). Therefore these studies suggest HHPD-41 is a short term stimulator of food intake in the Siberian hamster, similar to NPY. Toshinai et al., (2010) demonstrated a similar short term effect of ICV infusion of NERP-2, a N-terminal VGF derived peptide, on food intake in the rat. This effect was mediated by the orexin system (Toshinai et al., 2010). Interestingly, NERP-2 initially increased body temperature and oxygen consumption in anaesthetised rats, as well as locomotor activity in a separate study (Toshinai et al., 2010). This duality of increased food intake and energy expenditure is not limited to VGF; derivatives of CART also have opposing effects on food intake with parallel changes in energy expenditure (see section 6.1.2).

However despite the initial short-term (0-1hr) opposing effects on food intake, the longer-term effect (6-24hrs) of ICV infusion of HHPD-41 was a reduction in food intake, similar to TLQP-21 treatment. Whether these inhibitory effects on food intake would be additive, suggesting different receptors/mechanisms, or via similar mechanisms (and therefore not additive) is still to be established. These studies identify HHPD-41 as a novel peptide involved in the hypothalamic regulation of food intake and provide important information with regards the neuronal network which underlies the regulation of energy homeostasis.

6.1.2 The over-expression of VGF mRNA in the hypothalamus of Siberian hamsters and mice demonstrates a function beyond food intake

Having established the roles of VGF derived peptides in food intake, the studies in chapter 4 demonstrated that hypothalamic over-expression of VGF mRNA resulted in a reduction in body weight, associated with increased food intake and energy expenditure. In the Siberian hamster these effects were associated with an increase in BAT weight. Previously surgical denervation or excision of

BAT in mice had been shown to decrease oxygen consumption and increase body weight (Dulloo and Miller, 1984).

In the mouse, long term hypothalamic over-expression of VGF mRNA had no effect on BAT weight, but reduced epididymal fat. Previous studies have demonstrated a reduction in epididymal fat as a consequence of increased metabolic rate (Adams et al., 2006). Bartolomucci et al., (2006) demonstrated ICV infusion of TLQP-21 increased resting energy expenditure in mice. There was also an increase in epinephrine and an up-regulation of BAT β 2-AR and WAT PPAR- δ , β 3-AR and UCP-1, which were independent of activity and TH status. Furthermore, ICV infusion of NERP-2 significantly increased oxygen consumption in the rat (Toshinai et al., 2010). WAT is similarly innervated to BAT (Vaughan et al., 2014)) and long term the changes in gene expression demonstrated by Bartolomucci et al., (2006) following ICV infusion of TLQP-21 would be expected to result in a decrease in WAT weight, whilst the increase in UCP-1 would appear to imply 'beiging' of the tissue (i.e. increased numbers of brown adipocytes and/or mitochondria), resulting in a more metabolically active animal (see Figure 4.6.4.2 A which demonstrates an increase in oxygen consumption over the course of the study). The results, despite being in different species, are therefore largely consistent, although the proposed mechanism of action differs. This is similar to the TLQP-21 studies conducted in mice and Siberian hamsters, while the overall effect of ICV infusion of the VGF derived peptide is catabolic, energy expenditure is increased in the mouse, while food intake is reduced in the Siberian hamster.

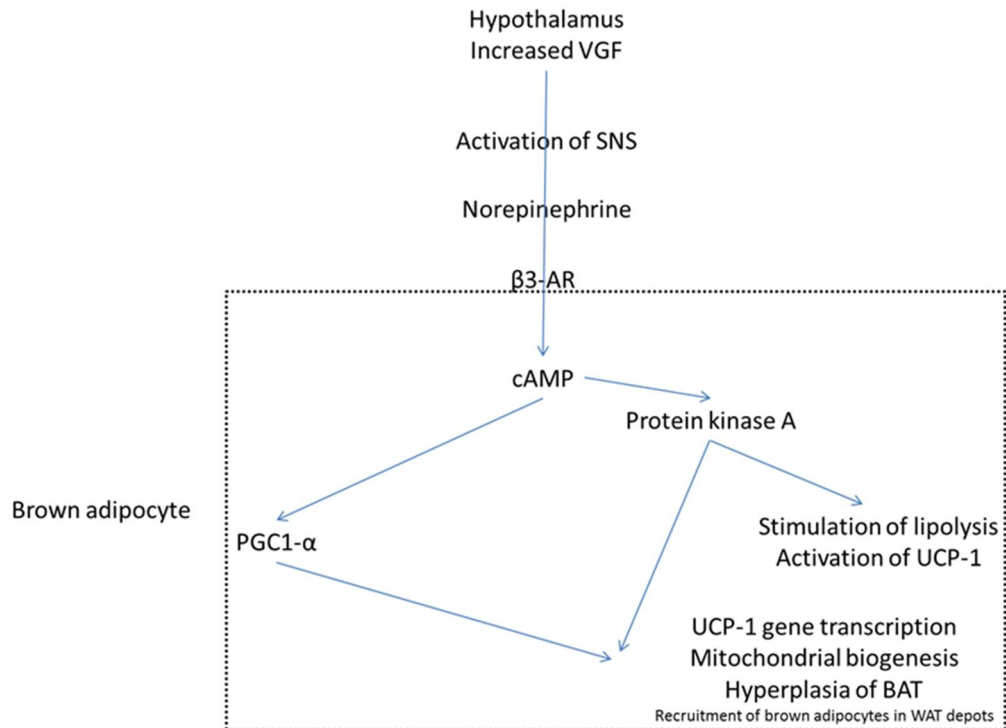


Figure 6.1.2: **A possible mechanism for the activation of BAT by VGF.** Increased hypothalamic VGF possibly results in the activation of the SNS and subsequent norepinephrine release. Indeed, $VGF^{-/-}$ demonstrate increased adrenal norepinephrine and epinephrine content – a possible compensatory mechanism for the global deletion of the gene throughout development (Fargali et al., 2014), while ICV infusion TLQP-21 up-regulates β -AR and UCP-1 in adipose tissue (Bartolomucci et al., 2006). Norepinephrine binds to the β 3-adrenoreceptor (β 3-AR) resulting in an increase in cAMP levels, which rapidly activate protein kinase A (PKA). Activation of UCP-1 results in increased fatty acid oxidation within the mitochondria of BAT (Lopez et al., 2013). PGC1- α is a powerful co-transcriptional activator for nuclear hormone receptor induced transcription of genes involved in thermogenesis, resulting in mitochondrial biogenesis and the recruitment of brown adipocytes in WAT depots (Crowley et al., 2002; Lee et al., 2014).

Similar to VGF, CART is widely distributed throughout the periphery and CNS, particularly the hypothalamus, and has a number of opposing roles (Murphy, 2006). CART co-localises with orexigenic and anorectic neurotransmitters in the hypothalamus, similar to VGF (Saderi et al., 2014). ICV infusion of CART₅₅₋₁₀₂ reduced food intake in rats fed normal chow (similar to TLQP-21 in the Siberian hamster), including in a second group fasted for 24 hours (Kristensen et al.,

1998). However, this reduction in food intake was associated with an increase in lipid oxidation, a decrease in fat storage (effects similar to the gene expression changes in the TLQP-21 treated mice (Bartolomucci et al., 2006)) and body weight gain in rats (Rohner-Jeanrenaud et al., 2002). ICV administration of CART reduces gastric motility, emptying and secretion (Asakawa et al., 2001) and Severini et al., (2009) demonstrated that ICV infusion of TLQP-21 in the rat reduced gastric emptying by 40%. Counter intuitively, $CART^{-/-}$ mice were normal in comparison to wild type littermates (Bannon et al., 2000). Although when transferred to a HFD, $CART^{-/-}$ mice displayed increased food intake, body weight and fat mass. Similarly the phenotype of the $VGF^{-/-}$ mouse closely matches the phenotype of TLQP-21 treated mice; a possible result of the global deletion of VGF throughout development and deletion of several opposing bioactive peptides.

Conversely to its anorectic effects, CART stimulates the release of AgRP and NPY from *ex-vivo* hypothalamic explants (Dhillon et al., 2002). Furthermore, Abbott et al., (2001) demonstrated that injection of $CART_{55-102}$ into distinct hypothalamic areas (including the PVN, VMN, DMN and ARC) increased food intake (similar to HHPD-41). Murphy (2006), proposed that these consequences are less contradictory if CARTs role is to increase food intake and heat production. Chronic delivery of CART into the ARC of rats increases food intake and BAT UCP-1 expression – a similar effect to the over-expression of VGF in the Siberian hamster. Over-expression of CART in the ARC also increased food intake, however these animals demonstrated greater weight loss in response to a 24 hour fast, suggesting increased energy expenditure (Kong et al., 2000). Indeed, ICV infusion of CART into the PVN up-regulates UCP-1 expression in BAT and both UCP-2 and UCP-3 expression in WAT and muscle (Wang et al., 2000). Again this is a similar effect to VGF over-expression in the mouse. Furthermore, the over-expression of CART in the ARC of rats resulted in increased cumulative food intake due to an increased thermogenic response

in BAT (Kong et al., 2003). The VGF over-expression studies in the Siberian hamster and mouse also displayed a similar phenotype.

6.1.3 VGF over-expression in disrupted models of energy homeostasis

Over-expression of VGF mRNA in Siberian hamsters switched to SD maintain significantly increased food intake, however this response was attenuated by switching to SD. Daily food intake and daily food intake per gram bodyweight were no longer significantly increased, although cumulative food intake (per gram body weight) was significantly increased. The Siberian hamster in SD has an increased capacity for thermogenesis (Barrett et al., 2005). Furthermore, the thermogenic capacity of BAT is increased in the Syrian hamster exposed to SD (McElroy et al., 1986), while Demas et al., (2002) demonstrated an increase in UCP-1 and PPAR- γ in Siberian hamsters in SD. Taken together these studies suggest BAT was more active in SD. This might then explain why the effects of over-expression of VGF mRNA are attenuated in SD. Similarly, mice increase norepinephrine induced thermogenesis in response to HFD, an effect which was not observed in UCP-1^{-/-} mice (Feldman et al., 2009). Akin to the Siberian hamster transferred to SD, mice transferred to a high fat diet increase BAT activity. This might explain why the effects of over-expression of VGF mRNA were attenuated by the HFD. Over-expression of VGF mRNA increased energy expenditure in the Siberian hamster in LD and mice fed a normal diet. The capacity for further increases in energy expenditure in response to a challenge (SD in the Siberian hamster; HFD in the mouse) is reduced by the over-expression of VGF mRNA, whose energy expenditure is already increased. Subsequently body weight gain was significantly increased in the mouse VGF treated group. The hypothesis that hypothalamic VGF increases BAT activation is further supported by the Watson et al., (2009) study which demonstrated VGF^{-/-} mice were cold intolerant.

There is, however, an alternative hypothesis for the attenuated effect of VGF over-expression in response to SD in the Siberian hamster and HFD in the mouse. In response to SD, PC1/3 and PC2 gene expression in the hypothalamus of Siberian hamsters has been shown to be increased within the ARC (Helwig et al., 2006). These enzymes produce the VGF derived peptides from the pro-peptide, as well as a number of other neuropeptides from their parent polypeptides. It is therefore possible that the panel of VGF derived peptides produced as a result of over-expression of the gene changes in response to photoperiod. Similarly, leptin regulates the hypothalamic expression of PC1 and PC2 expression in the mouse, increasing PC1 and PC2 promoter activity and protein expression in hypothalamic neurones. Secondly, fasted rats, which have low leptin levels, have decreased PC1 and PC2 gene and protein expression in the PVN. These levels are restored by exogenous administration of leptin to fasted rats (Sanchez et al., 2004). In response to HFD, C57Bl/6J mice become leptin resistant (Lin et al., 2000), therefore the panel of peptides produced from the VGF pro-peptide may change. Indeed, Chakraborty et al., (2006) demonstrated a change in VGF derived peptides in response to HFD.

Over-expression of VGF mRNA, however, did not mirror the results from peptide studies conducted in chapter 3 of this thesis or those performed by Bartolucci et al. (2006) and Jethwa et al. (2007). Given that VGF mRNA is up-regulated in response to fasting in the mouse (Hahm et al., 1999) and the metabolic responses proposed by Sadri et al., (2014), the fact that the over-expression was constant and long-term may account for this unusual phenotype. Furthermore, the production of multiple bioactive peptides, with opposing activities, may offer another explanation for the phenotype of Siberian hamsters and mice which over-express VGF mRNA. A similar paradox, in addition to the one outlined for CART, is found in POMC studies. Its derivatives, namely α MSH and β -endorphin, reduce and increase food intake respectively (Raffin-Sanson et al., 2003). POMC^{-/-} mice are obese (Yaswen et al., 1999) and ICV infusion of β -endorphin increased food intake, as did selective deletion of

the β -endorphin coding sequence from the mouse POMC gene (Appleyard et al., 2003).

6.1.4 Thyroid hormone represses endogenous VGF expression and promoter activity *in vitro*

Having demonstrated a novel role for VGF within the hypothalamus in regulating energy expenditure, the studies in chapter 5 identified novel regulators of the gene *in vitro*. VGF gene expression is reduced in the ARC in response to SD (Barrett et al., 2006), as are the components of the RA signalling pathway (Barrett et al., 2006; Ross et al., 2005). *In vitro* RA treatment of the SH-SY5Y cell line increased endogenous VGF expression and promoter activity. Given that over-expression of VGF mRNA in the Siberian hamster significantly increases food intake, it is proposed that the reduction in RA and subsequently VGF is a possible mechanism for the seasonal regulation of appetite in the Siberian hamster. Furthermore a possible TRE was identified within the *vgf* promoter. T3 treatment of the SH-SY5Y cell line repressed endogenous VGF expression and promoter activity. Removal of the potential TRE from the *vgf* promoter construct nullified the effects of T3. TREs have been previously shown to function in combination with RAR/RXR (de Luca et al., 1991); heterodimerisation favours the recruitment of activators, while homodimerisation favours suppressors of transcriptional activity (Cheung et al., 2010). Inferred from these observations is a possible mechanism for the seasonal regulation of appetite in the Siberian hamster (see Figure 5.7.3). Therefore it is hypothesised the inability of TR to heterodimerise with RAR/RXR results in the repression of the VGF gene in SD; a possible mechanism for the seasonal regulation of appetite. In addition, these studies also identified a possible VDRE and demonstrated increased endogenous VGF expression and promoter activity in response to treatment of the cell line with 1,25D3. Vitamin D was recently implicated in the regulation of energy metabolism and adipocyte biology *in vivo* (Wong et al., 2009).

6.2 MAIN IMPLICATIONS, LIMITATIONS AND FUTURE WORK

While no experimental model is perfect, the number of transgenic and knockout models has enhanced our understanding of the complex aetiology of obesity, which involves genetic, metabolic, behavioural and environmental factors. Indeed these models have improved our knowledge of the physiological and molecular mechanisms affecting energy homeostasis. The data presented within this thesis raises important questions with respect to our understanding of the regulation of energy homeostasis and therefore have potential implications for the design of pharmaceuticals for the treatment of obesity.

These studies demonstrate further scientific work is warranted. A physiological assessment of the VGF derived peptides in response to starvation, refeeding and high fat diet, along with photoperiod in the Siberian hamster may further elucidate the data obtained to date. Utilising liquid chromatography and mass spectrometry, as opposed to antibodies which do not detect specific VGF derived peptides, may be advantageous and informative. Whilst HHPD-41 and TLQP-21 are produced by the proteolytic cleavage of TLQP-62, the most abundant of the VGF derived peptides in the rat hypothalamus (Bartolomucci et al., 2007), HHPD-41 may itself be cleaved to produce AQEE-30. AQEE-30 evoked dose-dependent thermal hyperalgesia (Riedl et al., 2009) and penile erection in rats (Succu et al., 2004).

Similarly, the inability to confirm the different peptides produced by over-expression of VGF mRNA is a limitation of these studies. No VGF derived peptide specific antibody is currently available; antisera are limited to C or N terminal sequences (Brancia et al., 2010), which bind to a number of different peptides and therefore lack the required specificity. More generally, however, the technique relies upon obtaining large blocks of tissue, which may not reveal

the differences in small populations of cells. Further detailed studies are required before a definitive conclusion can be reached.

Over-expression of VGF mRNA in the hypothalamus, rather than specific nuclei within the hypothalamus, may obscure the intricacies of VGF's function, similar to the VGF^{-/-} mouse. The total ablation of a gene in all tissues in a global knockout model is often disadvantageous; knockout models are often lethal. They may also result in a permanent and/or compensatory change during development. For example, the ICV administration of the CART peptide resulted in reduced food intake in rats, and an antibody against CART increased food intake (Kristensen et al., 1998). However, the over-expression of CART in the ARC of rats resulted in increased cumulative food intake due to an increased thermogenic response in BAT (Kong et al., 2003). A further example of this is NPY, a potent stimulator of food intake, but NPY^{-/-} mice have a normal phenotype (Erickson et al., 1997). Therefore, over-expression or knockdown of the VGF gene within specific subsets of hypothalamic neurones utilising *Cre* recombinase technology or optogenetics would be a better strategy to investigate the role of VGF (Saper, 2010).

Studies conducted at thermoneutrality in the Siberian hamster and mouse may further elucidate the role of VGF in thermogenesis; Feldmann et al., (2009) demonstrated UCP-1 ablation was sufficient to induce obesity in mice exempt from thermal stress. To defend body temperature, mice increase their metabolism and food intake (Golozobova et al., 2004). This effect may obscure the effects of VGF over-expression and account for the differing mechanism of action when compared to the Siberian hamster. In response to a cold environment, mice increase UCP-1 expression and heat production in BAT (Shabalina et al., 2010). Again the effects of VGF over-expression in mice held at 4°C may be obscured. Alternatively a short term fast, which decreases BAT turnover (Matamala et al., 1996) may not occur in mice which over-express VGF

mRNA. These studies would further support the role of VGF in energy expenditure. Denervation of BAT and WAT in Siberian hamsters and mice respectively, which over-express VGF mRNA may also demonstrate its role in energy expenditure.

A chronic ICV infusion study of HHPD-41 (similar to TLQP-21 study conducted by Jethwa et al., 2007) may demonstrate a role in the regulation of body weight. The reduction in food intake 6-24hrs following acute ICV infusion of HHPD-41 would suggest a reduction in body weight following chronic (daily) infusion of the VGF derived peptide. Similarly, the effects of ICV infusion in SD would further elucidate its role in food intake. Furthermore, a study in mice and rats akin to the Bartolomucci et al., (2006) and Toshinai et al., (2010) would further substantiate its role in food intake. Further experimentation is required to assess whether the initial increase in food intake, and subsequent decrease, is the only effect of HHPD-41 administration. Boss-Williams and Bartness (1996) and Day and Bartness (2003) noted an increase in food hoarding in the Siberian hamster in response to treatment with NPY and AgRP respectively. Furthermore, Severini et al., (2009) demonstrated that TLQP-21 reduced gastric motility in rats post ICV infusion. This, however, could not be accurately assessed in the chosen model of the Siberian hamster as the species has the ability to store food within their cheek pouches (Warner et al., 2010).

Recently, two possible receptors have been identified for the VGF derived peptide TLQP-21 (see Chapter 3.7 DISCUSSION) (Chen et al., 2013; Hannedouche et al., 2013). However, the Chen et al., (2013) model did not elicit a response to TLQP-62, suggesting there might be multiple receptors for this and other VGF derived peptides. Given the outlined changes in the proteolytic enzymes which act upon the VGF pro-polypeptide and the Sadari et al., (2014) data which demonstrated VGF mRNA expression in both AgRP/NPY and POMC neurones, further work to identify the receptors involved is required.

The endogenous expression of the VGF gene and promoter analysis yielded interesting and novel data, including some potential regulatory factors and a possible mechanism for VGFs role in the response to SD. However, isolation of the Siberian hamster VGF promoter and gene is required to confirm this initial work with the mouse promoter. Electrophoretic mobility shift assays (EMSAs), in order to determine the presence of the possible TRE and VDRE interactions with their respective receptors are required. Furthermore these EMSAs could determine the proposed interaction with RA as a possible mechanism for the seasonal regulation of appetite in the Siberian hamster. Importantly, this validated promoter system could be utilised to screen for other potential regulators of the VGF gene and neuronal genes in general.

6.3 CLOSING REMARKS

At present there are no approved drugs that reduce appetite and manage weight which acts centrally. Indeed those who did such as sibutramine and rimonabant were withdrawn due to severe side effects (Ebling, 2014). The data reported in this thesis enhances our understanding of the role of VGF in regulating food intake and energy expenditure, and therefore energy homeostasis. However, further work is still required to identify feasible drug targets, given the prevalence and co-morbidities of obesity.

Appendix 1 – Buffers and Solutions

10mM PBS

Dissolve 8g NaCl, 0.2g KCl and 1.44g Na₂HPO₄ and 0.24g KH₂PO₄ in 1000ml water; adjust to pH 7.6 with dilute HCl.

1M CaCl₂

Dissolve 110.99g of anhydrous CaCl₂ in 800ml deionised water, adjust volume to 1000ml with water.

1M MgCl₂

Dissolve 203.30g of MgCl₂.6H₂O in 800ml water, adjust volume to 1000ml with water.

1M MgSO₄

Dissolve 120.37g of MgSO₄ in 800ml water, adjust volume to 1000ml with water.

2M NaOH

Dissolve 80g in 800ml water, adjust volume to 1000ml with water.

2M Tris-HCl

Dissolve 96.91g of Tris-HCl in 250ml water, adjust pH to 7.5 and volume to 400ml with water.

3M Sodium acetate

Dissolve 24.61g of sodium acetate in 100ml water.

1N NaOH

Dissolve 40g in 900ml water, adjust volume to 1000ml.

1,25D3

Dilute in cell culture medium from 10 μ M stock solutions, prepared in ethanol.

5xTBST

Dissolve 50g NaCl, 1g KCl and 125ml Tris (pH 7.5) in 800ml water, adjust volume to 950ml. Autoclave then add 50ml Tween-20 (final concentration 5%).

Agarose

Dissolve agarose (weight as appropriate for % gel) in TAE buffer (volume as appropriate for % gel).

BCIP

5-bromo-4-chloro-3-indolyl-phosphate, 4-toluidine, stock at 50mg/ml in dimethylformamide.

Blocking solution

1 x MABT (see below) with 20% goat serum and 2% Roche blocking reagent.

Diethyl-pyrocabonate-PBS

1 x PBS with diethyl-pyrocabonate (DEPC) added to 0.1%

Ethidium bromide

Add 50 μ l of 10mg/ml ethidium bromide to 1000ml water

Glucose

Dissolve 20g of glucose in 100ml water.

Glycerol

Mix 60ml of glycerol with 100ml water

Hybridisation buffer (hyb)

25ml formamide, 3.25ml SSC, 0.5ml EDTA (0.5M pH 8), 125 μ l yeast RNA (20mg/ml), 1ml Tween-20 (10%), 2.5ml CHAPS (10%), 100 μ l heparin (50mg/ml) and 17.5ml water.

LB

Dissolve 10g sodium chloride, 10g tryptone and 5g yeast extract in 1000ml water. Autoclave. Add antibiotic, once cooled, as appropriate.

LB agar

Dissolve 10g sodium chloride, 10g tryptone, 5g yeast extract and 15g bacto-agar in 1000ml water. Add antibiotic, once cooled, as appropriate.

MABT

100mM maleic acid, 150mM NaCl, 0.1% Tween-20, pH to 7.5 with NaOH

NBT

4-nitro blue tetrazolium chloride at 75mg/ml in 70% dimethylformamide

NGF

Dissolve in RPMI medium, supplemented with 100µg/ml BSA.

NMTT

1ml 5M NaCl, 2.5ml Tris (2M pH 9.5), 1.25ml MgCl₂ (2M), 5ml Tween-20 (10%) and 40.25ml water

NZY + broth

Dissolve 10g NZ amine, 5g yeast, 5g sodium chloride in 1000ml water, pH adjusted to 7.5 using 2M NaOH

PBSTw

PBS with 0.1% Tween-20

PFA

Add 40g PFA to 800ml PBS (at 60°C), add 1N NaOH until a clear solution forms. Cool and filter solution, adjust volume to 1000ml with PBS. Recheck pH, adjust with dilute HCl to 6.9.

RA

A 3mg/ml solution was prepared in DMSO and stored at -20°C (light-protected). RA was diluted with RPMI as required.

T3

Dissolve 1mg of T3 in 1ml 1N NaOH, add to 49ml RPMI for a 20µg/ml stock solution. Dilute as appropriate in culture medium.

TAE

Tris-acetate-ethylenediamine tetraacetic acid buffer comprised a final concentration of 40mM Tris-HCl, 1mM EDTA (pH 8.0) and 1.142 ml glacial acetic acid in 1000ml water.

Washing buffer

25ml formamide, 2.5ml SSC and 0.5ml Tween-20.

REFERENCES

Abbott CR, Rossi M, Wren AM, Murphy KG, Kennedy AR, Stanley SA, Zollner AN, Morgan DG, Morgan I, Ghatei MA, Small CJ & Bloom SR (2001) Evidence of an orexigenic role for cocaine- and amphetamine-regulated transcript after administration into discrete hypothalamic nuclei. *Endocrinology* 142, 3457-3463.

Adam CL, Moar KM, Logie TJ, Ross AW, Barrett P, Morgan, PJ & Mercer JG (2000) Photoperiod regulates growth, puberty and hypothalamic neuropeptide and receptor gene expression in female Siberian hamsters. *Endocrinology* 141 4349-4356.

Adams SH, Lei C, Jodka CM, Nikoulina SE, Hoyt JA, Gedulin B, Mack CM & Kendall ES (2006) PYY[3-36] administration decreases the respiratory quotient and reduces adiposity in diet-induced obese mice. *Journal of Nutrition* 136 195-201.

Agholme L, Lindstrom T, Kagedal K, Marcusson J & Hallbeck M (2010) An in vitro model for neuroscience - differentiation of SH-SY5Y cells into cells with morphological and biochemical characteristics of mature neurons. *Journal of Alzheimer's Disease* 20 1069-1082.

Ahima RS, Prabakaran D, Mantzoros C, Qu D, Lowell B, Maratos-Flier E & Flier JS (1996) Role of leptin in the neuroendocrine response to fasting. *Nature* 382 250-252.

Ahima RS (2008) Revisiting leptin's role in obesity and weight loss. *Journal of Clinical Investigation* 118 2380-2383.

Ahima RS & Antwi DA (2008) Brain regulation of appetite and satiety. *Endocrinology and Metabolism Clinics of North America* 34 811-823.

Ahlman H & Nilsson (2001) The gut as the largest endocrine organ in the body. *Annals of Oncology* 12 s63-68.

Air El, Benoit SC, Clegg DJ, Seeley RJ & Woods SC (2002) Insulin and leptin combine additively to reduce food intake and body weight in rats. *Endocrinology* 143 2449-2452.

Alkemada A (2010) Central and peripheral effects of thyroid hormone signalling in the control of energy metabolism. *Journal of Neuroendocrinology* 22 56-63.

Anand B & Brobeck J (1951) Localisation of a feeding centre in the hypothalamus of the rat. *Proceedings for the Society of Experimental Biology and Medicine* 77 323-324.

Archer ZA, Moar KA, Logie TJ, Reilly L, Stevens V, Morgan PJ & Mercer JG (2007) Hypothalamic neuropeptide gene expression during recovery from food restriction superimposed on short-day photoperiod-induced weight loss in the Siberian hamster. *American Journal of Physiology* 293 1094-1101.

Asakawa A, Inui A, Yuzuriha H, Nagata T, Kaga T, Ueno N, Fujino MA & Kasuga M (2001) Cocaine-amphetamine-regulated transcript influences energy metabolism, anxiety and gastric emptying in mice. *Hormone Metabolism Research* 33 554-558

Atchison RW, Casto BC & Hammon WM (1965) Adenovirus-associated defective virus particles. *Science* 149 754-756.

Baggio LL & Drucker DJ (2007) Biology of incretins: GLP-1 and GIP. *Gastroenterology* 132 2131-2157.

Balthasar N1, Coppari R, McMinn J, Liu SM, Lee CE, Tang V, Kenny CD, McGovern RA, Chua SC Jr, Elmquist JK & Lowell BB (2004) Leptin receptor signalling in POMC neurons is required for normal body weight homeostasis. *Neuron* 42 983-991.

Bandsma RH, Sokollik C, Chami R, Cutz E, Brubaker PL, Hamilton JK, Perlman K, Zlotkin S, Sigalet DL, Sherman PM, Martin MG & Avitzur Y (2013) From diarrhea to obesity in prohormone convertase 1/3 deficiency: age-dependent, clinical, pathologic, and enteroendocrine characteristics. *Journal of Clinical Gastroenterology* 47 834-843.

Bannon AW, Seda J, Carmouche M, Richards WG, Fan W, Jarosinski M, McKinzie AA, Douglass J (2000) Biological functions of CART: Data with CART eptide and CART knockout mice. *Society of Neuroscience Abstracts* 26, 2041.

Barker SB (1951) Mechanisms of action of the thyroid hormone. *Physiology Reviews* 31 205-243.

Branca C, Cocco C, D'Amato F, Noli B, Sanna F, Possenti R, Argiolas A & Ferri GL (2010) Selective expression of TLQP-21 and other VGF peptides in gastric neuroendocrine cells and modulation by feeding. *The Journal of Endocrinology* 207, 329-341.

Barrett P, Ross AW, Balik A, Littlewood PA, Mercer JG, Moar KM, Sallmen T, Schuhler S, Ebling FJP, Ubeaud C & Morgan PJ (2005) Photoperiodic regulation of histamine H3 receptor and VGF mRNA in the arcuate nucleus of the Siberian hamster. *Endocrinology* 146 1930-1939.

Barrett P, Ivanova E, Graham ES, Ross AW, Wilson D, Ple H, Mercer JG, Ebling FJP, Schuhler S, Dupre SM, Loudon ASI & Morgan PJ (2006) Photoperiodic regulation of GPR50, Nestin and CRBP1 in tanycytes of the third ventricle

ependymal layer of the Siberian hamster. *Journal of Endocrinology* 191 687-698.

Barrett, P, Ebling FJ, Schuhler S, Wilson D, Ross, AW, Warner A, Jethwa P, Boelen A, Visser TJ, Ozanne DM, Archer ZA, Mercer JG & Morgan PJ (2007) Hypothalamic thyroid hormone catabolism acts as a gatekeeper for the seasonal control of body weight and reproduction. *Endocrinology* 148 3608-3617.

Bartlet A, Bruns OT, Reimer R, Hohenberg H, Ittrich H, Peldschus K, Kaul MG, Tromsdorf UI, Weller H, Waurisch C, Eychmuller A, Gordts PL, Rinninger F, Bruegelmann K, Freund B, Nielsen P, Merkel M & Heeren J (2011) Brown adipose tissue activity controls triglyceride clearance. *Nature Medicine* 17 200-205.

Bartolomucci A, La Corte G, Possenti R, Locatelli V, Rigamonti AE, Torsello A, Bresciani E, Bulgarelli I, Rizzi R, Pavone F, D'Amto FR, Severini C, Mignogna G, Giorgi A, Schinina ME, Elia G, Brancia C, Ferri GL, Conti R, Ciani B, Pascucci T, Dell'Omo G, Muller EE, Levi A & Moles A (2006) TLQP-21, a VGF derived peptide, increases energy expenditure and prevents the early phase of diet induced obesity. *Proceedings in the National Academy of Sciences* 103 14584-14589.

Bartolomucci A, Bresciani E, Bulgarelli I, Rigamonti AE, Pascucci T, Levi A, Possenti R, Torsello A, Locatelli V, Muller EE & Moles A (2009) Chronic intracerebroventricular injection of TLQP-21 prevents high fat diet induced weight gain in fast weight gaining mice. *Genes and Nutrition* 4 49-57.

Baybis M & Salton SR (1992) Nerve growth factor rapidly regulates VGF gene transcription through cycloheximide sensitive and insensitive pathways. *Federation of European Biochemical Societies Letters* 308 202-206.

Benonmar Y, Berthou F, Vacher CM, Bailleux V, Gertler A, Djiane J & Taouis M (2009) Leptin But Not Ciliary Neurotrophic Factor (CNTF) Induces Phosphotyrosine Phosphatase-1B Expression in Human Neuronal Cells (SH-SY5Y): Putative Explanation of CNTF Efficacy in Leptin-Resistant State. *Endocrinology* 150 1182-1191.

Benson DL & Salton SR (1996) Expression and polarisation of VGF in developing hippocampal neurons. *Developmental Brain Research* 96 219-228.

Bernardis LL & Bellinger LL (1987) The dorsomedial hypothalamic nucleus revisited: 1986 update. *Brain Research* 434 321-381.

Berthoud HR (2008) The vagus nerve, food intake and obesity. *Regulatory Peptides* 149 15-25.

Bi S, Chen J, Behless RR, Hyn J, Kopin AS & Moran TH (2007) Differential body weight and feeding responses to high fat diets in rats and mice lacking cholecystokinin 1 receptors. *Regulatory, Integrative and Comparative Physiology* 239 55-63.

Bianco AC & Kim BW (2006) Deiodinases: implications of the local control of thyroid hormone action. *Journal of Clinical Investigation* 116 2571-2579.

Bjursell M, Ahnmark A, Bohlooly-Y M, William-Olsson, Rhedin M, Peng XR, Ploj K, Gerdin AK, Arnerup G, Elmgren A, Berg AL, Oscarsson J & Linden D (2007) Opposing effects of adiponectin receptors 1 and 2 on energy metabolism. *Diabetes* 56 583-593.

Blevins JE & Ho JM (2013) Role of oxytocin signaling in the regulation of body weight. *Reviews in Endocrine and Metabolic Disorders* 14 311-329.

Boelen A, Wiersinga WM & Fliers E (2008) Fasting induces changes in the hypothalamus-pituitary-thyroid axis. *Thyroid* 18 123-129.

Boender AJ, Koning NA, van den Heuvel JK, Juijendijk MCM, van Rozen AJ, la Fleur SE & Adan RAH (2014) AAV-Mediated Gene Transfer of the Obesity-Associated Gene *Etv5* in Rat Midbrain Does Not Affect Energy Balance or Motivated Behavior. *PLOS One* 9 e94159-e94159.

Bonni A, Ginty DD, Dudek H, & Greenberg ME (1995) Serine 133-phosphorylated CREB induces transcription via a cooperative mechanism that may confer specificity to neurotrophin signals. *Molecular Cellular Neuroscience* 6 168-183.

Boss-Williams KA & Bartness TJ (1996) NPY stimulation of food intake in Siberian hamsters is not photoperiod dependent. *Physiol Behav* 59 157-164.

Brady LS, Smith MS, Gold PW & Herkenham M (1990) Altered expression of hypothalamic neuropeptide mRNAs in food restricted and food deprived rats. *Neuroendocrinology* 52 441-447.

Brent GA, Williams GR, Harney JW, Forman BM, Samuels HH, Moore DD & Larsen PR (1992) Capacity for cooperative binding of thyroid hormone (T3) receptor dimers defines wild type T3 response elements. *Molecular Endocrinology* 6 502-514.

Brewer LD, Thiabault V, Chen KC, Langub MC, Landfield PW & Porter NM (2001) Vitamin D hormone confers neuroprotection in parallel with downregulation of L-type calcium channel expression in hippocampal neurons. *Journal of Neuroscience* 21 98-108.

Broadwell RD & Brightman MW (1976) Entry of peroxidase into neurons of the central and peripheral nervous system from extracerebral and cerebral blood. *Journal of Comparative Neurology* 166 257-283.

Brown DM, Donaldson K, Borm PJ, Schins RP, Denhardt M, Gilmour P, Jimenez LA & Stone V (2004) Calcium and ROS-mediated activation of transcription factors TNF- α cytokine gene expression in macrophages exposed to ultrafine particles. *Lung Cellular and Molecular Physiology* 286 344-353.

Calle C, Maestro B & Garcia-Arencibia M (2008) Genomic actions of 1,25-dihydroxyvitamin D₃ on insulin receptor gene expression, insulin receptor number and insulin activity in the kidney, liver and adipose tissue of streptozotocin-induced diabetic rats. *BMC Molecular Biology* 9 1-12.

Cannon B & Nedergaard J (2004) Brown adipose tissue: function and physiological significance. *Physiological Reviews* 84 277-359.

Canu N, Possenti R, Rinaldi AM, Trani E & Levi A (1997) Molecular cloning and characterisation of the human VGF promoter region. *Journal of Neurochemistry* 68 1390-1399.

Cassina V, Torsello A, Tempestini A, Salerno D, Brogioli D, Tamiazzo L, Bresciani E, Martinez J, Fehrentz JA, Verdie P, Omeljaniuk RJ, Possenti R, Rizzi L, Locatello V & Mantegazza F (2013) Biophysical characterisation of a binding site for TLQP-21, a naturally occurring peptide which induces resistance to obesity. *Biochimica et Biophysica Acta* 1828 455-460.

Celli A, Treves C & Stio M (1999) Vitamin D receptor in SH-SY5Y human neuroblastoma cells and effect of 1,25-dihydroxyvitamin D₃ on cellular proliferation. *Neurochemistry International* 34 117-124.

Cerchia L, D'Alessio A, Amabile G, Duconge F, Pestourie C, Tavitian B, Libri D & de Franciscis V (2006) An Autocrine Loop Involving Ret and Glial Cell-Derived Neurotrophic Factor Mediates Retinoic Acid-Induced Neuroblastoma Cell Differentiation. *Molecular Cancer Research* 4 481-488.

Chaing PM, Ling J, Jeong YH, Price DL, Aja SM & Wong PC (2010) Deletion of TDP-43 down-regulates Tbc1d1, a gene linked to obesity, and alters body fat metabolism. *Proceedings of the National Academy of Sciences United States of America* 107 16320-16324.

Chakraborty TR, Tkalych O, Nanno D, Garcia AL, Devi LA & Salton SR (2006) Quantification of VGF- and pro-SAAS-derived peptides in endocrine tissues and the brain, and their regulation by diet and cold stress. *Brain Research* 1089 21-32.

Chan HY, Xing X, Kraus P, Yap SP, Ng P, Lim SL & Lufkin T (2011) Comparison of IRES and F2A-Based Locus-Specific Multicistronic Expression in Stable Mouse Lines. *PLoS One* 6 e28885.

Chang DS, Su H, Tang GL, Brevetti LS, Sarkar R, Wang R, Kan YW & Messina LM (2003) Adeno-associated viral vector-mediated gene transfer of VEGF normalizes skeletal muscle oxygen tension and induces arteriogenesis in ischemic rat hindlimb. *Molecular Therapy* 7 44-51.

Chemelli RM, Willie JT, Sinton CM, Elmquist JK, Scammell T, Lee C, Richardson JA, Williams SC, Xiong Y, Kisanunke Y, Fitch TE, Nakazato M, Hammer RE, Saper CB & Yanagisawa M (1999) Nacrolepsy in rexin knockout mice: Molecular genetics of sleep regulation. *Cell* 98 437-451.

Chen C, Zhou Z, Zhong M, Zhang Y, Li M, Zhang L, Qu M, Yang J, Wang Y & Yu Z (2012) Thyroid hormone promotes neuronal differentiation of embryonic neural stem cells by inhibiting STAT3 signaling through TR α 1. *Stem Cells and Development* 21 2667-2681.

Chen YA, Pristera MA, Swanwick KK, Hamada Y, Rice ASC & Okuse K (2013) Identification of a receptor for neuropeptide VGF and its role in neuropathic pain. *Journal of Biological Chemistry* 288 34638-34646.

Chernogubova E, Hutchinson DS, Nedergaard J & Bengtsson T (2005) Alpha1- and beta1-adrenoceptor signaling fully compensates for beta3-adrenoceptor deficiency in brown adipocyte norepinephrine-stimulated glucose uptake. *Endocrinology* 146 2271-2284.

Cheung CC, Clifton DK & Steiner RA (1997) POMC neurons are direct targets for leptin in the hypothalamus. *Endocrinology* 138 4489-4492.

Cheung SY, Leonard JL & Davis PJ (2010) Molecular aspects of thyroid hormone actions. *Endocrine Reviews* 31 139-170.

Cheung YT, Lau WK, Yu MS, Lai CS, Yeung SC, So KF & Chang RC (2009) Effects of all-trans-retinoic acid on human SH-SY5Y neuroblastoma as in vitro model in neurotoxicity research. *Neurotoxicology* 30 127-135.

Chin LS, Li L & Greengard P (1994) Neuron specific expression of the synapsin II gene is directed by a specific core promoter and upstream regulatory elements. *Journal of Biological Chemistry* 269 18507-18513.

Chiorini JA, Kim F, Yang L & Kotin RM (1999) Cloning and characterization of adeno-associated virus type 5. *Journal of Virology* 73 1309-1319.

Cho KO, Skarnes WC, Minsk B, Palmieri S, Jackson-Grusby L & Wagner JA (1989) Nerve growth factor regulates gene expression by several distinct mechanisms. *Molecular Cell Biology* 9 135-143.

Clark JT, Kalra PS, Crowley WR & Kalra SP (1984) Neuropeptide Y and human pancreatic polypeptide stimulate feeding behaviour in rats. *Endocrinology* 115 427-427 1984

Cocco C, Brancia C, Pirisi I, D'Amato F, Noli B, Possenti R & Ferri FL (2007) VGF metabolic-related gene: Distribution of its derived peptides in mammalian pancreatic islets. *The Journal of Histochemistry and Cytochemistry* 55 619-628.

Colnot S, Lambert M, Blin C, Thomasset M & Perret C (1995) Identification of DNA sequences that bind retinoid X receptor-1,25(OH)₂D₃-receptor heterodimers with high affinity. *Molecular and Cellular Endocrinology* 113 89-98.

Coppola A, Lui ZA, Andrews ZB, Paradis E, Roy MC, Friedman JM, Ricquier D, Richard D, Horvath TL Gao XB & Diano S (2007) A central thermogenic-like mechanism in feeding regulation: an interplay between arcuate nucleus T₃ and UCP-2. *Cell Metabolism* 5 21-33.

Costa-e-Sousa RH & Hollenberg AN (2012) Minireview: The neural regulation of the hypothalamic-pituitary-thyroid axis. *Endocrinology* 153 4128-4135.

Cowley MA, Smart JL, Rubinstein M, Cerdán MG, Diano S, Horvath TL, Cone RD & Low MJ (2001) Leptin activates anorexigenic POMC neurons through a neural network in the arcuate nucleus. *Nature* 411 480-484.

Crowley VE, Yeo GS & O'Rahilly S (2002) Obesity therapy: altering the energy intake and expenditure balance sheet. *Nature Reviews: Drug Discovery* 1, 276-286.

Cuende J, Moreno S, Bolanos JP & Almeida A (2008) Retinoic acid downregulates Rae1 leading to APC(Cdh1) activation and neuroblastoma SH-SY5Y differentiation. *Oncogene* 27 3339-3344.

Cypress AM, Lehman S, Williams G, Tal I, Rodman D, Goldfine AB, Kuo FC, Plamer EL, Tseng YH, Doria A, Kolodny GM & Kahn CR (2009) Identification and Importance of Brown Adipose Tissue in Adult Humans. *The New England Journal of Medicine* 360 1509-1517.

D'Arcangelo G, Habas R, Wang S, Halegoua S & Salton SR (1996) Activation of codependent transcription factors is required for transcriptional induction of the vgf gene by nerve growth factor and Ras. *Molecular Cell Biology* 16 4621-4631.

Das KP, Freudenrich TM & Mundy WR (2004) Assessment of PC12 cell differentiation and neurite growth: a comparison of morphological and neurochemical measures. *Neurotoxicology and Teratology* 26 397-406.

Davis PJ, Leonard JL & Davis FB (2008) Mechanisms of nongenomic actions of thyroid hormone. *Frontiers in Neuroendocrinology* 29 211-218.

Day DE & Bartness TJ (2004) Agouti-related protein increases food hoarding more than food intake in Siberian hamsters. *American Journal of Physiology. Regulatory, Integrative and Comparative Physiology* 286 38-45.

de Backer MWA, Fitzsimons CP, Bans MAD, Lujendijk MCM, Garner KM, Vreugdenhil E & Adan RAH (2010) An adeno-associated viral vector transduces the rat hypothalamus and amygdala more efficiently than a lentiviral vector. *BMC Neuroscience* 11 1-8.

de Backer MW, la Fleur SE & Adan RA (2011) Both overexpression of AgRP or NPY in the PVN or LH induce obesity in a neuropeptide and nucleus specific manner. *European Journal of Pharmacology* 660 148-155.

de Felipe P & Ryan MD (2004) Targeting of proteins derived from self-processing polyproteins containing multiple signal sequences. *Traffic* 5 616-626.

de Luca LM (1991) Retinoids and their receptors in differentiation, embryogenesis, and neoplasia. *FASEB J* 5 2924-2933.

de Sliva A & Bloom SR (2012) Gut Hormones and Appetite Control: A Focus on PYY and GLP-1 as Therapeutic Targets in Obesity. *Gut and Liver* 6 10-20.

Decherf S, Seugnet I, Kouidhi S, Lopez-Juarez A, Clerget-Froidevaux MS & Demeneix BA (2010) Thyroid hormone exerts negative feedback on hypothalamic type 4 melanocortin receptor expression. *PNAS* 107 4471-4476.

Denroche HC, Huynh FK & Kieffer TJ (2012) The role of leptin in glucose homeostasis. *Journal of Diabetes Investigation* 3 115-129.

Dhillon WS, Small CJ, Stanley SA, Jethwa PH, Seal LJ, Murphy KG, Ghatei MA & Bloom SR (2002) Hypothalamic interactions between neuropeptide Y, agouti-related protein, cocaine- and amphetamine-regulated transcript and alpha-melanocyte-stimulating hormone in vitro in male rats. *Journal of Neuroendocrinology* 14 725-730.

Dhillon WS, Small CJ, Gardiner JV, Bewick GA, Whitworth EJ, Jethwa PH, Seal LJ, Ghatei MA, Hinson JP & Bloom SR (2003) Agouti-related protein has an inhibitory paracrine role in the rat adrenal gland. *Biochemical and Biophysical Research Communications* 301 102-107.

Di Rocco G, Pennuto M, Illi B, Canu N, Filocamo G, Trani E, Rinaldi AM, Possenti R, Mandolesi G, Sirinian MI, Jucker R, Levi A & Nasi S (1997) Interplay of the E box, the cyclic AMP response element, and HTF4/HEB in transcriptional regulation of the neurospecific, neurotrophin-inducible *vgf* gene. *Molecular Cellular Biology* 17 1244-1253.

Diano S, Farr SA, Beniot SC, McNay EC, da Silva I, Horvath B, Gaskin FS, Nonaka N, Jaeger LB, Banks WA, Morley JE, Pinto S, Sherwin RS, Xu L, Yamada KA, Sleeman MW, Tschop MH & Horvath TL (2006) Ghrelin controls hippocampal spine synapse density and memory performance. *Nature Neuroscience* 9 381-388.

Dietrich M & Horvath T (2010) Neural regulation of food intake and energy balance. *Nature Reviews Neuroscience Poster*, August.

Dietrich M & Horvath T (2012) Limitations in anti-obesity drug development: the critical role of hunger-promoting neurons. *Nature Reviews Drug Discovery* 11 675-691.

Djazayery AD, Miller DS & Stock MJ. (1978) Energy balances in obese mice. *Ntr Metab* 23 357-367.

Doerksen LF, Bhattacharya A, Kannan P, Pratt D & Tainsky MA (1996) Functional interaction between a RARE and an AP-2 binding site in the regulation of the human HOX A4 gene promoter. *Nucleic Acids Research* 24 2849-2856.

Dolnikoff M, Martin-Hidalgo A, Machado UF, Lima FB & Herrera E (2001) Decreased lipolysis and enhanced glycerol and glucose utilization by adipose tissue prior to development of obesity in monosodium glutamate (MSG) treated-rats. *International Journal of Obesity* 25 426-433.

Donnelly ML, Luke G, Mehrotra A, Li X, Hughes LE, Gni D & Ryan MD (2001) Analysis of the aphtovirus 2A/2B polyprotein cleavage mechanism indicates not a Proteolytic reaction but a novel translational effect: a putative ribosomal skip. *The Journal of General Virology* 82 1013-1025.

Dulloo AG & Miller DS (1984) Energy balance following sympathetic denervation of BAT. *Canadian Journal of Physiology and Pharmacology* 62 235-240.

Egleson KL, Fairfull LD, Salton SR & Levitt P (2001) Regional differences in neurotrophin availability regulate selective expression of VGF in the developing limbic cortex. *Journal of Neuroscience* 21 9315-9324.

Earthman CP, Beckman LM, Masodkar K & Sibley SD (2012) The link between obesity and low circulating 25-hydroxyvitamin D concentrations: considerations and implications. *International Journal of Obesity* 36 387-396.

Ebling FJP, Arthurs OJ, Turney BW & Cronin AS (1998) Seasonal neuroendocrine rhythms in the male Siberian hamster persist following monosodium glutamate-induced lesions of the arcuate nucleus in the neonatal period. *Journal of Neuroendocrinology* 10 701-712.

Ebling FJP & Barrett P (2008) The regulation of seasonal changes in food intake and body weight. *Journal of Neuroendocrinology* 20 827-833.

Ebling FJP, Wilson D, Wilson D, Wood J, Hughes D, Mercer JG, Morgan PJ & Barrett P (2008) Localisation of the TRH secretory system in the Siberian hamster. *Journal of Neuroendocrinology* 20 576-586.

Ebling FJP (2014) On the value of seasonal mammals for identifying mechanisms underlying the control of food intake and body weight. *Hormones and Behavior* 66 56-65.

Egawa M, Yoshimatsu H & Bray GA (1991) Neuropeptide Y suppresses sympathetic activity to interscapular brown adipose tissue in rats. *American Journal of Physiology* 260 328-334.

Ellis C, Moar KM, Logie TJ, Ross AW, Morgan PJ & Mercer JG (2008) Diurnal profiles of hypothalamic energy balance gene expression with photoperiod manipulation in the Siberian hamster, *Phodopus sungorus*. *American Journal of Physiology: Regulatory, Integrative and Comparative Physiology* 294 R1148-11453.

Elmqvist JK (2001) Hypothalamic pathways underlying the endocrine, autonomic, and behavioral effects of leptin. *International Journal of Obesity and Related Metabolic disorders* 25 s78-82.

Encanis M, Iglesias M, Liu Y, Wang H, Muhaisen A, Cena V, Gallego C & Comella JX (2000) Sequential treatment of SH-SY5Y cells with retinoic acid and brain-derived neurotrophic factor gives rise to fully differentiated, neurotrophic factor dependent, human neuron like cells. *Journal of Neurochemistry* 75 991-1003.

Erickson JC, Ahima RS, Hollopeter G, Flier JS & Palmiter RD (1997) Endocrine function of neuropeptide Y knockout mice. *Regulatory Peptides* 70, 199-202.

Ernst MB, Wunderlich CM, Hess S, Paehler M, Mesaros A, Koralov SB, Kleinriders A, Husch A, Münzberg H, Hampel B, Alber J, Kloppenburg P, Brüning JC & Wunderlich FT (2009) Enhanced Stat3 activation in POMC neurons

promotes negative feedback inhibition of leptin and insulin signalling in obesity. *Neuroscience Journal* 29 11582-11593.

Fadel J, Bubser M & Deutch AY (2002) Differential activation of orexin neurons by antipsychotic drugs associated with weight gain. *Journal of Neuroscience* 22 6742-6746.

Farooqi IS, Yeo GS, Keogh JM, Aminian S, Jebb SA, Butler G, Cheetham T & O'Rahilly S (2000) Dominant and recessive inheritance of morbid obesity associated with melanocortin 4 receptor deficiency. *The Journal of Clinical Investigation* 106 271-279.

Farooqi IS & O'Rahilly S (2006) Genetics of obesity in humans. *Endocrinological Reviews* 27 710-717.

Fekete C & Lechan RM (2007) Negative feedback regulation of hypophysiotropic thyrotropin releasing hormone (TRH) synthesizing neurons: role of neuronal afferents and type 2 deiodinase. *Frontiers in Neuroendocrinology* 28 97-114.

Feldmann HM, Golozoubova V, Cannon B & Nedergaard J (2009) UCP1 ablation induces obesity and abolishes diet-induced thermogenesis in mice exempt from thermal stress by living at thermoneutrality. *Cell Metabolism* 9 203-209.

Feletou M, Galizzi J & Levens N (2006) NPY receptors as drug targets for the central regulation of body weight. *CNS and Neurological Disorders Drug Targets* 5 263-274.

Ferri GL, Levi A & Possenti (1992) A novel neuroendocrine gene product: selective VGF8a gene expression and immune-localisation of the VGF protein in endocrine and neuronal populations. *Molecular Brain Research* 13 139-43.

Ferri GL, Gaudio RM, Cossu M, Rinaldi AM, Polak JM, Berger P & Possenti R (1995) The VGF protein in rat adenohypophysis: Sex differences and changes during the estrous cycle and after gonadectomy. *Endocrinology* 136 2244-2251.

Flatt J (2001) Macronutrient composition and food selection. *Obesity Research* 9 256-262.

Foresight Tackling Obesity: Future Choices Project (2007)
http://www.foresight.gov.uk/obesity/obesity_final/08.pdf Accessed 23rd May 2011

Fargali S, Garcia AL, Sadahiro M, Jiang C, Janssen WG, Lin WJ, Cogliani V, Elste A, Mortillo S, Cero C, Veitenheimer B, Graiani G, Pasinetti GM, Mahata SK, Osborn JW, Huntley GW, Phillips GR, Benson DL, Bartolomucci A & Salton SR (2014) The granin VGF promotes genesis of secretory vesicles, and regulates

circularizing catecholamine levels and blood pressure. *FASEB Journal* 28, 2120-2133.

Francis K, Lewis BM, Akatsu H, Monk PN, Cain SA, Scanlon MF, Morgan BP, Ham J & Gasque P (2003) Complement C3a receptors in the pituitary gland: a novel pathway by which an innate immune molecule releases hormones involved in the control of inflammation. *The Federation of American Societies for Experimental Biology Journal* 17 2266-2268.

Frayling TM (2007) A common variant in the FTO gene is associated with body mass index and predisposes to childhood and adult obesity. *Science* 316 889-894.

Friedman JM & Halaas JL (1998) Leptin and the regulation of body weight in mammals. *Nature* 395 763-770.

Funato H, Tsai AL, Willie JT, Kisanuki Y, Williams SC, Sakurai T & Yanagisawa M (2009) Enhanced orexin receptor 2 signalling prevents DIO and improves insulin sensitivity. *Cell Metabolism* 9 64-76.

Furler S, Paterna JC, Weibel M & Bueler H (2001) Recombinant AAV vectors containing the foot and mouth disease virus 2A sequence confer efficient bicistronic gene expression in cultured cells and rat substantia nigra neurons. *Gene Therapy* 8 864-873.

Gao G, Vandenberghe LH & Wilson JM (2005) New recombinant serotypes of AAV vectors. *Current Gene Therapy* 5 285-297.

Gardiner JV, Kong WM, Ward H, Murphy KG, Dhillo WS & Bloom SR (2005) AAV mediated expression of anti-sense neuropeptide Y cRNA in the arcuate nucleus of rats results in decreased weight gain and food intake. *Biochemical and Biophysical Research Communications* 327 1088-1093.

Garza JC, Kim CS, Liu J, Zhang W & Lu XY (2008) Adeno-associated virus-mediated knockdown of melanocortin-4 receptor in the paraventricular nucleus of the hypothalamus promotes high-fat diet-induced hyperphagia and obesity. *Journal of Endocrinology* 197 471-482.

Gauthier K, Plateroti M, Harvey CB, Williams GR, Weiss RE, Refetoff S, Willott JF, Sundin V, Roux JP, Malaval L, Hara M, Samarut J & Chassande O (2001) Genetic analysis reveals different functions for the products of the thyroid hormone receptor alpha locus. *Molecular and Cellular Biology* 21 4748-4760.

German JP, Wisse BE, Thaler JP, Oh-I S, Sarruf DA, Ogimoto K, Kaiyala KJ, Fischer JD, Matsen ME, Taborsky GJ Jr, Schwartz MW & Morton GJ (2010) Leptin Deficiency Causes Insulin Resistance Induced by Uncontrolled Diabetes. *Diabetes* 59 1626-1634.

Gibbs J, Young RC & Smith GP (1973) Cholecystokinin decrease food intake in rats. *Journal of Comparative Physiology and Psychology* 84 488-495.

Gillies GE, Linton EA & Lowry PJ (1982) Corticotropin releasing activity of the new CRF is potentiated several times by vaspressin. *Nature* 299 355-357.

Glass CK & Rosenfeld MG (2000) The coregulator exchange in transcriptional functions of nuclear receptors. *Genes and Development* 15 121-141.

Gold E (1977) Hypothalamic-pituitary function tests: current status. *Postgraduate Medicine* 62 105-114.

Golozoubova V1, Gullberg H, Matthias A, Cannon B, Vennström B & Nedergaard J (2004) Depressed thermogenesis but competent brown adipose tissue recruitment in mice devoid of all hormone-binding thyroid hormone receptors. *Molecular Endocrinology* 18, 384-401.

Goya L & Timiras PS (1991) Characterisation of nuclear T3 receptors in human neuroblastoma cells SH-SY5Y: Effect of differentiation with sodium butyrate and nerve growth factor. *Neurochemical Research* 16 113-116.

Grieger JC & Samulski (2005) Packaging capacity of adeno-associated virus serotypes: impact of larger genomes in infectivity and postentry steps. *Journal of Virology* 79 9933-9944.

Hagan MM, Rushing PA, Pritchard IM, Schwartz MW, Strack AM, Van der Ploeg LH, Woods SC & Seeley RJ (2000) Longer term orexigenic effects of AgRP involve mechanisms other than melanocortin receptor blockade. *Am J Physiol Regul Integr Comp Physiology* 279 47-52.

Hahn S, Mizuno TM, Wu TJ, Wisor JP, Priest CA, Kozak CA, Boozer CN, Peng B, McEvoy RC, Good P, Kelley KA, Takahashi JS, Pintar JE, Roberts JL, Mobbs CV & Salton SR (1999) Targeted deletion of the Vgf gene indicates that the encoded secretory peptide precursor plays a novel role in the regulation of energy balance. *Neuron* 23 537-48.

Hahn S, Fekete C, Mizuno T, Windsor J, Yan H, Boozer CN, Lee C, Elmquist JK, Lechan RM, Mobbs CV & Salton SR (2002) VGF is required for obesity induced by diet, gold thioglucose treatment and agouti and is differentially regulated in proopiomelanocortin and neuropeptide Y containing arcuate neurons in response to fasting. *The Journal of Neuroscience* 22 6929-6938.

Halford J, Wanninayake S & Blundell J (1998) Behavioural satiety sequence (BSS) for the diagnosis of drug action in food intake. *Pharmacology, Biochemistry and Behaviour* 61 159-168.

Hannedouche S, Beck V, Leighton-Davies J, Beibel M, Roma G, Oakeley EJ, Lannoy V, Bernard J, Hamon J, Barbieri S, Preuss I, Lasbennes MC, Sailer AW, Suply T, Seuwen K, Parker CN & Bassilana F (2013) Identification of the C3a (C3AR1) as the target of the VGF-derived peptide TLQP-21 in rodent cells. *Journal of Biological Chemistry* 288 27434-27443.

Haussler MR, Whitfield GK, Haussler CA, Hsieh JC, Thompson PD, Selznick SH, Dominguez CE & Jurutka PW (1998) The nuclear vitamin D receptor: biological and molecular regulatory properties revealed. *Journal of Bone and Mineral Research* 13 325-349.

Havel PJ (2001) Peripheral signals conveying metabolic information to the brain: short-term and long-term regulation of food intake and energy homeostasis. *Experimental Biology and Medicine* 226 963-977.

Hawley R, Scheibe R & Wagner J (1992) NGF induces the expression of the VGF gene through a cAMP response element. *The Journal of Neuroscience* 12 2573-2581.

Hazlerigg D & Loudon A (2008) New Insights into Ancient Seasonal Life Timers. *Current Biology* 18, R795-R804.

Health Survey for England (2005)
<http://www.dh.gov.uk/en/publicationsandstatistics/pubishedsurvey/healthsurveyforengland/healthsurveyresults/index.htm> Accessed 23rd May 2011

Hellen CU & Sarnow P (2001) Internal ribosome entry sites in eukaryotic mRNA molecules. *Genes and Development* 15 1593-1612.

Herwig A, Wilson D, Logie TJ, Boelen A, Morgan PJ, Mercer JG & Barrett P (2009) Photoperiod and acute energy deficits interact on components of the thyroid hormone system in hypothalamic tanycytes of the Siberian hamster. *American Journal of Physiology* 296 1307-1315.

Herwig A, de Vries EM, Bolborea M, Wilson D, Mercer JG, Ebling FJP, Morgan PJ & Barrett P (2013) Hypothalamic Ventricular Ependymal Thyroid Hormone Deiodinases Are an Important Element of Circannual Timing in the Siberian Hamster (*Phodopus sungorus*). *PLoS ONE* 8 e62003.

Herwig A, Petri I & Barrett P (2012) Hypothalamic gene expression rapidly changes in response to photoperiod in juvenile Siberian hamsters (*Phodopus sungorus*). *Journal of Neuroendocrinology* 24, 991-998.

Hetherington A & Ranson S (1940) Hypothalamic lesions and adiposity in the rat. *Anatomical Records* 78 149.

Hevroni D, Rattner A, Bundman M, Lederfein D, Gabarah A, Mangelus M, Silverman MA, Kedar H, Naor C, Kornuc M, Hanoch T, Seger R, Theill LE, Nedivi E, Richter-Levin G & Citri Y (1998) Hippocampal plasticity involves extensive gene induction and multiple cellular mechanisms. *Journal of Molecular Neuroscience* 10 75-98.

Heymsfield S, Greenberg A, Fujioka K, Dixon RM, Kushner R, Hunt T, Lubina JA, Patane J, Self B, Hunt P & McCamish M (1999) Recombinant leptin for weight loss in obese and lean adults: a randomised, controlled, dose escalation trial. *The Journal of the American Medicinal Association* 282 1567-1575.

Hill JW, Elias CF, Fukuda M, Williams KW, Berglund ED, Holland WL, Cho YR, Chuang JC, Xu Y, Choi M, Lauzon D, Lee CE, Coppari R, Richardson JA, Zigman JM, Chua S, Scherer PE, Lowell BB, Brüning JC & Elmquist JK. (2010) Direct insulin and leptin action on POMC neurons is required for normal glucose homeostasis and fertility. *Cell Metabolism* 11 286-297.

Hillman JB, Tong J & Tschop M 2011 Ghrelin biology and its role in weight-related disorders. *Discovery Medicine* 11, 521-528.

Holst JJ & Deacon CF (2013) Is there a place for incretin therapies on obesity and prediabetes? *Trends in Endocrinology and Metabolism* 24 145-152.

Huo L, Gamber K, Greeley S, Silva J, Huntoon N, Leng XH & Jorbaek C (2009) Leptin dependent control of glucose balance and locomotor activity in POMC neurons. *Cell Metabolism* 9 537-547.

Ibrahimi A, Vande Velde G, Reumers V, Toelen J, Thiry I, Vandequette C, Vets S, Deroose C, Bormans G, Baekelandt V, Debyser Z & Gijssbers R (2009) Highly efficient multicistronic lentiviral vectors with peptide 2A sequences. *Human Gene Therapy* 20 845-860.

Ishiguro H, Kim KT, Joh TH & Kim KS (1993) Neuro-specific expression of the human dopamine β -hydroxylase gene requires both cAMP-response element and a silencer region. *Journal of Biological Chemistry* 268 17987-17994.

Ishii S, Kamegai J, Tamura H, Shimizu T, Sugihara H & Oikawa S (2003) Hypothalamic neuropeptide Y/Y1 receptor pathway activated by a reduction in circulating leptin, but not an increase in circulating ghrelin, contributes to hyperphagia associated with triiodothyronine-induced thyrotoxicosis. *Neuroendocrinology* 78 321-330.

Ivankovic-Dikic I, Gronroos E, Blaukat A, Barth BU & Dikic I (2000) Pyk2 and FAK regulate neurite outgrowth induced by growth factors and integrins. *Nature Cell Biology* 2 574-581.

James WP, Caterson ID, Coutinho W, Finan N, van Gaal LF, Maggioni AP, Torp-Pederson C, Sharma AM, Shepherd GM, Rode RA, Renz CL & Investigators S (2010) Effect of sibutramine on cardiovascular outcomes in overweight and obese subjects. *The New England Journal of Medicine* 363 905-917.

Jang SK, Krausslich HG, Nicklin MJ, Duke GM, Palmenberg AC & Wimmer E (1998) A segment of the 5' nontranslated region of encephalomyocarditis virus RNA directs internal entry of ribosomes in vitro translation. *Journal of Virology* 62 2636-2343.

Jethwa P, Warner A, Nilaweera K, Brameld JM, Keyte JW, Carter WG, Bolton N, Bruggaber M, Morgan PJ, Barrett P & Ebling FJ (2007) VGF derived peptide, TLQP-21, regulates food intake and body weight in Siberian hamsters. *Endocrinology* 148 4044-4055.

Jethwa PH & Ebling FJP (2008) Role of VGF-derived peptides in the control of food intake, body weight and reproduction. *Neuroendocrinology* 88 80-87.

Jethwa PH, Barrett P, Turnbull Y, Enright RA, Warner A, Murphy M & Ebling FJ (2009) The role of histamine 3 receptors in the control of food intake in a seasonal model of obesity: the Siberian hamster. *Behavioural Pharmacology* 20 155-165.

Jethwa PH, Warner A, Fowler MJ, Murphy M, de Backer MW, Adan RAH, Barrett P, Brameld JM & Ebling FJP (2010) Short-days induce weight loss in Siberian hamsters despite overexpression of the agouti-related peptide gene. *Journal of Neuroendocrinology* 22 564-575.

Kadowaki S & Normal AW (1984) Dietary vitamin D is essential for normal insulin secretion from the perfused rat pancreas. *Journal of Clinical Investigation* 73 759-766.

Kalra SP (1997) Appetite and body weight regulation: is it all in the brain? *Neuron* 19 227-230.

Kalra SP, Dube MG, Pu S, Xu B, Horvath TL & Kalra PS (1999) Interacting appetite-regulating pathways in the hypothalamic regulation of body weight. *Endocrine Reviews* 20 68-100.

Kay MA, Glorioso JC & Naldini L (2001) Viral vectors for gene therapy: the art of turning infectious agents into vehicles of therapeutics. *Nature Medicine* 7 33-40.

Keen-Rhinehart E, Kalra SP & Kalra PS (2005) AAV-mediated leptin receptor installation improves energy balance and the reproductive status of obese female Koletsky rats. *Peptides* 26 2567-2578.

Kennedy GC (1953) The role of depot fat in the hypothalamic control of food intake in the rat. *Proceedings of the Royal Society of London* 140 578-596.

Kim B, Leventhal PS, Saltiel AR & Feldman EL (1997) Insulin like growth factor I mediated neurite outgrowth in vitro requires mitogen activated protein kinase activation. *Journal of Biological Chemistry* 272 21268-21273.

Kim KB, Kim BW, Choo HJ, Kwon YC, Ahn BY, Choi JS, Lee JS & Ko YG (2009) Proteome analysis of adipocyte lipid rafts reveals that gC1qR plays essential roles in adipogenesis and insulin signal transduction. *Proteomics* 9 2373-2382.

Kim KB, Yi JS, Nguyen N, Lee JH, Kwon YC, Ahn BY, Cho H, Kim YK, Yoo HJ, Lee JS & Ko YG (2011) Cell-surface receptor for complement component C1q (gC1qR) is a key regulator for lamellipodia formation and cancer metastasis. *Journal of Biological Chemistry* 286 23093-23101.

Kim MS, Rossi M, Abusnana S, Sunter D, Morgan DG, Small CJ, Edwards CM, Heath MM, Stanley SA, Seal LJ, Bhatti JR, Smith DM, Ghatei MA, & Bloom SR (2000) Hypothalamic localisation of the feeding effect of agouti-related peptide and alpha-melanocyte stimulating hormone. *Diabetes* 49 177-182.

Klos A, Tenner AJ, Johswick KO, Ager RR, Reis ES & Kohl J (2009) The role of anaphylatoxins in health and disease. *Molecular Immunology* 46 275-2766.

Knopper LD and Boily P (2000) The energy budget of captive Siberian hamsters, *Phodopus sungorus*, exposed to photoperiod changes: mass loss is caused by a voluntary decrease in food intake. *Physiology and Biochemical Zoology* 73 517-522.

Kobelt D, Aumann J, Fichtner I, Stein U, Schlag PM & Walther W (2010) Activation of the CMV-IE promoter by hyperthermia in vitro and in vivo: biphasic heat induction of cytosine deminase suicide gene expression. *Molecular Biotechnology* 46 197-205.

Kong W, Stanley S, Gardiner J, Abbott C, Murphy K, Seth A, Connoley I, Ghatei M, Stephens D & Bloom S (2003) A role for arcuate cocaine and amphetamine-regulated transcript in hyperphagia, thermogenesis, and cold adaptation. *FASEB Journal* 17, 1688-1690.

Könner AC, Janoschek R, Plum L, Jordan SD, Rother E, Ma X, Xu C, Enriori P, Hampel B, Barsh GS, Kahn CR, Cowley MA, Ashcroft FM & Brüning JC (2007) Insulin action in AgRP-expressing neurons is required for suppression of hepatic glucose production. *Cell Metabolism* 5 438-449.

Korhonen R, Kankaanranta H, Lahti A, Ladhe M, Knowles RG & Moilanen E (2001) Bi-directional effects of elevation of intracellular calcium on the expression of inducible nitric-oxide synthase in J774 macrophages exposed to

low and to high concentrations of endotoxin. *The Biochemical Journal* 354 351-358.

Kozak M (1987) An analysis of 5'—noncoding sequences from 699 vertebrate messenger RNAs. *Nucleic acids research* 15 8125-8148

Kraly FS, Carty WJ, Resnick S & Smith GP (1978) Effect of CCK on meal size and intermeal interval in the sham-feeding rat. *Journal of Comparative and Physiological Psychology* 92 697-707.

Kristensen P, Judge ME, Thim L, Ribel U, Christjansen KN, Wulff BS, Clausen JT, Jensen PB, Madsen OD, Vrang N, Larsen PJ & Hastrup S (1998) Hypothalamic CART is a new anorectic peptide regulated by leptin. *Nature* 393 72-76.

Laslop A, Mahata SK, Wolkersdorfer M, Mahata M, Srivastava M, Seidah NG, Fischer-Colbrie R & Winkler H (1994) Large dense-core vesicles in rat adrenal after reserpine: levels of mRNAs of soluble and membrane-bound constituents in chromaffin and ganglion cells indicate a biosynthesis of vesicles with higher secretory quanta. *Journal of Neurochemistry* 62 2448-2456.

Lavenius E, Gestblom C, Johansson I, Nanberg E & Pahlman S (1995) Transfection of TRK-A into human neuroblastoma cells restores their ability to differentiate in response to nerve growth factor. *Cell Growth and Differentiation* 6 727-736.

Lechan RM & Fekete C (2004) Feedback regulation of thyrotropin-releasing hormone (TRH): mechanisms for the non-thyroidal illness syndrome. *Journal of Endocrinological Investigation* 27 105-119.

Lechan RM & Fekete C (2006) The TRH neuron: a hypothalamic integrator of energy metabolism. *Progress in Brain Research* 153 209-235.

Lee YH, Jung YS & Choi D (2014) Recent advance in brown adipose tissue physiology and its therapeutic potential. *Experimental & Molecular Medicine* 46 e78.

Leibowitz SF & Wortley KE (2004) Hypothalamic control of energy balance; different peptides, different functions. *Peptides* 25 473-504.

Leinninger GM (2009) Location Location Location: the CNS sites of leptin action dictate its regulation of homeostatic and hedonic pathways. *International Journal of Obesity* 33 14-17.

Lenard NR & Berthoud HR (2008) Central and peripheral regulation of food intake and physical activity. *Obesity* 16 s11-22

Levi A, Eldridge JD & Paterson BM (1985) Molecular cloning of a gene sequence regulated by nerve growth factor. *Science* 229 393-395.

Levi A, Ferri GL, Watson E, Possenti R & Salton SR (2004) Processing, distribution, and function of VGF, a neuronal and endocrine peptide precursor. *Cellular and Molecular Neurobiology* 24 517-533.

Lewis SA & Cowan NJ (1986) Anomalous placement of introns in a member of the intermediate filament multigene family: an evolutionary conundrum. *Molecular and Cellular Biology* 6 1529-1534.

Li BS, Zhang L, Gu J, Amin ND & Pant HC (2000) Integrin alpha(1) beta(1)-mediated activation of cyclin-dependent kinase 5 activity is involved in neurite outgrowth and human neurofilament protein H Lys-Ser-Pro tail domain phosphorylation. *Journal of Neuroscience* 20 6055-6062.

Li L, Suzuki T, Mori N & Greengard P (1993) Identification of a functional silencer element involved in neuron specific expression of the synapsin I gene. *Proceedings of the National Academy of Sciences of the USA* 90 1460-1464.

Liebling DS, Eisner JD, Gibbs J & Smith GP (1975) Intestinal satiety in rats. *Journal of Comparative and Physiological Psychology* 89 955-965.

Lin S, Thomas TX, Storlien LH & Huang XF (2000) Development of high fat diet-induced obesity and leptin resistance in C57BL/6J mice. *International Journal of Obesity* 24 639-646.

Lin S, Boey D & Herzog H (2004) NPY and Y receptors lessons from transgenic and knockout models. *Neuropeptides* 38 189-200.

Lin HV, Plum L, Ono H, Gutiérrez-Juárez R, Shanabrough M, Borok E, Horvath TL, Rossetti L & Accili D. (2010) Divergent regulation of energy expenditure and hepatic glucose production by insulin receptor in agouti related protein and POMC neurons. *Diabetes* 59 337-346

Loiler SA, Conlon TJ, Song S, Tang Q, Warrington KH, Agarwal A, Kapturczak M, Li C, Ricordi C, Atkinson MA, Muzyczka N & Flotte TR (2003) Targeting recombinant adeno-associated virus vectors to enhance gene transfer to pancreatic islets and liver. *Gene Therapy* 10 1551-1558.

López M, Varela L, Vázquez MJ, Rodríguez-Cuenca S, González CR, Velagapudi VR, Morgan DA, Schoenmakers E, Agassandian K, Lage R, Martínez de Morentin PB, Tovar S, Nogueiras R, Carling D, Lelliott C, Gallego R, Oresic M, Chatterjee K, Saha AK, Rahmouni K, Diéguez C & Vidal-Puig A (2010) Hypothalamic AMPK and fatty acid metabolism mediate thyroid regulation of energy balance. *Nature Medicine* 16 1001-1008.

Lopez M, Alvarez CV, Nogueiras R & Dieguez C (2013) Energy balance regulation by thyroid hormones at central level. *Trends in Molecular Medicine* 19, 418-427.

LoPresti P, Poluha W, Poluha DK, Drinkwater E & Ross AH (1992) Neuronal differentiation triggered by blocking cell proliferation. *Cell Growth and Differentiation* 3 627-635.

Lowell BB, Susulic V, Hamann A, Lawitts JA, Himms-Hagen J, Boyer BB, Kozak LP & Flier JS (1993) Development of obesity in transgenic mice after genetic ablation of brown adipose tissue. *Nature* 366 740-742.

Lubrano-Bertheliet C, Cavazos M, Le Stunff C, Haas K, Shapiro A, Zhang S, Bougneres P & Vaisse C (2003) The human MC4R promoter: Characterisation and role in obesity. *Diabetes* 52 2996-3000.

Maestro B, Davila N, Carranza MC & Calle C (2003) Identification of a Vitamin D response element in the human insulin receptor gene promoter. *The Journal of Steroid Biochemistry and Molecular Biology* 84 223-230.

Mahata SK, Mahata M, Fischer-Colbrie R & Winkler H (1993) In situ hybridisation: mRNA levels of secretogranins II, VGF and peptidylglycine alpha-amidating monooxygenase in brain of salt loaded rats. *Histochemistry* 99 287-293.

Maia AL, Goemann IM, Meyer EL & Wajner SM (2011) Type 1 iodothyronine deiodinase in human physiology and disease. *Journal of Endocrinology* 209 283-297.

Mamane Y, Chan CC, Lavalley G, Morin N, Xu LJ, Huang J, Gordon R, Thomas W, Lamb J, Schadt EE, Kennedy BP & Mancini JA (2009) The C3a anaphylatoxin receptor is a key mediator of insulin resistance and functions by modulating adipose tissue macrophage infiltration and activation. *Diabetes* 58 2006-2017.

Mandel RJ, Manfredsson FP, Foust KD, Rising A, Reimsnider S, Nash K & Burger C (2006) Recombinant adeno-associated viral vectors as therapeutic agents to treat neurological disorders. *Molecular Therapy* 13 463-483.

Mandolesi G, Gargano S, Pennuto M, Illi B, Molfetta R, Soucek L, Mosca L, Levi A, Jucker R & Nasi S (2002) NGF-dependent and tissue-specific transcription of *vgf* is regulated by a CREB-p300 and bHLH factor interaction. *The Federation of European Biochemical Societies Letters* 510 50-56.

Marsh DJ, Miura GI, Yagaloff KA, Schwartz MW, Barsh GS & Palmiter RD (1999) Effects of neuropeptide Y deficiency on hypothalamic agouti related protein expression and responsiveness to melanocortin analogues. *Brian Res* 848 66-77.

Martin P, Albagli O, Poggi MC, Boulukos KE & Pognonec P (2006) Development of a new bicistronic retroviral vector with strong IRES activity. *BMC Biotechnology* 6 4.

Martin B, Ji S, Maudsley S & Mattson M (2010) Control laboratory rodents are metabolically morbid: why it matters. *PNAS* 107 6127-6133.

Martinez-Salas E (1999) Internal ribosome entry site biology and its use in expression vectors. *Current Opinion in Biotechnology* 10 458-464.

Massoud TF, Singh A and Gambhir SS (2008) Noninvasive molecular neuroimaging using reporter genes: part II, experimental, current, and future applications. *American Journal of Neuroradiology* 29 409-418.

McElroy JF & Wade GN (1986) Short photoperiod stimulates brown adipose tissue growth and thermogenesis but not norepinephrine turnover in Syrian hamsters. *Physiology and Behavior* 37 307-311.

Meiri KF, Pfenninger KH & Willard MB (1986) Growth-associated protein, GAP-43, a polypeptide that is induced when neurons extend axons, is a component of growth cones and corresponds to pp 46, a major polypeptide of a subcellular fraction enriched in growth cones. *Proceedings of the National Academy of Sciences United States of America* 83 3537-3541.

Mercer JG, Mora KM, Ross AW, Hoggard N & Morgan PJ (2000) Photoperiod regulates arcuate nucleus POMC, AgRP and leptin receptor mRNA in the Siberian hamster hypothalamus. *Am J Physiol Regul Integr Comp Physiol* 278 271-281.

Mercer JG, Moar KM, Logie TJ, Findlay PA, Adam CL & Morgan PJ (2001) Seasonally inappropriate body weight induced by food restriction: effect on hypothalamic gene expression in male Siberian hamsters. *Endocrinology* 142 4173-4181.

Mesaros A, Koralov SB, Rother E, Wunderlich FT, Ernst MB, Barsh GS, Rajewsky K & Brüning JC (2008) Activation of Stat3 signalling in AgRP neurons promotes locomotor activity. *Cell Metabolism* 7 236-238.

Mingozzi F & High KA (2011) Therapeutic *in vivo* gene transfer for genetic disease using AAV: progress and challenges. *Nature Reviews Genetics* 12 341-355.

Mizuguchi H, Xu Z, Ishii-Watabe A, Uchida E & Hayakawa T (2000) IRES-dependent second gene expression is significantly lower than cap-dependent first gene expression in a bicistronic vector. *Molecular Therapy* 1 376-382.

Morley JE, Hernandez EN & Flood JF (1987) Neuropeptide Y increases food intake in mice. *Am J Physiol Regul Integr Comp Physiol* 253 516-522.

Morris BJ (1989) Neuronal localisation of neuropeptide Y gene expression in the rat brain. *Journal of Comparative Neurology* 290 358-368.

Morris DL & Rui L (2009) Recent advances in understanding leptin signaling and leptin resistance. *American Journal of Physiology. Endocrinology and Metabolism* 297 1247-1259.

Morris MJ, Tortelli CF, Filippis A & Proietto J (1998) Reduced BAT function as a mechanism for obesity in the hypophagic, neuropeptide Y-deficient monosodium glutamate treated rat. *Regulatory Peptides* 75-76 441-447.

Morrison C & Berthoud H (2007) Neurobiology of nutrition and obesity. *Nutritional Reviews* 65 517-534.

Morton GJ & Schwartz MW (2011) Leptin and the CNS Control of Glucose Metabolism. *Physiological Reviews* 91 389-411.

Moss A, Ingram R, Kockh S, Theodorou A, Low L, Baccei M, Hathway GJ, Costigan M, Salton SR & Fitzgerald M (2008) Origins, actions and dynamic expression patterns of the neuropeptide VGF in rat peripheral and central sensory neurons following peripheral nerve injury. *Molecular Pain* 4 62.

Murphy KG (2006) Dissecting the role of cocaine- and amphetamine-regulated transcript (CART) in the control of appetite. *Briefings in Functional Genomics and Proteomics* 4 95-111.

Murphy KG & Bloom SR (2006) Gut hormones and the regulation of energy homeostasis *Nature* 444 854-859.

Murphy M, Jethwa PH, Warner A, Barrett P, Nilaweera KN, Brameld JM & Ebling FJP (2012) Effects of manipulating hypothalamic tri-iodothyronine concentrations on seasonal body weight and torpor cycles in Siberian hamsters. *Endocrinology* 153 101-112.

Mutch DM & Clement K (2006) Unraveling the genetics of human obesity. *PLoS Genetics* 29 e188.

Nedergaard J, Golozobova V, Matthias A, Asadi A, Jacobsson A & Cannon B (2001) UCP1: the only protein able to mediate adaptive non-shivering thermogenesis and metabolic inefficiency. *Biochimica et Biophysica acta* 154 82-106.

Nedergaard J, Bengtsson T & Cannon B (2007) Unexpected evidence for active brown adipose tissue in adult human. *American Journal of Physiology: Endocrinology and Metabolism* 293, e444-452.

Nedivi E, Basi GS, Akey IV & Pate Skene JH (1992) A neuronal specific GAP-43 core promoter located between unusual DNA elements that interact to regulate its activity. *Journal of Neuroscience* 12 691-704.

Norman AW, Frankel JB, Heldt AM & Grodsky GM (1980) Vitamin D deficiency inhibits pancreatic secretion of insulin. *Science* 209 823-825.

Nuclear Receptors Nomenclature Committee (1999) A unified nomenclature system for the nuclear receptor superfamily. *Cell* 97 161-163.

O'Connor TM (2000) The stress response and the HPA axis. *QJM* 93 323-333.

Oermann E, Bidmon HJ, Witte OW & Zilles K (2004) Effects of 1 α ,25 dihydrovitamin D₃ on the expression of HO-1 and GFAP in glial cells of the photothrombotically lesioned cerebral cortex. *Journal of Chemical Neuroanatomy* 28 225-238.

Olafsdottir G, Svansson V, Ingvarsson EM & Torsteinsdottir S (2008) In vitro analysis of expression vectors for DNA vaccination of horses: the effect of a Kozak sequence. *Acta Veterinaria Scandinavica* 50 1-7.

Olszewski PK, Cedernaes J, Olsson F, Levine AS & Schioth HB (2008) Analysis of the network of feeding neuroregulators using the Allen Brain Atlas. *Neuroscience Behavioural Reviews* 32 5 945-56

Ono H, Hoshino Y, Yasuo S, Watanabe M, Nakane Y, Murai A, Ebihara S, Korf HW & Yoshimura T (2008) Involvement of thyrotropin in photoperiodic signal transduction in mice. *Proc Natl Acad Sci USA* 105 18238-18242

Opstal-van Winden AW, Vermeulen RC, Peeters PH, Beijnen JH & van Gils CH (2012) Early diagnostic protein biomarkers for breast cancer: how far have we come? *Breast Cancer Research Treatment* 134 1-12.

Orava J, Nummenmaa L, Nojonen T, Viljanen T, Parkkola R, Nuutila P & Virtanen KA (2014) Brown adipose tissue function is accompanied by cerebral activation in lean but not obese humans. *Journal of Cerebral Blood Flow and Metabolism* 34 1018-1023.

Orlando FA, Goncalves CG, George ZM, Halverson JD, Cunningham PR & Meguid MM (2005) Neurohormonal pathways regulating food intake and changes after Roux-en-Y gastric bypass. *Surgery for Obesity and Related Diseases* 1 486-495.

Ouellet V, Labbe SM, Blondin DP, Phoenix S, Guerin B, Haman F, Turcotte EE, Richard D & Carpentier AC (2012) Brown adipose tissue oxidative metabolism contributes to energy expenditure during acute cold exposure in humans. *Journal of Clinical Investigation* 122 545-552.

Pahlman S, Odelstad L, Larsson E, Grotte G & Nilsson K (1981) Phenotypic changes of human neuroblastoma cells in culture induced by TPA. *International Journal of Cancer* 28 583-589.

Pahlman S, Ruusala AL, Abrahamsson L, Odelstad L & Nilsson K (1983) Kinetics and concentration effects of TPA-induced differentiation of cultured human neuroblastoma cells. *Cell Differentiation* 12 165-170

Pahlman S, Ruusala AL, Abrahamsson L, Matteson ME & Esscher T (1984) Retinoic acid-induced differentiation of cultured human neuroblastoma cells; a comparison with phorbol ester induced differentiation. *Cell Differentiation* 14 135-144.

Pan J, Kao YL, Joshi S, Jeetendran S, Dipette D & Singh US (2005) Activation of Rac1 by phosphatidylinositol 3-kinase in vivo: role in activation of mitogen-activated protein kinase (MAPK) pathways and retinoic acid-induced neuronal differentiation of SH-SY5Y cells. *Journal of Neurochemistry* 93 571-583.

Parker JA & Bloom SR (2012) Hypothalamic neuropeptides and the regulation of appetite. *Neuropharmacology* 63 18-30.

Patel H, Qi Y, Hawkins E, Hileman SM, Elmquist JK, Imai Y & Ahima RS (2006) Neuropeptide Y deficiency attenuates responses to fasting and high fat diet in obesity prone mice. *Diabetes* 55 3091-3098.

Patel N, Reiss U, Davidoff AM & Nathwani AC (2014) Progress towards gene therapy for haemophilia B. *International Journal of Hematology* 99, 372-376.

Payne AJ, Gerdes BC, Kaja S and Koulen P (2013) Insert sequence length determines transfection efficiency and gene expression levels in bicistronic mammalian expression vectors. *International Journal of Biochemistry and Molecular Biology* 4, 201-208.

Pelleymounter MA, Cullen MJ & Wellman CL (1995) Characteristics of BDNF-induced weight loss. *Experimental Neurology* 131 229-238.

Piccioli P, Di Luzio A, Amann R, Schuligoi R, Surani MA, Donnerer J & Cattaneo A (1995) Neuroantibodies: Ectopic expression of a recombinant anti-substance P antibody in the central nervous system of transgenic mice. *Neuron* 15 373-384.

Poluha W, Poluha DK & Ross AH (1995) TrkA neurogenic receptor regulates differentiation of neuroblastoma cells. *Oncogene* 10 185-189.

Possenti R, Eldridge JD, Paterson BM, Grasso A, & Levi A (1989) A protein induced by NGF in PC12 cells is stored in secretory vesicles and released through the regulated pathway. *European Molecular Biology Organization Journal* 8 2217-2223.

Possenti R, Di Rocco G, Nasi S & Levi A (1992) Regulatory elements in the promoter region of *vgf*, a nerve growth factor inducible gene. *Proceedings of the National Academy of Sciences of the USA* 89 3815-3819.

Possenti R, Muccioli G, Petrocchi P, Cero C, Cabassi A, Vulchanova L, Riedl MS, Manieri M, Frontini A, Giordano A, Cinti S, Govini P, Graiani G, Quaini F, Ghe C, Bresciani E, Bulgarelli I, Torsello A, Locatelli V, Sanghez V, Larsen BD, Petersen JS, Palanza P, Parmigiani S, Moles A, Levi A & Bartolomucci A (2012) Characterisation of a novel peripheral pro-lipolytic mechanism in mice. Role of VGF-derived peptide TLQP-21. *Biochemical Journal* 441 511-522.

Ravussin Y, Xiao C, Gavrolova O & Reitman ML (2014) Effect of intermittent cold exposure on brown fat activation, obesity and energy homeostasis in mice. *PLoS One* 9, e85876.

Riedl MS, Braun PD, Kitto KF, Roiko SA, Anderson LB, Honda CN, Fairbanks CA & Vulchanova L (2009) Proteomic analysis uncovers novel actions of the neurosecretory protein VGF in nociceptive processing. *Journal of Neuroscience* 29 1337-13388.

Ren X, Zhang T, Hu J, Ding W & Wang X (2010) Triptolide T10 enhances AAV-mediated gene transfer in mice striatum. *Neuroscience Letters* 479 187-191.

Robson AJ, Rousseau K, Loudon ASI & Ebling FJP (2002) Cocaine and amphetamine-related transcript (CART) mRNA regulation in the hypothalamus in lean and obese rodents. *Journal of Neuroendocrinology* 14 697-709.

Rohner-Jeanrenaud F, Craft LS, Bridwell J, Suter TM, Tinsley FC, Smiley DL, Burkhart DR, Statnick MA, Heiman ML, Ravussin E & Caro JF (2002) Chronic central infusion of cocaine- and amphetamine-regulated transcript (CART 55-102): effects on body weight homeostasis in lean and high-fat-fed obese rats. *International Journal of Obesity* 26, 143-149.

Rosenbaum M & Leibel RL (2010) Adaptive thermogenesis in humans. *International Journal of Obesity* 34 s47-s55.

Rosner B (2006) *Fundamentals of Biostatistics*. Thomson Brooks/Cole. ISBN 0534418201.

Ross AW, Webster CA, Mercer JG, Moar KM, Ebling FJ, Schuhler S, Barrett P & Morgan PJ (2004) Photoperiodic regulation of hypothalamic retinoid signalling: association of retinoid X receptor gamma with body weight. *Endocrinology* 145 13-20.

Ross AW, Helfer G, Russell L, Darras VM & Morgan PJ (2011) Thyroid hormone signalling genes are regulated by photoperiod in the hypothalamus of F344 rats. *PLoS One* 6 21351.

Roth J, Roland B, Cole RL, Trevaskis JL, Weyer C, Koda JE, Anderson CM, Parkes DG & Baron AD (2008) Leptin responsiveness restored by amylin agonism in diet induced obesity: Evidence from nonclinical and clinical studies. *Proceedings of the National Academy of Sciences* 105 7257-7262.

Rothman RB & Baumann MH (2009) Appetite suppressants, cardiac value disease and combination pharmacotherapy. *American Journal of Therapeutics* 16 354-364.

Rousseau K, Atcha Z, Cagampang FRA, Le Rouzic P, Stirland JA, Ivanov TR, Ebling FJP, Klingenspor M & Loudon AS (2002) Photoperiodic regulation of leptin resistance in the seasonally breeding Siberian hamster (*Phodopus sungorus*). *Endocrinology* 143 3083-3095.

Ryan MS & Drew J (1994) Foot and mouth disease virus 2A oligopeptide mediated cleavage of an artificial protein. *The EMBO Journal* 13 928-933.

Saderi N, Buijs FN, Salgado-Delgado R, Merkenstein M, Basualdo MC, Ferri GL, Escobar C & Buiks RM (2014) A role for VGF in the hypothalamic arcuate and paraventricular nuclei in the control of energy homeostasis. *Neuroscience* 265 184-95.

Sahu A (2004) A hypothalamic role in energy balance with special emphasis on leptin. *Endocrinology* 145 2613-2620.

Sainsbury A & Zhang L (2010) Role of the arcuate nucleus of the hypothalamus in regulation of body weight during energy deficit. *Molecular and Cellular Endocrinology* 316 109-119.

Sakurai T, Amemiya A, Ishii M, Matsuzaki I, Chemelli RM, Tanaka H, Williams SC, Richardson JA, Kozlowski GP, Wilson S, Arch JR, Buckingham RE, Haynes AC, Carr SA, Annan RS, McNulty DE, Liu WS, Terrett JA, Elshourbagy NA, Bergsma DJ & Yanagisawa M (1998) Orexins and orexin receptors: a family of hypothalamic neuropeptides and G-protein coupled receptors that regulate feeding behaviour. *Cell* 92 573-585.

Salton SR (1991) Nucleotide sequence and regulatory studies of VGF, a nervous system-specific mRNA that is rapidly and relatively selectively induced by nerve growth factor. *Journal of Neurochemistry* 57 991-996.

Salton SR, Fischberg DJ & Dong KW (1991) Structure of the gene encoding VGF, a nervous system-specific mRNA that is rapidly and selectively induced by nerve growth factor in PC12 cells. *Molecular Cell Biology* 11 2355-2349.

Silva JE (1995) Thyroid hormone control of thermogenesis and energy balance. *Thyroid* 5 481-492.

Sanchez VC, Goldstein J, Stuart RC, Hovanesian V, Huo L, Munzberg H, Friedman TC, Bjorbaek C & Nillni EA 2004 Regulation of hypothalamic prohormone convertases 1 and 2 and effects on processing of prothyrotropin-releasing hormone. *Journal of Clinical Investigation* 114 357-369.

Saper CB (2010) A treasure trove of gene expression patterns. *Nature Neuroscience* 13, 658-659.

Satoh T, Yamada M, Iwasaki T & Mori M (1996) Negative regulation of the gene for preprothyrotropin-releasing hormone from the mouse by thyroid hormone requires additional factors in conjunction with thyroid hormone receptors. *Journal of Biological Chemistry* 271 27919-27926.

Schuhler S & Ebling F (2006) Role of melanocortin in the long term regulation of energy balance: Lessons from a seasonal model. *Peptides* 37 301-309.

Schuhler S, Warner A, Finney N, Bennett GW, Ebling FJ & Brameld JM 2007 Thyrotrophin-releasing hormone decreases feeding and increases body temperature, activity and oxygen consumption in Siberian hamsters. *Journal of Neuroendocrinology* 19 239-249.

Schulz TJ & Tseng YH (2013) Brown adipose tissue: development, metabolism and beyond. *The Biochemical Journal* 453 167-178.

Schwartz MW, Baskin DG, Kaiyala KJ & Woods SC (1999) Model for the regulation of energy balance and adiposity by the central nervous system. *The American Journal of Clinical Nutrition* 69 584-596.

Schwartz GJ (2000) The role of gastrointestinal vagal afferents in the control of food intake: current prospects. *Nutrition* 16 866-873.

Schwartz MW, Woods SC, Porte D Jr, Seeley RJ & Baskin DG (2000) Central nervous system control of food intake. *Nature* 404 661-671.

Schwartz MW, Woods SC, Seeley RJ, Barsh GS, Baskin DG & Leibel RL (2003) Is the energy homeostasis system inherently biased towards weight gain? *Diabetes* 52, 232-238.

Scrocchi LA, Hill ME, Saleh J, Perkins B & Drucker DJ (2000) Elimination of GLP-1R signalling does not modify body weight gain. *Diabetes* 49 1552-1560.

Senese R, Cioffi F, de Lange P, Goglia F & Lanni A (2014) Thyroid: biological actions of 'nonclassical' thyroid hormones. *Journal of Endocrinology* 221 R1-R12.

Severini C, La Crote G, Importa G, Broccardo M, Agostini S, Petrella C, Sibila V, Pagani F, Guidobono F, Bulgarelli I, Ferri GL, Brancia C, Rinaldi AM, Levi A & Possenti R (2009) In vitro and in vivo pharmacological role of TLQP-21, a VGF derived peptide, in the regulation of rat gastric motor functions. *British Journal of Pharmacology* 157 984-993.

Shabalina IG, Hoeks J, Kramarova TV, Schrauwen P, Cannon B & Nedergaard J (2010) Cold tolerance of UCP1-ablated mice: a skeletal muscle mitochondria switch toward lipid oxidation with marked UCP3 up-regulation not associated with increased basal, fatty acid- or ROS-induced uncoupling or enhanced GDP effects. *Biochimica et Biophysica Acta* 1797 968-980.

Sharma M, Sharma O & Pant HC (1999) CDK-5-mediated neurofilament phosphorylation in SHSY5Y human neuroblastoma cells. *Journal of Neurochemistry* 73 79-86.

Simpson KA, Martin NM & Bloom SR (2009) Hypothalamic regulation of food intake and clinical therapeutic applications. *Arquivos Brasileiro Endocrinologia e Metabologia* 53 120-128.

Simpson PB, Bacha JI, Palfreyman EL, Woolacott AJ, McKernan RM & Kerby J (2001) Retinoic acid evoked-differentiation of neuroblastoma cells predominates over growth factor stimulation: an automated image capture and quantitation approach to neuritogenesis. *Analytical Biochemistry* 298 163-169.

Skaper SD (2012) The neurotrophin family of neurotrophic factors: an overview. *Methods in Molecular Biology* 846 1-12

Small CJ, Liu YL, Stanley SA, Connoley IP, Kennedy A, Stock MJ & Bloom SR (2003) Chronic CNS administration of Agouti-related protein (Agrp) reduces energy expenditure. *International Journal of Obesity and Related Metabolic Disorders* 27 530-533.

Smith GP, Jermone C & Norgren R (1985) Afferent axons in the abdominal complex vagus mediate satiety effect of cholecystokinin in rats. *American Journal of Physiology* 249 638-641.

Snyder SE, Pintar JE & Salton SR (1998) Developmental expression of VGF mRNA in the prenatal and postnatal rat. *The Journal of Comparative Neurology* 394 64-90.

Snyder SE, Peng B, Pintar JE & Salton SR (2003) Expression of VGF mRNA in developing neuroendocrine and endocrine tissues. *The Journal of Endocrinology* 179 227-235.

South EH & Ritter RC (1988) Capsaicin application to central or peripheral vagal fibres attenuates CCK satiety. *Peptides* 9 601-612.

Stanley BG, Anderson KC, Grayson MH & Leibowitz SF (1985) Repeated hypothalamic stimulation with neuropeptide Y increases daily carbohydrate and fat intake and body weight gain in female rats. *Physiology and Behavior* 46 173-177.

Stanley S, Wynne K, McGowan B & Bloom S (2005) Hormonal regulation of food intake. *Physiological Reviews* 85 1131-1158.

Statistics on Obesity, Physical Activity and Diet, England (2014) Health and Social Care Information Centre - www.hscic.gov.uk Accessed 14 March 2014

Steiner DF (1998) The proprotein convertases. *Current Opinion Chemical Biology* 2 31-39.

Stephens TW, Basinski M, Bristow PK, Blue-Valleskey JM, Burgett SG, Craft L, Hale J, Hoffman J, Hsiung HM & Krisauciunas A (1995) The role of neuropeptide Y in the antiobesity action of the obese gene product. *Nature* 377 530-532.

Stumpf WE, Bidmon HJ, Li L, Pilgrim C, Bartke A, Mayerhofer A & Heiss C (1992) Nuclear receptor sites for vitamin D-soltriol in midbrain and hindbrain of Siberian hamster (*Phodopus sungorus*) assessed by autoradiography. *Histochemistry* 98 155-164.

Succu S, Cocco C, Mascia MS, Melis T, Melis MRN, Possenti R, Levi A, Ferri GL & Argiolas A (2004) Pro-VGF-derived peptides induce penile erection in male rats: possible involvement of oxytocin. *European Journal of Neuroscience* 135 2742-2748.

Sun BD, Chen YT, Bird A, Amalfitano A & Koeberl DD (2003) Long-term correction of glycogen storage disease type II with a hybrid Ad-AAV vector. *Molecular Therapy* 7 193-201.

Sun Y, Asnicar M, Saha PK, Chan L & Smith RG (2006) Ablation of ghrelin improves the diabetic but not the obese phenotype of ob/ob mice. *Cell Metabolism* 3 379-386.

Surwit RS, Kuhn CM, Cochrane C, McCubbin JA & Feinglos MN (1988) Diet-induced type II diabetes in C57BL/6J mice. *Diabetes* 37 1163-1167.

Suzuki K, Jayasena CN & Bloom SR (2012) Obesity and appetite control. *Experimental Diabetes Research* 1-19.

Sweetman D, Golkane K, Rathjen T, Oustanina S, Braun T, Dalmay T & Munsterberg A (2008) Specific requirements of MRFs for the expression of muscle specific microRNAs, miR-1, miR-206 and miR-133. *Developmental Biology* 321, 491-494.

Takada J, Fonseca-Alaniz MH, de Campos TB, Andreotti S, Campana AB, Okamoto M, Borges-Silva CD, Machado UF & Lima FB (2008) Metabolic recovery of adipose tissue is associated with improvement in insulin resistance in a model of experimental diabetes. *Journal of Endocrinology* 198 51-60.

Takeda E, Miyamoto K, Kubota M, Minami H, Yokota I, Saijo T, Naito E, Ito M & Kuroda Y (1994) Vitamin D-dependent rickets type II: regulation of human osteocalcin gene expression in cells with defective vitamin D receptors by 1,25-dihydroxyvitamin D-3, retinoic acid, and triiodothyronine. *Biochimica et Biophysica Acta* 1227 195-199.

Tartaglia LA, Dembrski M, Weng X, Deng N, Culpepper J, Devos R, Richards GJ, Campfeld LA, Clark FT, Deeds J, Muir C, Sanker S, Moriarty A, Moore KJ, Smutko JS, Mays GG, Woolf EA, Monroe CA & Tepper RI (1995) Identification and expression cloning of a leptin receptor, OB-R. *Cell* 83 1263 - 1267.

Thakker-Varia S, Behnke J, Doobin D, Dalal V, Thakkar K, Khadim F, Wilson E, Palmieri A, Antila H, Rantamaki T1 & Alder J (2014) VGF (TLQP-62)-induced neurogenesis targets early phase neural progenitor cells in the adult hippocampus and requires glutamate and BDNF signalling. *Stem Cell Research* 12 762-777.

Tieu K, Zuo DM & Yu PH (1999) Differential effects of staurosporine and retinoic acid on the vulnerability of the SH-SY5Y neuroblastoma cells. *Journal of Neuroscience Research* 58 426-435.

Tong Q, Ye CP, Jones JE, Elmquist JK & Lowell BB (2008) Synaptic release of GABA by AgRP neurons is required for normal regulation of energy balance. *Nature Neuroscience* 11 998-1000.

Tokuyama K & Himms-Hagen J (1989) Adrenalectomy prevents obesity in glutamate-treated mice. *Am J Physiol Endocrinol Metab* 257: 139-144

- Toshinai K & Nakazato M (2009) Neuroendocrine regulatory peptide-1 and -2: Novel bioactive peptides processed from VGF. *Cellular and Molecular Life Sciences* 66 1939-1945.
- Trani E, Ciotti T, Rinaldi AM, Canu N, Ferri GL, Levi A & Possenti R (1995) Tissue-specific processing of the neuroendocrine protein VGF. *Journal of Neurochemistry* 65 2441-2449.
- Trani E, Giorgi A, Canu N, Amadoro G, Rinaldi AM, Halban PA, Ferri GL, Possenti R, Schinina ME & Levi A (2002) Isolation and characterisation of VGF peptides in rat brain. Role of PC1/3 and PC2 in the maturation of VGF precursor. *Journal of Neurochemistry* 81 565-574.
- Trichas G, Begbie J & Srinivas S (2008) Use of the viral 2A peptide for bicistronic expression in transgenic mice. *BMC Biology* 6 1-13.
- Trivedi P, Yu H, MacNeil DJ, van der Ploeg LH & Guan XM (1998) Distribution of orexin receptor mRNA in the rat brain. *Federation European Biochemical Societies Letters* 438 71-75.
- Tsukahara F, Uchida Y, Ohba K, Ogawa A, Yoshioka T & Muraki T (1998) The effect of acute cold exposure and norepinephrine on the uncoupling protein gene expression in brown adipose tissue of monosodium glutamate-obese mice. *Japanese Journal of Pharmacology* 77 247-249.
- Tsujino N & Sakurai T (2013) Role of orexin in modulating arousal, feeding, and motivation. *Frontiers in Behavioural Neuroscience* 18 28.
- Tups A, Stohr S, Helwig M, Barrett P, Krol E, Schachtner J, Mercer JG & Klingenspor M (2012) Seasonal leptin resistance is associated with impaired signalling via JAK2-STAT3 but not ERK, possibly mediated by reduced hypothalamic GRB2 protein. *Journal of Comparative Physiology* 182, 553-567.
- van den Pol AN, Decavei C, Levi A & Paterson B (1989) Hypothalamic expression of a novel gene product, VGF: Immunocytochemical analysis. *The Journal of Neuroscience* 9 4122-4137.
- van der Lans AA, Hoeks J, Brans B, Vijgen GH, Visser MG, Vosselman MJ, Hansen J, Jorgensen JA, Wu J, Mottaghy FM, Schrauwen P & van Marken Lichtenbelt WD (2013) Cold acclimation recruits human brown fat and increases nonshivering thermogenesis. *Journal of Clinical Investigation* 123, 3395-403.
- Van Heek M, Compton DS, France, CF, Tedesco RP, Fawzi AB, Graziano MP, Sybertz EJ, Strader CD & Davis HR Jr (1997) Diet-induced obese mice develop

peripheral but not central resistance to leptin. *Journal of Clinical Investigation* 99 385-390.

Van Vliet KM, Blouin V, Brument N, Agbandje-McKenna M & Snyder RO (2008) The role of the adeno-associated virus capsid in gene transfer. *Methods in Molecular Biology* 437, 51-91.

Varela L & Horvath TL (2012) Leptin and insulin pathways in POMC and AgRP neurons that modulate energy balance and glucose homeostasis. *EMBO Reports* 13, 1079-1086.

Vaisse C, Halaas JL, Horvath CM, Darnell JE Jr, Stoffel M & Friedman JM (1996) Leptin activation of Stat3 in the hypothalamus of wild-type and ob/ob mice but not db/db mice. *Nature Genetics* 14 95-97.

Vaughan CH, Zarebidaki E, Ehlen JC & Bartness TJ (2014) Analysis and measurement of the sympathetic and sensory innervations of white and brown adipose tissue. *Methods in Enzymology* 537, 199-225.

Velloso LA & Schwartz MW (2011) Altered hypothalamic function in diet induced obesity. *International Journal of Obesity* 35 1455-1465.

Wade GN & Bartness TJ (1984) Effects of photoperiod and gonadectomy on food intake, body weight and body composition in Siberian hamsters. *American Journal of Physiology* 246 26-30.

Wang C, Billington CJ, Levine AS & Kotz CM (2000) Effect of CART in the hypothalamic paraventricular nucleus on feeding and uncoupling protein gene expression. *Neuroreport* 11, 3251-3255.

Wang JY, Wu JN, Cherng TL, Hoffer BJ, Borlongan CV & Wang Y (2001) Vitamin D(3) attenuates 6-hydroxydopamine-induced neurotoxicity in rats. *Brain Research* 904 67-75.

Watanabe M, Yasuo S, Watanabe T, Yamamura T, Nakao N, Ebihara S & Yoshimura T (2004) Photoperiodic regulation of type 2 deiodinase gene in Djungarian hamster: possible homologies between avian and mammalian photoperiodic regulation of reproduction. *Endocrinology* 145 1546-1549.

Watson E, Hahm S, Mizuno TM, Windsor J, Montgomery C, Scherer PE, Mobbs CV & Salton SR (2005) VGF ablation blocks the development of hyperinsulinemia and hyperglycemia in several mouse models of obesity. *Endocrinology* 146 5151-5163.

Watson E, Fagali S, Okamoto H, Sadahiro M, Gordon RE, Chakraborty T, Sleeman MW & Salton SR (2009) Analysis of knockout mice suggests a role for

VGF in the control of fat storage and energy expenditure. *BMC Physiology* 28 1-20.

Westerterp K (2004) Diet Induced thermogenesis. *Nutrition and Metabolism* 1 1-5.

Williams G, Bing C, Cai XJ Harrold JA, King PJ & Liu XH (2001) The hypothalamus and the control of energy homeostasis: different circuits, different purposes. *Physiological Behaviour* 74 683-701.

Williams KW & Elmquist JK (2011) Lighting up the hypothalamus: coordinated control of feeding behaviour. *Nature Neuroscience* 14 277-278.

Willyard C (2014) Heritability: The family roots of obesity. *Nature* 508 s58-60.

Wong KE, Szeto FL, Zhang W, Ye H, Kong J, Zhang Z, Sun XJ and Li YC (2009) Involvement of the vitamin D receptor in energy metabolism: regulation of uncoupling proteins. *American Journal of Physiology* 296 820-828.

Woods SC, Lotter EC, McKay LD & Porte D Jr (1979) Chronic intracerebroventricular infusion of insulin reduces food intake and body weight of baboons *Nature* 282 503-505.

Woods SC, Lutz TA, Geary N & Langhans W (2006) Pancreatic signals controlling food intake; insulin, glucagon and amylin. *Philosophical Transactions of the Royal Society of London, Series B Biological Sciences* 361 1219-1235.

Woods SC & D'Alessio DA (2008) Central Control of Body Weight and Appetite. *Journal of Clinical Endocrinology and Metabolism* 93 s37-50.

Wren AM, Small CJ, Ward HL, Murphy KG, Dakin CL, Taheri S, Kennedy AR, Roberts GH, Morgan DG, Ghatei MA & Bloom SR (2000) The novel hypothalamic peptide ghrelin stimulates food intake and growth hormone secretion. *Endocrinology* 141 4325-28.

Wren AM, Small CJ, Abbott CR, Jethwa PH, Kennedy AR, Murphy KG, Stanley SA, Zollner AN, Ghatei MA & Bloom SR (2002) Hypothalamic actions of neuromedin U. *Endocrinology* 143 4227-4234.

Xie HR, Hu LS & Li GY (2010) SH-SY5Y human neuroblastoma cell line: in vitro cell model of dopaminergic neurons in Parkinson's disease. *Chinese Medical Journal* 123 1086-1092.

Yamada T, Katagiri H, Ishigaki Y, Oigahara T, Imai J, Uno K, Hasegawa Y, Gao J, Ishihara H, Niiijima A, Mano H, Aburatani H, Asano T & Oka Y (2006) Signals from intra-abdominal fat modulate insulin and leptin sensitivity through different

mechanisms: Neuronal involvement in food-intake regulation. *Cell Metabolism* 3 223-229.

Yamaguchi H, Sasaki K, Satomi Y, Shimbara T, Kageyama H, Mondal MS, Toshinai K, Date Y, Gonzalez LJ, Shioda S, Takao T, Nakazato M & Minamino N (2007) Peptidomic identification and biological validation of neuroendocrine regulatory peptide-1 and -2. *Journal of Biological Chemistry* 282 26354-26360.

Yamashita H, Inenaga K, Kawata M & Sano Y (1983) Phasically firing neurons in the supraoptic nucleus of the rat hypothalamus: immunocytochemical and electrophysical studies. *Neuroscience Letters* 37 87-82.

Yen PM, Ando S, Feng X, Liu Y, Maruvada P & Xia X (2006) Thyroid hormone action at the cellular, genomic and target gene levels. *Molecular and Cellular Endocrinology* 246, 121-127.

Yu S, Levi L, Siegel R & Noy N (2010) Retinoic acid induces neurogenesis by activating both retinoic acid receptors (RARs) and peroxisome proliferator-activated receptor β/δ (PPAR β/δ). *Journal of Biological Chemistry* 287 42195-41205.

Zhang Y, Proenca R, Maffei M, Barone M, Leopold L & Friedman JM (1994) Positional cloning of the mouse obese gene and its human homologue. *Nature* 372 425-432.

Zhang JV, Ren PG, vsian-Kretchmer O, Luo CW, Rauch R, Klein C & Hsueh AJ (2005) Obestatin, a peptide encoded by the gherlin gene, opposes gherlin's effects on food intake. *Science* 310 996-999.

Zhang T, Hu J, Ding W & Wang X (2009) Doxorubicin augments rAAV-2 transduction in rat neuronal cells. *Neurochemistry International* 55 521-528.

Zhang XK & Kahl M (1993) Regulation of retinoid and thyroid hormone action through homodimeric and heterodimeric receptors. *TEM* 4 156-162.

Zhao Z, Lange DJ & Pasinetti GM (2008a) Vgf is a novel biomarker associated with muscle weakness in amyotrophic lateral sclerosis (ALS), with a potential role in disease pathogenesis, *International Journal of Medical Science* 5 92-99.

Zhao T, Szabo N, Ma J, Luo L, Zhou X & Alvarez-Bolado G (2008b) Genetic mapping of Foxb1-cell lineage shows migration from caudal diencephalon to telencephalon and lateral hypothalamus. *The European Journal of Neuroscience* 28 1941-1955.